INFORMATION TO USERS

This manuscript has been reproduced from the microfilm master. UMI films the text directly from the original or copy submitted. Thus, some thesis and dissertation copies are in typewriter face, while others may be from any type of computer printer.

The quality of this reproduction is dependent upon the quality of the copy submitted. Broken or indistinct print, colored or poor quality illustrations and photographs, print bleedthrough, substandard margins, and improper alignment can adversely affect reproduction.

In the unlikely event that the author did not send UMI a complete manuscript and there are missing pages, these will be noted. Also, if unauthorized copyright material had to be removed, a note will indicate the deletion.

Oversize materials (e.g., maps, drawings, charts) are reproduced by sectioning the original, beginning at the upper left-hand corner and continuing from left to right in equal sections with small overlaps.

ProQuest Information and Learning
300 North Zeeb Road, Ann Arbor, MI 48106-1346 USA
800-521-0600

ADSORPTION AND SYNERGISM IN SUPERSPREADING OF TRISILOXANE SURFACTANT–N-ALKYL PYRROLIDINONE MIXTURES ON POLYETHYLENE SUBSTRATES

BY

YONGFU WU

A dissertation
Submitted to the Graduate Faculty in Chemistry
in partial fulfillment of the
requirements for the degree of
Doctor of Philosophy,
The City University of New York

2002

This manuscript has been read and accepted for the Graduate Faculty in Chemistry in satisfaction of the dissertation requirement for the degree of Doctor of Philosophy.

6/4/02
Data

Chair of Examining Committee

8/20/02
Date

Executive Officer

Dr. Richard Pizer

Dr. Manilal Dahanayake

Dr. James Batteas

Supervisory Committee

The City University of New York

THE CITY UNIVERSITY OF NEW YORK

Abstract

Adsorption and Synergism in Superspreading of Trisiloxane Surfactant –N-alkyl Pyrrolidinone Mixtures on Polyethylene Substrates

by

Yongfu Wu

Advisor: Professor Milton J. Rosen

To investigate the mechanism(s) of synergism in superspreading, surface tensions, contact angles and adsorption isotherms of surfactant aqueous solutions have been measured. It was found that the adsorption of trisiloxane surfactant(L77) from its aqueous solution onto powered polyethylene can be remarkably enhanced by the addition of certain N-alkyl pyrrolidinones and that there is a significant attractive interaction between the surfactant molecules at the polyethylene/aqueous solution interface. The reductions in interfacial pressure at the liquid/air, solid/liquid and solid/air interfaces caused by the surfactant mixtures have been evaluated by use of the Gibbs equation. The surface tension at the liquid/air interface is always increased in the mixtures, indicating that there is no synergism at this interface upon the addition of N-alkyl pyrrolidinones. However, the interfacial pressure at the solid/liquid

interface is increased when L77 and the proper N-alkyl pyrrolidinone are mixed at a certain ratio, indicating that the mixtures can show synergistic effect at this interface. Compared with the changes at the liquid/air interface and the solid/liquid interface, the change at the solid/air interface is insignificant. The change in the spreading coefficients on polyethylene film of aqueous solutions of L77, when mixed with the N-alkyl pyrrolidinone is in almost the same order as that of their enhancement of the spreading.

In order to investigate the cause of the changes in interfacial tensions at the various interfaces produced by replacement of L77 by N-alkyl pyrrolidinone, interaction parameters (β) of L77 with the different pyrrolidinones at the various interfaces were determined. β^{σ}_{LA} for all mixtures was between 0 and −1, indicating that the interaction at the air/aqueous solution interfaces is very weak. However, the values of β^{σ}_{SL} were between −2.7 and −6.7 for the mixtures with those N-alkyl-pyrrolidinones that produce enhancement of the superspreading of aqueous solution of L77 on polyethylene, indicating a significant attractive interaction with L77 at the polyethylene/aqueous solution interface. The order of increasing negative β^{σ}_{SL} values is L77-C2,6P>L77-C6P>L77-C8P> L77-CHP> L77-C4P, which is exactly the same as the order of increasing enhancement of superspreading. This attractive interaction results in a remarkable enhancement of adsorption of L77 onto polyethylene from the aqueous solution of the mixtures.

Dedication

To My Mother

ACKNOWLEDGEMENTS

I will be forever grateful to Professor Milton J. Rosen. His excellent scientific guidance, greatest patience, encouragement, understanding, friendship and invaluable help have made this thesis a reality. Thanks here cannot fully express my deep appreciation from the bottom of my heart, but all of these will be long remembered.

I should also give my many thanks to Professor Richard Pizer for his very kind help in my study and research when he served as the Executive Officer of the Ph.D. program of the Graduate School and as a member of my thesis committee.

I thank very much Dr. Mannil Dahanayake and Dr. James Batteas, members of my thesis committee, for their valuable time and helpful advice.

I thank very much all members of my family, for their support, encouragement and unselfish sacrifice through the years of my study.

Finally, my thanks and good wishes to all the friendly people who provided friendship and valuable conversation in the Surfactant Research Institute over the years.

CONTENTS

LISTS OF TABLES

Tables

Tables A

Tables B

LIST OF FIGURES

Figures A

Figures B

CHAPTER 1

INTRODUCTION

1.1 General Aspects

It is well known that spreading of a liquid on a solid or wetting of a solid surface by a liquid is a basic component in many natural processes and commercial technologies. Some examples include the spreading of liquids such as coatings or inks on substrates ranging from clean metals to plastics, the penetration of inks into porous substrates such as paper, and the spreading of pesticide formulations on waxy weed leaf surfaces. Most application areas have their own specialized literatures[1-8] and test methods [9-16]. Over many years, the subject of the solid/liquid interface and related phenomena, such as wetting and spreading, has attracted considerable interest from chemists, especially surfactant chemists, and has been the focus of a wide range of investigations because of its theoretical and practical implications [17-24].

Recent work on the spreading behavior of the polysiloxane-based surfactants has found that aqueous solutions of certain trisiloxane surfactants have the ability to spread on hydrophobic surfaces to a much greater extent than aqueous solutions of hydrocarbon-based surfactants, even when the latter surfactants are excellent wetting agents for other substrates[25]. Such unusual spreading behavior is now often called "superspreading" or "superwetting". During the last decade, this spreading of aqueous trisiloxane surfactant solutions over low-energy hydrophobic surfaces has been of great interest to chemists[26-35] because of their extraordinary spreading ability. Superspreading is usually ascribed to the ability of the trisiloxane surfactant to decrease the surface tension of the aqueous spreading solution to 20-21 mN/m, which is significantly lower than the minimum tension of 25 mN/m attainable with an aqueous hydrocarbon chain surfactant.

Most noteworthy is the finding of "synergism" in the superspreading of aqueous mixtures of a trisiloxane surfactant and a hydrocarbon chain surfactant over hydrophobic substrates, such as Parafilm and polyethylene. Recent investigations in our laboratory[36,37] have revealed that certain surface active materials with short hydrophobic chains, such as N-butyl, hexyl-, octyl- and 2-ethyhexyl-pyrrolidinones, although their aqueous solutions do not spread significantly on hydrophobic surfaces, when mixed with aqueous solutions of

ethoxylated trisiloxane, such as SILWET L77, can remarkably enhance the spreading ability of the latter on Parafilm and polyethylene, even when the total concentration is kept constant.

We have found that this synergistic effect is not associated with any further lowering of the surface tension of the solutions. To date, various theories have been proposed to explain the superspreading behavior of trisiloxane aqueous solutions on low-energy hydrophobic surfaces, a great deal of work has been done, and a considerable number of papers have been published[38-50]. However, very few papers[36,51] have been published related to synergism in the superspreading of aqueous solutions of mixtures of trisiloxane surfactant and hydrocarbon chain surfactants. Consequently, the mechanism of such synergism is not yet understood. The purpose of this investigation was to elucidate the mechanism involved in the "superspreading" of certain trisiloxane surfactants, especially the phenomena leading to "synergism" in the superspreading.

1.2 Overview

1.2.1 Siloxane Surfactants

Siloxane surfactants consist of dimethysiloxane groups coupled to one or more polar groups[52]. Siloxane surfactants of the proper structure can lower

aqueous surface tension to smaller values than can be achieved by using hydrocarbon surfactants, to values as low as 20 mN/cm. The ability of siloxane surfactants to promote spreading plays an important role in their use in paints and coatings[52], personal care products[53-57], cosmetics[58-62], textiles[63], the lubrication oil industry[64] and agrochemicals as adjuvants for pesticides and herbicides[65-72]. Gradzielski et al.[73] attributed the good wetting properties of siloxane surfactants to low adhesive forces between individual molecules in interfacial films. Vick[53] found that the time to wet by the Draves wetting test depended on the size of the siloxane hydrophobic group and the length of the polyoxyethylene group – the most rapid wetting was observed for the surfactant with the shortest siloxane groups and the smallest EO groups.

1.2.2 Superspreading

The unique ability of certain low molecular weight siloxane surfactants to promote wetting and spreading of dilute aqueous solutions on hydrophobic surfaces such as Parafilm® and Polyethylene was discovered in the 1960s[74-78] and has been the subject of numerous patents and papers since then. The ability of the trisiloxane surfactants to promote spreading on waxy weed leaf surfaces such as Velvetleaf and Lambsquarter is the basis of their use as herbicide adjuvants or wetting agents.

The molecular structure of the trisiloxane surfactants, and the origin of the difference between the hydrocarbon and siloxane surfactants is illustrated in Figure 1.

Figure 1 shows that the surface active character of the trisiloxane surfactants is due to the methyl groups – the surface energy of a methyl-saturated surface is about 20 mN/m[79]. In contrast, most hydrocarbon surfactants contain alkyl or alkylaryl hydrophobic chains which consist of mostly $-CH_2-$ groups. The surface energy of such a surface is dominated by the methylene groups and for this reason hydrocarbon surfactants typically achieve surface tension of about 25 mN/m or higher. Thus, the lower surface tensions given by siloxane surfactants can be traced directly to the different surface energies of $-CH_3-$ vs .$-CH_2-$.

The need to better understand the superspreading of siloxane derivatives has prompted experimental investigations of a number of aqueous surfactant solutions and dispersions. Early work was aimed at spreading dynamics of aqueous surfactant solutions on strongly hydrophobic surfaces[80]. Recently, Zabkiewicz and Gaskin[81] , Gaskin and Kirwood[82], and Knoche et al.[83] reported that a trisiloxane surfactant denoted $M(D'E_8OMe)M$, can be used as a very effective wetting agent for water-based herbicides on fairly hydrophobic plant leaves, where $M=(CH_3)_3SiO$, $E_n =(OCH_2CH_2)_n$, $Me =CH_3$, and $D' =-Si-CH_3(R)$.

Figure 1. Hydrophobic Group Structures of

(a) A Typical Hydrocarbon Surfactant

(b) A Typical Trisiloxane Surfactant

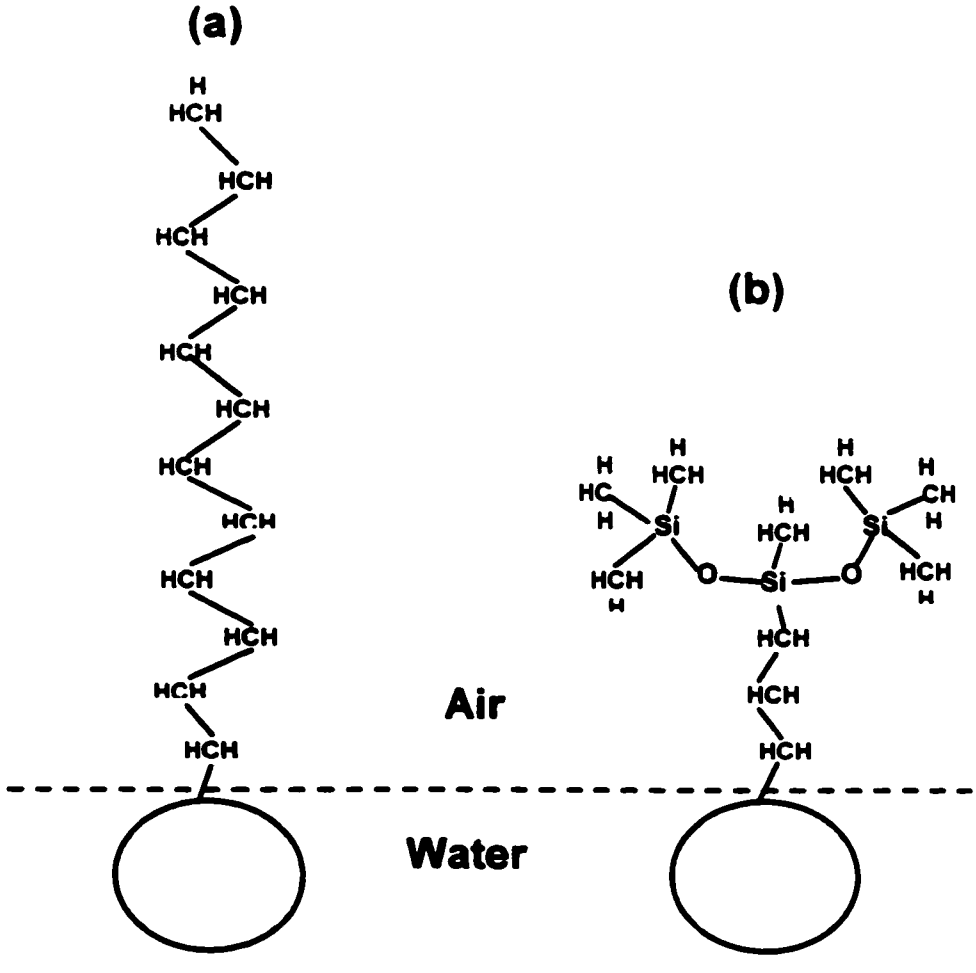

Table 1 lists the nomenclature and structure of a number of siloxane surfactants.

Table 1. Nomenclature and Structure of Silicone Surfactants

Surfactant[a]	Structure	Manufacture[b]
M(D'E_4OH)M	$(Me_3SiO)_2Si(Me)(CH_2)_3(OCH_2CH_2)_4OH$	DCC
M(D'E_8OH)M	$(Me_3SiO)_2Si(Me)(CH_2)_3(OCH_2CH_2)_8OH$	DCC
M(D'E_8OMe)M	$(Me_3SiO)_2Si(Me)(CH_2)_3(OCH_2CH_2)_8OMe$	OSi
M(D'E_8OAc)M	$(Me_3SiO)_2Si(Me)(CH_2)_3(OCH_2CH_2)_8OAc$	DCC
M(D'E_{12}OH)M	$(Me_3SiO)_2Si(Me)(CH_2)_3(OCH_2CH_2)_{12}OH$	DCC
MDM'E_8OH	$Me_3SiOSi(Me_2)OSi(Me)(CH_2)_3(OCH_2CH_2)_8OH$	DCC

[a] Me, CH_3; M, Me_3SiO; D', $Si(Me)(CH_2-$; E_n, $(OCH_2CH_2)_n$; Ac, $OC(C=O)CH_3$
[b] DCC, Dow Corning Corporation, Midland, MI; Osi, Osi Specialties, Inc.

Svitova et al.[28] measured interfacial tensions between a series of normal alkanes and 0.5 wt% solutions of M(D'E_8OH)M. Their results showed that the interfacial tension varied linearly with surfactant concentration in the bulk solution between about 0.025 mN/m for hexane to 0.4 mN/m for hexadecane. These small values indicate that trisiloxane surfactants are very effective at lowering interfacial tensions against low energy hydrocarbon substrates. Thus, the trisiloxane surfactants meet both criteria for spreading

over low energy hydrocarbon substrates – small surface and interfacial tensions. However, the actual spreading behavior exhibits a number of features which cannot be easily explained, e.g., the synergistic effect in superspreading without an association with a further lowering in surface tension.

Kanner et al[76] observed that "certain methysiloxane-polyether copolymers with low surface tension in aqueous solution spread rapidly to a thin film on low energy hydrophobic surfaces such as polyethylene and polystyrene", and that "the best wetting agents are based on siloxane hydrophobic groups containing 2 to 5 silicon atoms and have surface tension of 20-21 dyns per cm", and further, that "these wetting agents are also characterized by a rather specific solubility balance... for optimum wetting, a surfactant must have a limited but finite solubility in water".

Ananthapadmanabhan et al.[84,85] investigated the spreading behavior of several siloxane surfactants on Parafilm®. They also observed relationships between turbidity and spreading, equilibrium surface tension and spreading. These authors stated that "the structure itself of the SSI molecule plays a governing role in determining its superior properties". Much of the literature dealing with the spreading of the trisiloxane surfactants describes the spreading properties in terms of spreading area, spread diameter, or a spread index, which is a ratio to some benchmark condition. The spread area is usually defined as the area of a spread droplet after some fixed length of time.

Zhu et al. [25, 86] measured spreading rates of M(D'E_8OMe)M on Parafilm® using a video method. They found that the spread area increased linearly with time to a plateau value that was proportional to the surfactant concentration – the droplets spread until the inventory of surfactant to cover the air/aqueous solution and aqueous solution/substrate interface was exhausted. They also found a maximum in spreading rates as a function of surfactant concentration and showed that the spreading rate was linearly related to dispersion turbidity and sensitive to humidity. The dependence on humidity was taken to indicate the need for a pre-existing water film on the surface, and the rapid spreading was attributed to Marangoni effects[87].

The critical surface tension of wetting of Parafilm® is about 23dyn/cm [86]. Both M(D'E_8OMe)M and M(D'E_{12}OH)M, a more hydrophilic trisiloxane surfactant, have aqueous surface tensions above their CMC of about 20.5 dyn/cm. However, M(D'E_{12}OH)M does not wet Parafilm® at all. The reason for such big difference was not explained by the investigators. Zhu et al did not find any hydrocarbon surfactants which wet Parafilm®.

Lin et al.[26,88], working with M(D'E_8OH)M, confirmed the concentration maximum using a quartz crystal microbalance (QCM) to measure spreading rates on gold substrates whose surface energies were modified by mixtures with various ratios of $HS(CH_2)_{15}COOH$ to $HS(CH_2)_{15}CH_3$ and showed that there

was also a maximum in spreading rates as a function of substrate surface energy. They also discovered that $M(D'E_{12}OH)M$ spreads with similar characteristics, except that it is somewhat lower at its maximum value, and does not spread on Parafilm®.

Stoebe et al. [27,89,90] used an image analysis method to measure spreading rates (on gold-coated substrates whose surface energies were modified by mixtures with various ratio of $HS(CH_2)_{11}CH_2OH$ to $HS(CH_2)_{11}CH_3$) for solutions of several trisiloxane surfactants vs. surfactant concentration, substrates surface energy, relative humidity, and temperature. They also found that spread area increases linearly with time, and that there are maximum rates vs. concentration and substrate surface energy. They found that the sensitivity to humidity depended on the type of substrate – for Parafilm® the effect of humidity is strong, but for smoother surfaces it is much weaker.

Stoebe et al.[29] have also observed spreading by trisiloxane and hydrocarbon surfactants on mineral oil. The behavior was similar to that on solid surfaces, except that spreading rates are higher by a factor of 10 – 20 and there was not a concentration maximum. For the EO_4 homologues, they observed stepwise sprading events which correlated with disintegration of visible droplets of surfactant-rich phase.

CHAPTER 2

THEORETICAL BACKGROUND

2.1 Spreading Wetting

In spreading wetting (shown in Figure 2), a liquid in contact with a substrate spreads over the substrate and displaces another fluid, such as air, from the surface. For the spreading to occur spontaneously, the surface free energy of the system must decrease during the spreading process. When the area of an interface increases, the surface free energy at that interface increases; when the area decreases, the surface free energy decreases. In Figure 2, if the liquid spreads from C to B, covering an area a, then the decrease in surface free energy of the system due to decrease in area of the substrate/air interface is $a \times \gamma_{SA}$, where γ_{SA} is the interfacial free energy per unit area of the substrate in equilibrium with liquid-saturated air above it. At the same time the free energy of the system has been increased because of the increase in liquid-substrate and

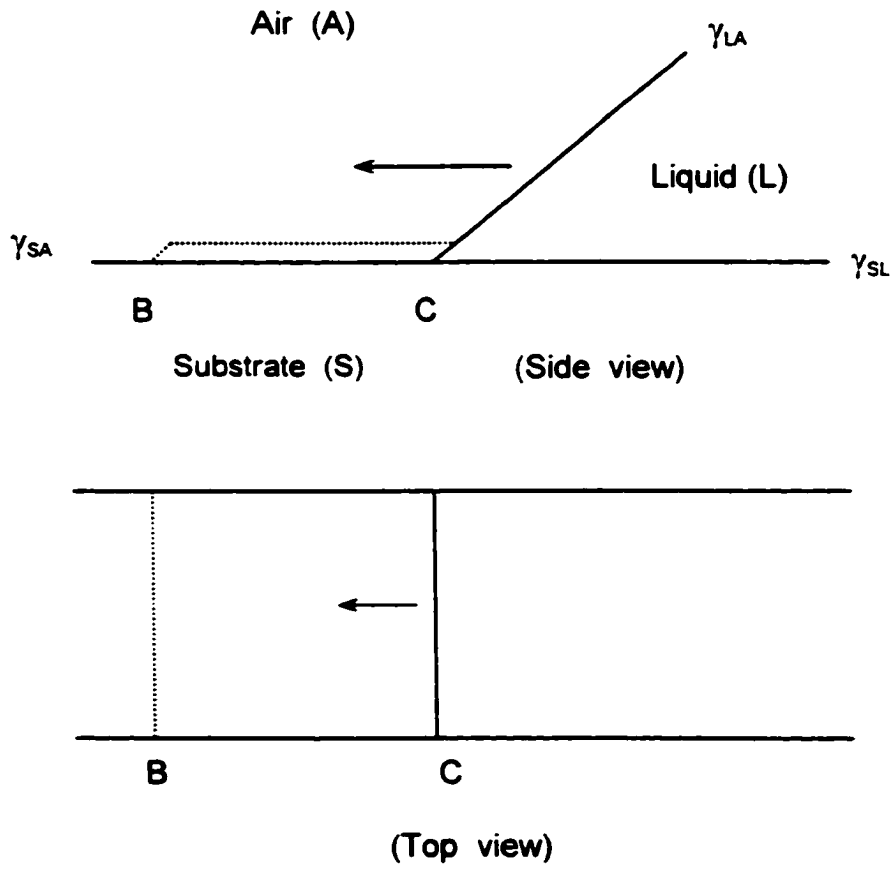

Figure 2. Spreading Wetting of a Liquid on a Solid Substrate

liquid-air interfaces. The increase in surface free energy of the system due to the increase in the liquid-substrate interface is $a \times \gamma_{SL}$, where γ_{SL} is the interfacial free energy per unit area at the liquid-substrate interface, and since the liquid-air interface has also been increased by area a, the increase in surface free energy due to increase in this interface is $a \times \gamma_{LA}$, where γ_{LA} is the

surface tension of liquid. Therefore, the total decrease in surface free energy per unit area of the system due to the spreading wetting, $-\Delta G_W/a$, is $\gamma_{SA}-(\gamma_{SL}+\gamma_{LA})$. If the quantity $\gamma_{SA}-(\gamma_{SL}+\gamma_{LA})$ is positive, the system decreases in surface free energy during the spreading process, and the process can then occur spontaneously. Otherwise, If the quantity $\gamma_{SA}-(\gamma_{SL}+\gamma_{LA})$ is negative, the system increases in surface free energy during the spreading process, and the process cannot occur spontaneously.

The quantity $\gamma_{SA}-(\gamma_{SL}+\gamma_{LA})$ is then a measure of the driving force behind the spreading process, and is usually called the spreading coefficient $S_{L/S}$. If $S_{L/S}$, as defined by

$$S_{L/S} = -\Delta G_W / a = \gamma_{SA}-(\gamma_{SL}+\gamma_{LA}) \qquad (1)$$

is positive, spreading process can occur spontaneously; if $S_{L/S}$ is negative, the liquid will not spread spontaneously over the substrate. Furthermore, it is expected that the more positive the spreading coefficient, the greater the spreading area made by liquid over substrate.

2.2 The Contact Angle

The contact angle, θ, that the liquid makes when it is at equilibrium with other phases in contact with it is related to the interfacial free energies per unit

area of those phases. When the liquid is in equilibrium with other two phases, gas and solid substrate, we can diagram the contact angle θ as shown in Figure 3.

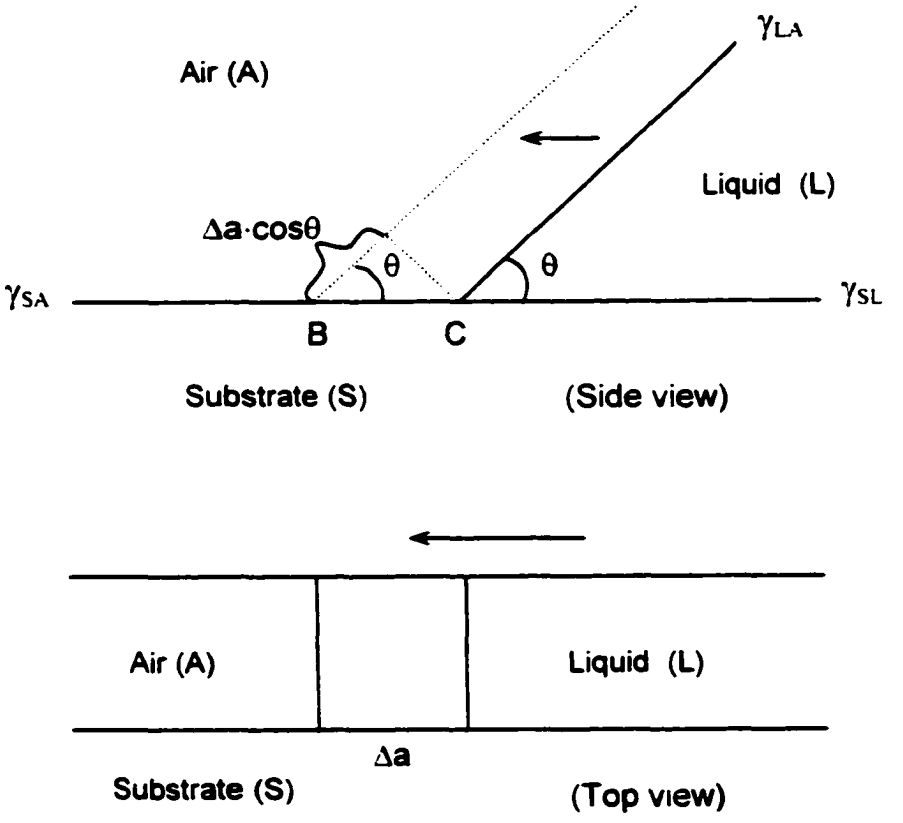

Figure 3. Contact Angle (θ) of a Liquid Made with a Solid Substrate

For a small reversible change in the position of the liquid on the surface so as to cause an increase in the liquid/solid interfacial area of Δa, there is a corresponding decrease Δa in the area of the solid/air interface and an increase in the liquid/air interface of $\Delta a \cdot \cos\theta$. Thus,

$$\Delta G_W = -\gamma_{SA} \cdot \Delta a + \gamma_{SL} \cdot \Delta a + \gamma_{LA} \cdot \Delta a \cdot \cos\theta \qquad (2)$$

As $\Delta a \rightarrow 0$, $\Delta G_W \rightarrow 0$, This means

$$-\gamma_{SA} \cdot da + \gamma_{SL} \cdot da + \gamma_{LA} \cdot da \cdot \cos\theta = 0 \qquad (3)$$

Therefore, $$\gamma_{LA} \cos\theta = \gamma_{SA} - \gamma_{SL} \qquad (4)$$

Equation (4) is generally called Young's equation and the quantity $\gamma_{LA} \cos\theta$, the adhesion tension. Note that γ_{SA}, the interfacial tension in equilibrium with the gas and solid phases in the system, is not γ_S, the free energy per unit area of the solid in a vacuum, but $\gamma_S - \pi$, where π is the reduction in interfacial free energy per unit area at the solid/air interface resulted from adsorption of vapor by liquid; that is, $\pi = \gamma_S - \gamma_{SA}$.

If the contact angle is larger than 0°, then the spreading coefficient cannot be positive or zero. Since $S_{L/S} = \gamma_{SA} - (\gamma_{SL} + \gamma_{LA}) = \gamma_{SA} - \gamma_{SL} - \gamma_{LA}$, and $\gamma_{SA} - \gamma_{SL} = \gamma_{LA} \cos\theta$ when $\theta > 0°$, substituting $\gamma_{LA} \cos\theta$ for $\gamma_{SA} - \gamma_{SL}$ yields:

$$S_{L/S} = \gamma_{LA} \cos\theta - \gamma_{LA} = \gamma_{LA}(\cos\theta - 1) \qquad (5)$$

When θ is finite, $(\cos\theta - 1)$ is always negative, and $S_{L/S}$, too, is always

negative. If the contact angle is 0, then $S_{L/S}$ may be zero or positive. In the either case, complete spreading wetting occurs.

2.3 Surface Tension

As described in part 2.1, the interfacial free energy is the minimum amount of work required to create that interface. The interfacial free energy per unit area is what we measure when we determine the interfacial tension between two phases. It is the minimum amount of work required to create unit area of the interface or to expand it by unit area. When we measure the surface tension of a liquid, we are measuring the interfacial free energy per unit area of the boundary between the liquid and the air above it. Also, as we calculated in part 2.1, when we expand an interface, the minimum work required to create the additional area, e.g., Δa, of that interface is equal to the product of the interfacial tension(γ) times the increase area of the interface, i.e., $W_{min} = \gamma \cdot \Delta a$. A surfactant is a substance that, when present at very low concentration in a system, has the property of adsorbing onto the surface or interface of the system and of altering to a marked degree the amount of work required to expand those interfaces. Surfactants usually act to reduce interfacial free energy rather than to increase it, although there are occasions when they are used to increase it.

It is well known that the molecules at a surface have higher potential

energies than those in the interior. This is because they interact more strongly with the molecules in the interior of the substance than they do with the widely spaced gas molecules above it. Work is therefore always required to bring a molecule from the interior to the surface.

Surfactants have a characteristic molecular structure consisting of a structural group that has very weak attraction for the solvent like water, known as hydrophobic group, together with a group that has strong attraction for the water, called the hydrophilic group. The typical structure of surfactants is shown in Figure 1. When a surfactant is dissolved in water, the presence of the hydrophobic group in the interior of water may cause distortion of the water molecules, increasing the free energy of the system. Meanwhile, the presence of the hydrophilic group prevents the surfactant molecules from being expelled completely from the water as a separate phase.

2.4 Adsorption of Surfactant Solution

As discussed in the previous part, one of the characteristic features of surfactants is their tendency to adsorb at interfaces in an oriented fashion. This adsorption has been intensively studied to determine (1) the concentration of surfactant at the interface; (2) the orientation of the surfactant at the interface; and (3) the energy changes such as ΔG, ΔH and ΔS in the system, resulting from the adsorption. These quantities are very important in research on

surfactants, since they provide information on the type and mechanism of any interactions involving the surfactant at the interface and the efficiency and effectiveness of its operation as a surface-active material. The efficiency is defined as a measure of the equilibrium concentration of surfactant in the liquid phase necessary to produce a given amount of effect, and the effectiveness is defined as the maximum effect that the surfactant can produce in that interfacial process irrespective of concentration.

2.4.1 Adsorption at the Air/Liquid Interface

2.4.1.1 Gibbs Surface

As discussed in the previous part, surfactant molecules have the tendency to concentrate at interfaces such as the air/liquid interface. However, the region of the interface is so small, compared with the bulk solution phase, that it is difficult to determine directly the amount of surfactant adsorbed per unit area of the air/liquid interface. A diagram of the interface is shown below.

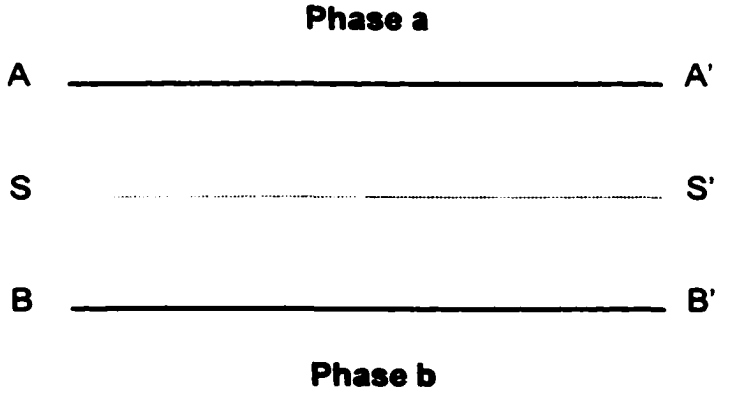

The phases above the plane A–A' and below the plane B–B' are homogeneous bulk phases a and b, e.g., air phase and bulk solution phase. The range between A–A' and B–B' is the interface or surface. In this range the compositions and properties are uniform within the plane that parallels to the A–A' and B–B' planes and continuously change along with the perpendicular direction of the planes. In the actual case, the boundaries between bulk and interfacial phases are not sharp, and the thickness of the surface is usually in the range of 1nm. It is very difficult to get information about the changes of the composition and properties in the direction of the bulk phase.

There are some different models used in the thermodynamic treatments of the interfacial phase. The Gibbs surface, the most convenient and widely accepted model, is an imaginary surface, that is a plane S–S' between A–A' and B–B' planes. It is a 2-dimensional geometry plane and is selected as the interfacial phase.

On the interface phase the composition is described by n_i^s called surface excess. The surface excess concentration Γ_i is a surface excess per unit area and represents the adsorption of component *i* on the surface

$$\Gamma_i = n_i^s / A \qquad (6)$$

In order to fix the position of the Gibbs surface, the usual convention is to set the dividing surface S–S' such that $\Gamma_1 = 0$ and adsorption of components other than 1 is called relative adsorption, Γ_i^1[91].

2.4.1.2 Gibbs Equation

The relationship between surface excess concentration of solute, C, and the slope of plot of surface tension vs. concentration, $d\gamma/dC$, is called the Gibbs equation.

The fundamental Gibbs equation for adsorption, derived by J. W. Gibbs[92] in 1878 from thermodynamic concepts[93], is as the following:

$$d\gamma = -S^S dT - \sum_i \Gamma_i d\mu_i \qquad (7)$$

where S^S corresponds to the surface entropy, Γ_i denotes the surface excess per unit area of component i and μ_i its chemical potential. Equation (7) is one of the fundamental equations of surface chemistry.

Considering a two-component system, such as a solute in a solvent, and at condition of constant temperature, Eq. (7) becomes

$$d\gamma = -\Gamma_1 d\mu_1 - \Gamma_2 d\mu_2 \qquad (8)$$

If the surface phase is chosen in a position that the surface excess of one component, usually solvent, is zero, i.e., $\Gamma_1 = 0$, then

$$d\gamma = -\Gamma_2^1 d\mu_2 \qquad (9)$$

At thermodynamic equilibrium of the system

$$\mu_2^s = \mu_2^b = \mu_2^0 + RT\ln f_2 C_2 \qquad (10)$$

where C_2 is the concentration and f_2 is activity coefficient of the solute in bulk solution phase. In dilute solution, f_2 is chosen as unity to a first approximation. Substituting Eq. (10) into Eq. (9) for μ gives

$$d\gamma = -\Gamma_2^1 RT d\ln C \qquad (11)$$

or

$$d\gamma = -RT\Gamma d\ln C \qquad (12)$$

For a surface active component the surface excess concentration, Γ_2^1, can be considered equal to the surface concentration, Γ, without significant error. Eq. (12) is the form in which the Gibbs equation is commonly used for nonionic surfactants containing no other materials. When γ is in dyn/cm and $R = 8.3143 \times 10^7 \text{ ergs} \cdot \text{mol}^{-1}\text{K}^{-1}$, then Γ is in mol/cm^2.

The area per molecule at the interface provides information on the degree of packing and the orientation of the adsorbed surfactant molecule, when compared with the dimensions of the molecule as obtained by use of molecular models. From the surface excess concentration, the area per molecule at the interface a_1^s, in square angstroms is calculated from the relation

$$a_1^s = \frac{10^{16}}{N\Gamma_1} \qquad (13)$$

where N = Avogardo's number and Γ_1 is in mol/cm^2.

The Gibbs equation for a mixture of two or more nonionic surfactants in dilute solution (10^{-2} M or less) can be written as:

$$d\gamma = -RT(\Gamma_1 d\ln C_1 + \Gamma_2 d\ln C_2) \qquad (14)$$

where Γ_1 is excess concentration at interface of component 1, Γ_2 is excess concentration at interface of component 2. C_1 is the concentration of component 1 in bulk solution phase, C_2 is the concentration of component 2 in bulk solution phase. If we use Γ_t stand for the total excess concentration at the interface of component 1 and component 2, C_t for the total concentration of component 1 and component 2 in the bulk solution phase, then

$$\Gamma_1 + \Gamma_2 = \Gamma_t \qquad (15)$$

and

$$C_1 + C_2 = C_t \qquad (16)$$

If we use x_1 as the mole fraction of component 1 in the bulk solution phase, the other one must be $(1 - x_1)$. Therefore,

$$C_1 = x_1 \cdot C_t \qquad (17)$$

$$C_2 = (1 - x_1) \cdot C_t \qquad (18)$$

Substituting Eq. (17) and (18) into (14) yields:

$$d\gamma = -RT\{\Gamma_1 d\ln(x_1 C_t) + \Gamma_2 d\ln[(1-x_1)C_t]\}$$

$$= -RT\{\Gamma_1 d(\ln x_1 + \ln C_t) + \Gamma_2 d[\ln(1-x_1) + \ln C_t]\}$$

$$= -RT\{\Gamma_1(d\ln x_1 + d\ln C_t) + \Gamma_2[d\ln(1-x_1) + d\ln C_t]\} \quad (19)$$

For a series of mixtures with different total concentrations, C_t, if the mole fractions of both components are fixed, they will not change with the adsorptions, e.g., the adsorption at the air/liquid interface is so small that the concentration of surfactants in the bulk solution phase at the equilibrium can be considered to be the same as initial concentration. Consequently, the mole fractions x_1 and $1-x_1$ are constants. Therefore

$$d\ln x_1 = d\ln(1-x_1) = 0 \quad (20)$$

Substituting Eq. (20) into Eq. (19) yields:

$$d\gamma = -RT[\Gamma_1 d\ln C_t + \Gamma_2 d\ln C_t]$$

$$= -RT(\Gamma_1 + \Gamma_2)d\ln C_t \quad (21)$$

Substituting Eq. (15) into Eq. (21) yields:

$$d\gamma = -RT\Gamma_t \cdot d\ln C_t \quad (22)$$

2.4.2 Adsorption at the Liquid/Solid Interface

2.4.2.1 Mechanisms of Adsorption

The adsorption of surfactants on solid surfaces is the basis for many technical applications of these substances. Generally, the following factors determine the extent and orientation of adsorption at the solid/liquid interface: (1) Types of solvent: aqueous or nonaqueous, and additives such as electrolytes, short chain alcohols, etc.. (2) Surface properties of the solid adsorbents where the solids differ according to the specific surface, porosity, and chemical composition. (3) Variation in surfactant structure with respect to type and size of the hydrophilic or hydrophobic group.

Adsorption may be influenced, in addition to the properties of the components, by parameters of the system, e.g., temperature and pH. Because of the variables cited, there are many different adsorption mechanisms that influence the enrichment of surfactant at the solid/liquid interface[94,95]. Rosen has classified the adsorption mechanism of ionic and nonionic surfactants as follows [96]:

1. *Ion exchange*: This mechanism involves the replacement of counter-ions adsorbed onto the substrates from solution by similarly charged surfactant ions.

2. *Ion pairing*: Adsorption of surfactant ions takes place from solution onto oppositely charged sites unoccupied by counterions.

3. *Hydrogen bonding*: Adsorption takes place by hydrogen bonding between substrate and adsorbate.

4. *Adsorption by polarization of π electrons*: Adsorption on solid surfaces is the result of attractive interaction forces between electron-rich aromatic nuclei of the adsorbate and positive sites located on the substrate.

5. *Adsorption by van der Waals dispersion forces*: Adsorption by this mechanism generally increases with increase in the molecular weight of the adsorbate. This mechanism may act as a supplementary mechanism to all other types of adsorption mechanisms.

6. In addition, adsorption may occur by "*alternating hydrophobic bonding*"[97, 98,99]. This mechanism takes place when the attractive forces of the surfactants become large enough to permit them to adsorb onto the solid surface by chain aggregation. By this mechanism, at higher surface coverage surfactant adsorption from the liquid phase may take place onto or adjacent to surfactants already adsorbed.

In view of the absence of charged sites, adsorption of nonionic surfactants onto solids generally follows mechanisms 3–6. Since the interaction forces between adsorbent and nonionic surfactant are small in comparison to ionic surfactants, the shapes of adsorption isotherms and adsorption thermodynamics are mainly affected by the molecular structure of surfactants.

2.4.2.2 Adsorption Isotherms

At the solid-liquid interface, the following information is of interest to researchers:

(1) the amount of surfactant absorbed per unit mass or unit area of the solid adsorbent, i.e., the surface concentration of the surfactant at a given temperature, since this is a measure of how much of the surface of the adsorbent has been covered, and hence changed, by the adsorption; (2) the equilibrium concentration of surfactant in the liquid phase required to produce a given surface concentration of surfactant at a given temperature, since this measures the efficiency with which the surfactant is adsorbed; (3) the concentration of surfactant on the adsorbent at surface saturation at a given temperature, since this determines the effectiveness with which the surfactant is adsorbed; (4) the orientation of the adsorbed surfactant and any other parameters that may shed light on the mechanism by which the surfactant is adsorbed, since a knowledge of the mechanism allows researchers to predict how a surfactant with a given molecular structure will adsorb at the interface; (5) the effect of adsorption on other properties of the adsorbent. An adsorption isotherm is a mathematical expression that relates the concentration of surfactant at the interface to its equilibrium concentration in the liquid phase. Since most of the desired information can be obtained from the adsorption

isotherm, determination of adsorption isotherms is very essential to the study of the performance of surfactants at the solid-liquid interface.

The fundamental equation for calculating the amount of one component (component 1) of a binary solution adsorbed onto a solid adsorbed is (Aveyard, 1973)

$$\frac{n_0 \Delta x_1}{m} = n_1^s x_2 - n_2^s x_1 \qquad (23)$$

where n_0 = the total number of moles of solution before adsorption

$\Delta x_1 = x_{1,0} - x_1$

$x_{1,0}$ = the mole fraction of component 1 before adsorption

x_1, x_2 = the mole fraction of component 1 and component 2 at adsorption equilibrium

m = the mass of the adsorbent, in grams

n_1^s, n_2^s = the number of moles of component 1 and component 2 adsorbed per gram of adsorbent at adsorption equilibrium.

When the liquid phase is a dilute solution of a surfactant (component 1) that is much more strongly adsorbed onto the solid adsorbent than the solvent (component 2), then $n_0 \Delta x_1 \approx \Delta n_1$ where Δn_1 = the change in the number of moles of component 1 in solution, $n_2^s \approx 0$, and $x_2 = 1$. Thus

$$n_1^s = \frac{\Delta n_1}{m} = \frac{\Delta C_1 V}{m} \qquad (24)$$

where $\Delta C_1 = C_{1,0} - C_1$

$C_{1,0}$ = the molar concentration (in moles/liter) of component before adsorption, in the liquid phase

V = the volume of the liquid phase, in liters.

For n_1^s to be determined with suitable accuracy, the values of ΔC_1, the change in the molar concentration of the surfactant solution upon adsorption, must be appreciable when compared to $C_{1,0}$, its initial concentration. For this to be so, the solid adsorbent must have a large surface area/gram, i.e., large specific area.

For dilute solutions of surfactant, the number of moles of surfactant adsorbed per unit mass of the solid substrate can be calculated from the concentrations of the surfactant in the liquid phase before and after the solution is mixed and shaken with the finely divided solid adsorbent. The mixture should be shaken until adsorption equilibrium has been reached. Then n_1^s is plotted against C_1 to yield the adsorption isotherm. A variety of analytical techniques are available for determining the change in concentration of the surfactant in the

solution, depending on the character and properties of the surfactant molecules to be analyzed.

The surfactant adsorption, Γ_{SL}, in mol/cm^2, of the surfactant can be calculated when a_s, the surface area per unit mass of the solid adsorbent, in cm^2/g (the specific surface area), is known.

$$\Gamma_{SL} = \frac{\Delta C_1 V}{a_s \times m} \qquad (25)$$

For solid substance that cannot be obtained in finely divided form, surface concentration can sometimes be calculated from contact angles. The determination of adsorption of surfactants onto planar solid surfaces will be discussed in section 2.4.2.6.

The adsorption isotherm can also be plotted in terms of Γ_{SL} as a function of C_1. The surface area per adsorbate molecule on the adsorbent, a_1^s, in square angstroms, is

$$a_1^s = \frac{10^{16}}{N\Gamma_{SL}} \qquad (26)$$

where N is Avogadro's number.

2.4.2.3 Types of Adsorption Isotherms

As discussed in the previous part, the nature of the adsorption mechanism may be deduced from the adsorption isotherm, in which the amount adsorbed is determined as a function of solution concentration. Adsorption isotherms may vary and have been classified by Giles et al.[99,100]. According to them, four characteristic classes are identified, based on the form of the initial part of the isotherm, with subgroups related to the behavior at higher concentrations. The isotherms are shown in Figure 4.

The L (Langmuir) class is the most common and is characterized by an initial region which is convex to the bulk phase concentration axis. The L2 isotherm reaches a plateau, and further adsorption above this value gives the L3 isotherm, and if that reaches a second plateau it is designated L4. The fifth L type shows a maximum and reflects a special set of circumstance – it is found with solutes that associate in solution and contain highly surface-active impurities (a maximum is not thermodynamically possible in a pure system).

For the S class the initial slope is concave to the bulk phase concentration axis, and this is frequently followed by a point of inflection leading to an S-shape isotherm. The H (high affinity) class results from extremely strong adsorption associated with chemisorption or other strong interactions at very low concentrations, giving an apparent intercept on the ordinate, e.g., stearic

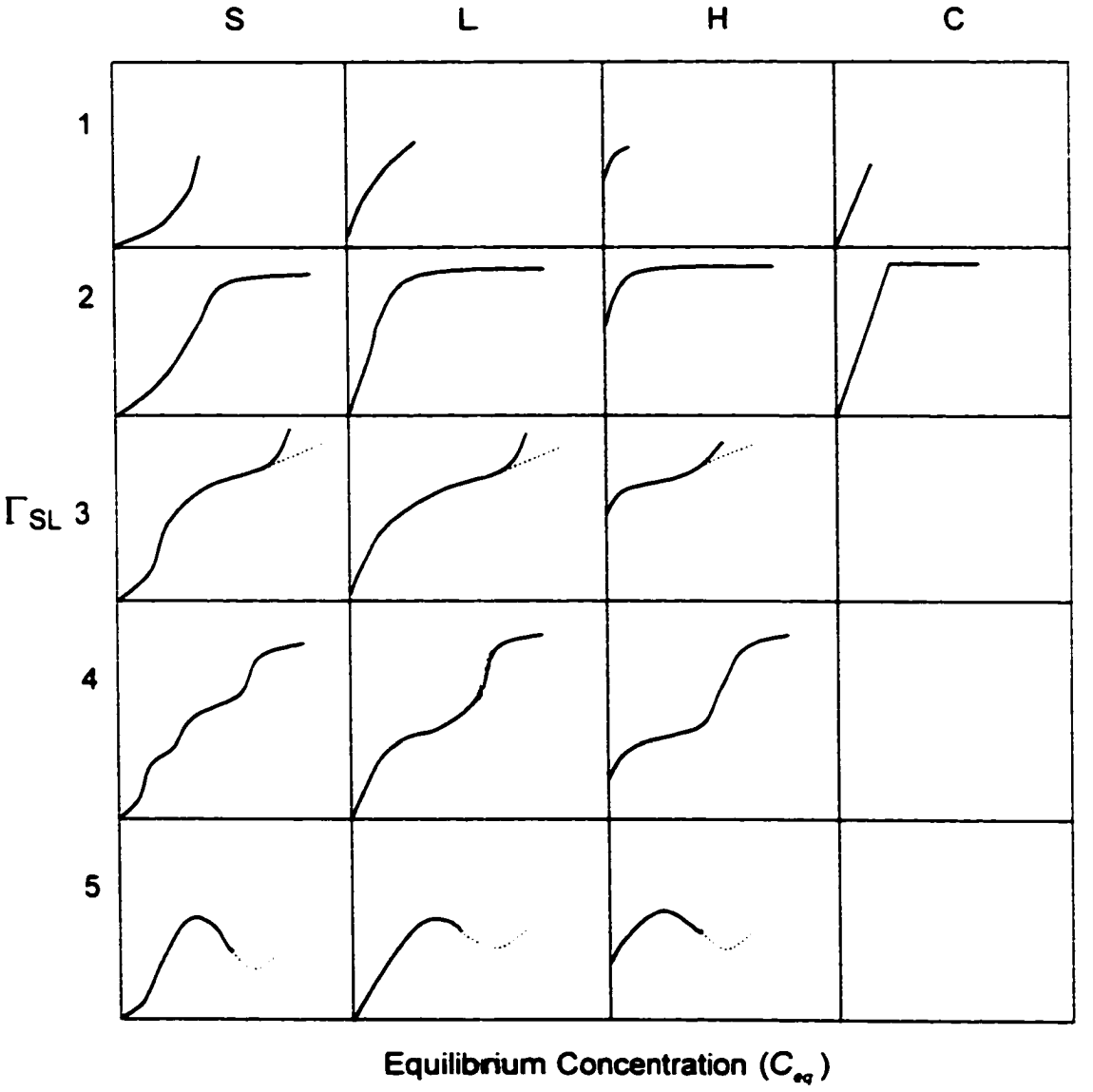

Figure 4. Classification of Adsorption Isotherms According to Giles et al.[100,101] (Letters indicate class and numbers indicate subgroup).

acid from benzene on metal powders. The C-type curves are found with micro-porous adsorbents, in which the number of adsorption sites remains constant

throughout the concentration range. As sites are covered, new sites appear and the surface available expands proportionally with the amount of solute adsorbed. Cases of C type linear adsorption have been found after an initial portion of L or H type. The inflections in subgroup 3 and the second in subgroup 4 may reflect a change in orientation of the adsorbed solute or the formation of a second layer.

However, for adsorption from dilute solution, the most frequent types of adsorption isotherms are as shown in Figure 5[102]. At low concentrations, the adsorption isotherms frequently may be expressed by either the Freundlich[103] or Langmuir relationship. The Freundlich equation is:

$$Q = kC^{1/n} \qquad (27)$$

where Q is the molar (or weight) adsorbed per unit weight of adsorbent, C is the molar (or weight) concentration of adsorbate in solution at equilibrium, and k and n are the experimental parameters which depend on the system of adsorbent and adsorbate.

The Langmuir equation, which originally was derived for the adsorption of gases on solids, may also be applied to adsorption from solution and will be discussed in Section 2.4.2.4.

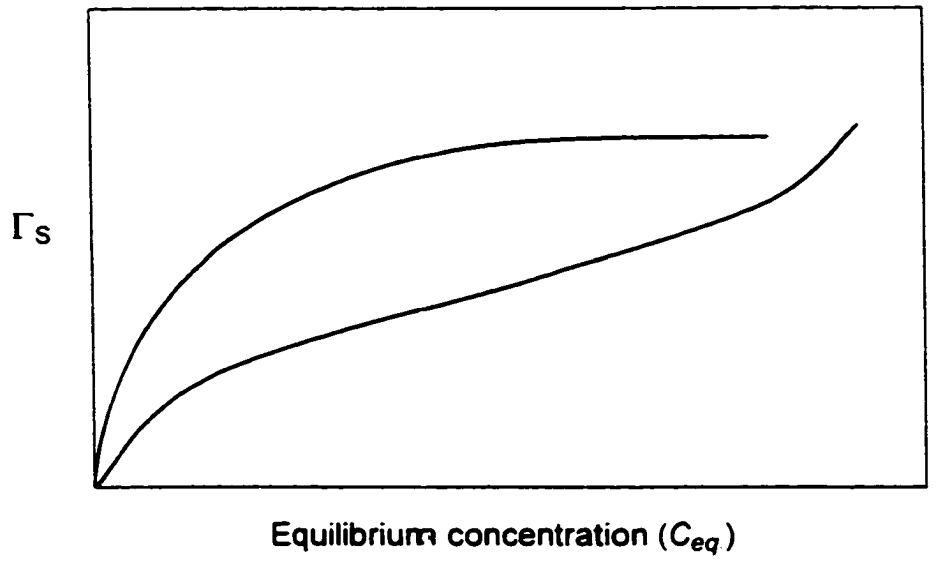

Figure 5. Examples of Frequently Observed Adsorption Isotherms

2.4.2.4 The Langmuir Adsorption Isotherm

A type of adsorption isotherm commonly observed in adsorption from solutions of surfactants is the Langmuir-type isotherm (Langmuir,1918), expressed by

$$\Gamma_{SL} = \frac{C_{eq}}{C_{eq} + a}\Gamma_{SL}^{m} \qquad (28)$$

where Γ_{SL} =the surface concentration of the surfactant, in mol/cm^2

Γ_{SL}^{m} =the maximum surface concentration of the surfactant, in mol/cm^2, at monolayer adsorption

C_{eq} = the concentration of the surfactant in the liquid phase at adsorption equilibrium,in mol/L

a = a constant $[= 55.3\exp(\Delta G^0 / RT)]$, in mol/L, at absolute temperature T, in the vicinity of room temperature and where ΔG^0 is the free energy at infinite dilution.

This type of adsorption is valid in theory only under the following conditions:

1. The adsorbent is homogeneous.
2. Both solute and solvent have equal molar surface areas.
3. Both surface and bulk phase exhibit ideal behavior, e.g., no solute-solute or solvent-solvent interactions in either phase.
4. The adsorption film is monolayer.

Many surfactant solutions show Langmuir-type behavior, even when these restrictions are not met [104].

2.4.2.5 Adsorption of Nonionic Surfactants

Nonionic surfactants are physically adsorbed, rather than chemisorbed. However, they differ from many other surface-active solutes in that quite small changes in concentration, temperature, or molecular structure of the adsorbate

can have a large effect on the adsorption. This is due to adsorbate–adsorbate and adsorbate–solvent interactions, which cause solute aggregation in the bulk solution and which lead to changes in orientation and packing of surfactants at the surface. A general scheme of the most likely orientation changes undergone by nonionic surfactants adsorbed from aqueous solution is shown in Figure 6[105]. The three isotherms corresponding to the different adsorption sequences are shown in Figure 7[105].

In the first stage of adsorption [Figure 6(I)] the surfactant is adsorbing on a surface where there are very few other adsorbate molecules and where consequently the adsorption amount of adsorbate increases almost linearly with the increase of the equilibrium concentration of solute in the bulk phase solution. Adsorption occurs because of van der Waals interaction (principally dispersion forces) and therefore, in the case of an aqueous solvent, it is determined mainly by the hydrophobic moiety of the surfactant. Nevertheless, the polar groups of the surfactant may have some interactions with the surface, and hydrophilic ethylene oxide groups can have a slight positive adsorption even on a non-polar adsorbent [106,107]. When the interaction is due to dispersion forces, the heats of adsorption are relatively small and correspond to the heat liberated by replacing surface solvent molecules with surfactant [108,109]. At this stage the adsorbate molecule tends to lie flat on the surface because its hydrophobic portion is positively adsorbed, as are most types of nonionic

hydrophilic head groups, especially large polyethylene oxide ones. With the molecule lying parallel to the surface, the adsorption energy will increase in

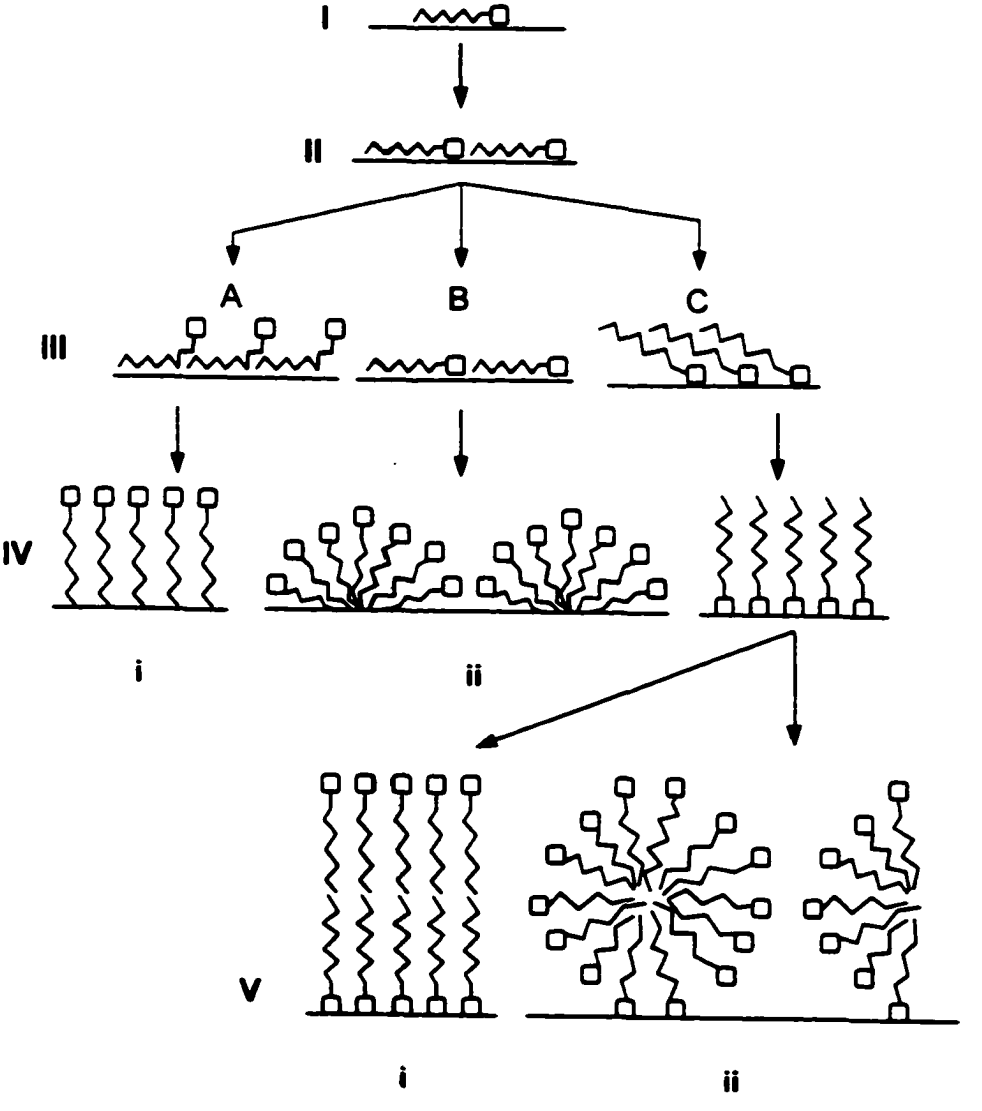

Figure 6. Model for the Adsorption of Nonionic Surfactants, showing the orientation of surfactant molecules at the surface[105].

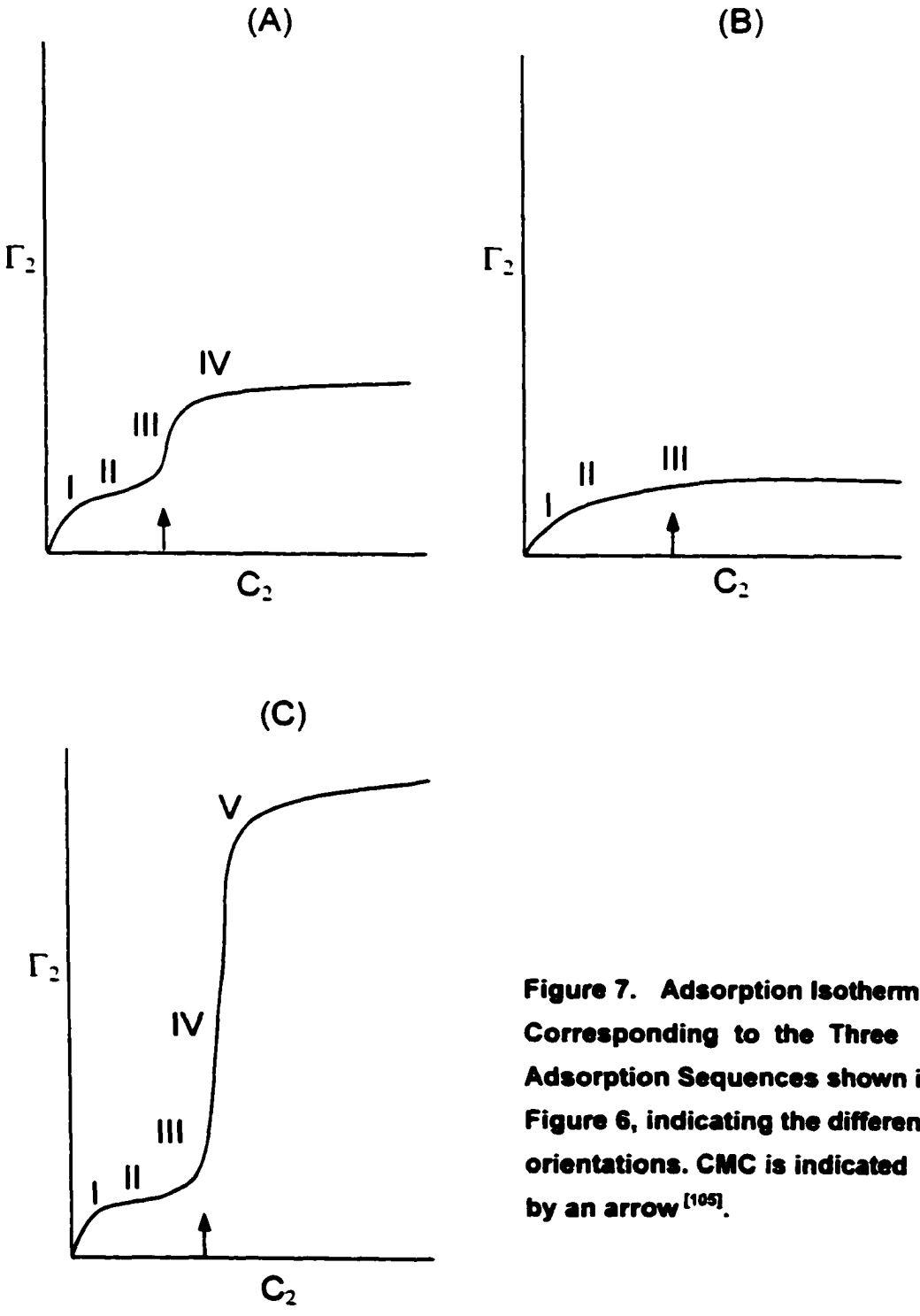

Figure 7. Adsorption Isotherms Corresponding to the Three Adsorption Sequences shown in Figure 6, indicating the different orientations. CMC is indicated by an arrow [105].

almost equal increments for each additional carbon atom in its alkyl chain, and the initial slope of the isotherm will increase correspondingly (Traube's rule). The same can also happen with each additional ethylene oxide group [107].

The approach to monolayer saturation with the molecules lying flat [Figure 6(II)] is accompanied by a gradual decrease in the slope of the adsorption isotherm. Although most of the "free" solvent molecules will have been displaced from the surface by the time the monolayer is complete, the surfactant itself will probably still be hydrated at this stage, so there will continue to be solvent molecules in the interfacial layer [109]. Increase in the size of the surfactant molecule by, for example, lengthening an alkyl or polyethylene oxide chain, will decrease the adsorption. On the other hand, increasing temperature should increase the adsorption because de-solvation reduces the effective size of the adsorbate[110,111]. In general, increasing temperature reduces the solubility of nonionic surfactants but increases their surface activity. This is also true for fatty alcohols [112,113].

The subsequent stages of adsorption are increasingly dominated by adsobate–adsorbate interactions, although it is the absorbate–adsorbent interactions that initially determine how the adsorption progresses when stage II is complete. The absorbate–adsorbent interaction depends on the nature of the

adsorbent and on the hydrophobic–hydrophilic balance in the surfactant. When the hydrophilic group is only weakly adsorbed, it will be displaced from the surface by the alkyl chains of adjacent molecules [Figure 6 (III)]. This can occur more readily when the adsorbent is non-polar or when the surfactant has a short polyethylene oxide chain rather than a long one. However, if there is a strong attraction between the hydrophilic group and the surface, such as may occur with polar adsorbents like silicates and oxides, the alkyl chain is displaced [Figure 6 (III)C]. The intermediate situation [Figure 6(III)B] occurs when neither type of displacement is favoured and the adsorbate then remains flat on the surface. In this case adsorption might not be expected to change with subsequent increase in surfactant concentration, except perhaps from a slight increase due to surfactant de-solvation. However, it has been suggested that multilayers of horizontally oriented adsorbate can be formed[114,115]. Nevertheless, apart from some adsorption data for smectite clay [115–117], there does not seem to be very much evidence for the existence of layers of nonionic surfactant molecules lying flat on the surface at high bulk solution concentration.

The change in amount adsorbed in the third stage of adsorption is unlikely to be large, but as the concentration of surfactant in the bulk solution approaches the C.M.C. (Critical Micelle Concentration), there will be a tendency

for the alkyl chains of the adsorbed molecules to aggregate. This will cause the molecules to become vertically oriented and there will be a large increase in adsorption (Stage IV). This increase is probably not entirely caused by the change in orientation. The lateral forces due to alkyl chain interactions in the adsorbed layer will compress the head group, and for an ethylene oxide chain this will result in a less coiled, more extended conformation. There may also be some de-solvation. However, even in the close-packed monolayer the ethenoxy chain will not be fully extended [118–120]. The longer the surfactant alkyl chain the greater will be the cohesion force and hence the smaller the surfactant cross sectional area. This may explain why saturation adsorption increases with chain length. With non-polar adsorbents, the adsorption energy of a methylene group is almost the same as its micellization energy[107], so the surface aggregation process can occur quite easily even at concentrations below the bulk solution C.M.C.. With polar adsorbents, however, the head group may be quite strongly bound to the surface, and partial detachment of a large ethenoxy chain from the surface, needed for close-packing of the alkyl chains [Figure 6(IV)C], may not be achieved until the surfactant concentration is above the C.M.C.. When the adsorption layer is like that shown in Figure 6(IV)C, the surface will be hydrophobic.

2.4.2.6 Adsorption on a Planar Solid Surface

As discussed in section of 2.4.2.2, for solid substances that cannot be obtained in finely divided form, the adsorption isotherms cannot be determined by the difference in concentration of the bulk solution phase between before and after adsorption equilibrium. However, the maximum adsorption amount on their planar surfaces (Γ_{max}^{SL}) can be determined from contact angles.

Values of Γ_{max}^{SL}, at the aqueous solution/solid interface, can be obtained from the maximum slopes of the $\gamma_{LA}\cos\theta$ vs logC curves. From Young's equation:

$$\gamma_{LA}\cos\theta = \gamma_{SA} - \gamma_{SL} \qquad (29)$$

where γ_{LA} = the surface tension at the liquid/vapor interface, in mN/m.

γ_{SA} = the surface tension at the solid/vapor interface, in mN/m.

γ_{SL} = the surface tension at the solid/liquid interface, in mN/m.

θ = the equilibrium contact angle which the liquid phase makes with the solid, measured in the liquid phase.

If we differentiate both sides of Young's equation by lnC, then we have the following equation:

$$\frac{d(\gamma_{LA}\cos\theta)}{d\ln C} = \frac{d\gamma_{SA}}{d\ln C} - \frac{d\gamma_{SL}}{d\ln C} \qquad (30)$$

From the Gibbs equation at the three interfaces, we have:

at the L/A interface, $d\gamma_{LA}/d\ln C = -nRT \cdot \Gamma_{LA}$ (31)

at the S/L interface, $d\gamma_{SL}/d\ln C = -nRT \cdot \Gamma_{SL}$ (32)

at the S/A interface, $d\gamma_{SA}/d\ln C = -nRT \cdot \Gamma_{SA}$ (33)

where Γ_{LA} = the adsorption at the liquid/vapor interface, in mol/cm^2,

Γ_{SL} = the adsorption at the solid/liquid interface, in mol/cm^2,

Γ_{SA} = the adsorption at the solid/vapor interface, in mol/cm^2

C = Surfactant concentration in bulk solution phase, in mol/L

n= 1 for nonionic surfactants

Substitution of Equations (31), (32) and (33) into Eq. (30) , at constant temperature, yields:

$$\frac{d(\gamma_{LA}\cos\theta)}{d\ln C} = -nRT\Gamma_{SA} - (-nRT\Gamma_{SL}) = nRT\Gamma_{SL} - nRT\Gamma_{SA} \qquad (34)$$

From which,

$$\Gamma_{SL} = \Gamma_{SA} + \frac{1}{nRT} \times \frac{d(\gamma_{LA}\cos\theta)}{d\ln C} \qquad (35)$$

It should be noted that because surfactants with hydrocarbon chains cannot lower the surface free energy of a solid, such as Parafilm®, polyethylene, or Teflon, therefore, it can be assumed that γ_{SA} is a constant for the planar solid surfaces with low surface free energy [121], i.e., $\frac{d\gamma_{SA}}{d\ln C} = 0$. According to Equation (30), $\Gamma_{LA} = 0$. Consequently,

$$\Gamma_{SL} = \frac{1}{nRT}\frac{d(\gamma_{LA}\cos\theta)}{d\ln C} \qquad (36)$$

But $\frac{d\gamma_{SA}}{d\ln C} \neq 0$ for surfactants with dimethylsiloxane or perfluoralkyl hydrophobic groups that can lower the surface free energy of a hydrocarbon solid. Therefore, only the values of $(\Gamma_{SL} - \Gamma_{SA})$ can be calculated from $\frac{1}{nRT}\frac{d(\gamma_{LA}\cos\theta)}{d\ln C}$ for those systems [51].

2.4.3 Adsorption at the Air/Hydrocarbon Solid Interface

As discussed in the previous section, the adsorption at the air/solid interface is not equal to 0 for surfactants with dimethylsiloxane or perfluoroIkyl hydrophobic groups that can lower the surface free energy of a hydrocarbon solid. According to Equation (35), and for nonionic surfactants, the adsorption at the air/hydrocarbon solid interface can be calculated as following:

$$\Gamma_{SA} = \Gamma_{SL} - \frac{1}{RT} \times \frac{d(\gamma_{LA} \cos\theta)}{d\ln C} \qquad (37)$$

Γ_{SL} can be obtained directly from an adsorption isotherm; Γ_{LA} can be calculated through the slope of a plot of γ_{LA} vs. ln C by use of the Gibbs equation (Eq. 31) and consequently Γ_{SA} can be calculated from Γ_{SL} and $\frac{d(\gamma_{LA} \cos\theta)}{d\ln C}$, the slope of the plot of $\gamma_{LA}\cos\theta$ vs. ln C.

2.4.4 Adsorption Free Energy

2.4.4.1 Standard Adsorption Free Energy at the A/L Interface

Standard adsorption free energy (ΔG^0_{ad}) at the air/aqueous solution interface have been calculated from the equation[122.123]:

$$\Delta G^0_{ad} = -RT \ln\left(\frac{d\pi}{dC}\right)_{C\to 0} \qquad (38)$$

where $$\left(\frac{d\pi}{dC}\right)_{C\to 0} = \alpha \text{ (Traube's constant)} \qquad (39)$$

which is the slope of plot of surface pressure, $\pi = \gamma^0_{LA} - \gamma_{LA}$, of the solution versus the concentration (C) of surfactant at very low concentration. Here, the

hypothetical standard states of the surface and bulk solution are defined as when the surfactant has a typical environment of an extremely low surface concentration at unit surface pressure.

However, good surface tension data in this concentration range are very difficult to obtain, since traces of impurities adsorbed from the air or present in the solvent or in the surfactant to be used can markedly affect the surface tension results. Therefore, there are only a few studies in the literature using this approach[123-126], since investigators of the effect of surfactant on the surface tension of solvents generally are interested in the region where surfactants show the maximum effect, rather than the region where they show little effect. Therefore, the utility of equation (38) is limited.

A new approach to calculate the standard adsorption free energy at the air/aqueous solution interface for individual surfactant solutions that is applicable to data in the high surface pressure region was proposed by Rosen and Aronson[127]. According to this method, a standard free energy of adsorption, ΔG_{ad}^{0}, at the air/aqueous solution interface can be calculated by the equation:

$$\Delta G_{ad}^{0} = RT \ln a_{\pi} - \pi \cdot A_{m}^{s} \qquad (40)$$

where a_π = activity of the surfactant in the aqueous phase at a surface pressure of π in the region of surface saturation, where $\Gamma_{LA} = \Gamma_{LA}^{max}$ and the molar area of the surfactant $A^S = A_{min}^S$.

The standard state of the surface phase is a hypothetical monolayer of the surfactant at its closest packing but at a surface pressure of zero. For nonionic surfactants at dilute concentration (<1x10^{-2} M) in the solution phase, the activity of surfactant in equation (40) can be substituted by its mole fraction, and equation (40) becomes

$$\Delta G_{ad}^0 = RT \ln(C_\pi / \omega) - \pi \cdot A_m^s \qquad (41)$$

where C_π =molar concentration of surfactant in the aqueous phase at a surface pressure of π and ω is the number of moles of water per liter of water. When C_π is in mol/L, π in mN/m(mJ/m^2), A_m^s in Å^2 per molecule, and $R = 8.314 J \cdot mol^{-1} \cdot K^{-1}$, equation (40) becomes

$$\Delta G_{ad}^0 (J/mol) = 2.303RT \log(C_\pi / \omega) - 6.023\pi \cdot A_m^s \qquad (42)$$

When the surface tension of the solvent has been reduced by 20 mN/m, i.e., π =20 mN/m, then the relation becomes

$$\Delta G_{ad}^0 = 2.303RT \cdot pC_{20} - 6.023 \times 20 A_m^s - 2.303RT \log \omega \qquad (43)$$

At saturated adsorption, $A_m^s = A_{min}$, equation (48) can be replaced by:

$$\Delta G_{ad}^0(J/mol) = -5710\,pC_{20} - 120.5A_{min} - 9951 \qquad (44)$$

where $R = 8.314 J \cdot mol^{-1} \cdot K^{-1}$, $T = 298.2$ K and $\omega = 55.3$ mol/L.

2.4.4.2 Standard Adsorption Free Energy at the L/S Interface

When adsorption follows the Langmuir equation (Eq. 28), determination of the values of Γ_{SL}^m and a permits calculation of the area of the adsorbed molecule at surface saturation and the free energy of adsorption at infinite dilution. To determine whether adsorption is following the Langmuir equation and to permit calculation of the values of Γ_{SL}^m and a, the equation is usually transformed into linear form by inverting it. Thus,

$$\frac{C_{eq}}{\Gamma_{SL}} = \frac{C_{eq}}{\Gamma_{SL}^m} + \frac{a}{\Gamma_{SL}^m} \qquad (45)$$

or

$$\frac{1}{\Gamma_{SL}} = \frac{a}{\Gamma_{SL}^m C_{eq}} + \frac{1}{\Gamma_{SL}^m} \qquad (46)$$

A plot of C_{eq}/Γ_{SL} versus C_{eq} [equation (45)] should be a straight line whose slope is $1/\Gamma_{SL}^m$ and whose intercept with the ordinate is a/Γ_{SL}^m. Alternatively, a

plot of $1/\Gamma_{SL}$ versus $1/C_{eq}$ [equation (46)] should be a straight line with slope $= a/\Gamma_{SL}^{m}$ and intercept with the ordinate is $1/\Gamma_{SL}^{m}$.

When the specific surface area of the solid adsorbent a_s is unknown, n_1^s may be plotted against C_1 and the Langmuir equation takes the form:

$$n_1^s = \frac{C_{eq}}{C_{eq} + a} n_m^s \qquad (47)$$

The linear forms are

$$\frac{C_{eq}}{n_1^s} = \frac{C_{eq}}{n_m^s} + \frac{a}{n_m^s} \qquad (48)$$

or

$$\frac{1}{n_1^s} = \frac{a}{n_m^s C_{eq}} + \frac{1}{n_m^s} \qquad (49)$$

From equation (45), $a = C_{eq}$ when $\Gamma_{SL} = \Gamma_{SL}^{m}/2$; from equation (48), when $n_1^s = n_m^s/2$. Therefore, a may also be determined from a plot of Γ_{SL} versus C_{eq} (or n_1^s versus C_{eq}) at the point where $\Gamma_{SL} = \Gamma_{SL}^{m}/2$ (or $n_1^s = n_m^s/2$), i.e., it equals the equilibrium surfactant concentration in the liquid phase required for one-half monolayer coverage of the adsorbent surface. In mol/L, $a = 55.3\exp(\Delta G^0/RT)$ in the vicinity of room temperature, and

$$-\log a = -\Delta G^0/2.303RT - 1.74 \qquad (50)$$

Since $-\log a$ is therefore a function of the free energy change involved in the transfer of the surfactant molecule from the liquid phase to the solid substrate, it is a suitable measure of the efficiency of adsorption of the surfactant when adsorption follows the Langmuir equation[127]. Therefore, the adsorption free energy at the solid/aqueous solution interface can be calculated by use of the equation:

$$\Delta G^0_{ad} = 2.303RT\log(a) - 4.01RT \qquad (51)$$

2.5 The Spreading Coefficient

As discussed in Section 2.1, the spreading coefficient of an aqueous solution over a solid substrate, $S_{L/S}$, is the surface free energy decrease per unit area as a result of the spreading:

$$S_{L/S} = \gamma_{SA} - \gamma_{SL} - \gamma_{LA} \qquad (52)$$

When $S_{L/S} \geq 0$, the spreading occurs spontaneously; when $S_{L/S} < 0$, spontaneous spreading does not occur and the liquid produces a contact angle, θ, with the substrate.

2.5.1 Change in Spreading Coefficient upon Mixing

For an L77 aqueous solution:

$$S^{L77}_{L/S} = \gamma^{L77}_{SA} - \gamma^{L77}_{SL} - \gamma^{L77}_{LA} \qquad (53)$$

When mixed with pyrrolidinone (or other surfactants):

$$S_{L/S}^{Mix} = \gamma_{SA}^{Mix} - \gamma_{SL}^{Mix} - \gamma_{LA}^{Mix} \qquad (54)$$

Therefore, the change of the spreading coefficient upon the addition of the pyrrolidinone is equal to:

$$S_{L/S}^{Mix} - S_{L/S}^{L77} = (\gamma_{SA}^{Mix} - \gamma_{SA}^{L77}) - (\gamma_{SL}^{Mix} - \gamma_{SL}^{L77}) - (\gamma_{LA}^{Mix} - \gamma_{LA}^{L77}) \qquad (55)$$

In equation (55), only the value of $(\gamma_{LA}^{Mix} - \gamma_{LA}^{L77})$ can be obtained directly from the plots of γ_{LA}^{Mix} vs. logC and γ_{LA}^{L77} vs. logC. However, the values of $(\gamma_{SA}^{Mix} - \gamma_{SA}^{L77})$ and $(\gamma_{SL}^{Mix} - \gamma_{SL}^{L77})$ cannot be obtained directly because direct interfacial tension measurements at the solid/air and solid/liquid interfaces are not available. However, they can be obtained indirectly.

The interfacial pressure, π, of a system is the difference between the interfacial tension of the solvent, γ^0 and the interfacial tension of the surfactant solution, γ. Therefore,

$$\pi = \gamma^0 - \gamma \qquad (56)$$

According to equation (56), for the L77 solution, the interfacial pressure at the solid/aqueous solution interface equals:

$$\pi_{SL}^{L77} = \gamma_{SL}^{Solv.} - \gamma_{SL}^{L77} \qquad (57)$$

Similarly, for the mixed surfactant solution, the interfacial pressure at the solid/aqueous solution interface then equals:

$$\pi_{SL}^{Mix} = \gamma_{SL}^{Solv} - \gamma_{SL}^{Mix} \qquad (58)$$

Equations (57) and (58) can be rearranged as below:

$$\gamma_{SL}^{L77} = \gamma_{SL}^{Solv} - \pi_{SL}^{L77} \qquad (59)$$

and

$$\gamma_{SL}^{Mix} = \gamma_{SL}^{Solv} - \pi_{SL}^{Mix} \qquad (60)$$

Subtraction of equation (59) from equation (60) yields:

$$\gamma_{SL}^{Mix} - \gamma_{SL}^{L77} = \pi_{SL}^{L77} - \pi_{SL}^{Mix} \qquad (61)$$

In the same fashion, we obtain the equation at the solid/air interface:

$$\gamma_{SA}^{Mix} - \gamma_{SA}^{L77} = \pi_{SA}^{L77} - \pi_{SA}^{Mix} \qquad (62)$$

Substitution of (61) and (62) into (55) yields the following:

$$S_{L/S}^{Mix} - S_{L/S}^{L77} = (\pi_{SA}^{L77} - \pi_{SA}^{Mix}) - (\pi_{SL}^{L77} - \pi_{SL}^{Mix}) - (\gamma_{LA}^{Mix} - \gamma_{LA}^{L77})$$

$$= -\Delta\gamma_{LA} + \Delta\pi_{SL} - \Delta\pi_{SA} \qquad (63)$$

where,

$$\Delta\gamma_{LA} = \gamma_{LA}^{Mix} - \gamma_{LA}^{L77} \qquad (64)$$

$$\Delta\pi_{SL} = \pi_{SL}^{Mix} - \pi_{SL}^{L77} \qquad (65)$$

$$\Delta\pi_{SA} = \pi_{SA}^{Mix} - \pi_{SA}^{L77} \qquad (66)$$

Thus, the effect of the addition of the N-alkyl-pyrrolidinone on the superspreading of the L77 solution (the difference between the spreading coefficients of the mixture and the L77 solution by itself) can be evaluated from the changes in surface tension at the liquid/air, and the changes in the interfacial pressures at the liquid/solid and solid/air interfaces.

2.5.2 Evaluation of $\Delta\pi_{SL}$

According to the Gibbs adsorption equation for the solid/liquid interface:

$$d\gamma_{SL} = - nRT\,\Gamma_{SL}\cdot d\ln C \qquad (67)$$

where γ_{SL} = the surface tension at the solid/liquid interface, in mN/m

Γ_{SL} = the adsorption at the solid/liquid interface, in mol/cm^2

C = concentration of surfactant in bulk solution below C.M.C in mol/L

T = temperature of the system, in K

n = 1 for nonionic surfactants

R = 8.3143 Joules·mol^{-1}·K^{-1}

If both sides of Eq. (67) are integrated and Eq. (56) is employed , then:

$$\int_{\gamma^0_{SL}}^{\gamma_{SL}} d\gamma_{SL} = \gamma_{SL} - \gamma^0_{SL} = -\pi_{SL} = -RT\int_0^C \Gamma_{SL}\cdot d\ln C \qquad (68)$$

Therefore, we obtain:

$$\pi_{SL} = RT\int_0^C \Gamma_{SL} \cdot d\ln C \qquad (69)$$

Applying equation (69) to the L77 aqueous solution and its mixed aqueous solution with pyrrolidinones, the following equations are obtained:

$$\pi_{SL}^{L77} = RT\int_0^{C_{L77}} \Gamma_{SL}^{L77} \cdot d\ln C_{L77} \qquad (70)$$

$$\pi_{SL}^{Mix} = RT\int_0^{C_{Total}} \Gamma_{SL}^{Total} \cdot d\ln C_{total} \qquad (71)$$

where, π_{SL}^{L77} is the surface pressure at the solid/aqueous solution interface caused by the L77 aqueous solution; C_{L77}, the concentration of L77 in the bulk solution by itself; Γ_{SL}^{L77}, the adsorption of L77 at the solid/aqueous solution interface. Similarly, π_{SL}^{Mix} is the surface pressure at the solid/aqueous solution interface caused by the mixed aqueous solution of L77 and pyrrolidinone; C_{total}, the total concentration of L77 and pyrrolidinone in the bulk solution; Γ_{SL}^{Total}, the total adsorption of L77 and pyrrolidinone at the solid/aqueous solution interface.

From their adsorption isotherms, Γ_{SL}^{Total} and Γ_{SL}^{L77} can be found as a function of $\ln(C_{total})$ and $\ln(C_{L77})$, respectively. Therefore, π_{SL}^{Mix} and π_{SL}^{L77} can be calculated from the plots of Γ_{SL}^{Total} vs. $\ln(C_{total})$ and Γ_{SL}^{L77} vs. $\ln(C_{L77})$, respectively. The

definite integrals in equations (70) and (71) are just the areas under the plots of Γ_{SL} vs. lnC from C equal 0 to C. In this fashion, the values of $(\pi_{SL}^{Mix} - \pi_{SL}^{L77})$ at the concentrations of C_{Total} and C_{L77} can be calculated(Figure 8, page 60).

2.5.3 Evaluation of $\Delta\pi_{SA}$

In the same fashion, we obtain:

$$\pi_{SA} = RT\int_0^C \Gamma_{SA} \cdot d\ln C \qquad (72)$$

where Γ_{LA} is the adsorption at the air/solid interface, C is the equilibrium concentration of the surfactant in the solution phase below the C.M.C..

2.6 Interaction and Synergism at the Interfaces

2.6.1 Interaction at the Air/Aqueous Solution Interface

The molecular interaction parameter between two surfactants at an the air/liquid interface can be evaluated by the following equations, which are based upon the application of nonideal solution theory to the thermodynamics of the system[129, 130]:

$$\frac{X_1^2 \ln(\alpha C_{12} / X_1 C_1^0)}{(1-X_1)^2 \ln[(1-\alpha)C_{12} / (1-X_1)C_2^0]} = 1 \qquad (73)$$

$$\beta_{LA}^{\sigma} = \frac{\ln(\alpha C_{12} / X_1 C_1^0)}{(1-X_1)^2} \qquad (74)$$

where α is the mole fraction of surfactant 1 in the total surfactant in the solution phase, (i.e., the mole fraction of surfactant 2 equals 1-α); X_1 is the mole fraction of surfactant 1 in the total surfactant in the adsorbed monolayer; C_1^0, C_2^0 and C_{12} are the solution phase molar concentrations of surfactant 1, 2 and their mixture, respectively, required to produce given surface tension values; β_{LA}^{σ} is the molecular interaction parameter for mixed monolayer formation at the same interface. Equation (73) can be solved numerically for X_1, when α, C_1^0, C_2^0 and C_{12} are obtained from experimental data. A negative value of β_{LA}^{σ} means a more attractive interaction or less repulsion between the two surfactant molecules in the monolayer at the air/liquid interface after mixing than before mixing, and the more negative the value of β_{LA}^{σ}, the stronger the attractive interaction or weaker the repulsion between the molecules after mixing. A value of zero indicates ideal mixing. A positive value of β_{LA}^{σ} indicates less attraction or more self-repulsion between the molecules after mixing in the monolayer than before mixing.

The conditions for synergism or negative synergism in surface tension reduction efficiency to exist are:[130,131]

Synergism	Negative Synergism
1. β_{LA}^{σ} must be negative	1. β_{LA}^{σ} must be positive
2. $\lvert\beta_{LA}^{\sigma}\rvert > \lvert Ln(C_1^0 / C_2^0)\rvert$	2. $\beta_{LA}^{\sigma} > \lvert Ln(C_1^0 / C_2^0)\rvert$

2.6.2 Interaction in Mixed Micelle Formation

The interaction parameter (β^M) between two surfactants in mixed micelle formation in aqueous solution can be evaluated by the following equations:

$$\frac{X_1^M \ln(\alpha C_{12}^M / X_1^M C_1^M)}{(1-X_1^M)^2 \ln[(1-\alpha)C_{12}^M /(1-X_1^M)C_2^M]} = 1 \qquad (75)$$

$$\beta^M = \frac{\ln(\alpha C_{12}^M / X_1^M C_2^M)}{(1-X_1^M)^2} \qquad (76)$$

where C_1^M, C_2^M and C_{12}^M are the critical micelle concentrations(C.M.C.) of individual surfactants 1, 2 and their mixture, respectively, at a given value of α ; α is the mole fraction of surfactant 1 in the total surfactant in the solution phase; X_1 is the mole fraction of surfactant 1 in the total surfactant in the mixed micelle; β^M is the molecular interaction parameter that measures the nature and extent of the interaction between the two different surfactant molecules in the mixed micelle. Equation (75) can be solved numerically for X_1, when α, C_1^M, C_2^M and C_{12}^M are obtained from experimental data. A negative value of β^M means more attractive interaction or less repulsion between the two surfactant molecules in the mixed micelle after mixing than before mixing, and the more negative the value of β^M , the stronger the attractive interaction or the weaker the repulsion between the molecules after mixing.

The conditions for synergism or negative synergism in surface tension reduction efficiency to exist are:[131,132]

Synergism	Negative Synergism
1. β^M must be negative	1. β^M must be positive
2. $\lvert\beta^M\rvert > \lvert\mathrm{Ln}(C_1^M / C_2^M)\rvert$	2. $\beta^M > \lvert\mathrm{Ln}(C_1^M / C_2^M)\rvert$

2.6.3 Interaction at the Solid/Aqueous Solution Interface

Interaction parameters (β_{SL}^{σ}) for mixed monolayers at the solid/aqueous solution interface can also be evaluated by the following equations:

$$\frac{X_1^2 \ln(\alpha C_{12} / X_1 C_1^0)}{(1-X_1)^2 \ln[(1-\alpha)C_{12} / (1-X_1)C_2^0]} = 1 \qquad (77)$$

$$\beta_{SL}^{\sigma} = \frac{\ln(\alpha C_{12} / X_1 C_1^0)}{(1-X_1)^2} \qquad (78)$$

where α is the mole fraction of surfactant 1 in the total surfactant in the solution phase, (i.e., the mole fraction of surfactant 2 equals 1-α); X_1 is the mole fraction of surfactant 1 in the total surfactant in the adsorbed monolayer; C_1^0, C_2^0 and C_{12} are the solution phase molar concentrations of surfactant 1, 2 and their mixture, respectively, obtained at the same value of the adhesion, $\gamma_{LA}\cos\theta$, for the case where the solid has a low-energy surface and the surfactant has a hydrocarbon chain in the molecule[121]. However, when the solid has a high-energy surface, or the surfactants have dimethyl siloxane

groups (or perfluoroalkyl hydrophobic groups) in the molecules, the values of C_1^0, C_2^0 and C_{12} must be obtained from the plots of π_{SL} versus lnC and at the same value of π_{SL}, interfacial pressure at the solid/aqueous interface[51], which are shown in Figure 8. Similarly, a negative value of β_{SL}^{σ} means an attractive interaction between the two surfactant molecules in the mixed monolayer at the air/liquid interface, and the more negative the value of β_{SL}^{σ}, the stronger the attractive interaction between the molecules.

2.6.4 Synergism in Interfacial Tension Reduction Effectiveness

Synergism in interfacial tension reduction effectiveness exists when the mixture of two surfactants at its critical micelle concentration(CMC) reaches a lower interfacial tension (or a larger interfacial pressure, π) value than that attained at the CMC of either individual surfactant. The conditions for synergism or negative synergism in interfacial tension reductive effectiveness to occur[132] are:

Synergism	Negative Synergism
1. $\beta^{\sigma} - \beta^{M}$ must be negative	1. $\beta^{\sigma} - \beta^{M}$ must be positive
2. $\left\|\beta^{\sigma} - \beta^{M}\right\| > \left\|Ln\left(\frac{C_1^{0.CMC}C_2^{M}}{C_2^{0.CMC}C_1^{M}}\right)\right\|$	2. $\beta^{\sigma} - \beta^{M} > \left\|Ln\left(\frac{C_1^{0.CMC}C_2^{M}}{C_2^{0.CMC}C_1^{M}}\right)\right\|$

where $C_1^{0.CMC}$, $C_2^{0.CMC}$ are the molar concentrations of surfactants 1 and 2, respectively, required to yield an interfacial tension equal to that of any mixture at its CMC.

At the point of maximum synergism or maximum negative synergism in interfacial tension reduction effectiveness, the composition of the mixed interfacial layer equals the composition of the mixed micelle. α^{*E}, the mole fraction of surfactant 1 in the solution phase (on a surfactant-only basis) at this point is obtained[132] by solving the following equation (79) numerically for X_1^{*E}, and substituting that value into equation (80) to calculate α^{*E}:

$$\frac{\gamma_1^{0.CMC} - K_1(\beta^\sigma - \beta^M)(1 - X_1^*)^2}{\gamma_2^{0.CMC} - K_2(\beta^\sigma - \beta^M)(X_1^*)^2} = 1 \qquad (79)$$

$$\alpha^{*E} = \frac{\frac{C_1^M}{C_2^M} \cdot \frac{X_1^*}{1 - X_1^*} \cdot \exp[\beta^M(1 - 2X_1^*)]}{1 + \frac{C_1^M}{C_2^M} \cdot \frac{X_1^*}{1 - X_1^*} \cdot \exp[\beta^M(1 - 2X_1^*)]} \qquad (80)$$

where K_1, K_2 are the slopes of the γ – lnC plots of the aqueous solutions of surfactants 1 and 2, respectively; $\gamma_1^{0.CMC}$, $\gamma_2^{0.CMC}$ are the interfacial tensions of surfactants 1 and 2, respectively, at their respective CMCs; C_1^M, C_2^M are the CMCs of surfactants 1 and 2, respectively.

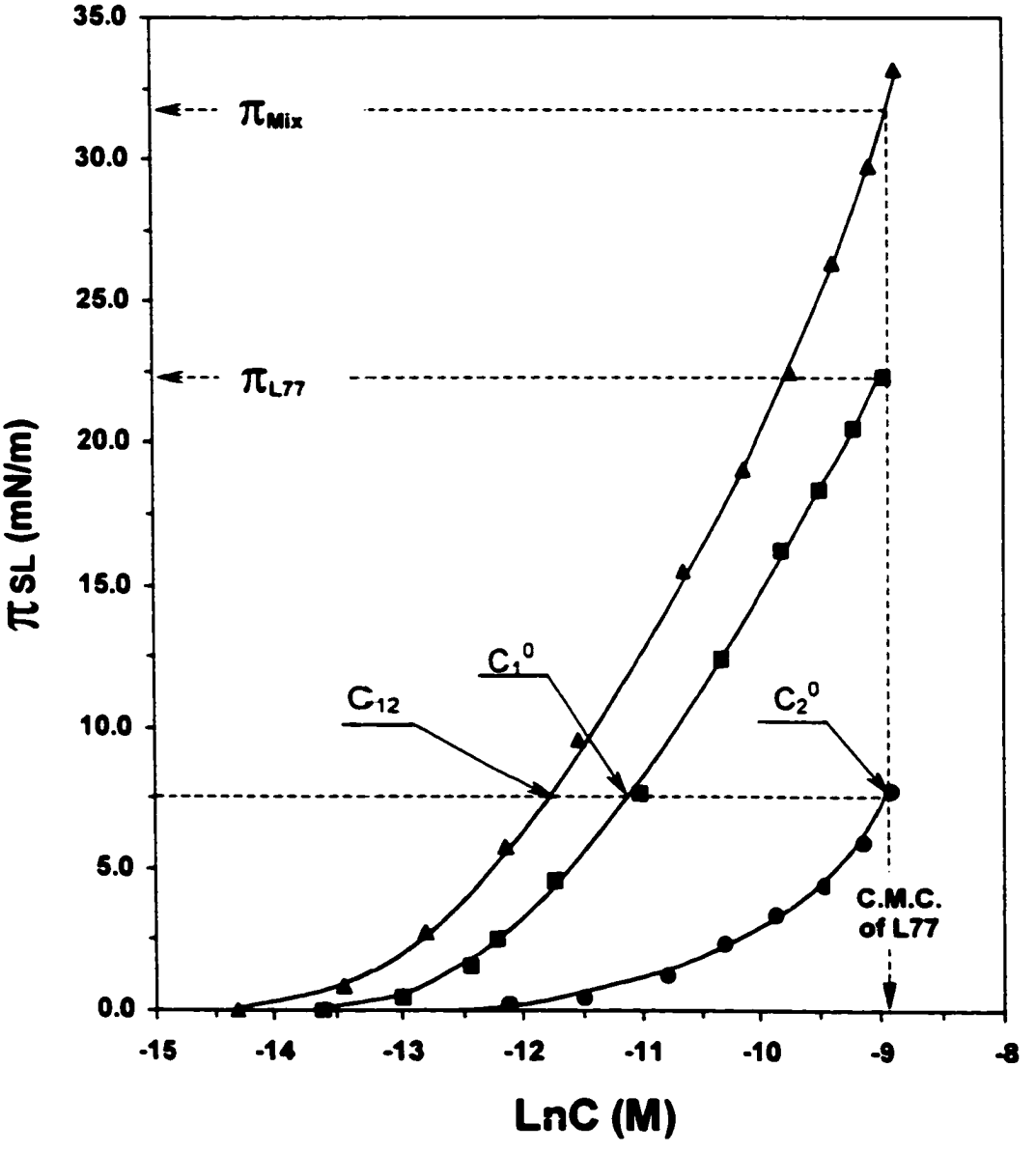

Figure 8. Plots of π_{SL} vs. LnC for Aqueous Solutions of L77, C2,6P and Their Mixture(phosphate buffer, pH=7.00): L77, ■; Mixture with α_{L77}: 0.381, ▲; C2,6P, ●. (Wu, Y. F.; Rosen, M. J. *Langmuir*, 2002, 18(6), 2205-2215)

CHAPTER 3

EXPERIMENTAL

3.1 Materials

The molecular structures of the surfactants investigated, trisiloxane surfactant and N-alkyl pyrrolidinones, are shown in Chart 1. The relevant physicochemical properties are listed in Table 2.

3.1.1 Trisiloxane Surfactant, L77

Trisiloxane Surfactant: SILWET L77, a commercial product, was supplied by OSI Specialties, Inc., Tarrytown, NY, courtesy of Dr. George Policello. Since the degradation of the siloxane backbone results in loss of surface activity of the trisiloxane, the aqueous SILWET L77 solution must be made with phosphate buffer, pH=7.00, to prevent hydrolysis as following[133]:

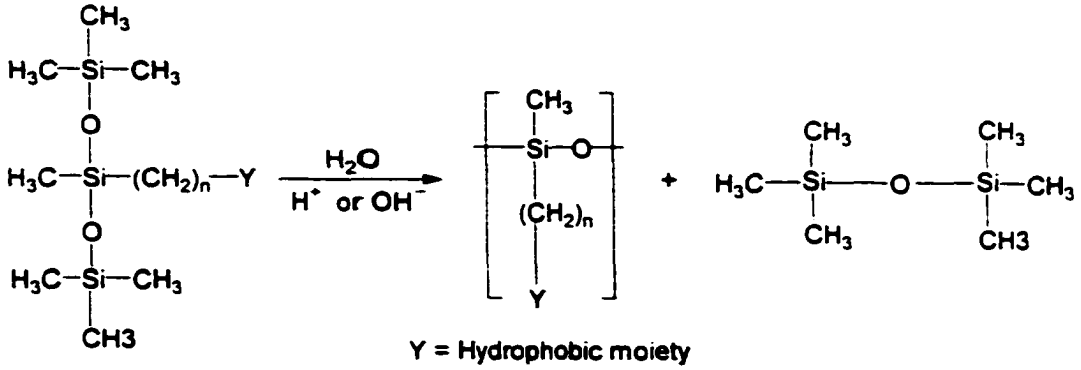

Y = Hydrophobic moiety

Chart 1. Molecular Structures of Surfactants Investigated

Trisiloxane-based Surfactant (SILWET L77)

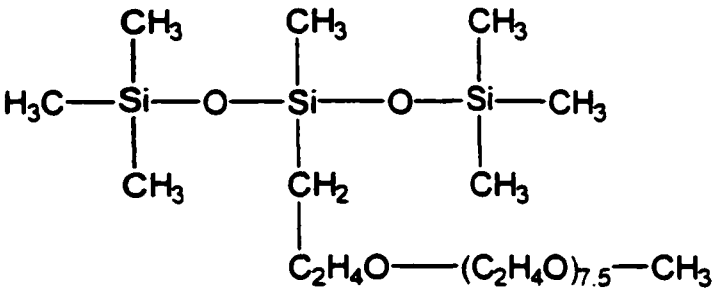

Hydrocarbon-based Surfactants (N-alkyl-Pyrrolidinones)

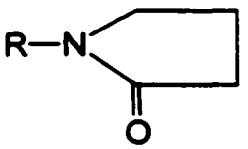

R		Symbol
$-C_4H_9$	N-butyl-Pyrrolidinone	C4P
$-CH_2CHC_4H_9$ (with C_2H_5)	N-(2-ethylhexyl)-Pyrrolidinone	C2,6P
$-C_6H_{13}$	N-hexyl-Pyrrolidinone	C6P
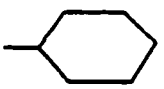	N-cyclohexyl-Pyrrolidinone	CHP
$-C_8H_{17}$	N-octyl-Pyrrolidinone	C8P
$-C_{10}H_{21}$	N-decyl-Pyrrolidinone	C10P

Table 2. Some Physicochemical Properties of L77 and the Pyrrolidinones

(In Phosphate Buffer Solution, pH =7.00, 25 °C)

Compound	M.W.	Solubility (M)	ε ($M^{-1}cm^{-1}$) (191 nm)	ε ($M^{-1}cm^{-1}$) (205 nm)	C.M.C. (M)
L77	700	7.15×10^{-4}	2050	1560	1.33×10^{-4}
C4P	141	No limit	7840	5930	N/A
CHP	169	0.155	8270	6220	N/A
C6P	167	6.95×10^{-2}	7750	5880	N/A
C2,6P	197	1.25×10^{-2}	8110	6180	N/A
C8P	197	5.05×10^{-3}	7940	5830	N/A
C10P	225	4.45×10^{-4}	7480	5770	N/A

3.1.2 N-Alkyl-Pyrrolidinones, CnP

N-Alkyl-Pyrrolidinones(CnP), the additives investigated, including: N-butyl-pyrrolidinone(C4P), N-hexyl- pyrrolidinone(C6P), N-cyclohexyl-pyrrolidinone (CHP), N-octyl- pyrrolidinone(C8P), N-2-(ethylhexyl)-pyrrolidinone(C2,6P) and N-decyl-pyrrolidinone(C10P), were supplied by ISP Corp., Wayne, N.J., courtesy of Dr. John Hornby. All were used without further purification.

3.1.3 Powdered Polyethylene

Polyethylene powder, was supplied by U.S.I. Chemicals, Co., Cincinnati, OH, specific area, 0.360 m^2/g, and was used for two purposes: (1) To make polyethylene films for measurement of spreading factors of aqueous solutions of trisiloxane surfactant L77, N-alkyl-pyrrolidinones and their mixtures. (2) To determine adsorption isotherms of trisiloxane surfactant L77, N-alkyl-pyrrolidinones and their mixtures from phosphate buffer aqueous solutions. Before the powder was used, it was cleaned very carefully. The procedures for the cleaning are described in Section 3.2.1.

3.1.4 Quartz-Condensed Water

The water used for the preparation of surfactant solutions was deionized first and then distilled twice. The last distillation was completed with alkaline

potassium permanganate ($KMnO_4$) solution and through a one-meter high Vigreaux column with quartz condenser and receiver. The specific conductivity of the quartz-condensed water is 1.1×10^{-6} $\Omega^{-1}cm^{-1}$ at 25 °C and the pH value is about 5.8.

3.1.5 Potassium Dihydrogen Phosphate

Potassium Dihydrogen Phosphate (KH_2PO_4), J. T. Baker Chemical Co., Phillispsburg, NJ

3.2 Preparations

3.2.1 Preparation of Polyethylene Film

Before the powder was used, it was cleaned by the following procedure: (1) Weigh about 20 grams of the powder using a clean, dry 250 mL Erlenmeyer flask, then wash it with about 100 mL spectroanalyzed methanol and stir it with an electromagnetic stirrer for about 1 hour. (2) After each washing, filter the methanol using a pressure filter, evaporate it using a hot water bath; then add 100 mL distilled water to dissolve the residue. (3) Check the surface tension of the residue solution, if the surface tension decreases to below ~65 mN/m after each washing, continue the washing till the surface tension reaches a constant, ~65 mN/m. (4) Dry the washed polyethylene powder in a vacuum desiccator over anhydrous phosphorus pentaoxide (P_2O_5) for a few weeks. Then the powder is ready to use.

The polyethylene film was made by melting a thin layer of the clean powder on a 10cm×10cm clean glass square with a small Bunsen burner flame. After the glass has cooled to room temperature, put it into a large clean beaker with about 1000 mL distilled water, then heat the beaker to around 70 °C to make the polyethylene film soft. Use a knife to cut the film along the edges of the glass very carefully without touching the central area of the side attached to the glass square and remove it from the glass. The side of the polyethylene film that had contacted the glass (which is much smoother than the other side) is used for measuring the spreading factors.

3.2.2 Verification of Hydrophobicity of the Polyethylene Film

The hydrophobicity of a solid surface is commonly measured by the contact angle which water makes with it [89]. Contact angle results of water on polyethylene surfaces at 25 °C vary from 88° to 107°, reported by different investigators[134-138]. For the polyethylene film made in this laboratory, the average advancing contact angle of distilled water at 25 °C was 97°. Due to oxidation by the oxygen in the environment, surface energy of the polyethylene film will change with time. As a result, the hydrophobicity of the film will change after being used many times. Therefore, it is necessary to examine the hydrophobicity of the film frequently. If the contact angle of water at room temperature is less than 90°, the film is no longer used for measuring spreading factors and contact angles of surfactant solutions. The methods to measure

spreading factor and contact angle are described in sections 3.3.4 and 3.3.6, respectively.

3.2.3 Preparation of Phosphate Buffer

The buffer solution was made with potassium dihydrogen phosphate (KH_2PO_4), sodium hydroxide(NaOH) solution and "quartz" water in the following manner: dissolve 13.61 grams of KH_2PO_4 with 100 mL "quartz" water in a 2000 mL volumetric flask, add 29.10 mL 2.00 M of NaOH solution, then dilute it with "quartz" water to the mark, shake it very well and then let it stand for 72 hours. After that, transfer the buffer solution to a clean 3000 mL beaker to measure its pH value. The equilibrium pH value is checked by a pH meter and adjusted to pH=7.00 with sodium hydroxide solution. The pH meter was calibrated by using two standard buffer solutions at pH=4.00 and 10.00.

3.2.4 Preparation of Surfactant Solutions

The stock solutions were made by dissolving surfactants in the pre-prepared buffer solution. All other surfactant solutions with different concentrations were made by diluting the stock solution with the buffer solution.

3.3 Measurements

3.3.1 Measurement of Spreading Factors

Four pieces of glass (about 0.5cm×0.5cm) were placed at the corners of a clean polyethylene film, which was mounted on an optically flat glass plate

(10cm×10cm) resting upon the horizontal mouth of a glass bottle. Using a microsyringe, which had previously been rinsed with the solution being tested, a 20 μL drop of the solution was placed on the polyethylene film. The stop watch was started and another 10cm×10cm glass square was immediately placed over the four pieces of glass so that the second piece of glass was parallel to the polyethylene film. After three minutes (when the solution has stopped spreading), an outline of the spread solution was traced onto the top glass. This area was then retraced onto standard white paper from which it was cut and weighed. The exact spreading area was then calculated from the mass of a piece of the same paper of known area, with the assumption that the paper has a constant mass per unit area.

After each measurement, the polyethylene substrate was thoroughly rinsed with methanol, tap water and distilled water, and was then put into boiling distilled water for at least 30 minutes in order to remove any adsorbed surfactant. The solutions, all at 1.0g/L total surfactant concentration, which is much above the CMC of the mixture, were made at 10%, 20%, 30% .....replacements of the trisiloxane surfactant by the N-alkyl-pyrrolidinone being tested. Each spreading measurement was done three to five times until the reproducibility was satisfactory, to ensure minimal relative error. The spreading area is the average of the areas obtained in each set of measurements. The

spreading factor (SF) is the ratio: spreading area of the surfactant solution / spreading area of the same volume of solvent.

3.3.2 Measurement of Surface Tension

Equilibrium surface tension measurements were made by the Wilhelmy plate technique with a Krüss K-12 tensiometer (Krüss GmbH, Hamburg). The plate is made of platinum-iridium with length of 19.9 mm and thickness of 0.2 mm. The instrument was calibrated against quartz-condensed water each day that measurements were made. At 25.0 °C, the surface tension of quartz-condensed water is 71.97 mN/m. Sets of measurements were taken until the change in surface tension was less than 0.08mN/m every 15 minutes. The temperature of the measurement cell was controlled by a water thermostat within ±0.1 °C.

The procedure for measuring surface tension is as follows:

1. Turn on the thermostat bath pump and its heat controller, adjust the temperature regulator to the desired value, 25 °C.
2. Turn on power of the K-12 tensiometer and the attached processor.
3. Turn the knob to its stop limit to make sure the balance locker is locked, then take down the platinum plate from its suspension carefully.
4. Rinse a clean sample vessel with the sample solution to be measured three times, then fill it with the sample solution to about 2/3 volume.

5. Insert the sample vessel into the thermostat vessel and wait until the temperature reaches the desired temperature.
6. Rinse the platinum plate with distilled water three times.
7. Heat the plate to red-hot with a Bunsen burner; cool it to room temperature for measurement.
8. Insert the plate into the suspension carefully, release the balance lock and wait until the plate stops vibrating. Now a number of "0.000 g" should appear on the LC-display of the tensiometer. Otherwise, the tensometer should be calibrated again.
9. On the LC-dispaly of the processor, use the keyboard to choose (1) Plate method; (2) Surface tension; (3) Series of measurements.
10. With the selection of "Series of Measurements", set "min. std. deviation" as 0.08 mN/m; "max. number of values" as 999"; "interval of measurements" as 900 sec.; "printer output" as "ON=1".
11. Move the vessel up towards the plate until the plate hangs just 1~2 mm above the solution surface.
12. Press the "START" key on the keyboard of the processor.

The results of surface tension will be taken and printed out every 15 minutes. The standard deviation of the measurements will calculated automatically after each measurement. When it less than 0.08 mN/m, the tensometer will stop measuring automatically.

3.3.3 Measurement of Contact Angle

Advancing contact angles were measured with a Contact Angle Image Goniometer and Image Analysis Attachment (Model 100-22, Ramé-Hart, Inc., Mountain Lakes, NJ). Seven drops of solution, each about 10μL, were applied to the polyethylene surface, which was placed in a thermostatic environmental chamber saturated with solvent vapor to retard droplet evaporation. Angles were measured on both sides of each of the seven drops for at least 1 hour at 25 °C. Equilibrium contact angle values were assumed to be obtained when no changes were observed for 15 min. The equilibrium contact angle values were reproducible within ±0.2°C.

The procedure for measuring the contact angle is described below:

1. Turn on the thermostat bath pump connected to circulating water for the sample chamber and its heat controller, adjust the temperature regulator to the desired value (25 °C).
2. Turn the computer on, load and run the image analysis program from the Window's system, or enter "R" in the 702 directory from DOS system.
3. Press any key to display an image and then press "L" key for a live image.
4. Rotate the measuring and baseline reticles on the microscope until they are horizontally coincidental.

5. Place a piece of clean polyethylene substrate (2cm×3cm), attached flat to a clean glass square of size identical to that of the base of the chamber.
6. Turn the related knobs, focus on the front edge of the substrate to make sure that it is parallel with the front edge of the leveling stage and vertically move the substrate until the top surface slightly covers the reticles.
7. Press "B" to check Baseline of the system. If the heights of the left and right sides differ from each other within 0.5 pixel, the baseline is ready for measuring. Otherwise, press "L" twice to live image and use the leveling screws below the chamber to re-level the substrate horizontally until a satisfactory baseline is achieved. Press "B" to store the latest baseline.
8. Use a micro-syringe to place 5 ~ 7 drops of solution to be tested of 10 μL volume, on the front edge of the substrate. Cover the chamber tightly to prevent the sample drops from evaporation.
9. Press "L" for a live image and turn related knob to move the image to the center of the screen, focus on one of the drops.
10. Adjust intensity of the screen to a proper contrast, e.g., light=250, dark=55, and fix these values for a set of measurements.
11. Press "A" for automatic scan. It performs both horizontal and vertical scans automatically on the left side and right side of a sessile drop. The readings of contact angle are shown on the screen.
12. Repeat. Press "A" to obtain new readings every 10 minutes until the corresponding values change by less than 0.3 ° after a 10 minute interval.

3.3.4 Measurement of Adsorption Isotherms

3.3.4.1 Preparation of Solution for Equilibrium Adsorption

Use analytical balance to weigh a dry and clean 50 mL plastic vial (Nalge Company, Rochester, NY), then weigh about 0.5 grams of clean polyethylene powder into it. Use a pipet to add 40.00 mL of surfactant(s) solution of known concentration to the vial. Cover it tightly and shake it vigorously to make the solution and polyethylene powder mix well. The vial is then placed on a shaking machine and shaken continuously for 12 hours in order to get adsorption equilibrium.

3.3.4.2 Separation of Adsorbate Solution and Absorbent Powder

The solution, after adsorption equilibrium, and the polyethylene powder were separated by use of a centrifuge (SORVALL RC JC Dupont) at speed of 15,000 rpm for about 1 hour. Use a clean pipet to transfer the separated solution to a dry, clean 50 mL beaker. The effectiveness of the separation was examined by UV absorbance at a visible wavelength, λ=600 nm. If the absorbance in a 1cm cuvette is less than 0.003, the separation is sufficient. The methods to measure UV absorbance are described in sections 3.3.7.4.

3.3.4.3 Two- Phase Titration for L77

The equilibrium concentration of the L77 was determined by two–phase titration[37,139,140], which is based upon the transfer of a dye–surfactant complex

between the aqueous phase and the organic phase. The organic–soluble complex of surfactant with a basic dye is destroyed by an anion and the dye is released into the aqueous phase and the color changes.

The procedures to titrate L77 with a standard solution of potassium tetrakis(4-chlorophenyl) borate (Lancaster Synthesis Ltd. Windham, NH) are the following: (1) transfer 10.00 ml of L77 unknown solution to a glass-stoppered, 100 mL Erlenmeyer flask, add 5.00mL of 6M KOH and 5.00 mL1,2-dichloroethane as oil phase to the flask, then add 3 drops of 1% Victoria Blue B (Fluka, Switzerland) methanol solution as indicator. The mixture is now blue. (2)Immediately shake the stoppered flask vigorously; the oil phase turns to pink color. (3)The mixture is then titrated with standard potassium tetrakis (4-chlorophenyl) borate solution (1.00×10^{-4}M), with shaking after each drop addition, until a slightly blue endpoint is reached. The percent error of the titration is less than 2%(see Appendix I for the error analysis). The calibration curve is shown in Figure 9. The N-alkyl-pyrrolidinones in the mixture do not interfere with the titration of L77 [37].

Figure 9 Two-Phase Titration Curve of L77 with Potassium Tetrakis (4-Chlorophenyl) Borate

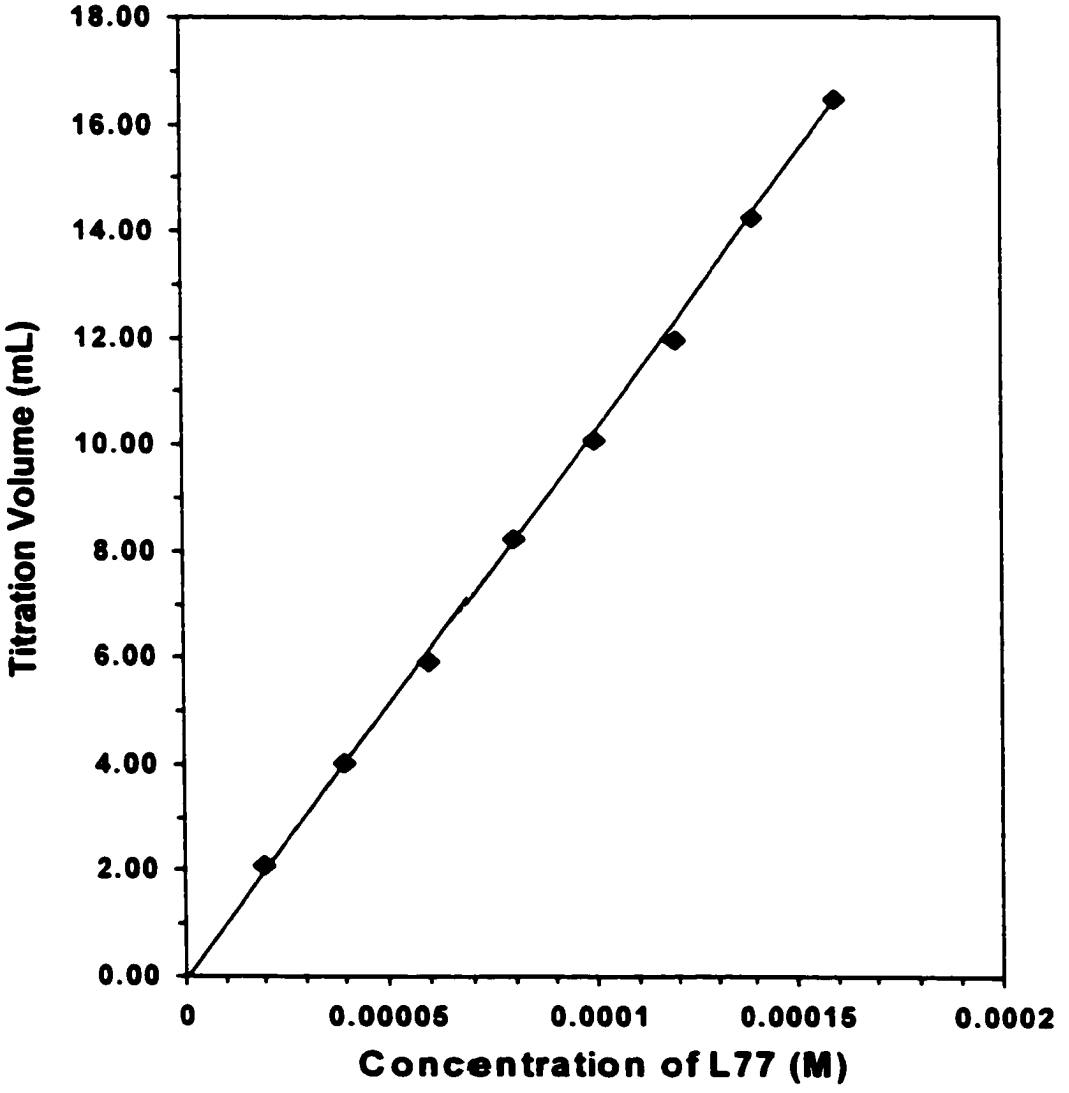

3.3.4.4 UV Absorbance for N-Alkyl-Pyrrolidinones

The equilibrium concentrations of pyrrolidinones were determined by measuring their UV absorbance (U-2001 UV/Vis Spectrophotometer, HITACHI) at λ=205 nm. For individual pyrrolidinone solutions, the unknown concentration can determined by the UV absorbance directly according to Beer's Law from a calibration curve. However, for binary mixtures of L77 and pyrrolidinone(CnP), when the concentration of pyrrolidinone is determined by UV absorbance, the contribution of L77 to the UV absorbance must be deducted. The calibration curves of L77 and C10P are shown in Figure 10 for example.

According to Beer's Law, the total absorbance for a multicomponent system is given by[141]:

$$A_{total} = A_1 + A_2 + \cdots + A_n = \varepsilon_1 bc_1 + \varepsilon_2 bc_2 + \cdots + \varepsilon_n bc_n \qquad (81)$$

where ε is decadic molar extinction coefficient of components, in $M^{-1}cm^{-1}$, which depends on the wavelength selected; b the length of cuvette, which is 1.00 cm; c the concentration of each components, in mol/L; the subscripts refer to components 1, 2,...,n. Therefore, the absorbance of pyrrolidinone(CnP) in the mixture with L77 can be calculated by

$$A_{CnP} = A_{total} - A_{L77} = A_{total} - \varepsilon_{L77} \cdot c_{L77} \qquad (82)$$

Figure 10. UV Calibration Curves of L77 and C10P at λ=205 nm

(In Phosphate Buffer Solution, pH=7.00, 25 °C)

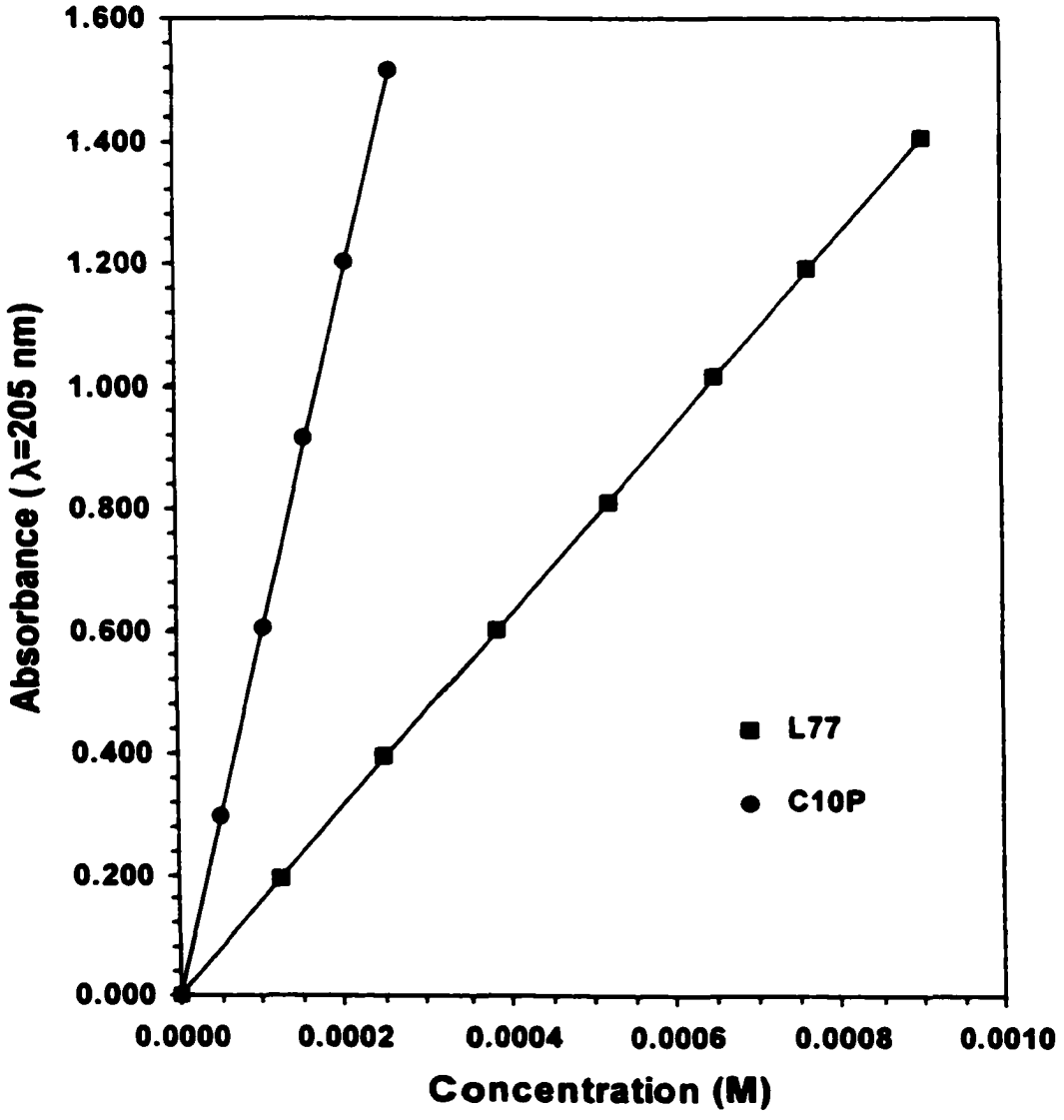

The value of ε_{L77} can be pre-determined, and C_{L77} can be titrated as described above. The data of the decadic molar extinction coefficients, ε, for L77, C4P, CHP, C6P, C2,6P, C8P and C10P at λ=205 nm are listed in Table 2, page 63.

The procedures to measure the UV absorbance are:

1. Turn the instrument on, check if the cartridge is installed inside the printer, turn the printer on.
2. Perform a self-diagnosis and automatic wavelength calibration.
3. After initialization, the "Main Menu" screen appears on the display, then select wavelength scan from the Main Menu.
4. Select the ABS (Absorbance) as the data acquisition mode.
5. Enter the wavelength scan test setup variables as: Strat WL: 400 nm; Stop WL: 200 nm; UP Scale: 2.500; LO Scale: -0.300; Scan Speed: 100 nm/min.
6. Select the instrumental setup and its variables as: Baseline: User; Response: Medium; Lamp Change WL: 340 nm; WI Lamp: ON; D2 Lamp: ON.
7. Collect a user baseline: Rinse two cuvettes thoroughly at least 3 times with distilled water, then do the same thing with buffer solution. Dry their outsides carefully with a Kimwipe, then place the cuvettes containing a reference (buffer) and blank solution (buffer) in both the reference (back) and sample (front) positions, cover the chamber completely. Highlight "User Baseline" on the screen in the WL Scan submenu list, then press "ENTER" key. Press

"FORWARD" key, the measurement screen appears with axes dimensioned for the impending scan. Press "START" key to begin collection of the background spectrum. The base line should be a nearly straight line. The data are stored in the baseline memory location and are used in all subsequent measurements until a new baseline replaces the current one.

8. Remove the sample cuvette and rinse it thoroughly at least 3 times with sample solution to be measured, then fill it with the sample solution and dry outsides. Place the sample cuvette in the front holder, cover the chamber. Press "START" to begin collection of absorbance.
9. Use the crosshair to trace the spectrum and acquire ABS data from the spectrum directly. Use the arrow keys to move the crosshair to 205 nm, the corresponding ABS value appears in the cursor windows. Repeat the wavelength scan 5~7 times, take the average of all measurements at this wavelength.

CHAPTER 4

RESULTS AND DISCUSSION

Part I

Adsorption at Various Interfaces

4.1 At the Air/Aqueous Solution Interface(Γ_{LA})

4.1.1 Adsorption of Individual Surfactants

The adsorption (Γ_{LA}) of surfactant at the air/aqueous solution interface can be obtained from the plot of surface tension (γ_{LA}) versus log C by use of equation (31). Data for these individual surfactants have been published. However, these published results were obtained with different solvents and by different techniques. In our laboratory, the adsorption of C2,6P, C8P and C10P at the air/liquid interface has been measured in "quartz" water or 0.1 M NaCl solution in quartz water[142]. In H. T. Davis' group, they measured surface tension of L77 in the media of quartz water, and then calculated the result of minimum areas per molecule at the air/aqueous solution[25]. However, the adsorption of these materials at the air/aqueous solution interface from

phosphate buffer solution have not been measured. In order to prevent hydrolysis of L77, all measurements on solutions of L77 and the N-alkyl pyrrolidinones were done in phosphate buffer solution at pH 7.00.

Figure A–1 shows plots of γ_{LA} vs. log C of L77, and of C4P, CHP, C6P, C2,6P, C8P, and C10P in phosphate buffer solution. The minimum areas per molecule at the air/aqueous solution, A_{min} in $Å^2$, calculated from the maximum slopes of the plots in Figure A–1 and equation (31), are listed in Table A–1. By comparing the results listed in Table A–1 with the available published data, it can be found that they are in good agreement with the results published by this laboratory and H. T. Davis' group. They also indicate that the phosphate buffer solution has no significant effect on the adsorption of the N-Alkyl-pyrrolidinone and trisiloxane surfactant at the air/aqueous solution interface.

The maximum adsorption ($\Gamma_{LA.Max}$), called the effectiveness of adsorption, of the trisiloxane surfactant L77 and N-alkyl-pyrrolidinones at the air/aqueous interface increases in the order: L77<C4P<CHP<C2,6P<C6P<C8P<C10P. L77 has the smallest adsorption at the interface because of its largest hydrophobic head group. On the other hand, the adsorption of N-alkyl-pyrrolidinones at the interface increases with the length of their hydrophobic chains, except for C2,6P which has a branched chain and consequently, a larger area per molecule at

the interface than C6P. C4P has the shortest hydrocarbon chain, and therefore the smallest adsorption at the interface, while C10P has the longest one, and the greatest adsorption. This is consistent with the well-known observation that the adsorption at the air/aqueous solution interface of surfactants with the same hydrophilic head group and homologous hydrocarbon chains increases with the length of the hydrocarbon chain.

Table A–1 also lists the pC_{20} (the negative log of the surfactant molar fraction, C_{20}, that reduces the surface tension of the solvent by 20 mN/m,) values, a measure of the efficiency of adsorption of the surfactant at the interface and ΔG^{0}_{ad} (standard free energy of adsorption) values calculated by use of equations(13) and(44). L77 has the greatest adsorption efficiency at the air/aqueous solution interface, although it has the lowest adsorption effectiveness at the interface. Its most negative standard free energy of adsorption at the interface indicates that it also possesses highest tendency to adsorb at the air/aqueous solution interface, compared to the investigated N-alkyl-pyrrolidinones. This is probably because of the lower surface free energy produced by the methyl groups in its hydrophobic group. For the N-alkyl-pyrrolidinones, their adsorption efficiency increases in the order: C4P<CHP<C6P<C2,6P<C8P <C10P, which is exactly the order of increasing in the length of the hydrocarbon chain in the molecule.

4.1.2 Adsorption of Surfactant Mixtures at the Air/Liquid Interface

(i) L77–C4P Mixtures: Figure B–1 shows plots of γ_{LA} vs. log C of L77, C4P and their mixed solutions at different mole fractions of L77. The results of adsorption at the air/aqueous solution interface are listed in Table A–2. In Table A–2, when the mole fraction of L77, α_{L77}, equals 1.000, the solution contains L77 only, when α_{L77} equals 0.000, the solution contains C4P only. The values of α_{L77} in the mixture solutions are the initial mole fractions of L77, before adsorption equilibrium. However, it is usually considered to be unchanged after adsorption equilibrium because the adsorption amount at this interface is so small that the concentration of the two components in the bulk solution phase remains the same as that before adsorption equilibrium. From the results, it can be seen that the total maximum adsorption of the mixtures increases slightly with decrease of α_{L77}, or with increase of mole fraction of C4P. This is due to the slightly larger maximum adsorption of C4P at the interface. Furthermore, it can be seen that total adsorption of the mixtures appears to reach a maximum at α_{L77}=0.209. However, this is within the experimental error of the measurements.

(ii) L77–CHP Mixtures: Figure B–2 shows plots of γ_{LA} vs. log C of L77, CHP and their mixed solutions at different mole fractions of L77. The results of adsorption at the air/aqueous solution interface are listed in the Table A–3.

From the results, it can be seen that the total maximum adsorption of the mixtures again increases with a decrease of α_{L77}, or with an increase of mole fraction of CHP, again due to the larger maximum adsorption of CHP at the interface(3.05×10^{-10} mol/cm^2).

(iii) L77–C6P Mixtures: Figure B–3 shows plots of γ_{LA} vs. log C of L77, C6P and their mixed solutions at different mole fractions of L77. The results of adsorption at the air/aqueous solution interface are listed in Table A–4. From the results, it can be seen that the total maximum adsorption of the mixtures increases with a decrease of α_{L77}, or with an increase of mole fraction of C6P. This is due to the larger maximum adsorption of C6P at the interface(3.71×10^{-10} mol/cm^2).

(iv) L77–C2,6P Mixtures: Figure B–4 shows plots of γ_{LA} vs. log C of L77, C2,6P and their mixed solutions at different mole fractions of L77. The results of adsorption at the air/aqueous solution interface are listed in Table A–5. From the results, it can be seen that the total maximum adsorption of the mixtures increases with a decrease of α_{L77}, or with an increase of mole fraction of C6P. This is due to the larger maximum adsorption of C2,6P at the interface(3.54×10^{-10} mol/cm^2).

(v) L77–C8P Mixtures: Figure B–5 shows plots of γ_{LA} vs. log C of L77, C8P and their mixed solutions at different mole fractions of L77. The results of adsorption at the air/aqueous solution interface are listed in Table A–6. From the results, it can be seen that the total maximum adsorption of the mixtures increases with decrease of α_{L77}, or with increase of mole fraction of C8P. This is due to the larger maximum adsorption of C8P at the interface(4.34×10^{-10} mol/cm^2).

(vi) L77–C10P Mixtures: Figure B–6 shows plots of γ_{LA} vs. log C of L77, C10P and their mixed solutions at different mole fractions of L77. The results of adsorption at the air/aqueous solution interface are listed in Table A–7. From the results, it can be seen that the total maximum adsorption of the mixtures increases with a decrease of α_{L77}, or with an increase of mole fraction of C10P. This is due to the larger maximum adsorption of C10P at the interface(4.45×10^{-10} mol/cm^2).

Summary: Plots of the total adsorptions of the mixtures at the air/aqueous solution interface are shown in Figure A–2. From the plots, it can be seen that, for the mixtures of the N-alkyl-pyrrolidinones and SILWET L77, the total surfactant adsorption at the air/aqueous solution interface increases with a decrease in the mole fraction of L77, but there is no linear relationship between

them. The increase in total surfactant adsorption of the mixture with an increase in the mole fraction of the N-alkyl-pyrrolidinones reflects the larger maximum adsorption value of the pyrrolidinone than of the L77. The concave shapes of the plots, however, indicate the total adsorption of the mixture is less than that expected from proportionate replacement of L77 by N-alkyl-pyrrolidinones.

Figure A-1. Surface Tension of L77 and Pyrrolidinones(CnP) at Air/Aqueous Solution Interface

(Phosphate Buffer Solution, pH=7.00, 25 °C)

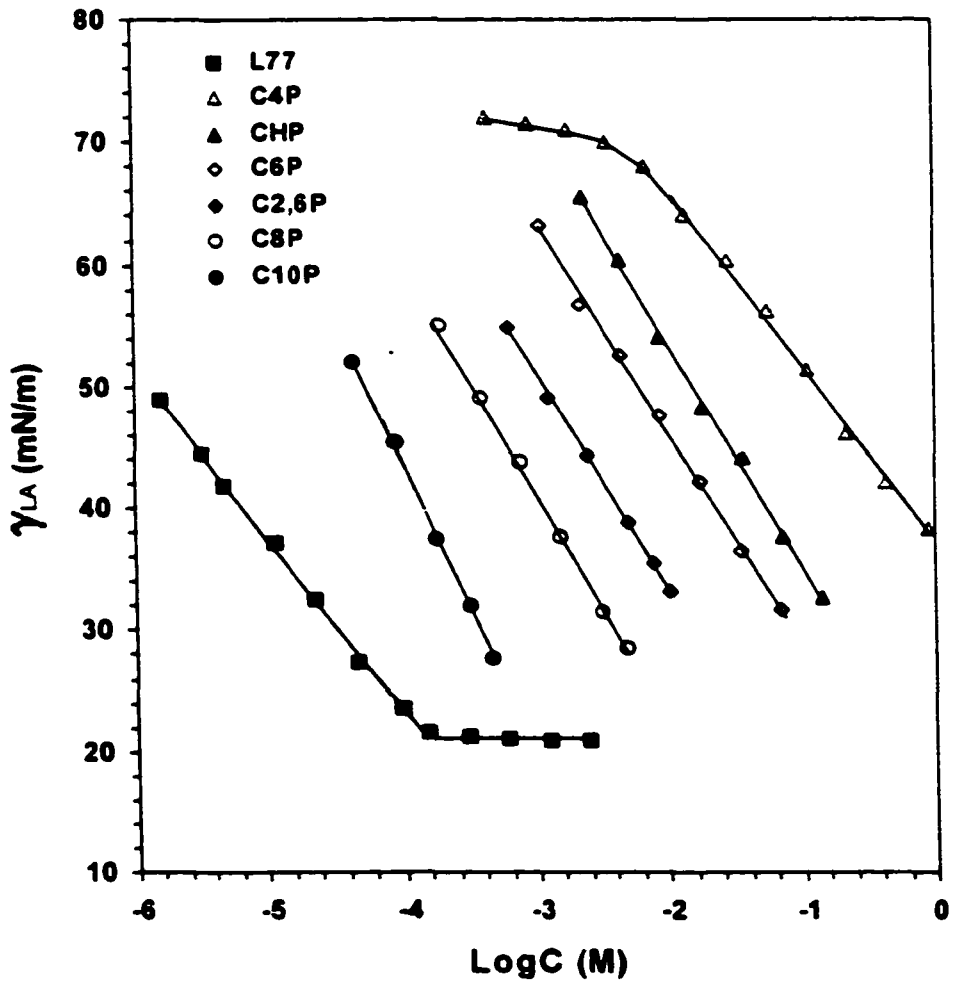

Table A-1. Interfacial Properties of L77 and the Individual N-Alkyl Pyrrolidinones at the Air/Aqueous Solution Interface

(In Phosphate Buffer Solution, pH ≈7.00, 25 °C)

Compounds	$\Gamma_{LA,max}$ (mol/cm^2)	A_{min} (Å^2)	pC_{20}	$\Delta G°_{ad}$ (kJ/mol)
L-77	2.52×10^{-10}	66.0	5.95	-51.9
C4P	2.60×10^{-10}	63.9	1.05	-23.7
CHP	3.05×10^{-10}	54.4	1.85	-27.1
C6P	3.71×10^{-10}	44.8	2.35	-28.8
C2,6P	3.54×10^{-10}	46.9	3.05	-33.0
C8P	4.34×10^{-10}	38.3	3.25	-33.1
C10P	4.45×10^{-10}	37.3	4.25	-38.7

Table A-2. Adsorption Results of the Mixtures of L77 and C4P at the Air/Aqueous Solution Interface

(In Phosphate Buffer Solution, pH =7.00, 25 °C)

α_{L77} (Ini.)	C4P (wt.%)	$\frac{d\gamma_{LA}}{d\log C}$	$\Gamma_{LA,max}$ (mol/cm^2)	$A_{LA,min}$ (Å^2)
1.000	0.0	-14.4	2.52×10^{-10}	65.9
0.805	4.7	-14.4	2.53×10^{-10}	65.6
0.611	11.4	-14.7	2.57×10^{-10}	64.6
0.475	18.2	-15.0	2.62×10^{-10}	63.4
0.313	30.7	-15.2	2.66×10^{-10}	62.4
0.209	43.3	-15.3	2.68×10^{-10}	62.0
0.110	62.0	-15.2	2.66×10^{-10}	62.4
0.029	87.1	-15.0	2.62×10^{-10}	63.4
0.000	100.0	-14.8	2.60×10^{-10}	63.9

Table A-3. Adsorption Results of the Mixtures of L77 and CHP at the Air/Aqueous Solution Interface

(In Phosphate Buffer Solution, pH =7.00, 25 °C)

α_{L77} (Ini.)	CHP (wt.%)	$\frac{d\gamma_{LA}}{d\log C}$	$\Gamma_{LA,max}$ (mol/cm^2)	$A_{LA,min}$ (Å^2)
1.000	0.0	-14.4	2.52×10^{-10}	65.9
0.838	4.4	-14.8	2.59×10^{-10}	64.1
0.694	9.5	-14.9	2.61×10^{-10}	63.6
0.581	14.7	-15.2	2.66×10^{-10}	62.4
0.407	25.8	-15.7	2.75×10^{-10}	60.4
0.253	41.3	-16.1	2.82×10^{-10}	58.9
0.115	64.7	-15.5	2.72×10^{-10}	61.0
0.058	79.5	-16.7	2.92×10^{-10}	56.9
0.000	100.0	-17.4	3.05×10^{-10}	54.4

Table A-4. Adsorption Results of the Mixtures of L77 and C6P at the Air/Aqueous Solution Interface

(In Phosphate Buffer Solution, pH =7.00, 25 °C)

α_{L77} (Ini.)	C6P (wt.%)	$\frac{d\gamma_{LA}}{d\log C}$	$\Gamma_{LA,max}$ (mol/cm^2)	$A_{LA,min}$ (Å^2)
1.000	0.0	-14.4	2.52×10^{-10}	65.9
0.868	4.5	-14.8	2.60×10^{-10}	63.9
0.735	8.0	-15.1	2.65×10^{-10}	62.7
0.574	15.2	-15.6	2.74×10^{-10}	60.6
0.417	25.2	-15.8	2.77×10^{-10}	59.9
0.243	42.9	-16.7	2.93×10^{-10}	56.7
0.152	57.4	-18.6	3.25×10^{-10}	51.1
0.028	89.3	-20.2	3.54×10^{-10}	46.9
0.000	100.0	-21.2	3.71×10^{-10}	44.8

Table A-5. Adsorption Results of the Mixtures of L77 and C2,6P at the Air/Aqueous Solution Interface

(In Phosphate Buffer Solution, pH =7.00, 25 °C)

α_{L77} (Ini.)	C2,6P (wt.%)	$\frac{d\gamma_{LA}}{d\log C}$	$\Gamma_{LA,max}$ (mol/cm^2)	$A_{LA,min}$ (Å^2)
1.000	0.0	-14.4	2.52×10^{-10}	65.9
0.825	5.6	-15.1	2.64×10^{-10}	62.9
0.651	13.1	-15.4	2.69×10^{-10}	61.7
0.501	21.9	-16.3	2.85×10^{-10}	58.3
0.381	31.4	-16.8	2.94×10^{-10}	56.5
0.220	49.9	-18.4	3.22×10^{-10}	51.6
0.096	72.6	-19.1	3.34×10^{-10}	49.7
0.025	91.6	-19.7	3.45×10^{-10}	48.1
0.000	100.0	-20.2	3.54×10^{-10}	46.9

Table A-6. Adsorption Results of the Mixtures of L77 and C8P at the Air/Aqueous Solution Interface

(In Phosphate Buffer Solution, pH =7.00, 25 °C)

α_{L77} (Ini.)	C8P (wt.%)	$\frac{d\gamma_{LA}}{d\log C}$	$\Gamma_{LA,max}$ (mol/cm^2)	$A_{LA,min}$ (Å^2)
1.000	0.0	-14.4	2.52×10^{-10}	65.9
0.906	2.8	-15.0	2.63×10^{-10}	63.1
0.791	6.9	-15.1	2.65×10^{-10}	62.7
0.660	12.7	-15.4	2.70×10^{-10}	61.5
0.535	19.7	-15.6	2.74×10^{-10}	60.6
0.375	31.9	-16.3	2.85×10^{-10}	58.3
0.222	49.7	-18.6	3.26×10^{-10}	50.9
0.085	75.2	-22.1	3.87×10^{-10}	42.9
0.000	100.0	-24.8	4.34×10^{-10}	38.3

Table A-7. Adsorption Results of the Mixtures of L77 and C10P at the Air/Aqueous Solution Interface

(In Phosphate Buffer Solution, pH =7.00, 25 °C)

α_{L77} (Ini.)	C10P (wt.%)	$\frac{d\gamma_{LA}}{d\log C}$	$\Gamma_{LA,max}$ (mol/cm^2)	$A_{LA,min}$ (Å^2)
1.000	0.0	-14.4	2.52×10^{-10}	65.9
0.867	4.7	-15.1	2.64×10^{-10}	62.9
0.707	11.8	-15.8	2.77×10^{-10}	59.9
0.575	19.2	-16.8	2.95×10^{-10}	56.3
0.435	29.5	-18.5	3.24×10^{-10}	51.2
0.307	42.0	-20.4	3.58×10^{-10}	46.4
0.186	58.4	-21.8	3.82×10^{-10}	43.5
0.077	79.4	-23.9	4.19×10^{-10}	39.6
0.000	100.0	-25.4	4.45×10^{-10}	37.3

Figure A-2. Total Adsorption $\Gamma_{LA,max}$ versus α_{L77} of L77, CnP, and Their Mixtures at the Air/Aqueous Solution Interface

(Phosphate Buffer Solution, pH=7.00, 25 °C)

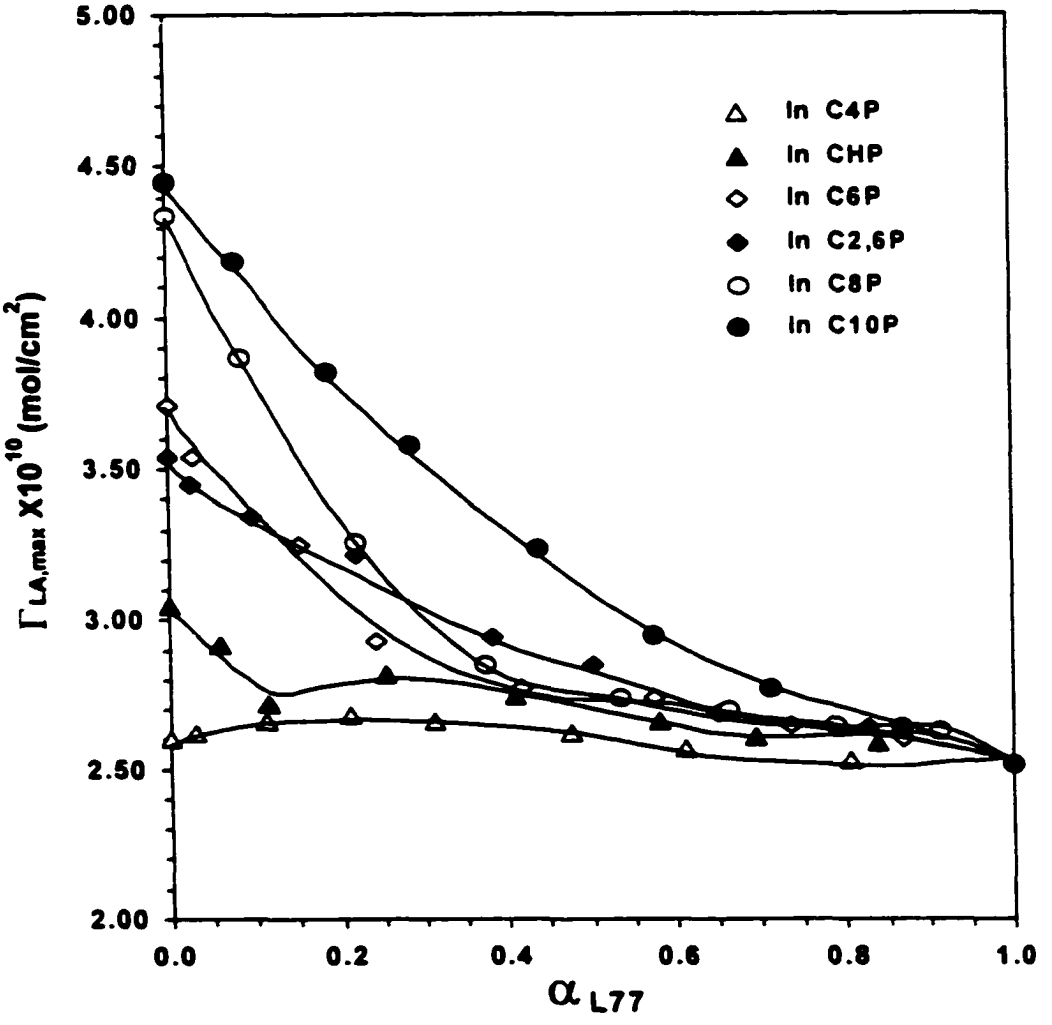

4.2 Adsorption at the Liquid/Solid Interface (Γ_{SL})

4.2.1 Adsorption of the Individual Surfactants

Unlike measurements of adsorption at the air/aqueous solution interface, which are calculated indirectly from surface tension data, adsorption of surfactants and their mixtures at the solid/aqueous solution interface was determined directly, as described in Section 3.3.4. Figure A–3 shows the adsorption isotherms of L77, C4P, CHP, C6P, C2,6P C8P and C10P on the surface of powdered polyethylene. All measurements were made on surfactant solutions in phosphate buffer at pH = 7.00 and were taken to sufficiently high concentration to ensure the formation of a monolayer at the solid/aqueous solution interface. All the adsorption isotherms with the exception of the C10P isotherms show Langmuir-type adsorption. The adsorption on the powdered polyethylene surface increases in the order: C4P < CHP < C6P < C2,6P < C8P < L77 < C10P. According to equation (45), C_{eq}/Γ_{SL} versus C_{eq} for L77, C4P, CHP, C6P, C2,6P C8P and C10P are plotted and shown in Figure A–4. The plots are linear for all the compounds except C10P. Table A–8 lists the adsorption free energies, calculated by using equation (51), surface concentrations of surfactant at monolayer adsorption, and correlation coefficients of the plot of C_{eq}/Γ_{SL} versus C_{eq} for L77 and the individual N-Alkyl

pyrrolidinones. From Table A–8, the absolute value of the negative adsorption free energy of the investigated surfactants decreases in the order: L77 > C8P ~ C6P > CHP ~ C2,6P > C4P > C10P. L77 has the most negative adsorption free energy at the solid/aqueous solution interface. This is probably due to the methyl groups its hydrophobic group. With the exception of C10P and C2,6P, this order for the pyrrolidinones is the same as that at the air/aqueous solution interface; the expected decrease, for the pyrrolidinones, with decrease in the alkyl chain length. Since C10P appears not to show true Langmuir-type adsorption, as shown by its poor correlation coefficient (R^2) of 0.802, for linearity of equation (45), the value of –31.8 kJ/mol, calculated from equation (51), is probably not correct. The reason for the relatively poorer adsorption of C2,6P at the solid/liquid interface than at the air/aqueous solution interface is not known, but may be related to its branched-chain structure. It is noteworthy that, although the adsorption tendency of C10P on powdered polyethylene may possibly be low, it has the highest adsorption effectiveness on polyethylene powder, showing the largest adsorption amount in Figure A–3.

4.2.2 Adsorption of Surfactant Mixtures at the Solid/Aqueous Solution Interface

As described in Chapter 3, the adsorption amounts of L77 and the pyrrolidinones(CnP) from their mixed solutions onto the polyethylene/aqueous

solution interface were measured by use of two phase titration and UV spectroscopy, respectively. In order to find the effect of the addition of a pyrrolidinone on the adsorption of L77 at the interface, the adsorptions of L77 and all N-alkyl-pyrrolidinones in their mixtures with different initial mole fractions of L77 were compared with their adsorption by themselves at the same equilibrium concentration.

Experimental data are listed in Table B–50 to Table B–91, including the fixed initial mole fraction of L77($\alpha_{L77,ini}$), initial total concentration($C_{ini,total}$), initial concentration of L77($C_{ini,L77}$), initial concentration of CnP($C_{ini,CnP}$), weight of the polyethylene powder used (g), adsorption amount of L77(Ads. L77), adsorption amount of CnP(Ads.CnP), total adsorption (Ads.Total) of L77 plus CnP, equilibrium concentration of L77($C_{eq.,L77}$), equilibrium concentration of CnP($C_{eq,CnP}$), total equilibrium concentration($C_{eq,total}$) of L77 plus CnP, mole fraction of L77 in the bulk solution phase at adsorption equilibrium($\alpha_{L77,eq.}$), and mole fraction of L77 in the adsorbed layer at adsorption equilibrium($X_{L77,eq.}$). In addition, the related adsorption isotherms are shown in Figure B–13 to Figure B–54. In these figures, all adsorption isotherms of individual L77 and individual CnP are the same, used for comparison of the adsorption of L77 and CnP from their mixed solutions. All solutions were made below or around the C.M.C. for L77and below their solubilities for N-alkyl-pyrrolidinones.

(i) L77–C4P Mixtures: The experimental data are listed in Table B–50 to Table B–56. The adsorption isotherms are shown in Figure B–13 to Figure B–19.

In Figures B–13 and B–14, it can be seen that for the mixtures, all with initial mole fractions, $\alpha_{L77,ini}$ 0.034 and 0.137, the adsorption amount of L77 is less than that of L77 individual at the same equilibrium concentration, the adsorption amount of C4P is almost the same as C4P individual at the same equilibrium concentration, the total adsorption of L77 and C4P in the mixtures is lower than the adsorption of L77 at the same equilibrium concentration. This is, because at these very small fixed initial mole fractions of L77 in the mixtures, the mixtures contain mainly C4P. Therefore, the adsorption of C4P from the mixtures is nearly the same as from pure C4P solutions. On the other hand, the number of moles of L77 in the mixture solutions is too small to reach the adsorption amount from L77 solution. Furthermore, there is no synergism in the adsorption from these mixtures with these fixed initial α_{L77} values, as indicated by the fact that the total mixed adsorption of L77 plus C4P is less than an L77 solution or C4P solution. From the corresponding Tables B–50 and B–51, it can be seen that the equilibrium mole fraction of L77 in the bulk solution phase changes with the equilibrium concentration. At low equilibrium concentrations, the values of $\alpha_{L77,eq.}$ is much less that of $\alpha_{L77,ini}$, meaning that L77 and C4P

were not adsorbed equally or proportionally onto the polyethylene/aqueous solution interface. L77 molecules were adsorbed at the interface much more than C4P. This can be explained by the much higher adsorption efficiency of L77 at solid/aqueous solution interface as discussed in the previous part. The equilibrium mole fraction of L77($\alpha_{L77,eq.}$) increases with an increase in the equilibrium concentration, becoming close to its initial value, but it is always smaller than its initial value. This is because there are always more L77 molecules adsorbed at the interface. However, the difference becomes smaller and smaller. This is because at the high equilibrium concentration, the adsorption amount is not large enough to change the initial concentration greatly. Consequently, it can not change the initial fixed mole fraction greatly. From the tables, it can also be seen that the mole fraction of L77 in the adsorbed layer is almost a constant at all equilibrium concentrations and much larger than that in the bulk solution phase, particularly at low equilibrium concentrations. This again can be explained as a result of the high adsorption efficiency of L77 at the solid/aqueous solution interface.

In Figures B–15 and B–16, it can be seen that when the mixed solutions of L77 and C4P were made at initial mole fractions of L77 of 0.243 and 0.353, adsorption of L77 and C4P from their mixture solution is larger than that from their individual solutions. That means if L77 and C4P are mixed in mole ratios of 1:3 or 1:2, both adsorptions at the polyethylene/aqueous solution interface of

L77 and C4P from their mixed solutions can be enhanced by each other. There is a synergistic effect on their adsorption. This is, the total adsorption is enhanced by the addition of C4P to the mixtures.

Figure B–17 shows the adsorption isotherms of L77 and C4P from their mixed solution onto the polyethylene with $\alpha_{L77,ini.}$=0.503. It can be seen that when L77 and C4P are mixed in 1:1 mole ratio, only the adsorption of L77 can be enhanced, however, the adsorption of C4P is almost the same as from its individual solution.

Figure B–18 shows the adsorption isotherms of L77 and C4P from their mixed solution onto the polyethylene with $\alpha_{L77,ini.}$=0.634. It can be seen that when L77 and C4P are mixed in about 2:1 mole ratio, the adsorption of L77 can be enhanced slightly. However, the adsorption of C4P is less than that from its individual solution. The reason might be that most of the adsorption sites on the polyethylene surface are occupied by L77 molecules, which results in a decrease in adsorption of C4P molecules at the polyethylene surface.

Figure B–19 shows the adsorption isotherms of L77 and C4P from their mixture solution with $\alpha_{L77,ini.}$=0.819 onto the polyethylene. It can be seen that when L77 and C4P are mixed in about 4:1 mole ratio, the adsorption of L77 from the mixture solution is nearly the same as from its individual solution, the

adsorption of C4P is much less than that from its individual solution, and approaches 0. Again, the reason might be that the mixed solution contains so much L77, a surfactant with much higher adsorption efficiency on polyethylene, that the behavior of this solution is very close to that of its individual solution. The adsorption sites on the solid surface are almost completely occupied by L77 molecules.

The adsorption results of the mixtures of L77 and C4P at various fixed initial L77 mole fractions are listed in Table A–9.

(ii) L77–CHP Mixtures: The experimental data are listed in Table B–57 to Table B–63. The adsorption isotherms are shown in Figures B–20 to B–26.

In Figure B–20, it can be seen that for the mixtures with fixed initial $\alpha_{L77,ini}$ =0.067, the adsorption amount of L77 is less than that of individual L77 at the same equilibrium concentration. The adsorption amount of CHP at very low concentration is almost the same as CHP, but it becomes lower at higher concentration. It reaches saturation at about 2×10^{-4} M. The saturated adsorption is about 1×10^{-10} mol/cm^2. The total adsorption of L77 and CHP in the mixtures is lower than the adsorption of L77 at the same equilibrium concentration, but it becomes larger at higher total concentration. An explanation is that, although this mixed solution contains only very little L77, its

tendency to adsorb at the solid interface is greater than that of CHP, but its concentration in the bulk solution is not high enough to establish a saturation adsorption. For CHP, although its concentration is high enough in the bulk solution, the adsorption sites on the polyethylene surface have been mainly occupied by the more active L77 molecules. As a result, its adsorption is still low and reaches saturation quickly. The related experimental data are listed in Table B–57.

Figure B–21 shows the adsorption isotherms of mixture with fixed initial $\alpha_{L77,ini}$=0.136. The difference from Figure B–20 is that the adsorption of L77 from the mixture is a little higher than from its individual solution. The adsorption of CHP still reaches saturation at low concentration, but the saturated adsorption amount is smaller than the previous one. This is because the amount of CHP is less, due to the higher fixed initial $\alpha_{L77,ini}$ in these solutions. The related experimental data are listed in Table B–58.

Figures B–22 to B–24 show the adsorption isotherms of mixtures with fixed initial $\alpha_{L77,ini}$ =0.285, 0.438, 0.602, respectively. From the adsorption isotherms, it can be seen that adsorption of L77 from the mixture is greater than from its individual solution, but the saturated adsorption of CHP is smaller than from its individual solution. However, the adsorption of CHP from the mixed solution at low concentration is higher than from its individual solution for the

mixtures of $\alpha_{L77,ini}$ =0.285 and 0.438. That means that when L77 and CHP were mixed at those initial mole fractions, synergism between these two different molecules occurred; both of their adsorptions onto the polyethylene surface were enhanced at low concentration. The related experimental data are listed in Tables B–59, B–60 and B–61.

Figure B–25 shows the adsorption isotherms of L77 and CHP onto polyethylene from their mixture with $\alpha_{L77,ini.}$=0.712. It can be seen that when L77 and CHP were mixed in this molar ratio, only the adsorption of L77 was enhanced; the adsorption of CHP was much less than from its individual solution. However, the total adsorption of the two surfactants on the polyethylene was still greater than that of L77. The related experimental data are listed in Table B–62.

Figure B–26 shows the adsorption isotherms of L77 and CHP onto the polyethylene from their mixture with $\alpha_{L77,ini.}$=0.850. It can be seen that when L77 and CHP are mixed in this molar ratio, the adsorption of L77 from the mixture is nearly the same as from its individual solution; the adsorption of CHP is almost equal to 0. The reason might be that such a mixed solution contains so much L77, a surfactant with much higher adsorption efficiency onto polyethylene, that the behavior of this solution is very close to that of its individual solution. The adsorption sites on the solid surface are almost occupied completely by L77

molecules; therefore, the adsorption of CHP at the solid surface is almost 0. The related experimental data are listed in Table B–63.

The adsorption results of the mixtures of L77 and CHP at various fixed initial L77 mole fractions are listed in Table A–10.

(iii) L77–C6P Mixtures: The fixed initial mole fractions of L77 used for mixed solutions of L77 and C6P($\alpha_{L77,ini}$) are 0.039, 0.172, 0.269, 0.441, 0.595, 0.751, 0.877. The experimental data are listed in Tables B–64 to B–70. The adsorption isotherms are shown in Figures B–27 to B–33.

In Figure B–27, it can be seen that for the mixtures with fixed initial $\alpha_{L77,ini}$=0.039, the adsorption amount of L77 is less than that of L77 individual at the same equilibrium concentration. The adsorption amount of C6P at low concentration is almost the same as C6P individual, but it becomes lower at higher concentration. It reaches saturation at about 5×10^{-5} M, the saturated adsorption is about 1.5×10^{-10} mol/cm^2. The total adsorption of L77 and C6P in the mixtures is lower than the adsorption of L77 individual at the same equilibrium concentration, but it becomes larger at higher total concentration. An explanation is that, although this mixed solution contains very little L77, its adsorption tendency at the solid interface is greater than that of C6P, but its concentration in the bulk solution is not high enough to establish a saturation

adsorption. For C6P, although its concentration is high enough in the bulk solution, the adsorption sites on the polyethylene surface have been mainly occupied by the more active L77 molecules. As a result, its adsorption is still low and reaches saturation quickly. The related experimental data are listed in Table B–64.

Figure B–28 shows the adsorption isotherms of mixture with fixed initial $\alpha_{L77,ini}$=0.172. The difference from Figure B–27 is that the adsorption of L77 from the mixture is a little higher than from its individual solution. The adsorption of C6P still gets saturated at low concentration, but the saturated adsorption amount is about 1.0×10^{-10} mol/cm^2, smaller than the previous one. This is because the amount of C6P is less, due to the higher fixed initial $\alpha_{L77,ini}$ in these mixtures. The related experimental data are listed in Table B–65.

Figures B–29 to B–31 show the adsorption isotherms of mixtures with fixed initial $\alpha_{L77,ini}$ =0.269, 0.441, 0.595, respectively. From the adsorption isotherms, it can be seen that the adsorption effectiveness of L77 from the mixed solutions is 3.4×10^{-10} mol/cm^2, 3.2×10^{-10} mol/cm^2 and 3.0×10^{-10} mol/cm^2, respectively, which is greater than from its individual solution, 2.7×10^{-10} mol/cm^2. But they decrease with an increase of the fixed initial mole ratio of L77. That means that when L77 and C6P were mixed in the above mole ratios of L77 to C6P, the mixtures showed synergism in the adsorption of L77 on the

polyethylene, and the maximum synergism was obtained at $\alpha_{L77,ini}$ =0.269. The saturated adsorptions of C6P from the mixed solutions are much smaller than from its individual solution. There is no synergism found in the adsorption of C6P on the polyethylene surface. The related experimental data are listed in Table B–66, Table B–67 and Table B–68.

Figure B–32 shows the adsorption isotherms of L77 and C6P onto polyethylene from their mixture solution with $\alpha_{L77,ini.}$=0.751. It can be seen that when L77 and C6P were mixed at this mole ratio, only the adsorption of L77 was enhanced, the adsorption of C6P was much less than it from its individual solution. However, the total adsorption of the two surfactants on the polyethylene was still greater than that of L77. The related experimental data are listed in Table B–69.

Figure B–33 shows the adsorption isotherms of L77 and C6P onto polyethylene from their mixture with $\alpha_{L77,ini.}$=0.877. It can be seen that when L77 and C6P are mixed in this mole ratio, the adsorption of L77 from the mixture solution is nearly the same as it is from its individual solution; the adsorption of C6P is almost equal to 0. The reason is that such mixed solution contains so much L77, a surfactant with much higher adsorption efficiency at polyethylene, that the behavior of this solution is very close to that of its individual solution. The adsorption sites on the solid surface are almost completely occupied by

L77 molecules. Therefore, the adsorption of C6P at the solid surface is almost 0. The related experimental data are listed in Table B–70.

The adsorption results of the mixtures of L77 and C6P at various fixed initial L77 mole fractions are listed in Table A–11.

(iv) L77–C2,6P Mixtures: The fixed initial mole fractions of L77 used for mixed solutions of L77 and C2,6P($\alpha_{L77,ini}$) are 0.036, 0.115, 0.246, 0.415, 0.530, 0.672, 0.836. The experimental data are listed in Tables B–71 to B–77. The adsorption isotherms are shown in Figures B–34 to B–40.

Figure B–34 shows the adsorption isotherms of L77, C2,6P from their mixed solutions and the total adsorption on powdered polyethylene. It can be seen that for the mixtures with fixed initial $\alpha_{L77,ini}$=0.036, the adsorption amount of L77 is less than that of L77 solution at the same equilibrium concentration. The adsorption amount of C2,6P at very low concentration is almost the same as C2,6P alone, but it becomes lower at higher concentration. Its adsorption reaches saturation at about 1.5×10^{-4} M, the saturated adsorption is about 1.35×10^{-10} mol/cm^2. The total adsorption of L77 and C2,6P in the mixtures is lower than the adsorption of L77 solution at the same equilibrium concentration, but it becomes larger at higher total concentration. An explanation is that, although this mixed solution contains very little L77, the adsorption tendency of

L77 at the solid interface is greater than that of C2,6P, but its concentration in the bulk solution is not high enough to establish a saturated adsorption. For C2,6P, although its concentration is high enough in the bulk solution, the adsorption sites on the polyethylene surface have been mainly occupied by the more active L77 molecules. As a result, its adsorption is still low and reaches saturation quickly. The related experimental data are listed in Table B–71.

Figure B–35 shows the adsorption isotherms of mixtures with fixed initial $\alpha_{L77,ini}$=0.115. The adsorption of L77 from the mixture at very low concentration is higher than from its individual solution, but the saturation adsorption is still lower. The adsorption of C2,6P from the mixture at low concentration (<4×10^{-5} M) is greater than from its individual solution, and reaches saturation at the concentration(~4×10^{-5} M). The saturated adsorption is about 1.0×10^{-10} mol/cm^2, which is smaller than from its individual solution. An explanation is that, the adsorption tendency of L77 onto the solid is greater than that of C2,6P, L77 molecules occupy most of adsorption sites on the solid surface and establish an adsorption equilibrium at the higher concentration. Therefore, both L77 and C2,6P reaches their saturation adsorption at the higher concentration. The related experimental data are listed in Table B–72.

Figure B–36 and Figure B–37 show the adsorption isotherms of L77 and C2,6P on polyethylene powder from their mixtures with fixed initial $\alpha_{L77,ini}$

=0.246, 0.415, respectively. From the adsorption isotherms, it can be seen that the adsorption of L77 from the mixed solutions is enhanced over whole range of concentration measured. The maximum adsorption of L77 from these two mixtures are 2.9×10^{-10} mol/cm^2, 3.7×10^{-10} mol/cm^2, respectively. They are greater than from its individual solution, 2.7×10^{-10} mol/cm^2. These mixtures show significant synergism in the adsorption of L77 on the polyethylene, and the maximum synergism is obtained at $\alpha_{L77,ini}$ =0.415. The adsorption of C2,6P from the mixture is enhanced at low concentrations, but its saturation adsorption from the mixed solutions are much lower than from its individual solution. The related experimental data are listed in Tables B–73 and B–74.

Figure B–38 and Figure B–39 show the adsorption isotherms of L77 and C2,6P onto powdered polyethylene from their mixtures with $\alpha_{L77,ini.}$=0.530 and 0.672. From the figures, it can be seen that the adsorption of L77 from the mixed solutions is enhanced remarkably over the whole range of concentrations measured. The maximum adsorptions for these two mixtures are 3.7×10^{-10} mol/cm^2, 3.4×10^{-10} mol/cm^2, respectively. They are greater than from its individual solution, 2.7×10^{-10} mol/cm^2. This means a significant synergism was produced between the molecules of L77 and C2,6P. However, the saturated adsorptions of C2,6P from these mixtures are only about 5.0×10^{-11} mol/cm^2 and 3.0×10^{-11} mol/cm^2, much lower than from its individual solution. The total

adsorption is much greater than that of L77 from its individual solution. This is due to the significant enhancement in the adsorption of L77 from the mixtures. The related experimental data are listed in Table B–75 and Table B–76.

Figure B–40 shows the adsorption isotherms of L77 and C2,6P onto polyethylene from their mixture with $\alpha_{L77,ini.}$=0.836. From the figure, it can be seen that when L77 and C2,6P are mixed in this mole ratio, the adsorption of L77 from the mixture at low concentrations (<2×10^{-5} M) is nearly the same as from its individual solution. The adsorption of L77 from the mixture increases slightly with an increase in equilibrium concentration. The adsorption of C2,6P is very small, or approaches 0. The total adsorption is almost the same as that of L77 from the mixed solution. The reason is that such mixed solutions contains so much L77 that the total adsorption is dominated by L77. The adsorption sites on the solid surface were almost completely occupied by L77 molecules. Therefore, the adsorption of C2,6P on the solid surface is almost 0. The related experimental data are listed in Figure B–77.

The adsorption results of the mixtures of L77 and C2,6P at various fixed initial L77 mole fractions are listed in Table A–12.

(v) L77–C8P Mixtures: The fixed initial mole fractions of L77 used for mixtures of L77 and C8P($\alpha_{L77,ini}$) are 0.094, 0.244, 0.401, 0.551, 0.672, 0.799,

0.908, respectively. The experimental data are listed in Tables B–78 to B–84. The adsorption isotherms are shown in Figures B–41 to B–46.

Figure B–41 shows the adsorption isotherms of L77, C8P from their mixture and the total adsorption on powdered polyethylene. From the figure, it can be see that for the mixture with fixed initial $\alpha_{L77,ini}$=0.094, the adsorption of L77 is lower than from its individual solution. The concentration of L77 in the bulk solution is not high enough to establish a saturated adsorption because of its very small mole fraction in the bulk solution. The adsorption of C8P from the mixture at very low concentration is almost the same as that from its individual solution. It reaches saturation at about 1.0×10^{-4} M, the saturation adsorption of C8P is about 1.55×10^{-10} mol/cm^2, much smaller from its individual solution. An explanation is that, although the concentration of C8P in bulk solution is high enough, the adsorption sites on polyethylene surface have been mainly occupied by L77 molecules. As a result, the adsorption of C8P is low. The total adsorption of L77 plus C8P in the mixtures is lower than that of L77 individual at low concentration, but it becomes larger due to the contribution of the adsorption of C8P from the mixture. The related experimental data are listed in Table B–78.

Figure B–42 shows the adsorption isotherms of mixture with fixed initial $\alpha_{L77,ini}$=0.244. The adsorption of L77 from the mixture over the whole range of

concentrations measured is higher than from its individual solution. The adsorption of C8P from the mixture at low concentrations is almost the same as from its individual solution, but the saturation adsorption is lower than from its individual solution. An explanation is that, although this mixed solution contains very little L77 and the adsorption tendency of L77 onto the solid interface is greater than that of C8P, however, comparing to C8P, it is not great enough to occupy completely the adsorption sites on the solid surface. Therefore, an adsorption equilibrium between the two surfactants at the solid/aqueous solution interface is established at an equilibrium concentration. This can be seen in this figure or found in Table B–79. The related experimental data are listed in Table B–79.

Figure B–43 shows the adsorption isotherms of L77 and C8P on polyethylene powder from their mixture with fixed initial $\alpha_{L77,ini}$ =0.401. From the adsorption isotherms, it can be seen that the adsorption of L77 from the mixed solutions is enhanced remarkably over the whole range of concentration measured. The maximum adsorption of L77 from mixture is about 3.6×10^{-10} mol/cm^2, which is greatly greater than from its individual solution, 2.7×10^{-10} mol/cm^2, and still increases slightly with an increase in its equilibrium concentration. This means that when L77 and C8P were mixed in this mole ratio, the mixture shows a significant synergism in the adsorption of L77 on powdered polyethylene. On the other hand, the adsorption of C8P from the

mixture is not enhanced. The saturation adsorption of C8P from the mixed solutions is only about 1.2×10^{-10} mol/cm^2, much lower than from its individual solution. The adsorption of C8P from the mixtures does not increase with its equilibrium concentration. The reason is that the adsorption of L77 is dominant at the solid/liquid interface, and, what is more, it is greatly enhanced by C8P in the mixture. Therefore, more adsorption sites on polyethylene surface are occupied L77 molecules. As a result, the adsorption of C8P at the interface reaches saturation quickly with low adsorption effectiveness. The related experimental data are listed in Table B–80.

Figures B–44, B–45 and B–46 show the adsorption isotherms of L77 and C8P onto powdered polyethylene from their mixture with $\alpha_{L77,ini.}$=0.551, 0.672 and 0.799, respectively. From the figures, it can be seen that the adsorption of L77 from the mixed solutions is almost the same as from the individual solution, but enhanced at higher concentrations. The adsorption of L77 from the mixture at higher concentration increases slightly with its equilibrium concentration. The maximum adsorption of L77 for these three mixtures are 3.3×10^{-10} mol/cm^2, 3.1×10^{-10} mol/cm^2 and 2.9×10^{-10} mol/cm^2, respectively. For C8P, its adsorption from the mixture is much lower than from its individual solution. The maximum adsorptions of C8P for these three mixtures are: 8.5×10^{-11} mol/cm^2, 5.5×10^{-11} mol/cm^2 and 3.0×10^{-11} mol/cm^2, respectively. This is because the equilibrium concentration of C8P in the bulk solution decreases with the increase of mole

ratio of L77. The total adsorption of the two surfactants on polyethylene is greater than that of L77 from its individual solution. This is due the contribution of the adsorption of C8P from the mixture solution. The related experimental data are listed in Tables B–81, B–82 and B–83.

Figure B–47 shows the adsorption isotherms of L77 and C8P onto powdered polyethylene from their mixture with $\alpha_{L77,ini.}$=0.908. It can be seen that when L77 and C8P are mixed in this mole ratio, the adsorption of L77 from the mixed solution over whole range of concentration is nearly the same as from its individual solution. The adsorption of C8P is very small, or approaches to 0. The total adsorption of the two surfactants is almost the same as that of L77 from the mixture. The reason is that this mixture contains so much L77 that the total adsorption is dominated by L77. The adsorption sites on the solid surface are almost completely occupied by L77 molecules. Therefore, the adsorption of C8P at the solid surface is almost 0. The related experimental data are listed in Table B–84.

The adsorption results of the mixtures of L77 and C8P at various fixed initial L77 mole fractions are listed in Table A–13.

(vi) L77–C10P Mixtures: The fixed initial mole fractions of L77 used for mixtures of L77 and C10P($\alpha_{L77,ini}$) are 0.064, 0.158, 0.271, 0.401, 0.554, 0.690,

0.855, respectively. The experimental data are listed in Tables B–85 to B–91. The adsorption isotherms are shown in Figures B–48 to B–54.

Figures B–48 and B–49 show the adsorption isotherms of L77, C10P from their mixture with fixed initial $\alpha_{L77,ini}$ =0.064, 0.158 and the total adsorption on powdered polyethylene. It is unexpected that the adsorption of L77 from the mixed solution is much lower than that from L77 individual solution. The adsorption of C10P at low concentration (<8.0×10^{-5} M) from the mixed solution is less than that from its individual solution, but it increases very quickly with the increase of equilibrium concentration and reaches an unusually high amount at higher concentration. For this unusually high adsorption, the reason may be that the concentration of C10P is very close to its solubility in the buffer solution, which is 4.5×10^{-4} mol/L, and there is a repulsive interaction between C10P and L77 molecules in the bulk solution phase (to be discussed later in this thesis) that results in a decrease in the solubility of C10P. Consequently, more molecules of C10P move to the interface. The available maximum adsorption of C10P from the mixed solution is about 2.75×10^{-9} mol/cm^2 for the mixture with $\alpha_{L77,ini}$ =0.064, 2.00×10^{-9} mol/cm^2 for the mixture with $\alpha_{L77,ini}$ =0.158, which correspond to areas of 6.0 Å^2 and 8.3 Å^2 per molecule of C10P at the polyethylene/aqueous solution interface. Based upon the area per molecule of C10P at the air/aqueous solution interface of 37.3 Å^2(Table A-1), a multilayer of C10P rather than a monolayer is formed at polyethylene/aqueous solution

interface. The adsorption isotherms of C10P do not reach a plateau, indicating that there is no saturation adsorption reached. The total adsorption of L77 and C10P for the mixtures is almost the same as that of C10P from the mixtures. This is because the concentration of L77 in the mixtures is very low. Therefore, the total adsorption is dominated by the adsorption of C10P. The related experimental data are listed in Tables B–85 to B–86.

Figures B–50 and B–51 show the adsorption isotherms of L77, C10P from their mixtures with fixed initial $\alpha_{L77,ini}$= 0.271 and 0.401and their total adsorption. It can be seen that the adsorption of L77 from the mixed solutions over the whole concentration range is lower than that from its individual solutions. The saturation adsorptions of L77 are only 1.0×10^{-10} mol/cm^2 and 1.2×10^{-10} mol/cm^2 for the two mixtures, respectively. The adsorption of C10P from the mixed solutions at low concentration (<1.0×10^{-4} M) is almost the same as from its individual solution, but it increases quickly with an increase in its equilibrium concentration. From the figures, the maximum adsorption of C10P for these two mixtures is about 1.55×10^{-9} mol/cm^2 for the mixture with $\alpha_{L77,ini}$ =0.271, 8.50×10^{-10} mol/cm^2 for the mixture with $\alpha_{L77,ini}$ =0.401, which decreases with an increase of $\alpha_{L77,ini}$. This is because the equilibrium concentration of C10P decreases with an increase in $\alpha_{L77,ini}$. The total adsorption of the mixtures is lower than that of C10P from its individual solution. This is because the

adsorption of L77 from the mixtures is too low to make the total adsorption higher. The related experimental data are listed in Tables B–87 to B–88.

Figures B–52 and B–53 show the adsorption isotherms of L77, C10P from their mixtures with fixed initial $\alpha_{L77,ini}$= 0.554, 0.690 and their total adsorption. It can be seen that the adsorption of L77 from the mixed solutions over the whole concentration range is smaller than from its individual solution. But the saturation adsorptions increase remarkably to 2.0×10^{-10} mol/cm^2 and 2.2×10^{-10} mol/cm^2 for the two mixtures, respectively. They are close to the saturation adsorption of L77 from its individual solution, and keep increasing with its equilibrium concentration. This is because the concentration of L77 in these two mixed solutions is high enough to make its adsorption at the solid/aqueous solution interface compatible with the adsorption of C10P at the same interface. The adsorption of C10P from the mixed solution at low concentration (<2.0×10^{-5} M) is higher, but becomes lower at higher concentrations. This is due to the more competitive adsorption of L77 at higher concentrations. The total adsorption of L77 and C10P over the whole concentration range is between the adsorption of L77 and C10P from their individual solutions. The related experimental data are listed in Tables B–89 to B–90.

Figure B–54 shows the adsorption isotherms of L77 and C10P from their mixed solutions with $\alpha_{L77,ini.}$=0.855 and the total adsorption onto powdered

polyethylene. The adsorption of L77 from the mixed solution is still slightly lower than from its individual solution, but very close to the saturation adsorption from its individual solution at high concentration. This is because this mixed solution contains mainly L77 and there is no synergism found in this system. Its adsorption behavior, therefore, is very similar to that of the L77 solution itself. The concentration of L77 in this mixed solution is high enough to establish an adsorption equilibrium at higher concentration. On the other hand, the mole fraction of C10P in this mixed solution is too small to make its concentration high enough to establish an adsorption plateau. In the figure, the maximum adsorption of C10P in this mixture is only about 9.5×10^{-11} mol/cm^2, decreases greatly with the initial mole fraction of L77. Same as before, the total adsorption of L77 plus C10P over the whole concentration range is between the adsorption of L77 and C10P from their individual solutions. The related experimental data are listed in Table B–91.

The adsorption results of the mixtures of L77 and C10P at various fixed initial L77 mole fractions are listed in Table A–14.

4.2.3 Enhancement of Adsorption from L77–CnP Surfactant Mixtures at the Aqueous Solution/Solid Interface

In order to describe the enhancement of L77 surfactant adsorption shown in the previous discussions, the maximum adsorption of L77, $\Gamma^{mix}_{SL,L77,max}$, from the mixed solutions with C4P, CHP, C6P, C2,6P, C8P and C10P, is plotted as function of equilibrium mole fraction of L77 in Figure A–5. From the figure, it appears the adsorption of L77 from the mixed solution onto the polyethylene powder surface is enhanced when its mole fraction exceeds 0.15, except for C10P. The extent (effectiveness) of enhancement caused by the pyrrolidinones decreases in the order: C2,6P > C8P > C6P > CHP > C4P. There is no enhancement found over the whole mole fraction range for C10P. Figure A–5 also indicates that the maximum enhancement of L77 occurs at different mole fractions of L77 for the different pyrrolidinones: from that figure, for C2,6P, it occurs at α_{L77} = 0.45; for C8P, at 0.35; for C6P, at 0.25; for CHP, at 0.35; for C4P, at 0.15. The larger the mole fraction of L77 in the mixture, the smaller the mole fraction of pyrrolidinone, and therefore, the higher its enhancement efficiency. Consequently, the efficiency of the pyrrolidinones in enhancing the adsorption of L77 on the polyethylene powder decreases in the order: C2,6P > C8P >CHP > C6P > C4P. From these results, it appears that, of the pyrrolidinones investigated, C2,6P, in both effectiveness and efficiency, is the best additive to enhance the adsorption of L77 on this hydrophobic low energy surface. Presumably, a branched alkyl chain is better than a linear alkyl chain for the enhancement. Among the prrolidinones with straight alkyl chains, the order of both efficiency and effectiveness increases with an increase in alkyl

chain length. However, again, C10P is fundamentally different from all other pyrrolidinones with straight alkyl chains in showing no enhancement of the adsorption of L77. The reason for such a large difference caused by the additional two carbon atoms in the alkyl chain is currently unknown.

The total surfactant adsorption at the polyethylene/aqueous solution interface from mixtures of L77 and pyrrolidniones with different L77 mole fractions is shown in Figure A–6. From this figure, it is seen that the total surfactant adsorption from the mixture is larger than the total ideal adsorption, i.e., the sum of the individual adsorptions multiplied by their mole fractions in the solution phase: $\Gamma_{SL}^{Total}(ideal) = \alpha_{1,eq} \cdot \Gamma_{SL}^{(1)} + (1-\alpha_{1,eq}) \cdot \Gamma_{SL}^{(2)}$. If the maximum enhancement by the pyrrolidinones of the total surfactant adsorption is compared with their ideal adsorption value, it can be seen that the enhancement of the pyrrolidinones decreases in the order: C2,6P > C8P > C4P > CHP > C6P. For C10P, where there is no enhancement of adsorption from the mixed solution, the total adsorption always decreases with the increase in L77 mole fraction. The maximum enhancement occurs at around α_{L77} =0.4 for C2,6P and C8P, at around α_{L77} =0.25 for C4P, CHP and C6P.

Figure A-3. Adsorption Isotherms of L77 and the Individual Pyrrolidinones(CnP) onto Powdered Polyethylene

(In Phosphate Buffer Solution, pH=7.00)

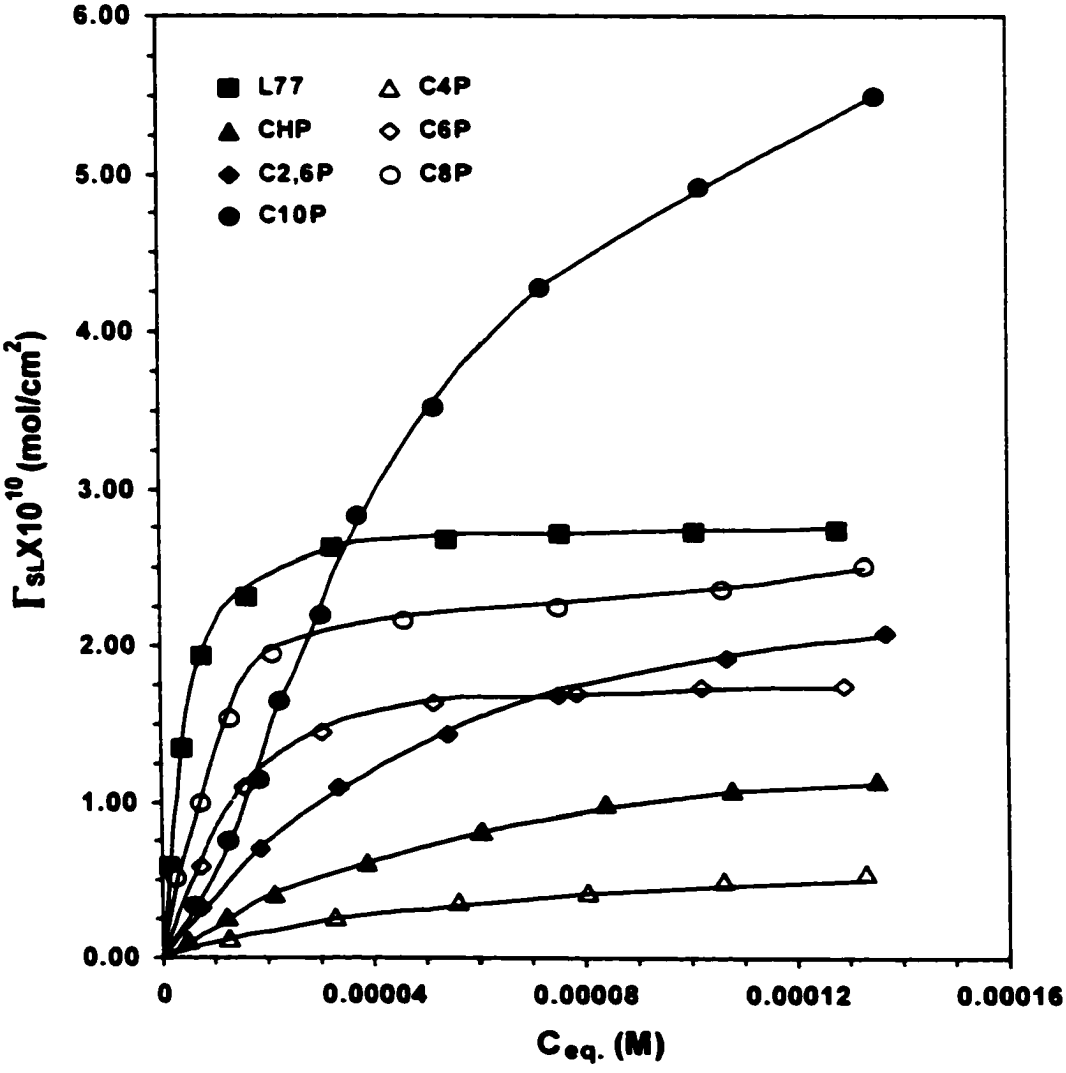

Figure A-4. Plots of ($C_{eq.}/\Gamma_{SL}$) versus C_{eq} for L77 and the Individual Pyrrolidinones(CnP) onto Powdered Polyethylene

(In Phosphate Buffer Solution, pH=7.00)

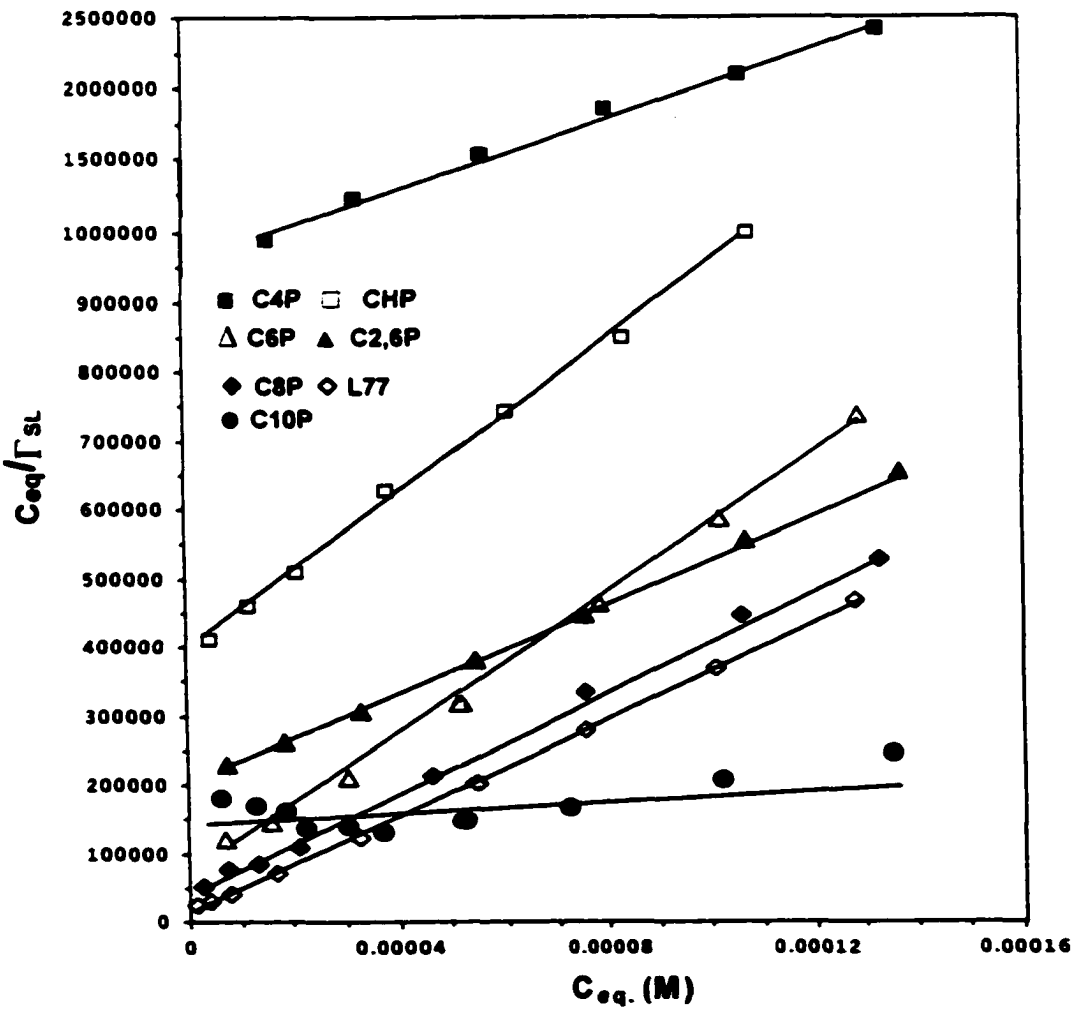

Figure A-5. Maximum Adsorption of L77, $\Gamma_{SL,L77max}$, vs. $\alpha_{L77,eq}$ for L77/CnP Mixtures at the Solid/Liquid Interface (In Phosphate Buffer Solution, pH=7.00)

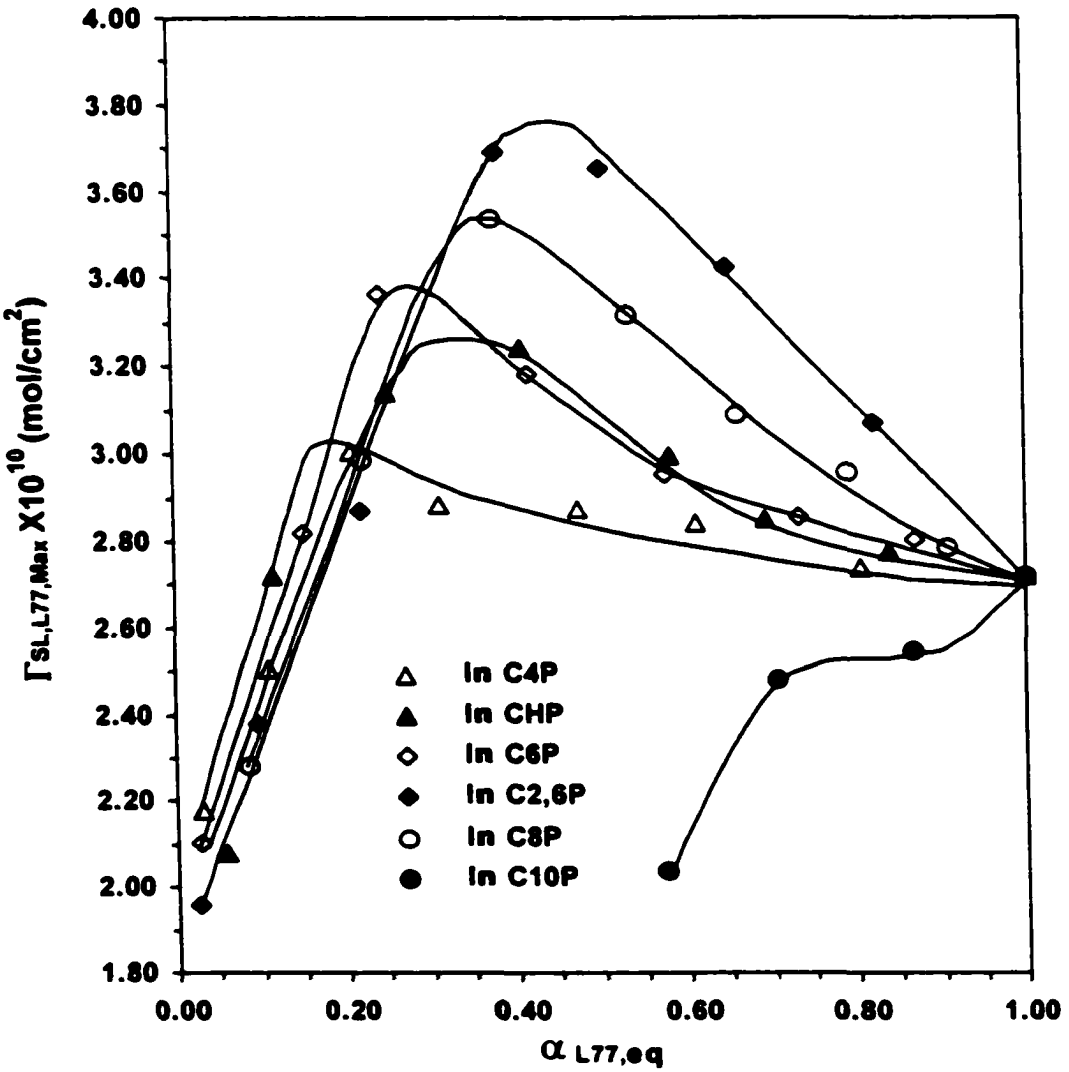

Figure A-6. Total Adsorption, $\Gamma_{SL,Total}$ vs. $\alpha_{L77,eq}$ for Mixtures of L77 and CnP at the Solid/Liquid Interface

(In Phosphate Buffer Solution, pH=7.00)

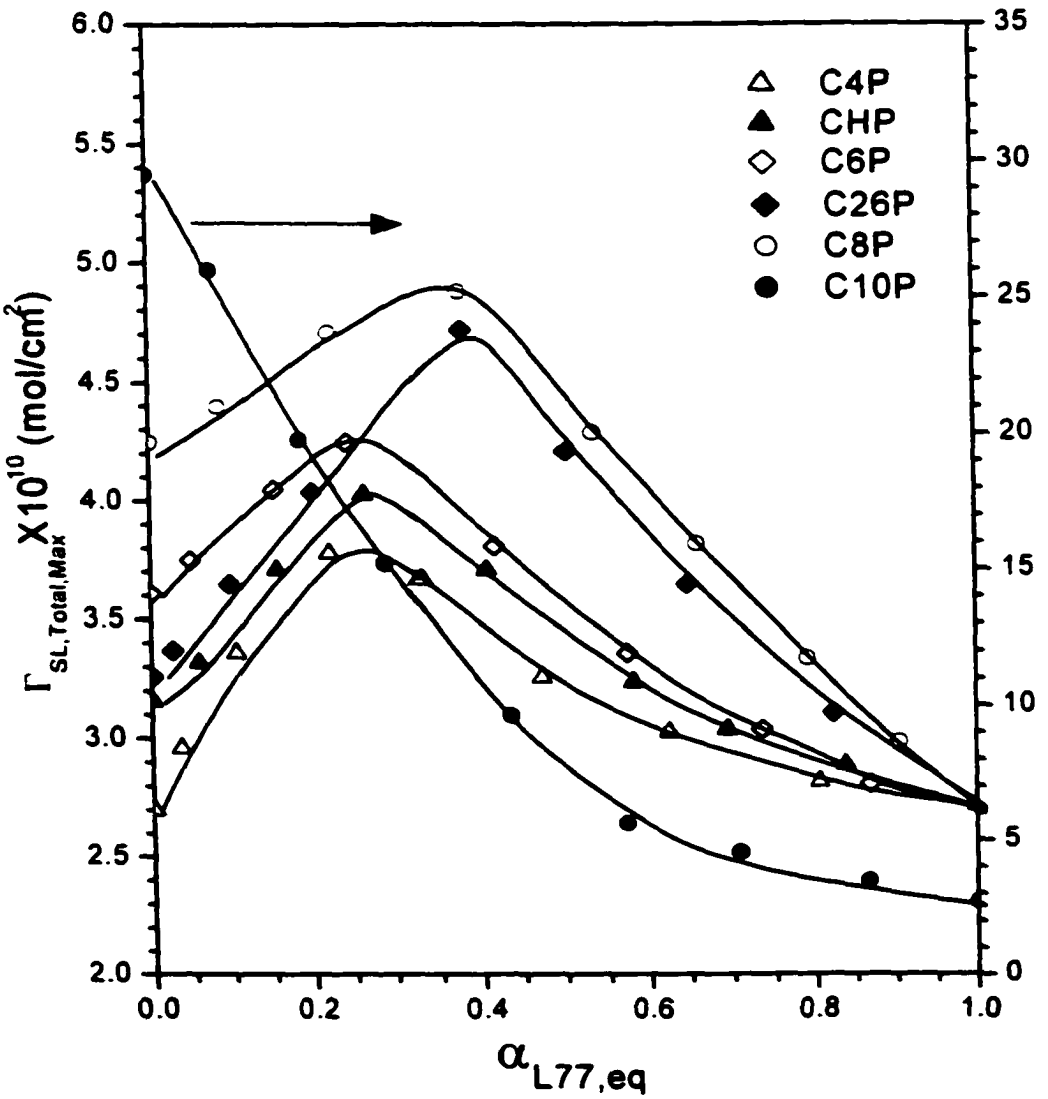

Table A-8. Adsorption Free Energies and Correlation Coefficients, $\Gamma_{SL,max}$, and A_{min} for L77 and Pyrrolidinones(CnP) on Powdered Polyethylene

(In Phosphate Buffer Solution, pH=7.00, 25 °C)

Compound	$\Delta G°_{ad}$ (kJ/mol)	$(C_{eq}/\Gamma_{SL}) \sim C_{eq}$ Correlation (R^2)	$\Gamma_{SL,\ max}$ (mol/cm^2)	A_{min} (Å^2)
L77	-40.9	1.000	2.72×10^{-10}	61.0
C4P	-33.2	0.998	2.70×10^{-10}	61.5
CHP	-34.0	0.994	3.16×10^{-10}	52.5
C6P	-38.4	1.000	3.61×10^{-10}	46.0
C2,6P	-33.9	0.994	3.26×10^{-10}	50.9
C8P	-38.7	0.998	4.25×10^{-10}	39.1
C10P	-31.8	0.802	a	N/A

[a] Non-Langmuir-type isotherm.

Table A-9. Adsorption Results of the Mixtures of L77 and C4P at the Powdered Polyethylene/Aqueous Solution Interface

(In Phosphate Buffer Solution, pH =7.00, 25 °C)

α_{L77} (Eq.)	$\Gamma_{SL,L77}$ (mol/cm^2)	$\Gamma_{SL,C4P}$ (mol/cm^2)	$\Gamma_{SL,Total}$ (mol/cm^2)	X_{L77} (Ads.layer)
0.029	2.18×10^{-10}	8.80×10^{-11}	3.06×10^{-10}	0.712
0.110	2.51×10^{-10}	8.40×10^{-11}	3.35×10^{-10}	0.751
0.209	3.01×10^{-10}	9.10×10^{-11}	3.92×10^{-10}	0.768
0.313	2.88×10^{-10}	8.00×10^{-11}	3.68×10^{-10}	0.781
0.473	2.87×10^{-10}	3.90×10^{-11}	3.26×10^{-10}	0.879
0.611	2.84×10^{-10}	1.40×10^{-11}	2.98×10^{-10}	0.953
0.805	2.74×10^{-10}	8.00×10^{-12}	2.82×10^{-10}	0.972
1.000	2.72×10^{-10}	0.000	2.72×10^{-10}	1.000

Table A-10. Adsorption Results of the Mixtures of L77 and CHP at the Powdered Polyethylene/Aqueous Solution Interface

(In Phosphate Buffer Solution, pH =7.00, 25 °C)

α_{L77} (Eq.)	$\Gamma_{SL,L77}$ (mol/cm^2)	$\Gamma_{SL,CHP}$ (mol/cm^2)	$\Gamma_{SL,Total}$ (mol/cm^2)	X_{L77} (Ads.layer)
0.058	2.08×10^{-10}	1.15×10^{-10}	3.23×10^{-10}	0.645
0.115	2.72×10^{-10}	9.50×10^{-11}	3.67×10^{-10}	0.741
0.253	3.14×10^{-10}	8.90×10^{-11}	4.13×10^{-10}	0.780
0.407	3.24×10^{-10}	5.10×10^{-11}	3.75×10^{-10}	0.864
0.581	2.99×10^{-10}	2.50×10^{-11}	3.24×10^{-10}	0.923
0.694	2.85×10^{-10}	1.00×10^{-11}	2.95×10^{-10}	0.966
0.838	2.78×10^{-10}	5.00×10^{-12}	2.83×10^{-10}	0.982
1.000	2.72×10^{-10}	0.000	2.72×10^{-10}	1.000

TableA-11. Adsorption Results of the Mixtures of L77 and C6P at the Powdered Polyethylene/Aqueous Solution Interface

(In Phosphate Buffer Solution, pH =7.00, 25 °C)

α_{L77} (Eq.)	$\Gamma_{SL,L77}$ (mol/cm^2)	$\Gamma_{SL,C6P}$ (mol/cm^2)	$\Gamma_{SL,Total}$ (mol/cm^2)	X_{L77} (Ads.layer)
0.028	2.10×10^{-10}	1.65×10^{-10}	3.75×10^{-10}	0.561
0.152	2.82×10^{-10}	1.13×10^{-11}	3.95×10^{-10}	0.713
0.243	3.37×10^{-10}	8.80×10^{-11}	4.25×10^{-10}	0.793
0.417	3.18×10^{-10}	5.40×10^{-11}	3.72×10^{-10}	0.854
0.574	2.96×10^{-10}	2.70×10^{-11}	3.23×10^{-10}	0.916
0.735	2.85×10^{-10}	9.00×10^{-12}	2.94×10^{-10}	0.970
0.868	2.80×10^{-10}	5.00×10^{-12}	2.85×10^{-10}	0.982
1.000	2.72×10^{-10}	0.000	2.72×10^{-10}	1.000

TableA-12. Adsorption Results of the Mixtures of L77 and C2,6P at the Powdered Polyethylene/Aqueous Solution Interface

(In Phosphate Buffer Solution, pH =7.00, 25 °C)

α_{L77} (Eq.)	$\Gamma_{SL,L77}$ (mol/cm^2)	$\Gamma_{SL,C2,6P}$ (mol/cm^2)	$\Gamma_{SL,Total}$ (mol/cm^2)	X_{L77} (Ads.layer)
0.025	1.96×10^{-10}	1.41×10^{-10}	3.37×10^{-10}	0.582
0.097	2.38×10^{-10}	1.20×10^{-10}	3.58×10^{-10}	0.665
0.220	2.87×10^{-10}	1.07×10^{-10}	3.94×10^{-10}	0.729
0.381	3.69×10^{-10}	1.03×10^{-10}	4.72×10^{-10}	0.782
0.503	3.65×10^{-10}	6.20×10^{-11}	4.27×10^{-10}	0.856
0.650	3.42×10^{-10}	3.30×10^{-11}	3.75×10^{-10}	0.912
0.823	3.07×10^{-10}	1.10×10^{-11}	3.18×10^{-10}	0.966
1.000	2.72×10^{-10}	0.000	2.72×10^{-10}	1.000

TableA-13. Adsorption Results of the Mixtures of L77 and C8P at the Powdered Polyethylene/Aqueous Solution Interface

(In Phosphate Buffer Solution, pH =7.00, 25 °C)

α_{L77} (Eq.)	$\Gamma_{SL,L77}$ (mol/cm^2)	$\Gamma_{SL,C8P}$ (mol/cm^2)	$\Gamma_{SL,Total}$ (mol/cm^2)	X_{L77} (Ads.layer)
0.085	2.28×10^{-10}	2.11×10^{-10}	4.39×10^{-10}	0.520
0.222	2.98×10^{-10}	1.68×10^{-10}	4.66×10^{-10}	0.640
0.375	3.54×10^{-10}	1.34×10^{-10}	4.88×10^{-10}	0.725
0.535	3.32×10^{-10}	9.10×10^{-11}	4.23×10^{-10}	0.785
0.660	3.09×10^{-10}	5.60×10^{-11}	3.65×10^{-10}	0.847
0.791	2.96×10^{-10}	3.10×10^{-11}	3.27×10^{-10}	0.905
0.906	2.79×10^{-10}	2.00×10^{-11}	2.99×10^{-10}	0.933
1.000	2.72×10^{-10}	0.000	2.72×10^{-10}	1.000

TableA-14. Adsorption Results of the Mixtures of L77 and C10P at the Powdered Polyethylene/Aqueous Solution Interface

(In Phosphate Buffer Solution, pH =7.00, 25 °C)

α_{L77} (Eq.)	$\Gamma_{SL,L77}$ (mol/cm^2)	$\Gamma_{SL,C10P}$ (mol/cm^2)	$\Gamma_{SL,Total}$ (mol/cm^2)	X_{L77} (Ads.layer)
0.077	6.20×10^{-11}	2.60×10^{-9}	2.66×10^{-9}	0.023
0.185	8.40×10^{-11}	1.98×10^{-9}	2.06×10^{-9}	0.041
0.307	1.01×10^{-10}	1.50×10^{-9}	1.60×10^{-9}	0.063
0.434	1.22×10^{-10}	8.38×10^{-10}	9.60×10^{-10}	0.127
0.572	2.04×10^{-10}	3.61×10^{-10}	5.65×10^{-10}	0.361
0.707	2.48×10^{-10}	2.07×10^{-11}	4.55×10^{-10}	0.546
0.865	2.55×10^{-10}	9.30×10^{-11}	3.48×10^{-10}	0.733
1.000	2.72×10^{-10}	0.000	2.72×10^{-10}	1.000

4.3 Adsorption at the Air/Solid Interface (Γ_{SA})

As discussed above, although adsorption of surfactant at the air/liquid and solid/liquid interfaces is very important in the process of spreading, the adsorption of surfactant at the solid/air interface may also play an important role in the spreading, since adsorption at the solid/air interface in such manner as to decrease interfacial tension at the air/solid interface will decrease the value of the spreading coefficient and consequently will be unfavorable to the tendency to spread. It has not been studied much, due to the difficulty in determining the adsorption at the solid/air interface. To date, only one publication dealing with the adsorption of surfactant at the solid/air interface has been found. Tiberg, F. and Cazabat, A. M.[38] reported that spreading of nonionic siloxane poly-(ethylene oxide) surfactants at the solid-air interface occurs through an autophobic thin precursor film growing at the foot of the nonwetting main drop. In the current study, the adsorption of L77, N-alkyl-pyrrolidinones(CnP) and their mixtures onto the polyethylene/air interface, obtained through use of Equation(37): $\Gamma_{SA} = \Gamma_{SL} - \frac{1}{RT} \times \frac{d(\gamma_{LA} \cos\theta)}{d\ln C}$, and the assumption of the applicability of adsorption on the powdered polyethylene to adsorption on a planar film of the same polyethylene, is described.

Contact angles of L77, the pyrrolidinones, and their mixed solutions on the planar polyethylene surface were measured. The adhesion tension, $\gamma_{LA}\cos\theta$ was plotted versus logC to get the slope of the plot. The plots for L77, CnPs and their mixtures are shown in Figures B–7 to B–12. The related experimental data are listed in Tables B–1 to B–49. The values of Γ_{SA}, calculated by use of equation (37), together with the slope of $\gamma_{LA}\cos\theta$ vs. logC plots and the valuesof Γ_{SL}(expt.) and Γ_{SL}(SA=0) for these the mixtures of L77 and CnPs, are listed in Tables A–15 to A–20.

(i) L77–C4P Mixtures: Figure B–7 shows plots of $\gamma_{LA}\cos\theta$ vs. logC of L77, C4P and their mixed solutions with different mole fractions of L77. The results of adsorption at the air/polyethylene interface are listed in Table A–15. The results show that the adsorption of L77 and the mixtures at the air/polyethylene interface is smaller by one order of magnitude than that at the air/aqueous solution and solid/aqueous solution interfaces. For individual C4P, its adsorption at the air/solid interface is smaller by two orders of magnitude. This result is consistent with the concept that, on solids with low surface energies such as Parafilm, paraffin, Teflon and polyethylene, $d\gamma_{SA}/d\ln C=0$ for surfactants with hydrocarbon chains (hydrophobic groups that can not lower the surface free energy of the solid), and from Equation(37), since $\Gamma_{SA}=0$,

$\Gamma_{SL} = \frac{1}{nRT}\frac{d(\gamma_{LA}\cos\theta)}{d\ln C}$. But $d\gamma_{SA}/d\ln C \neq 0$ for surfactants with dimethylsiloxane or perfluoralkyl hydrophobic groups that can lower the surface free energy of polyethylene. Therefore, only the values of $(\Gamma_{SL} - \Gamma_{SA})$ can be calculated from $\frac{1}{nRT}\frac{d(\gamma_{LA}\cos\theta)}{d\ln C}$ for those systems.

$\Gamma_{SL}(SA=0)$, adsorptions of L77, C4P and their mixtures with various α_{L77} at the polyethylene substrate/aqueous solution interface, calculated using $\Gamma_{SL} = \frac{1}{nRT}\frac{d(\gamma_{LA}\cos\theta)}{d\ln C}$, based upon the assumption that $\Gamma_{SA}=0$, are also listed in Table A–15. In the table, only for C4P ($\alpha_{L77}=0.000$) solution are $\Gamma_{SL}(SA=0)$ values and the experimental results, Γ_{SL}[expt.], obtained from the adsorption isotherms, very close to each other. The derivation is only 1.5% for C4P, which is less than the experimental error (see Appendix I for analysis of experimental errors). Therefore, the assumption that $\Gamma_{SA}=0$ is valid for C4P. On the other hand, there is a significant difference between Γ_{SL}[expt.] and Γ_{SL}[SA=0] for L77 and the L77–C4P mixtures, indicating that the assumption of $\Gamma_{SA}=0$ is not valid for L77 and L77–C4P mixtures at the air/polyethylene interface.

(ii) L77–CHP Mixtures: Figure B–8 shows plots of $\gamma_{LA}\cos\theta$ vs. logC of L77, CHP and their mixed solutions with different mole fractions of L77. The

results of adsorption at the air/polyethylene interface are listed in Table A–16. The adsorption of L77 and the mixtures at the air/solid interface is smaller by one order of magnitude than that at the air/aqueous solution and solid/aqueous solution interfaces. For CHP, its adsorption at the air/solid interface is 0. These results are consistent with the considerations discussed before.

Results of Γ_{SL}[SA=0] for L77, CHP and their mixtures with various α_{L77} at the polyethylene substrate/aqueous solution interface are also listed in Table A–16. In the table, only for CHP (α_{L77}=0.000) solution are Γ_{SL}[SA=0] results and the experimental results, Γ_{SL}[expt.], obtained from the adsorption isotherms, exactly the same. Therefore, the assumption that Γ_{SA}=0 is also valid for CHP. On the other hand, there is a significant difference between Γ_{SL}[expt.] and Γ_{SL}[SA=0] for L77 and the mixtures of L77 and CHP.

(iii) L77–C6P Mixtures: Figure B–9 shows plots of $\gamma_{LA}\cos\theta$ vs. logC of L77, C6P and their mixed solutions with different mole fractions of L77. The results of adsorption at the air/polyethylene interface are listed in Table A–17. The results show that the adsorption of L77 and the mixtures at the air/solid interface is smaller by one order of magnitude than that at the air/aqueous solution and solid/aqueous solution interfaces. For C6P, its adsorption at the

air/solid interface is smaller by two orders of magnitude. These results are consistent with the considerations discussed previously.

Results of Γ_{SL}[SA=0] for L77, C6P and their mixtures with various α_{L77} at the polyethylene substrate/aqueous solution interface are also listed in Table A–17. In the table, only for C6P (α_{L77}=0.000) solution are Γ_{SL}[SA=0] results and the experimental results, Γ_{SL}[expt.], obtained from the adsorption isotherms, almost the same. Therefore, the assumption that Γ_{SA}=0 is also valid for C6P. On the other hand, there is a significant difference between Γ_{SL}[expt.] and Γ_{SL}[SA=0] for L77 and the mixtures of L77 and C6P.

(iv) L77–C2,6P Mixtures: Figure B–10 shows plots of $\gamma_{LA}\cos\theta$ vs. logC of L77, C2,6P and their mixed solutions with different mole fractions of L77. The results of adsorption at the air/polyethylene interface are listed in Table A–18. From the results, it can be found that the adsorption of L77 and the mixtures at the air/solid interface is smaller by one order of magnitude than that at the air/aqueous solution and solid/aqueous solution interfaces. For C2,6P and the mixture with α_{L77}=0.025, their adsorptions at the air/solid interface are smaller by two orders of magnitude. These results are consistent with the considerations as discussed previously.

Results of Γ_{SL}[SA=0] for L77, C2,6P and their mixtures with various α_{L77} at the polyethylene substrate/aqueous solution interface are also listed in Table A–18. In the table, it can be found that for C2,6P (α_{L77}=0.000) and the mixture with α_{L77}=0.025, the values of Γ_{SL}[SA=0] and experimental results, Γ_{SL}[expt.], obtained from the adsorption isotherms, are almost the same. Therefore, the assumption that Γ_{SA}=0 is also valid for C2,6P and the mixture containing mainly C2,6P. On the other hand, there is a significant difference between Γ_{SL}[expt.] and Γ_{SL}[SA=0] for L77 and other mixtures.

(v) L77–C8P Mixtures: Figure B–11 shows plots of $\gamma_{LA}\cos\theta$ vs. logC of L77, C8P and their mixed solutions with different mole fractions of L77. The results of adsorption at the air/polyethylene interface are listed in Table A–19. From the results, it can be found that the adsorption of L77 and the mixtures at the air/polyethylene interface is smaller by one order of magnitude than that at the air/aqueous solution and solid/aqueous solution interfaces. For C8P, its adsorption at the air/solid interface is smaller by two orders of magnitude. These results are also consistent with the considerations discussed previously.

Results of Γ_{SL}[SA=0] for L77, C8P and their mixtures with various α_{L77} at the polyethylene substrate/aqueous solution interface are also listed in Table A–19. In the table, it can be found that the values of Γ_{SL}[SA=0] and

experimental results, Γ_{SL}[expt.], obtained from the adsorption isotherms, are almost the same only for C8P solution (α_{L77}=0.000). Therefore, the assumption that Γ_{SA}=0 is only valid for C8P. On the other hand, there is a significant difference between Γ_{SL}[expt.] and Γ_{SL}[SA=0] for L77 and the mixtures.

(vi) L77–C10P Mixtures: Figure B–12 shows plots of $\gamma_{LA}\cos\theta$ vs. logC of L77, C10P and their mixed solutions with various mole fractions of L77. The results of adsorption at the air/polyethylene interface are listed in Table A–20. From the results, the adsorptions of C10P and the mixtures at the air/solid interface, except for the mixture with α_{L77}=0.867, are too large to be believable. The reason may be that, because the adsorption of C10P at the solid/aqueous solution interface is not Langmuir type, the calculation of Γ_{SA} by equation(37) is not correct.

Summary: The adsorption of L77 and its mixtures with N-alkyl-pyrrolidinones at the air/polyethylene interface is smaller than that at the air/aqueous solution and polyethylene/aqueous solution interfaces by one order of magnitude, but it is not zero. This is to be expected in the case of L77 and its mixtures with the pyrrolidinones, since dimethyl siloxane hydrophobic groups can lower the free energy of the polyethylene surface.

For C10P, the adsorption at the air/solid interface are too large to be believable. The reason may be that, because the adsorption of C10P at the polyethylene/aqueous solution interface is not Langmuir type, the calculation of Γ_{SA} by the Gibbs equation, which is based upon monolayer adsorption at the interface, is not correct.

Table A-15. Adsorption Results of the Mixtures of L77 and C4P at the Air/Polyethylene Interface($\Gamma_{SA,Total}$)

(In Phosphate Buffer Solution, pH =7.00, 25 °C)

α_{L77} (Ini.)	$\frac{d(\gamma_{LA}\cos\theta)}{d(\log C)}$	Γ_{SL} (expt.) (mol/cm^2)	Γ_{SL}(SA=0) (mol/cm^2)	$\Gamma_{SA,total}$ (mol/cm^2)
1.000	14.8	2.72×10^{-10}	2.59×10^{-10}	1.30×10^{-11}
0.805	15.2	2.82×10^{-10}	2.66×10^{-10}	1.60×10^{-11}
0.611	15.8	2.98×10^{-10}	2.77×10^{-10}	2.10×10^{-11}
0.475	16.3	3.26×10^{-10}	2.85×10^{-10}	4.10×10^{-11}
0.313	17.8	3.68×10^{-10}	3.12×10^{-10}	5.60×10^{-11}
0.209	19.1	3.92×10^{-10}	3.34×10^{-10}	5.80×10^{-11}
0.110	17.2	3.35×10^{-10}	3.01×10^{-10}	3.40×10^{-11}
0.029	15.6	3.06×10^{-10}	2.73×10^{-10}	3.30×10^{-11}
0.000	15.2	2.70×10^{-10}	2.66×10^{-10}	0.40×10^{-11}

Table A-16. Adsorption Results of the Mixtures of L77 and CHP at the Air/Polyethylene Interface($\Gamma_{SA,Total}$)

(In Phosphate Buffer Solution, pH =7.00, 25 °C)

α_{L77} (Ini.)	$\frac{d(\gamma_{LA}\cos\theta)}{d(\log C)}$	Γ_{SL} (expt.) (mol/cm^2)	Γ_{SL}(SA=0) (mol/cm^2)	$\Gamma_{SA,total}$ (mol/cm^2)
1.000	14.8	2.72×10^{-10}	2.59×10^{-10}	1.30×10^{-11}
0.838	15.5	2.83×10^{-10}	2.71×10^{-10}	1.20×10^{-11}
0.694	16.0	2.95×10^{-10}	2.80×10^{-10}	1.50×10^{-11}
0.581	16.8	3.24×10^{-10}	2.94×10^{-10}	3.00×10^{-11}
0.407	18.7	3.75×10^{-10}	3.27×10^{-10}	4.80×10^{-11}
0.253	20.3	4.03×10^{-10}	3.55×10^{-10}	4.80×10^{-11}
0.115	18.4	3.67×10^{-10}	3.22×10^{-10}	4.50×10^{-11}
0.058	17.7	3.23×10^{-10}	3.10×10^{-10}	1.30×10^{-11}
0.000	17.4	3.05×10^{-10}	3.05×10^{-10}	0.000

Table A-17. Adsorption Results of the Mixtures of L77 and C6P at the Air/Polyethylene Interface($\Gamma_{SA,Total}$)

(In Phosphate Buffer Solution, pH =7.00, 25 °C)

α_{L77} (Ini.)	$\frac{d(\gamma_{LA}\cos\theta)}{d(\log C)}$	Γ_{SL} (expt.) (mol/cm^2)	Γ_{SL} (SA=0) (mol/cm^2)	$\Gamma_{SA,total}$ (mol/cm^2)
1.000	14.8	2.72×10^{-10}	2.59×10^{-10}	1.30×10^{-11}
0.868	15.3	2.85×10^{-10}	2.68×10^{-10}	1.70×10^{-11}
0.735	15.7	2.94×10^{-10}	2.75×10^{-10}	1.90×10^{-11}
0.574	17.2	3.23×10^{-10}	3.01×10^{-10}	2.20×10^{-11}
0.417	19.3	3.71×10^{-10}	3.38×10^{-10}	3.30×10^{-11}
0.243	21.2	4.25×10^{-10}	3.71×10^{-10}	5.40×10^{-11}
0.152	21.4	3.95×10^{-10}	3.75×10^{-10}	2.00×10^{-11}
0.028	20.5	3.75×10^{-10}	3.59×10^{-10}	1.60×10^{-11}
0.000	20.9	3.71×10^{-10}	3.66×10^{-10}	0.50×10^{-11}

Table A-18. Adsorption Results of the Mixtures of L77 and C2,6P at the Air/Polyethylene Interface($\Gamma_{SA,Total}$)

(In Phosphate Buffer Solution, pH =7.00, 25 °C)

α_{L77} (Ini.)	$\frac{d(\gamma_{LA}\cos\theta)}{d(\log C)}$	Γ_{SL} (expt.) (mol/cm^2)	Γ_{SL} (SA=0) (mol/cm^2)	$\Gamma_{SA,total}$ (mol/cm^2)
1.000	14.8	2.72×10^{-10}	2.59×10^{-10}	1.30×10^{-11}
0.825	16.6	3.18×10^{-10}	2.91×10^{-10}	2.70×10^{-11}
0.651	18.5	3.75×10^{-10}	3.24×10^{-10}	5.10×10^{-11}
0.501	20.9	4.27×10^{-10}	3.66×10^{-10}	6.10×10^{-11}
0.381	22.8	4.72×10^{-10}	3.99×10^{-10}	7.30×10^{-11}
0.220	21.5	3.94×10^{-10}	3.76×10^{-10}	1.80×10^{-11}
0.096	19.7	3.58×10^{-10}	3.45×10^{-10}	1.30×10^{-11}
0.025	18.8	3.37×10^{-10}	3.29×10^{-10}	0.80×10^{-11}
0.000	18.4	3.26×10^{-10}	3.22×10^{-10}	0.40×10^{-11}

Table A-19. Adsorption Results of the Mixtures of L77 and C8P at the Air/Polyethylene Interface($\Gamma_{SA,Total}$)

(In Phosphate Buffer Solution, pH =7.00, 25 °C)

α_{L77} (Ini.)	$\frac{d(\gamma_{LA}\cos\theta)}{d(\log C)}$	Γ_{SL} (expt.) (mol/cm^2)	Γ_{SL} (SA=0) (mol/cm^2)	$\Gamma_{SA,total}$ (mol/cm^2)
1.000	14.8	2.72×10^{-10}	2.59×10^{-10}	1.30×10^{-11}
0.906	15.7	2.99×10^{-10}	2.75×10^{-10}	2.40×10^{-11}
0.791	16.9	3.27×10^{-10}	2.96×10^{-10}	3.10×10^{-11}
0.660	18.8	3.65×10^{-10}	3.29×10^{-10}	3.60×10^{-11}
0.535	21.9	4.23×10^{-10}	3.83×10^{-10}	4.00×10^{-11}
0.375	23.6	4.88×10^{-10}	4.13×10^{-10}	7.50×10^{-11}
0.222	23.8	4.66×10^{-10}	4.17×10^{-10}	4.90×10^{-11}
0.085	23.6	4.39×10^{-10}	4.13×10^{-10}	2.60×10^{-11}
0.000	24.2	4.32×10^{-10}	4.24×10^{-10}	0.80×10^{-11}

Table A-20. Adsorption Results of the Mixtures of L77 and C10P at the Air/Polyethylene Interface($\Gamma_{SA,Total}$)

(In Phosphate Buffer Solution, pH =7.00, 25 °C)

α_{L77} (Ini.)	$\frac{d(\gamma_{LA}\cos\theta)}{d(\log C)}$	Γ_{SL} (expt.) (mol/cm^2)	Γ_{SL} (SA=0) (mol/cm^2)	$\Gamma_{SA,total}$ (mol/cm^2)
1.000	14.8	2.72×10^{-10}	2.59×10^{-10}	1.30×10^{-11}
0.867	16.7	3.48×10^{-10}	2.92×10^{-10}	5.60×10^{-11}
0.707	18.2	4.55×10^{-10}	3.19×10^{-10}	1.36×10^{-10}
0.575	19.3	5.65×10^{-10}	3.38×10^{-10}	2.27×10^{-10}
0.435	21.4	9.60×10^{-10}	3.75×10^{-10}	5.85×10^{-10}
0.307	23.5	16.0×10^{-10}	4.11×10^{-10}	1.19×10^{-9}
0.186	24.1	20.6×10^{-10}	4.22×10^{-10}	1.64×10^{-9}
0.077	24.4	26.6×10^{-10}	4.27×10^{-10}	2.23×10^{-9}
0.000	25.6	30.5×10^{-10}	4.48×10^{-10}	2.60×10^{-9}

CHAPTER 4

RESULTS AND DISCUSSION (Continued)

Part II

Superspreading and Interactions

4.4 Superspreading

4.4.1 Spreading Factor(SF)

In order to measure the spreading ability of a surfactant solution on a solid substrate, a parameter, called the spreading factor: (SF), was used. It is defined as the ratio of the spreading area of the surfactant solution to that of the solvent of the same volume. When such a spreading factor is larger than 25, the spreading is usually called "superspreading".

4.4.2 Synergism in Superspreading

In measurements of the spreading, a series of solutions (total concentration always 1.0g/L) with different %wt. replacement of trisiloxane L77 by pyrrolidinones were used. In order to make the results more convenient for comparison with other results, such as adsorption at the solid/liquid interface, the mass percent of replacement of L77 by pyrrolidinone was converted to the mole fraction of L77 in the mixture. Plots of spreading factor (SF) vs. mole fraction of L77 (α_{L77}) for aqueous mixtures of L77 and pyrrolidinones on the polyethylene substrate are shown in Figure A-7. The points at α_{L77} = 0.000 and α_{L77} = 1.000 correspond to individual N-alkyl-pyrrolidinone in buffer solution and individual L77 in buffer solution, respectively.

The data in Figure A–7 show that all the pyrrolidinones (C4P, CHP, C6P, C2,6P, C8P and C10P) in buffer solution have very small spreading factors (2 ~3), meaning that the spreading abilities of all the pyrrolidinones, by themselves, on polyethylene film are very poor. On the other hand, the trisiloxane, L77, in buffer solution has a very large spreading factor, around 150, indicating its superspreading ability on the polyethylene film. There is a small difference among the measured spreading factors for L77 because they were measured on different days with different humidity and temperature.

Most significant in Figure A–7 is the finding of a synergistic effect in the spreading of the mixtures of trisiloxane L77 and certain pyrrolidinones. From the plots of spreading factor (SF) vs. α_{L77}, one can see that the mixtures of L77 with C4P, CHP, C6P, C2,6P or C8P show a nonideal spreading on the polyethylene substrate. When the mole fraction of L77 is larger than about 0.25, the spreading factors of the mixed solutions are larger than that of the L77 solution itself.

The effectiveness of superspreading enhancement by the pyrrolidinone (the maximum SF value of the mixture) is different for the different pyrrolidinones. SF_{max} = 164 for the mixture with C4P; 180 with CHP; 210 with C6P; 213 with C8P; 234 with C2,6P. Therefore, the effectiveness of the pyrrolidinones in enhancing the spreading of trisiloxane L77 on the polyethylene substrate decreases in the order: C2,6P > C8P, C6P > CHP > C4P. It is noteworthy that the mixtures of L77 with C10P show no synergistic effect at all; the plot of spreading factor vs. α_{L77} for the mixtures of L77 with C10P is almost linear over the whole range of mole fractions of L77. It appears that spreading of the mixture of L77 and C10P on the polyethylene film is ideal.

In order to explain these results, the effect on the spreading coefficient, $S_{L/S} = \gamma_{SA} - (\gamma_{SL} + \gamma_{LA})$ (equation (1)) of the replacement of some of the L77 in the spreading solution by N-alkyl pyrrolidinone was determined.

4.4.3 Change in the Spreading Coefficient ($\Delta S_{L/S}$)

The change in the spreading coefficient of L77 upon the replacement of some of it by N-alkyl pyrrolidinone is given by the relationship(Equations 63–66, Chapter 2):

$$\Delta S_{L/S} = S_{L/S}^{Mix} - S_{L/S}^{L77} = -\Delta\gamma_{LA} + \Delta\pi_{SL} - \Delta\pi_{SA}$$

where,

$$\Delta\gamma_{LA} = \gamma_{LA}^{Mix} - \gamma_{LA}^{L77}$$

$$\Delta\pi_{SL} = \pi_{SL}^{Mix} - \pi_{SL}^{L77}$$

$$\Delta\pi_{SA} = \pi_{SA}^{Mix} - \pi_{SA}^{L77}$$

4.4.3.1 Results of $\Delta\gamma_{LA}$

According to equation(64) and the previous discussion, the value of $(\gamma_{LA}^{Mix} - \gamma_{LA}^{L77})$ can be obtained directly from the plots of γ_{LA}^{Mix} vs. logC and γ_{LA}^{L77} vs. logC. The plots for systems of L77–C4P, L77–CHP, L77–C6P, L77–C2,6P, L77–C8P and L77–C10P are shown in Figures B–1 to B–6. From the figures, it can seen that the surface tension of mixture solutions for all systems is higher that of L77 itself at the same concentration. The surface tension always increases with the decrease in the mole fraction of L77 when concentration (or log C) is the same.

An example of the determination of $\Delta\gamma_{LA}$ is shown in Figure A–8, the plot of γ_{LA} vs. logC for L77 itself and the mixed surfactant solution containing C8P at a mole fraction of α_{L77}=0.375. Since the concentrations (1.0g/L) used in the measurement of their superspreading is above their C.M.C.s, both γ_{LA}^{L77} and γ_{LA}^{Mix} are constant, which are 20.5 mN/m and 22.3 mN/m, respectively, and consequently, the value of $(\gamma_{LA}^{Mix} - \gamma_{LA}^{L77})$ is a constant, equal to 1.8 mN/m. All results of $\Delta\gamma_{LA}$ for these systems are listed in Tables A–21 to A–26. All $\Delta\gamma_{LA}$ values are positive, which means that the surface tension of the mixed solution above the C.M.C. of L77 is always greater than that of the L77 solution over all the concentrations used in the measurements. There is no synergistic effect at the air/aqueous solution interface over whole concentration range.

4.4.3.2 Results of $\Delta\pi_{SL}$

Unlike $\Delta\gamma_{LA}$ that can be obtained directly from the experimental data, the reduction of interfacial tension at the solid/aqueous solution interface can only be obtained indirectly from their adsorption isotherms. The method for calculating $\Delta\pi_{SL}$ is as discussed in Chapter 2.

The plots of $\Gamma_{SL,Total}$ vs. lnC for systems of L77–C4P, L77–CHP, L77–C6P, L77–C2,6P, L77–C8P and L77–C10P are shown in Figures B–55 to

B–60. In order to calculate π_{SL} by use of Equation (69), $\pi_{SL} = RT\int_0^C \Gamma_{SL} \cdot d\ln C$, these curves are fitted by use of the software of Origin®6.0. The fitted polynomial functions are listed in Appendix II. The area enclosed by the curves and the X axis is then calculated through the fitted function of the curves. It should be noted that although adsorption of surfactants at the solid/liquid interface cannot be zero if the equilibrium concentration of surfactants at bulk solution phase is not zero, the resultant error in the calculated areas is insignificant.

Plots of π_{SL}^{L77}, π_{SL}^{CnP} and π_{SL}^{Mix} vs. lnC for all of the above systems are shown in Figures B–61 to B–66. Values of $\Delta\pi_{SL}$ are obtained from these figures in the following manner(the mixture of L77 and C8P with α_{L77}=0.375 is used as an example): In Figure A–9, at the C.M.C. of L77 (ln(CMC). = –8.94), π_{SL}^{Mix} and π_{SL}^{L77} equal 32.6 mN/m and 22.5 mN/m, respectively. Thus, the reduction in interfacial tension ($\pi_{SL}^{Mix} - \pi_{SL}^{L77}$) for this mixture at the C.M.C. of L77 equals 10.1 mN/m. This means that the addition of C8P to the aqueous solution of L77 at a mole fraction of α_{L77}=0.375 results in an additional decrease in amount of 10.1 mN/m in the interfacial tension at the solid/liquid interface. It is of benefit to the spreading of the aqueous solution on the polyethylene surface because it will make the spreading coefficient ($S_{L/S}$) of the solution more

positive. Values of $\Delta\pi_{SL}$ for L77 and its mixtures with C4P, CHP, C6P, C2,6P C8P and C10P at different mole fractions of L77 are listed in Tables A–21 to A–26. Except for initial α_{L77} values of 0.115 or less, the $\Delta\pi_{SL}$ values for the L77 mixtures with C4P, CHP, C6P, C2,6P and C8P are all positive, indicating reduction of the solid/liquid interfacial tension. By contrast, all the L77 mixtures with C10P (Table A–26) show negative values of $\Delta\pi_{SL}$, indicating increase in the solid/liquid interfacial tension.

4.4.3.3 Results of $\Delta\pi_{SA}$

As discussed in Chapter 2, π_{SA} can be calculated via equation(72), $\pi_{SA} = RT\int_0^C \Gamma_{SA} \cdot d\ln C$, where Γ_{SA} is the adsorption at the air/solid interface, C is the equilibrium concentration of the surfactant in the solution phase below the C.M.C.. As discussed in the previous part of this chapter, Γ_{SA} for L77, pyrrolidinones and all their mixtures is smaller by one or two orders of magnitude than that at the air/aqueous solution interface (Γ_{LA}) or at the solid/aqueous solution interface (Γ_{SL}) at all surfactant concentrations. Since, from the above equation, π_{SA} is directly proportional to Γ_{SA}, it can be concluded that π_{SA} will be smaller by one order of magnitude than π_{LA} and π_{SL}, and, consequently, that $\Delta\pi_{SA}$ must be smaller by one order of magnitude than $\Delta\pi_{LA}$

and $\Delta\pi_{SL}$. Therefore, compared with $\Delta\pi_{LA}$ and $\Delta\pi_{SL}$, the effect of $\Delta\pi_{SA}$ on the change in the spreading coefficient ($S_{L/S}^{Mix} - S_{L/S}^{L77}$) is negligible.

Consequently, from Equation (63), we have:

$$S_{L/S}^{Mix} - S_{L/S}^{L77} \approx \Delta\pi_{SL} - \Delta\gamma_{LA} \qquad (83)$$

The results of ($S_{L/S}^{Mix} - S_{L/S}^{L77}$) for L77 and the mixtures with C4P, CHP, C6P, C2,6P, C8P and C10P at different mole ratios of L77 are also listed in Tables A–21 to A–26. From the data in those tables, the increase in the value of the interfacial pressure at polyethylene/aqueous solution interface ($\Delta\pi_{SL}$) upon the addition of the N-alkylpyrrolidinone is the dominant factor in increasing the value of the spreading coefficient.

4.4.3.4 Relationship between Spreading Coefficient($S_{L/S}$) and Spreading Factor(SF)

From Tables A–21 to A–26, it is seen that the spreading coefficients of the mixed solutions are greater than that of the solution of L77 by itself for the mixtures with C4P, CHP, C6P, C2,6P and C8P when the mole fraction of L77 is larger than a certain value, e.g., 0.313 for L77–C4P, 0.253 for L77–CHP, 0.152 for L77–C6P, 0.220 for L77–C2,6P, 0.375 for L77–C8P. That means that if the

pyrrolidinone, except for C10P, is mixed with L77 at a proper mole fraction, it can make the spreading coefficient of the mixture more positive than that of the L77 by itself. That is, the free energy decrease per unit area of the mixed solution upon spreading (Equation 1) becomes larger than that of the solution of L77 by itself. Consequently, the solution will spread on the polyethylene substrate to a larger area than that obtained with L77 by itself. The larger the value of $(S_{L/S}^{Mix} - S_{L/S}^{L77})$, the more positive the spreading coefficient of the mixed solution, and the greater should be the spreading area. It has been shown that the spreading coefficient is proportional to the spreading rate of pure liquids on homogeneous smooth solids[143]. If we can assume that this applies also to solutions, and since there was a constant amount of spreading time (3 minutes) used in this study, the larger the (positive) spreading coefficient, the larger will be the spreading area.

From the values of $(S_{L/S}^{Mix} - S_{L/S}^{L77})$ in Tables A–21 to A–26, the order of maximum increase in the spreading coefficient by the pyrrolidinones is: C8P > C2,6P > C6P > CHP > C4P. This is almost the same as the order of their maximum enhancement of the spreading factor, C2,6P > C8P > C6P > CHP > C4P, shown in Figure A–7. In view of the very different experimental techniques involved in the calculation of the values of $(S_{L/S}^{Mix} - S_{L/S}^{L77})$ and the measurement of the spreading factors, the data correlate well with each other.

It is difficult to compare spreading coefficient($S_{L/S}$) with spreading factor(SF) directly because the values of $S_{L/S}$ itself are not available at present. However, the relationship between the change in spreading coefficient ($S^{Mix}_{L/S} - S^{L77}_{L/S}$) and the change in spreading factor(SF_{mix}–SF_{L77}) can be found from the above results, and it is shown in Figure A–10. There is a good linear relationship between them. The correlation coefficients (R^2) for all systems are very close to 1. That means the parameter of $\Delta S_{L/S}$ for a mixed spreading solution can be replaced by the parameter of ΔSF, and the latter one can be obtained easily by experiment.

4.5 Interactions between Molecules of L77 and Pyrrolidinoes

In order to investigate the cause of the changes in tensions at the various interfaces produced by replacement of L77 by N-alkyl pyrrolidinone, interaction parameters (β^{σ}) at the various interfaces were determined.

4.5.1 Interaction Parameters at the Air/Liquid Interface (β^{σ}_{LA})

Molecular interactions between L77 and pyrrolidinones C4P, C6P, CHP, C2,6P, C8P and C10P at the air/aqueous solution interface at pH=7.00 in phosphate buffer were evaluated by use of Equations (73) and (74):

$$\frac{X_1^2 \ln(\alpha C_{12} / X_1 C_1^0)}{(1-X_1)^2 \ln[(1-\alpha)C_{12}/(1-X_1)C_2^0]} = 1, \qquad \beta^{\sigma}_{LA} = \frac{\ln(\alpha C_{12} / X_1 C_1^0)}{(1-X_1)^2}$$

Determinations of the values of C_1^0, C_2^0 and C_{12} are shown in Figure A–8. Results of the molecular interaction parameter, β_{LA}^{σ}, at the air/liquid interface, between L77 and pyrrolidinones are listed in Table A–27.

From the results, it appears that the mixtures all exhibit very weak interactions at the air/aqueous solution interface. The L77–C10P mixture shows a very weak repulsion between the two surfactant molecules. This is consistent with the $\Delta\gamma_{LA}$ results listed in Tables A–21 to A–26, which indicate that there is no synergism at the air/aqueous solution interface. In addition, the results of minimal area per molecule at the air/aqueous solution interface, $A_{LA,min}$, listed in Tables A–2 to A–7, are also evidence for the very weak interactions between L77 and pyrrolidinones. The area per molecule for all mixtures is between L77 and the individual pyrrolidinone, indicating that there is no significant attractive or repulsive interaction between L77 and pyrrolidinones at the air/aqueous solution interface. Furthermore, these results can be verified by comparing these mixtures with the nonionic mixture of $C_{12}(OE)_8OH$–$C_{12}(OE)_3OH$[144]. In this binary mixture, both surfactants are nonionic, and their interaction parameter (β_{L1}^{σ}) at the air/aqueous solution interface is only –0.2 at 25 °C.

4.5.2 Interaction Parameters in the Micelle(β^M) in the Aqueous Phase

Molecular interactions between L77 and pyrrolidinones: C4P, C6P, CHP, C2,6P, C8P and C10P in micelle formed in phosphate buffer solution at pH=7.00 have been evaluated by use of Equations (75) and (76):

$$\frac{X_1^M \ln(\alpha C_{12}^M / X_1^M C_1^M)}{(1-X_1^M)^2 \ln[(1-\alpha)C_{12}^M/(1-X_1^M)C_2^M]} = 1, \qquad \beta^M = \frac{\ln(\alpha C_{12}^M / X_1^M C_2^M)}{(1-X_1^M)^2}$$

Determinations of the values of C_1^M, C_2^M and C_{12}^M are shown in Figure A–8. The interaction parameters(β^M) are only approximate, since the values of the CMC for the pyrrolidinones are not available due to their limited solubilities in the buffer solution. The calculations are based upon use of their maximum solubilities as the CMC values for the individual pyrrolidinones. The results are listed in Table A–27.

From the results, it can be seen that L77 and all pyrrolidinones, except for C10P, show weak attractive interactions in their mixed micelles with L77. However, there is no synergism found in reduction of the surface tension because one of the conditions under which synergism exists, that β^σ must be more negative than β^M [145], is not met. This can be verified by the surface tension data for these mixtures.

4.5.3 Interaction Parameters at the Solid/Liquid Interface (β^{σ}_{SL})

Interaction parameters at the aqueous solution/polyethylene interface (β^{σ}_{SL}) have also been calculated by use of Equations (77) and (78) and through the adsorption isotherms of the two individual surfactants and their mixtures. The plots of π_{SL} vs. lnC are obtained from adsorption isotherms and shown in Figures B–61 to B–66 for systems L77–C4P, L77–CHP, L77–C6P, L77–C2,6P, L77–C8P and L77–C10P, respectively. The values of $\ln(C_1^0)$, $\ln(C_2^0)$ and $\ln(C_{12})$ are taken from the plots of π_{SL} vs. LnC at the same value of π_{SL} as shown in Figure A–8. To obtain the concentrations, the largest common π_{SL} value is best, because it corresponds to higher values of C_1^0, C_2^0 and C_{12}, and consequently, smaller relative errors for the concentrations. That is quite similar to the procedure used in calculating β^{σ}_{LA}. However, for use in Equations (77) and (78), the value of α_1, the equilibrium mole fraction of L77 in the bulk solution phase, is generally not equal to its initial value, because it changes with adsorption of the surfactants onto the solid surface. This is different from the calculation for β^{σ}_{LA} and β^{M}, where adsorption at the air/aqueous solution interface is insignificant. But α_1 can be plotted as a function of lnC (C: total equilibrium concentration) by use of the data listed in Tables B–50 to B–91. The C_1^0, C_2^0,

C_{12} and the equilibrium α_1 values for the relevant lnC_{12} value are substituted in Equations (77) and (78) to calculate β^{σ}_{SL} values. These are listed in Table A–28.

From the table, it can be seen that the results of β^{σ}_{SL}(expt) for all mixtures, except for L77–C10P, are negative, meaning that there is an attractive interaction between L77 and pyrrolidinones C4P, CHP, C6P, C2,6P and C8P, while the mixture of L77 and C10P has a small positive interaction parameter, indicating weak repulsive interaction. The more negative the interaction parameters, the stronger the attraction. The order of negative β^{σ}_{SL} values is C2,6P > C6P > C8P > CHP > C4P .This is exactly the same order as the decrease in the enhancement of the spreading factor observed above (shown in Figure A–7). For C10P, there is no enhancement found in the spreading factor when it is added to L77 aqueous solution at any mole ratio.

The attractive interactions between L77 and pyrrolidinones C4P, CHP, C6P, C2,6P and C8P are also consistent with the remarkable enhancement of the adsorption of L77 onto powdered polyethylene(shown in Figure A–5). The maximum enhancements by the pyrrolidinones are in the order: C2,6P > C8P > C6P > CHP > C4P, which is almost the same as the order of interactions listed above. Such interactions result in a more packed monolayer at the polyethylene/aqueous interface. Perhaps the structural similarity between the branched hydrophobic group in the L77 molecule and the branched

hydrocarbon chain in C2,6P molecule accounts for the finding that their interaction is the greatest.

4.5.4 Comparison of Calculated and Measured Mole Fraction of L77 at the Solid/Liquid Interface

Equation (77) was used above to calculate the values of X_1, the mole fraction of L77 in the total surfactant at the solid/ liquid interface. Since this value can also be obtained from the adsorbed amount of the two surfactants from their mixture onto powdered polyethylene as described before, this permits evaluation of the validity and accuracy of equation (77), which is based upon the assumptions of nonideal solution theory.[131,145]

Table A–28 lists the calculated values of X_1(calcd), obtained from equation (77), and the interaction parameter, β^{σ}_{SL}(calcd), calculated by substitution of X_1(calcd) and α_1 into equation (78), and the values of X_1(expt), obtained from the adsorption isotherm data, and the values of β^{σ}_{SL}(expt), obtained by use of X_1(expt) in equation (78). Considering the complexity of the calculations, the agreement between the values of X_1(calcd) and those of X_1(expt) is considered good validation of the nonideal solution treatment of the adsorption data. The values of β^{σ}_{SL}(calcd.) are also considered to be in good agreement with those of β^{σ}_{SL}(expt).

4.5.5 Synergism in Reduction of Interfacial Tension Effectiveness at the Solid/Liquid Interface

Similar to the situation at the air/liquid interface, the maximum synergism in reduction of interfacial tension effectiveness at the polyethylene/aqueous solution interface can also be evaluated by Equations (79) and (80). However, the values of K_1 and K_2 should be the slopes of the γ_{SL}–lnC plots of the aqueous solutions of L77 and pyrrolidinones, respectively. Due to the difficulty in availability of the values of γ_{SL}, it is not possible at present to numerically solve Equation (79) to obtain the value of X_1^*, the equilibrium mole fraction of L77 in the adsorbed monolayer at the polyethylene/aqueous solution interface at the point of maximum synergism in this respect.

Although there is difficulty in obtaining X_1^* mathematically, the experimental data for X_1^* are available from the adsorption isotherms. The values of X_1^* corresponding to the experimental mole fraction($\alpha_1^{*,E}$), at which the maximum interfacial tension reduction (π_{SL}^{Max}) is obtained, may be used to calculate $\alpha^{*,E}$(calcd) by use of Equation (80). The related results are listed in Table A–29.

In Table A–29, π_{SL}^{Max} is the maximum interfacial tension reduction effectiveness at the polyethylene/aqueous solution interface and it is obtained

from the plots of π_{SL} – lnC (shown in Figures B–61 to B–66) at the point of LnC.M.C of L77. In Equation (80), C_1^M is the C.M.C. of L77, which is 1.33×10^{-4} M, while C_2^M was approximated by use of the maximum solubilities of the pyrrolidinones, listed in Table 2. It can be seen that the calculated results are quite close to the experimental results. This agreement is another good validation of the nonideal solution treatment of the adsorption results. For the system of L77–C10P, the maximum interfacial tension reduction effectiveness was only found at the ratio of $\alpha^{*,E}$(expt) equal to 1.000. This means their mixtures do not show any synergism in spreading.

In addition, the values of $(\beta^{\sigma}_{SL}-\beta^{M})$, calculated from the previous results are listed in Table A–29. As mentioned above, one of the conditions under which synergism in interfacial tension reduction effectiveness will occur at the solid/liquid interface is if β^{σ}_{SL} is more negative than β^{M}, that is if $(\beta^{\sigma}_{SL}-\beta^{M})$ is negative. In the table, the values for the systems of L77–C4P, L77–CHP, L77–C6P, L77–C2,6P and L77–C8P are negative, and synergism in interfacial tension reduction effectiveness is observed. For the system L77–C10P, this value is positive, and no synergism is observed.

Figure A-7. Spreading Factor(SF) vs. Mole Fraction of L77(α_{L77}) for Aqueous Mixtures of L77 and Pyrrolidinones(CnP) on the Polyethylene Substrate

(In Phosphate Buffer Solution, pH=7.00, 25°C)

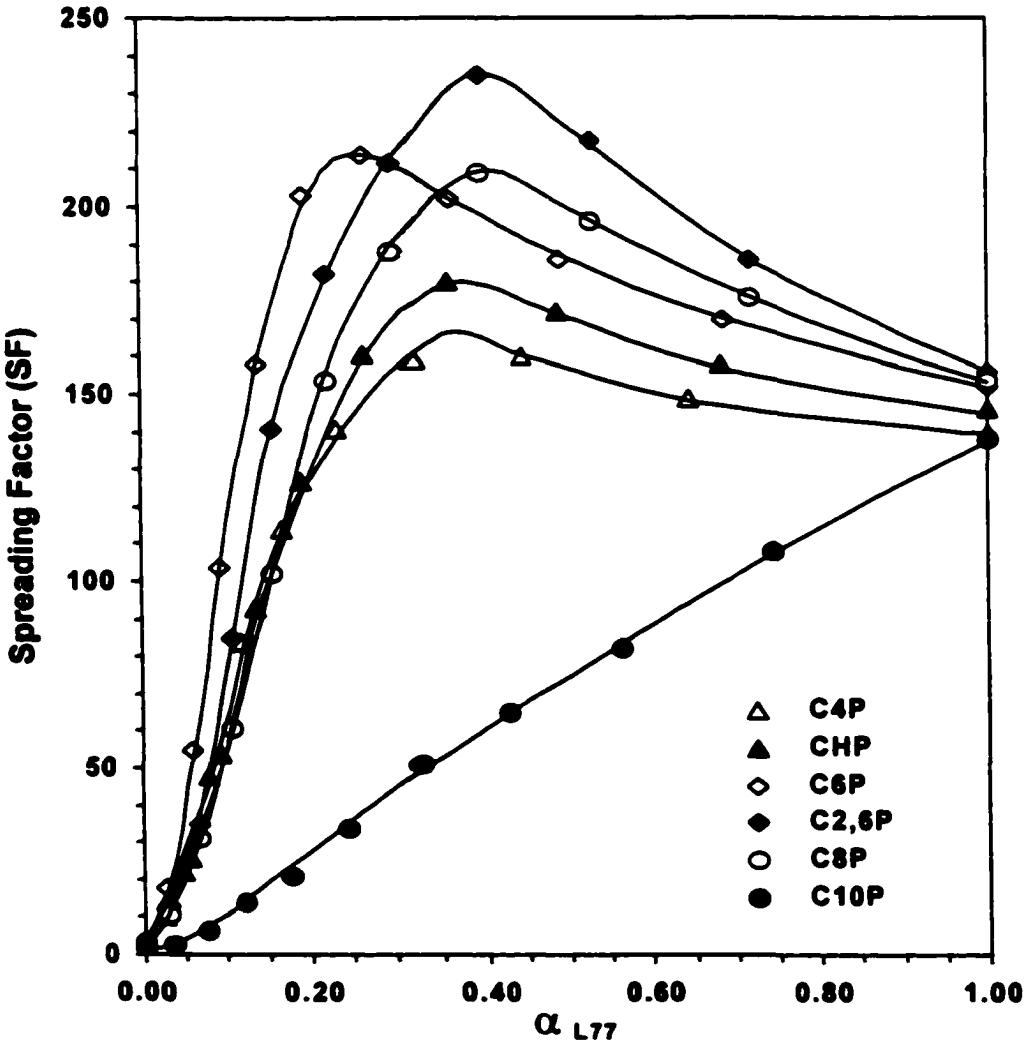

Figure A-8. Plots of γ_{LA} vs. logC for L77, C8P and Their Mixture(α_{77}=0.375)

(Phosphate Buffer Solution, pH=7.00, 25 °C)

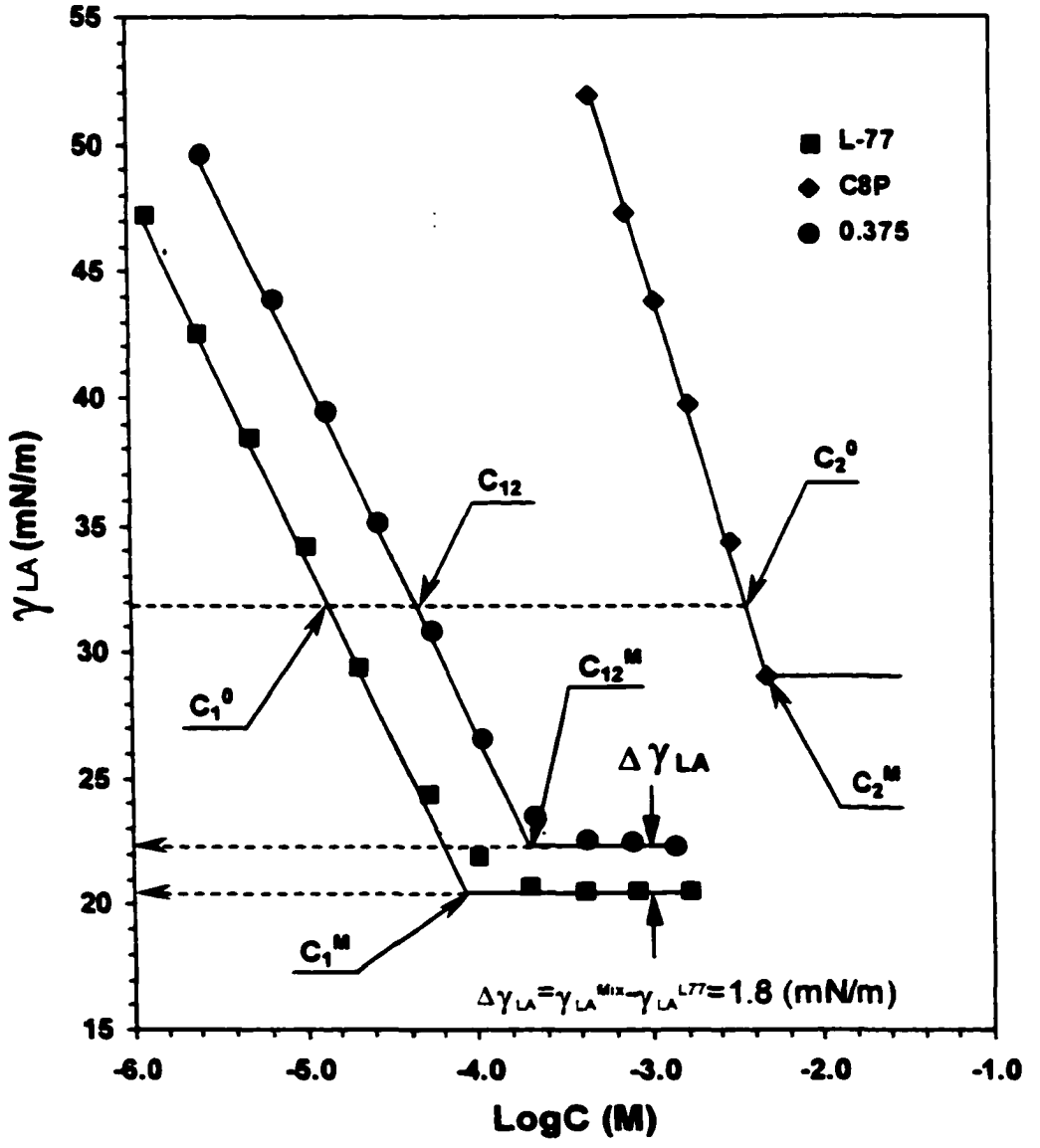

Figure A-9. Plots of π_{SL} vs. lnC for L77, C8P and Their Mixture(α_{77}=0.375) at the Polyethylene/Aqueous Solution Interface

(Phosphate Buffer Solution, pH=7.00, 25 °C)

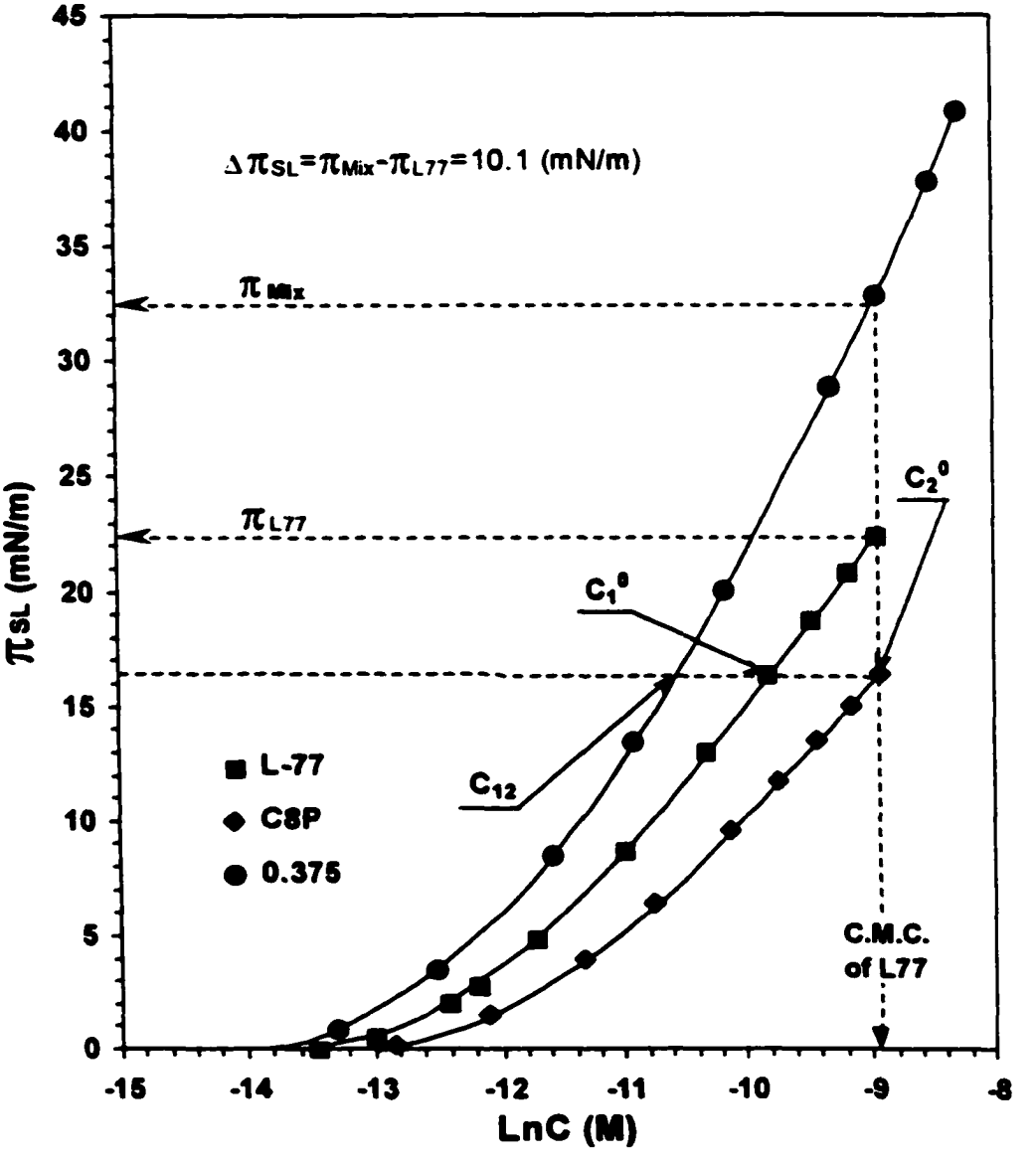

Figure A-10. Linear Relationship between Change in Spreading Factor(SF) and Spreading Coefficient($S_{L/S}$) for Mixtures of L77 and Pyrrolidinones(CnP)

(In Phosphate Buffer Solution, pH=7.00, 25°C)

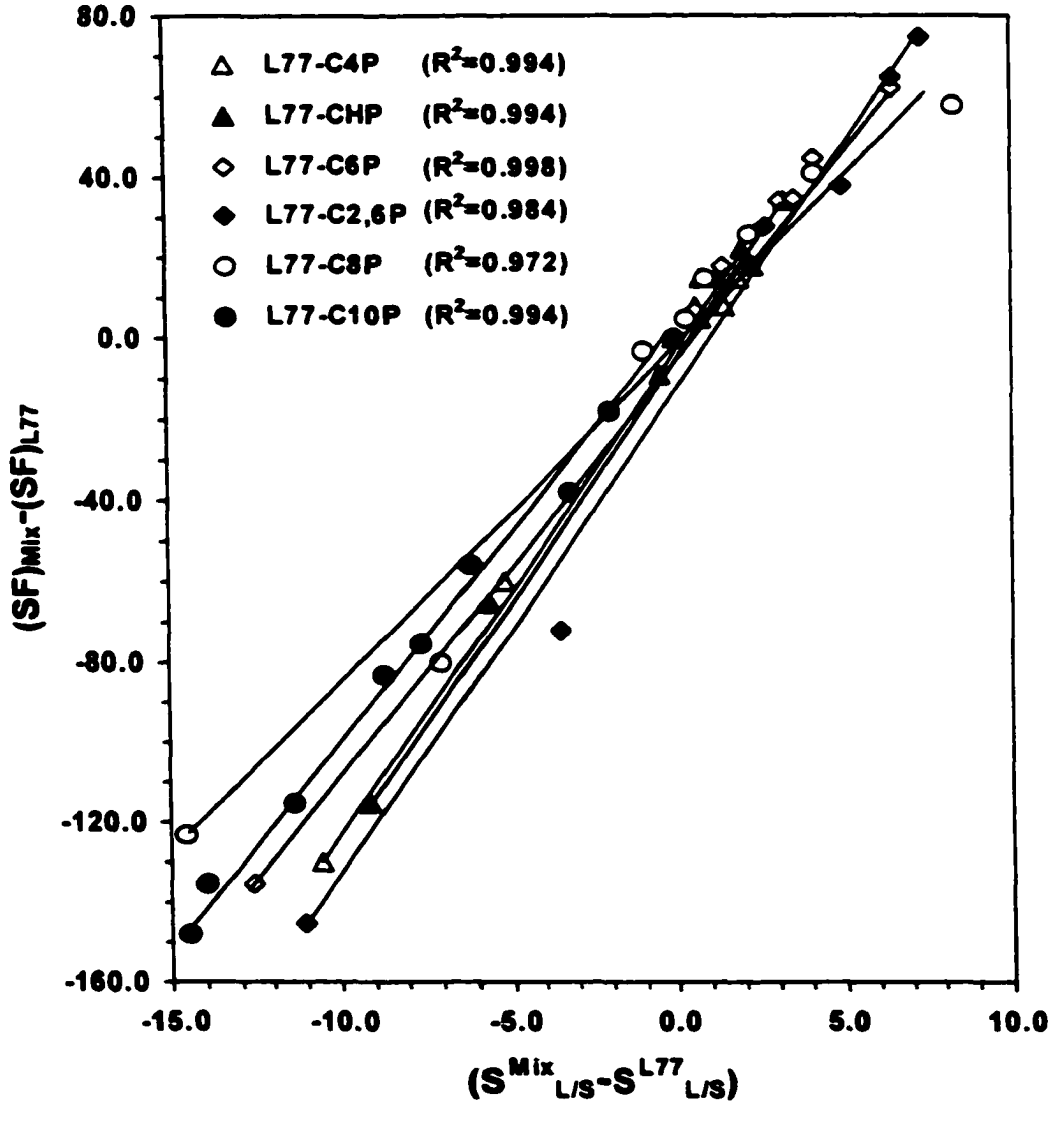

Table A-21. Results of Change in the Interfacial Tension, Spreading Coefficient and Spreading Factor for Mixtures of L77 and C4P

(In Phosphate Buffer Solution, pH =7.00, 25 °C)

α_{L77} (eq.)	$\Delta\gamma_{LA}$ (mN/m)	$\Delta\pi_{SL}$ (mN/m)	$S^{Mix}_{L/S}-S^{L77}_{L/S}$ (mN/m)	$(SF)_{Mix}-(SF)_{L77}$
1.000	0	0	0	0
0.805	0.3	1.1	0.8	5
0.611	0.6	2.1	1.5	8
0.475	1.4	3.6	2.4	18
0.313	2.1	4.0	1.9	15
0.209	2.4	1.9	-0.5	-9
0.110	2.9	-2.3	-5.2	-60
0.029	4.0	-6.6	-10.6	-130
0.000	18.4	-21.0	-39.4	-138

Table A-22. Results of Change in the Interfacial Tension, Spreading Coefficient and Spreading Factor for Mixtures of L77 and CHP

(In Phosphate Buffer Solution, pH =7.00, 25 °C)

α_{L77} (eq.)	$\Delta\gamma_{LA}$ (mN/m)	$\Delta\pi_{SL}$ (mN/m)	$S^{Mix}_{L/S}-S^{L77}_{L/S}$ (mN/m)	$(SF)_{Mix}-(SF)_{L77}$
1.000	0	0	0	0
0.838	0.2	0.9	0.6	8
0.694	0.4	1.7	1.3	15
0.581	1.0	3.0	2.0	22
0.407	1.5	4.8	3.3	34
0.253	2.2	3.0	0.8	15
0.115	3.2	-2.1	-5.6	-65
0.058	4.8	-4.3	-9.1	-115
0.000	11.8	-12.2	-24.0	-132

Table A-23. Results of Change in the Interfacial Tension, Spreading Coefficient and Spreading Factor for Mixtures of L77 and C6P

(In Phosphate Buffer Solution, pH =7.00, 25 °C)

α_{L77} (eq.)	$\Delta\gamma_{LA}$ (mN/m)	$\Delta\pi_{SL}$ (mN/m)	$S^{Mix}{}_{L/S}-S^{L77}{}_{L/S}$ (mN/m)	$(SF)_{Mix}-(SF)_{L77}$
1.000	0	0	0	0
0.868	0.2	0.8	0.6	7
0.735	0.3	1.7	1.4	18
0.574	1.1	4.3	3.2	34
0.417	1.3	5.5	4.2	45
0.243	2.0	8.5	6.5	52
0.152	2.3	5.9	3.6	15
0.028	4.7	-7.9	-12.6	-135
0.000	10.4	-14.1	-24.5	-142

Table A-24. Results of Change in the Interfacial Tension, Spreading Coefficient and Spreading Factor for Mixtures of L77 and C2,6P

(In Phosphate Buffer Solution, pH =7.00, 25 °C)

α_{L77} (eq.)	$\Delta\gamma_{LA}$ (mN/m)	$\Delta\pi_{SL}$ (mN/m)	$S^{Mix}_{L/S}-S^{L77}_{L/S}$ (mN/m)	$(SF)_{Mix}-(SF)_{L77}$
1.000	0	0	0	0
0.825	0.2	2.5	2.3	18
0.651	0.3	5.3	5.0	38
0.503	1.0	7.5	6.5	65
0.381	1.6	9.0	7.4	75
0.220	1.8	4.5	2.7	28
0.097	2.6	-0.9	-3.5	-82
0.025	5.0	-6.1	-11.1	-145
0.000	12.3	-14.0	-26.3	-155

Table A-25. Results of Change in the Interfacial Tension, Spreading Coefficient and Spreading Factor for Mixtures of L77 and C8P

(In Phosphate Buffer Solution, pH =7.00, 25 °C)

α_{L77} (eq.)	$\Delta\gamma_{LA}$ (mN/m)	$\Delta\pi_{SL}$ (mN/m)	$S^{Mix}{}_{US}-S^{L77}{}_{US}$ (mN/m)	$(SF)_{Mix}-(SF)_{L77}$
1.000	0	0	0	0
0.906	0.1	0.4	0.3	5
0.791	0.2	1.1	0.9	15
0.660	0.3	2.5	2.2	26
0.535	0.7	4.9	4.2	41
0.375	1.8	10.1	8.3	62
0.222	2.3	1.3	-1.0	-3
0.085	3.0	-4.0	-7.0	-80
0.000	8.1	-6.5	-14.6	-103

Table A-26. Results of Change in the Interfacial Tension, Spreading Coefficient and Spreading Factor for Mixtures of L77 and C10P

(In Phosphate Buffer Solution, pH =7.00, 25 °C)

α_{L77} (eq.)	$\Delta\gamma_{LA}$ (mN/m)	$\Delta\pi_{SL}$ (mN/m)	$S^{Mix}{}_{L/S}-S^{L77}{}_{L/S}$ (mN/m)	$(SF)_{Mix}-(SF)_{L77}$
1.000	0	0	0	0
0.865	0.4	-1.6	-2.0	-18
0.707	0.9	-2.3	-3.2	-38
0.572	1.4	-4.7	-6.1	-56
0.434	1.8	-5.8	-7.6	-75
0.307	2.2	-6.5	-8.7	-83
0.185	3.1	-8.3	-11.4	-115
0.077	4.5	-9.5	-14.0	-135
0.000	8.0	-6.5	-14.5	-148

Table A-27. Interactions between L77 and Pyrrolidinones at the Air/Liquid Interface and in Micelle

(In Phosphate Buffer Solution, pH =7.00, 25 °C)

System	X_1^{LA}	β^{σ}_{LA}	X_1^{M}	β^{M}	$\beta^{\sigma}_{LA}-\beta^{M}$
L77–C4P	0.78	–0.43	0.76	–0.82	0.39
L77–CHP	0.76	–0.57	0.72	–1.24	1.81
L77–C6P	0.76	–0.82	0.69	–1.56	2.38
L77–C2,6P	0.75	–0.67	0.66	–1.83	2.50
L77–C8P	0.67	–0.40	0.65	–1.75	2.15
L77–C10P	0.62	0.14	0.55	0.10	0.04

Table A-28. Interactions between L77 and Pyrrolidinones at the Polyethylene/Aqueous Solution Interface

(In Phosphate Buffer Solution, pH =7.00, 25 °C)

System	α_1	β^{σ}_{SL} (expt)	β^{σ}_{SL} (calcd)	X^{I}_{SL} (expt)	X^{I}_{SL} (calcd)
L77–C4P	0.046	–3.5	–2.7	0.77	0.74
L77–CHP	0.105	–4.2	–3.6	0.71	0.68
L77–C6P	0.145	–5.9	–5.4	0.64	0.62
L77–C2,6P	0.182	–6.8	–6.7	0.55	0.55
L77–C8P	0.269	–5.5	–5.1	0.42	0.49
L77–C10P	0.295	1.2	0.7	0.44	0.51

Table A-29.. Maximum Synergism in Interfacial Tension Reduction for Aqueous L77–Pyrrolidinone Mixtures at the Polyethylene/Aqueous Solution Interface

(In Phosphate Buffer Solution, pH =7.00, 25 °C)

System	π_{SL}^{Max} (mN/m)	$\alpha^{*,E}$ (expt)	$\alpha^{*,E}$ (calcd)	$\beta^{\sigma}_{SL}-\beta^{M}$	Synergism
L77	22.5	1.00	1.00	N/A	N/A
L77–C4P	26.5	0.31	0.34	–2.7	observed
L77–CHP	27.3	0.41	0.39	–3.0	observed
L77–C6P	31.0	0.24	0.27	–4.4	observed
L77–C2.6P	31.5	0.38	0.41	–4.9	observed
L77–C8P	32.6	0.38	0.36	–3.7	observed
L77–C10P	22.5	1.00	N/A	1.1	not observed

CHAPTER 5

MECHANISMS OF SUPERSPREADING AND SYNERGISM IN THE SUPERSPREADING

5.1 Mechanism of Superspreading

Aqueous solutions of trisiloxane surfactant, SILWET L77, exhibit superior wetting properties on hydrophobic substrates. Although this phenomenon of superspreading has been known for decades and received extensive coverage in the scientific literature in recent years. its mechanism is still not well understood. In this chapter, a postulated mechanism is proposed, which is based on the unique molecular structure and the leading film[146] formed around the droplet in the process of spreading.

The molecular structure of SILWET L77 is shown in the previous chapter of this dissertation. A space filling model of the SILWET L77 molecule, as well as a picture of the vertical view from top of the molecule are shown in Figures A-11 and A-12. From its unique low surface tension at the air/aqueous solution

interface, it is reasonable to assume that the methyl groups attached to the silicon are exposed to the air and the long polyether chain is entirely in the water.

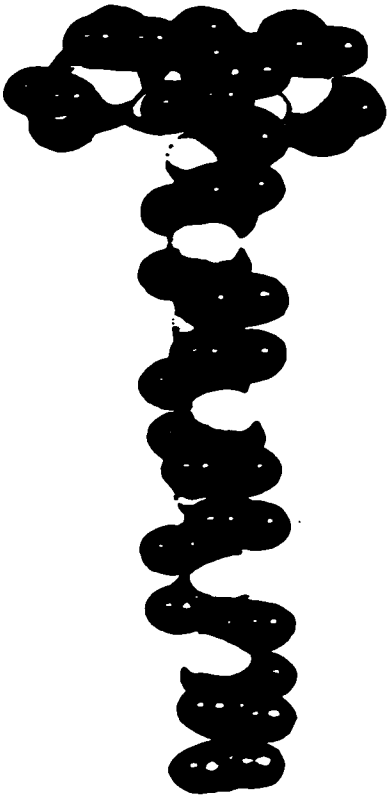

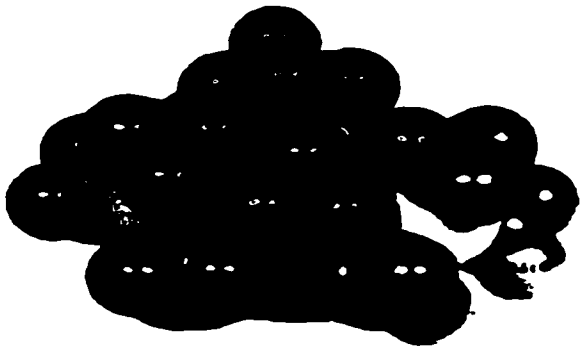

Figure 12. Vertical View from Top of the Model of SILWET L77

Figure 11. A Space Filling Model of the SILWET L77

Paradoxically, the structure of L77 with its compact hydrophobic group and extended hydrophilic chain seems like an "inversion" of the structure of a

regular ionic surfactant, which possesses a compact polar head group and a long hydrophobic alkyl chain. In the case of L77, the silicon backbone provides a means to expose a dense layer of $-CH_3$ groups on the surface, resulting in a lower surface tension than available with the $-CH_2-$ groups of an alkyl chain, because $-CH_3$ groups have lower surface free energies than $-CH_2$ groups [79].

When a liquid spreads on a solid surface, a precursor film (leading film) is formed surrounding the drop due to the Marangoni Effect [87]. A surface tension gradient at the edge of the drop is the driving force for spreading. A picture of a droplet of aqueous solution of $C_{12}E_{10}$ on a bare, oxidized silicon wafer is shown in Figure 13 [147]. A SEM picture of a drop of cooled glass on Fernico metal (which has the same coefficient of thermal expansion) is shown in Figure 14[148]. As the spreading front stretches, concentration of the solution in the precursor film decreases because of the adsorption of surfactant at the solid/aqueous solution interface. Consequently, the surface tension increases at the front relative to the top of the droplet, thereby establishing a surface tension gradient. The greater the adsorption at the solid/aqueous solution interface, the higher the gradient, the faster the spreading and the larger the ultimate coverage of the surface.

Figure 13. Picture of a Droplet of Aqueous Solution of C12E10 on a Bare, Oxidized Silicon Wafer, showing precursor film around the droplet [147].

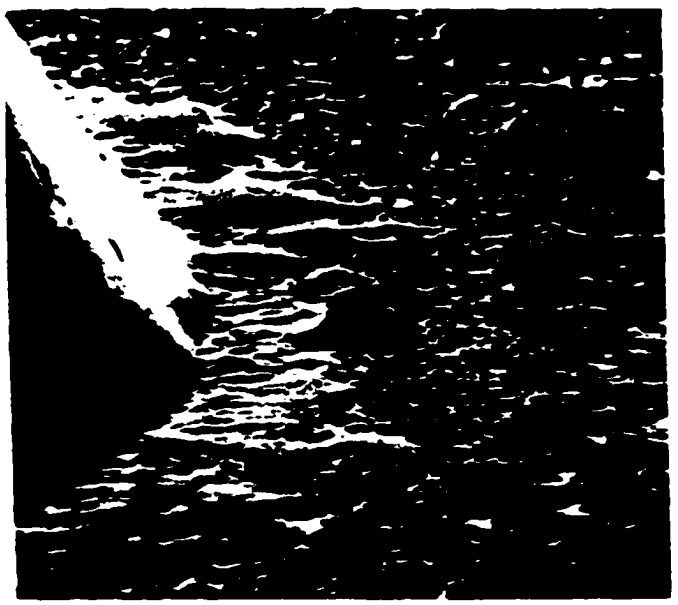

Figure 14. A SEM Picture(×130) of a Drop of Cooled Glass on Fernico Metal, showing precursor film around the droplet [148].

A proposed mechanism to explain the superspreading of L77 is elucidated in Figure 15.

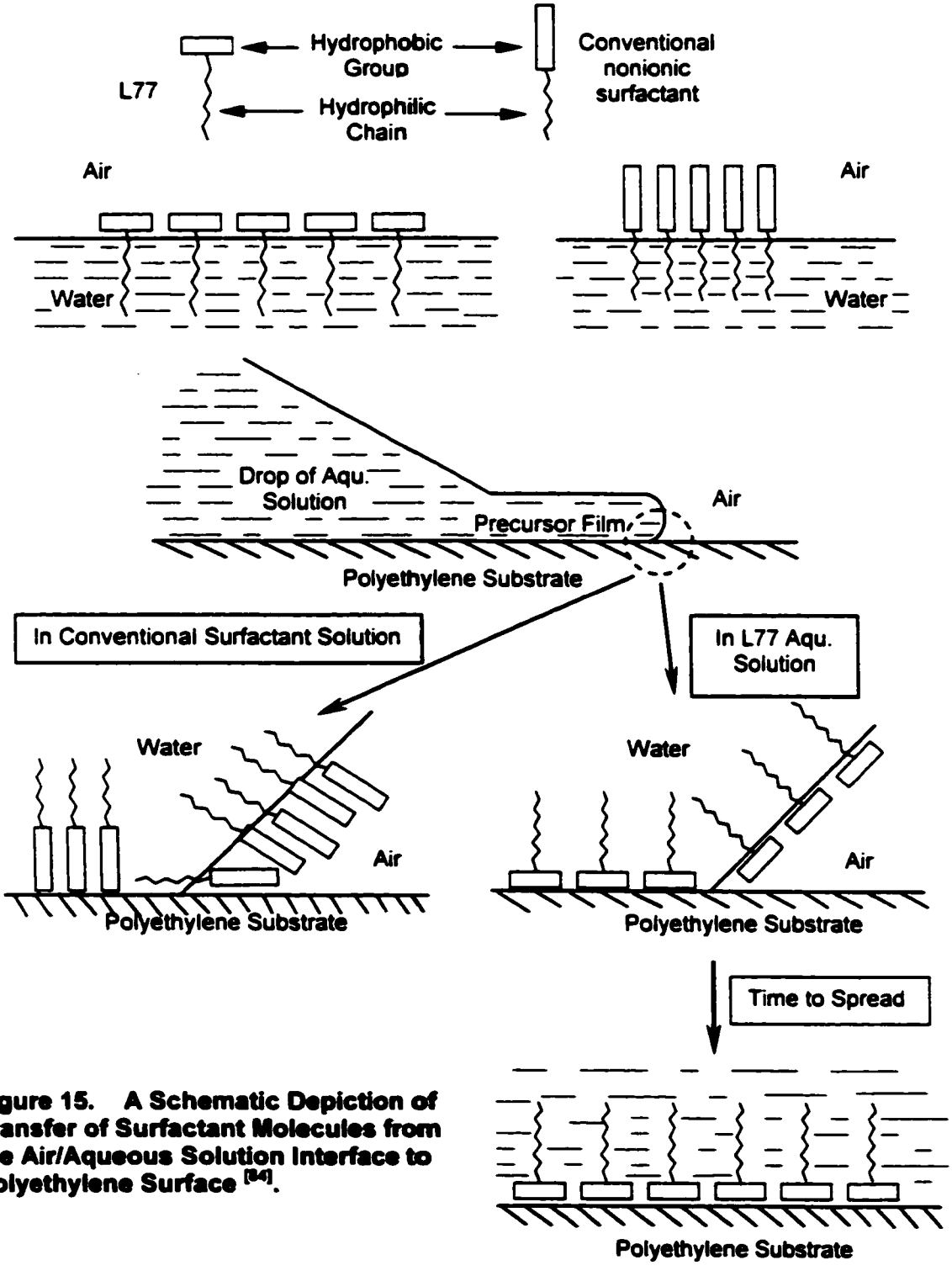

Figure 15. A Schematic Depiction of Transfer of Surfactant Molecules from the Air/Aqueous Solution Interface to Polyethylene Surface [84].

In Figure15, it is shown that the progressive advance of L77 aqueous solution can be likened to "molecular zippering" of the polyethylene/aqueous solution interface. Conventional surfactants tend to lie flat on the surface exposing hydrophobic patches which impede spreading.

As discussed in the previous part of this dissertation, the low surface tension criterion is not the only one governing the spreading characteristics of surfactant solutions. The unique structure of L77 must play an important role in determining its superspreading behavior. The extraordinary ability of trisiloxane surfactant L77 to spread on hydrophobic surfaces may be related to the short, compact structure of its hydrophobic group, which facilitates a transfer of surfactant molecules from the air/aqueous solution interface to the solid surface. In Figure 15, the advancing contact angle of the precursor film is shown, on a molecular scale, as being obtuse[25]. Because of the short, compact nature of the hydrophobic group, L77 molecules are readily transferred from the air/ aqueous solution interface to the polyethylene/aqueous solution interface, facilitating progressive advance of the precursor film. The surface tension gradient is maintained until the spreading reaches equilibrium.

This behavior can be contrasted to that observed with conventional surfactants in which the cumbersome hydrophobic groups impede the

molecular transfer and the spreading process. According to the proposed mechanism, it can be predicted that the longer the hydrophobic chain, the more difficult will be the transfer of surfactant molecules from the air/aqueous solution interface to the solid/aqueous solution interface, and therefore, the less tendency of spreading on the solid surface. Couzis[149] and his co-workers reported that trisiloxane surfactants are able to remove the highly energetic water layer near the hydrophobic surfaces. However, the conventional polyethoxylate surfactants(C_iE_j) are not able to remove this interfacial water layer effectively.

5.2 Mechanism of Synergism in Superspreading

As discussed in Part I of Chapter 4, the adsorption of L77 and the total adsorption of the surfactant mixtures at the polyethylene/aqueous solution interface can be enhanced by the addition of pyrrolidinones, except for C10P, to the L77. This means that the addition of pyrrolidinones with short hydrocarbon chains can make the adsorbed molecules more closely packed at the polyethylene/aqueous solution interface, which results in an additional reduction of the interfacial tension at the interface. On the other hand, the adsorption of L77 at the air/aqueous solution interface is not enhanced by the addition of pyrrolidinones. However, the addition of pyrrolidinones with short hydrocarbon

chains to the aqueous solution of L77 may make the film at the air/ aqueous solution interface, specially the precursor film of spreading, more flexible and easier to bend. Kabalnov reported that many spreading agents have very short and highly branched hydrocarbon tail structures to facilitate good spreading [48]. For further explanation, the precursor films of superspreading of aqueous solutions on polyethylene surface for L77 alone are shown in Figure 16 and Figure 17, a mixture of L77 and a pyrrolidinone with a short straight hydrocarbon chain, such as C8P, are shown in Figure 18 and Figure 19, and a mixture of L77 and a pyrrolidinone with a branched hydrocarbon chain, such as C2,6P, are shown in Figure 20 and Figure 21.

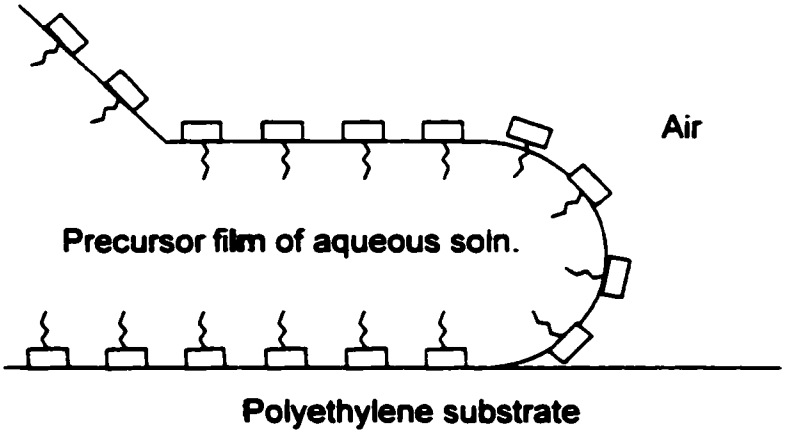

Figure 16. Precursor Film of Aqueous Solution of L77 Alone on Polyethylene Substrate. Adsorption of L77 at the interfaces of air/aqueous solution and polyethylene/aqueous solution are almost the same.

As discussed in the previous part, the reason for superspreading of L77 on a hydrophobic surface such as polyethylene film is due to its unique molecular

structure with a compact hydrophobic group, rather than a long hydrocarbon chain in a conventional surfactant molecule. The precursor film is shown in Figure 16. It can be seen that the bend of the precursor film in the direction of advance spreading will mainly depend upon the distance between the hydrophilic chains of the L77 molecules, as shown in Figure 17. Obviously, the larger the distance between the two hydrophilic chains, the easier will be the bend of the precursor film in the spreading direction.

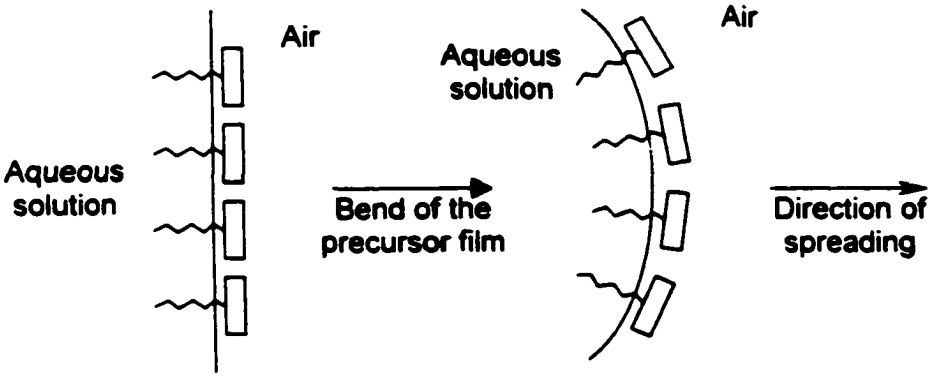

Figure 17. Bend of Precursor Film of Aqueous Solution of L77 in the Direction of Advance Spreading. The larger the distance between the hydrophilic chains of the two L77 molecules, the easier will it be to bend.

According to the experimental results, for mixtures of L77 and pyrrolidinone with a short straight hydrocarbon chain such as C8P, the adsorption of the mixture at the polyethylene/aqueous solution interface is greater than that at air/aqueous solution interface because the adsorption of L77 at the former interface is enhanced by the addition of pyrrolidinones except for C10P. At the air/aqueous solution interface, there is no enhancement of the

adsorption. The adsorption of L77 decreases because some of the adsorbed L77 molecules are replaced by pyrrolidinone molecules at the interface. This is shown in Figure 18. Therefore, the distance between the hydrophilic chains of two L77 molecules becomes larger, which makes it easier to bend the precursor film in the direction of spreading. This is shown in Figure 19. The experimental data have evidenced this change in the distance between the two hydrophobic chains of L77 molecules. As an approximation, this change can be evaluated in the following manner. The minimum area of L77 per molecule in absence of pyrrolidinone is 66 $Å^2$. Assume it occupies a square area at the air/aqueous solution interface, the distance between the two hydrophobic chains equals the square root of 66 $Å^2$, which is 8.1 Å. In the mixture with a pyrrolidinone, e.g., C8P, the total adsorption of L77 and C8P at the air/aqueous solution interface increases to 2.8×10^{-10} mol/cm^2 because of the contribution from the larger

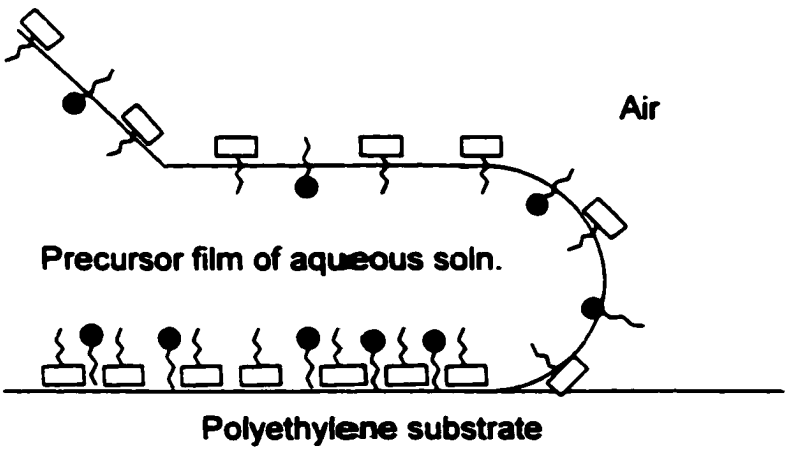

Figure 18. Precursor Film of Aqueous Solution of Mixture of L77 and Pyrrolidinone Having a Short Straight Hydrocarbon Chain on Polyethylene Substrate. Adsorptions of L77 at the polyethylene/aqueous solution interface is enhanced; at the air/aqueous solution interface, it decreases.

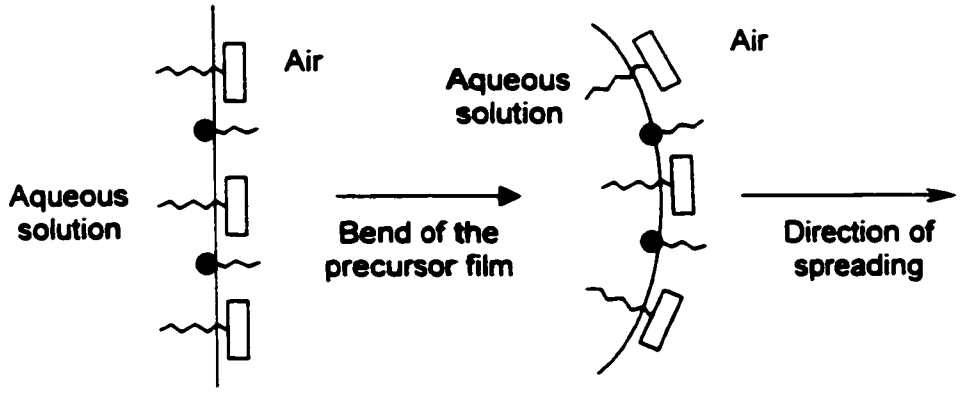

Figure 19. Bend of Precursor Film of Aqueous Solution of L77 and Pyrrolidinone Having a Short Straight Hydrocarbon Chain on Polyethylene Substrate in the Direction of Spreading. The distance between the hydrophilic chains of two L77 molecules becomes larger.

adsorption of C8P at the air/aqueous solution interface. The average minimum area per molecule is therefore 59 $Å^2$. In the adsorbed monolayer at the interface, the mole fraction of L77 is 0.62. Therefore, the average area occupied by each L77 molecule equals 95 $Å^2$. With the same assumption of a square occupied by each L77 molecule, the distance between the two hydrophobic chains of L77 is 9.8 Å, which is larger than that in absence of C8P. On the other hand, the hydrophilic group of the pyrrolidinones is much smaller than the hydrophilic group of L77. The space between the hydrophilic groups of L77 is large enough to accommodate it.

For mixtures of L77 and the pyrrolidinone with a branched hydrocarbon chain, C2,6P, the enhancement of adsorption at the polyethylene/aqueous solution interface caused by C2,6P is the greatest among the pyrrolidinoes studied. The possible packing model for the mixture of L77 and C2,6P at the polyethylene/ aqueous solution interface is shown in Figure 20. The branched hydrophobic chain works as a bridge to link each two L77 molecules at this interface. In this way, both L77 and C2,6P molecules have optimal packing and reach a maximum enhancement of adsorption at the interface. This packing model can be verified by the results of the mole fraction of L77 at the polyethylene/aqueous solution interface. The experimentally determined X^{l}_{SL} (expt) and calculated X^{l}_{SL} (calcd) are the same, both of them are 0.55 [51], which are pretty close to the value of 0.5, obtained from the proposed packing model. The experimentally determined mole fractions of L77, X^{l}_{SL} (expt), in the mixtures with other pyrrolidiniones are: C4P, 0.77; CHP, 0.71; C6P, 0.64; C8P, 0.55; C10P, 0.40. At the interface air/aqueous solution, the change in the adsorption is the same as that of other pyrrolidinones as described before, there is no enhancement of adsorption at this interface and some of the adsorbed L77 molecules are replaced by C2,6P molecules. Therefore, the distance between the hydrophilic chains of two L77 molecules becomes larger, which makes it easier to bend the precursor film in the direction of spreading. This is shown in Figure 21. In addition, because of the branched

hydrophobic chain in C2,6P molecules, the side in the air at the air/aqueous solution interface is more crowded relative to other pyrrolidinones, which is also

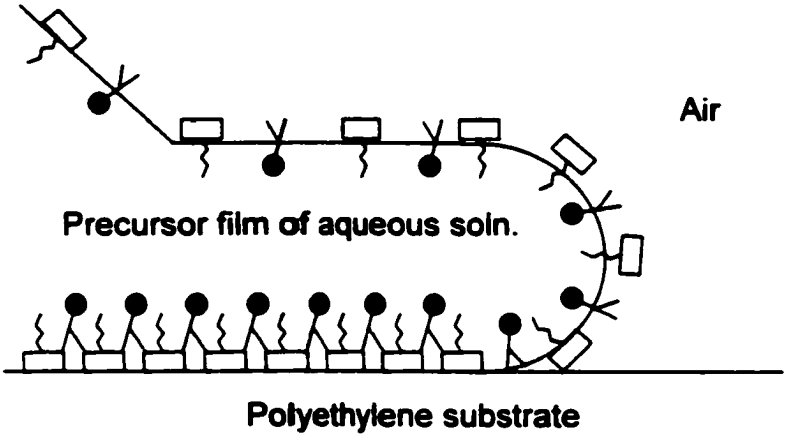

Figure 20. Precursor Film of Aqueous Solution of Mixture of L77 and C2,6P on Polyethylene Substrate. The branched hydrophobic chains in C2,6P molecules link each two molecules of L77 to make the molecules pack best at the polyethylene/aqueous solution interface.

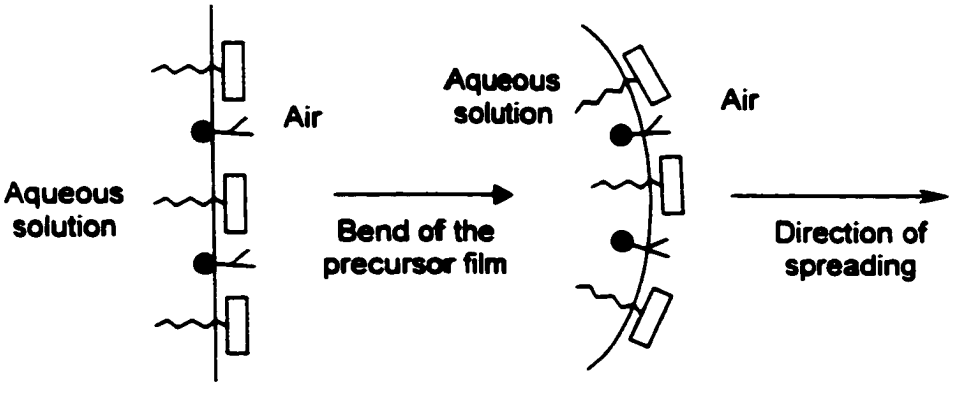

Figure 21. Bend of Precursor Film of Aqueous Solution of L77 and C2,6P on Polyethylene Substrate in the Direction of Advance Spreading. The branched hydrocarbon chains make an additional contribution to bend the precursor film in the direction of spreading.

shown in Figure 21, it makes an additional contribution to bend the precursor film in the direction of spreading, which cannot be produced by other used pyrrolidinones with a short straight hydrocarbon chain. Combined both unique properties of C2,6P as described above, the mixture of L77 and C2,6P shows the greatest synergistic effect in superspreading on polyethylene film. As of the mixture of L77 and CHP, although the hydrocarbon group of CHP, cyclohexyl group, is nearly as bulky as C2,6P, it is not able to enhance the adsorption of L77 at polyethylene/aqueous solution interface, a dominant factor governing the spreading, as high as C2,6P. Therefore, the synergism of mixture of L77 and CHP is less than that of mixture of L77 and C2,6P.

5.3 The Lack of Synergism Found in Mixtures of L77 and C10P

Apparently, there is a maximum in the length of the hydrocarbon chain of pyrrolidinones that can enhance the superspreading of L77 on the polyethylene substrate. Except for CHP and C2,6P, whose hydrocarbon chains are not straight chain, C4P, C6P, C8P, and C10P are exact homologues, whose hydrophobic chains each increase by two $-CH_2$ groups. Their hydrophobicities can be related to their solubilities in water; the lower solubility, the higher the hydrophobocity of the molecule. Figure 22 shows the logarithm of solubility (mole/L) of the homologues in the phosphate buffer solution. It can be seen that the logarithm of the solubility(mole/L) of the homologues decreases linearly with increase in the number of carbon atoms in the alkyl chain. Noteworthy is that

the solubilities(mole/L) of C4P, C6P and C8P are higher than that of L77, but the solubility(mole/L) of C10P is lower than that of L77. It means that the hydrophobicity of C10P is higher than that of L77. This may account for its greater adsorption than that of L77 at the aqueous solution/ polyethylene interface [37].

Figure 22. Plot of Logarithm of Solubility(M) vs. the Number of Carbon Atoms in Alkyl Chain

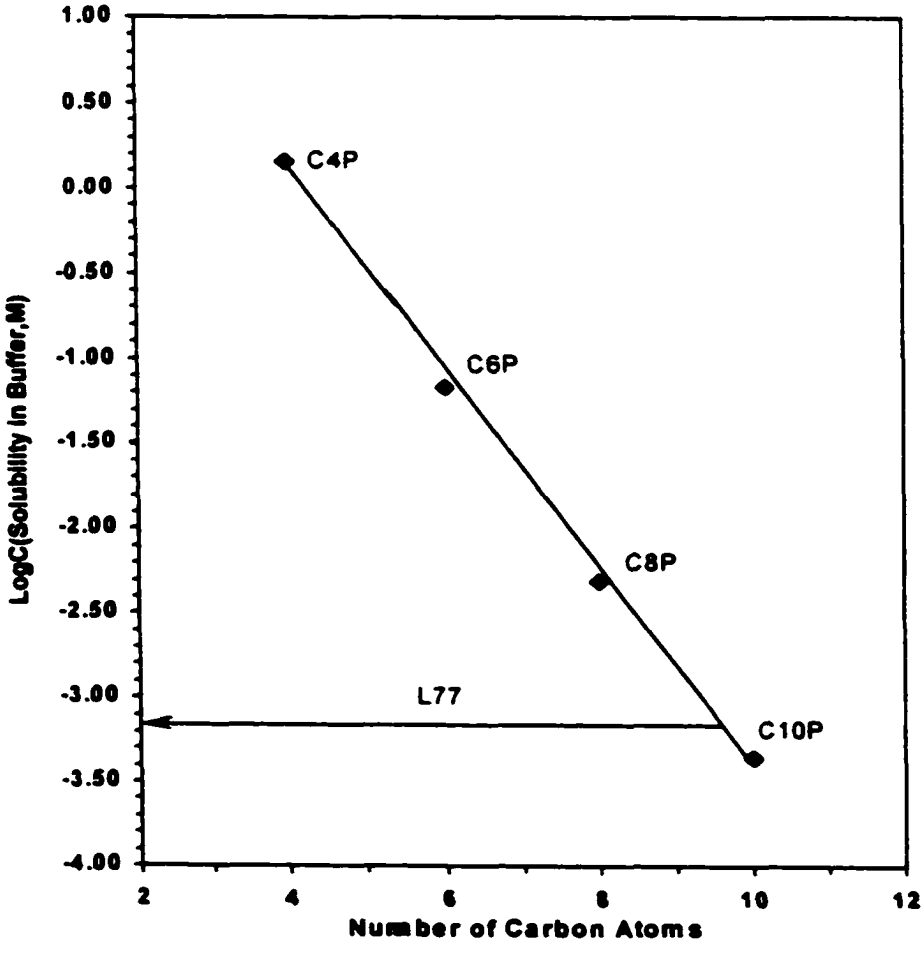

Because of the competitive adsorption of C10P, the polyethylene/aqueous solution interface, when contacted with the mixture of L77 and C10P, will be mainly occupied by C10P molecules, as shown in Figure 23, rather than by the L77 molecules observed in the mixtures with other pyrrolidinones. This has been confirmed by experimental data of mole fraction of L77 (X_{SL}^{l}) at the interface of polyethylene/aqueous solution. For the mixture of L77 and C10P, X_{SL}^{L77} (expt) = 0.40; for all the other mixtures, X_{SL}^{L77} (expt) is greater than 0.50. Thus, the interfacial tension at the polyethylene/aqueous solution interface, reduced mainly by C10P, cannot be as low as where reduced mainly by L77, in the other mixtures. Consequently, the spreading cannot be enhanced effectively.

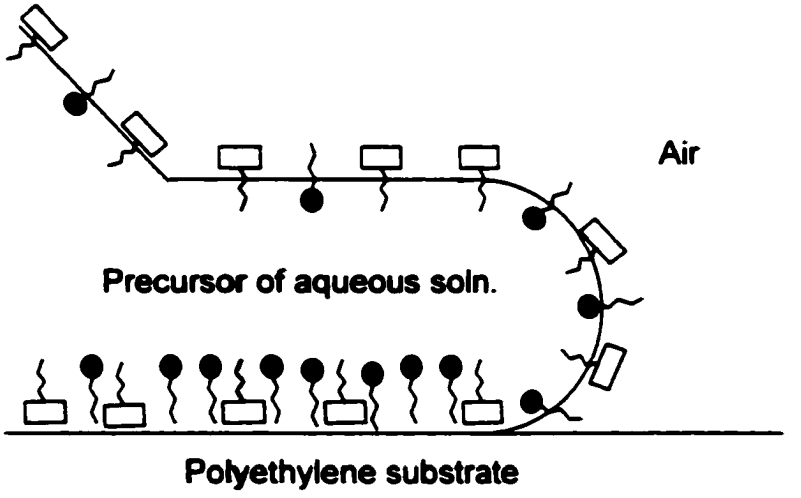

Figure 23. Precursor Film of Aqueous Solution of Mixture of L77 and C10P on Polyethylene Substrate. The mole fraction of L77 at the polyethylene/aqueous solution interface is 0.4, the greater portion of this interface is occupied by C10P.

Also, the most competitive adsorption of C10P relative to other pyrrolidinones results in a smallest mole ratio of L77 to C10P at air/aqueous solution interface. From the experimental results[51], it can be seen that for mixtures of L77 and pyrrolidinones, L77 and C10P, X_{LA}^{I}=0.62; L77 and C8P X_{LA}^{I}=0.67; L77 and C2,6P, X_{LA}^{I}=0.75; L77 and C6P, X_{LA}^{I}=0.76; L77 and CHP, X_{LA}^{I}=0.76; L77 and C4P, X_{LA}^{I}=0.78. Because a pretty large portion of the interface is occupied by C10P molecules, with the longest straight hydrocarbon chains relative to the other pyrrolidinones, it impedes the transfer of surfactant molecules from the air/aqueous solution interface to the polyethylene/ aqueous solution interface because of the greater difficult of bending of the precursor film. Consequently, the spreading of the mixture is not enhanced.

CONCLUSIONS

Adsorption effectiveness (Γ_{LA}) of the individual surfactant at the air/aqueous solution interface decreases in the order: C10P > C8P > C6P > C2,6P > CHP > C4P > L77. For N-alkylpyrrolidinones with different alkyl chain lengths, the adsorption at the air/aqueous solution interface increases, as expected, with length of the alkyl chain. L77, although it has the smallest adsorption at air/aqueous solution interface, has the lowest $\gamma_{c.m.c.}$. Therefore, the value of $\gamma_{c.m.c}$ is not necessarily consistent with the adsorption effectiveness at the air/aqueous solution interface, but depends as well on the molecular characteristics of the surfactant. However, L77 has the greatest adsorption efficiency (pC_{20}, $-\Delta G^{0}_{ad}$) at the air/aqueous solution interface among the compounds investigated. Mixtures of L77 and an N-alkyl-pyrrolidinone show little, if any, enhancement of the total surfactant adsorption of the mixture at that interface.

Adsorption amounts of the individual surfactants on powdered polyethylene surfaces decrease in the order: C10P > L77 > C8P > C2,6P > C6P > CHP > C4P, with adsorption of the pyrrolidinones on the polyethylene surface

decreasing, as expected, with a decrease in the number of carbon atoms in the alkyl chain of the pyrrolidinones. The adsorption isotherms of all surfactants except C10P are of Langmuir type, with the absolute values of their (negative) standard adsorption free energies decreasing in the order: L77 > C8P > C6P > CHP > C2,6P > C4P. There is considerable enhancement of the adsorption of L77 in the mixed solutions onto the powdered polyethylene surface upon the addition to the solution of the pyrrolidinones and, except for C10P, reduction in the adsorption of the pyrrolidinones. The enhancement effectiveness by the pyrrolidinones of L77 adsorption at the polyethylene/aqueous solution interface is in the order: C2,6P > C8P > C6P > CHP > C4P; the enhancement efficiency is in the order: C2,6P > C8P > CHP> C6P > C4P.

There is also enhancement of the total adsorption of surfactant at the polyethylene/aqueous solution interface in the L77-pyrrolidinone mixtures. The enhancement effectiveness of the pyrrolidinones decreases in the order: C2,6P > C8P > C4P > CHP > C6P ; the enhancement efficiency in the order: C2,6P ~ C8P > C6P ~ CHP > C4P. C10P causes no enhancement of total surfactant adsorption.

Since adsorption of individual surfactants and their mixtures at the solid/air interface is smaller by one order of magnitude than that at the air/aqueous solution and solid/aqueous solution interfaces and there is almost

no enhancement of the total adsorption of the surfactants at the air/aqueous solution interface upon addition of the pyrrolidinones, enhancement of the adsorption at the solid/aqueous solution interface, and especially of L77, appears to be the most significant effect of this addition.

The change in the values of the spreading coefficient on polyethylene of an aqueous solution of the ethoxylated trisiloxane L77 upon addition of an N-alkyl pyrrolidinone can be approximated from the difference between the change in interfacial pressure at the polyethylene/aqueous solution interface and the change in the surface tension of the aqueous solution. The increase in the value of the former is the dominant factor in increasing the value of the spreading coefficient.

The change in the spreading coefficient on the polyethylene of an aqueous solution of L77 upon addition of different N-alkyl pyrrolidinones is in about the same order as their enhancement of its spreading factor on polyethylene. There is a good linear relationship between the change in spreading coefficient and the change in spreading factor. The slope of the plots for all mixtures is almost a constant, meaning it is related to the surface energy of the substrate.

Interactions of L77 with the different N-alkyl pyrrolidinones investigated at the aqueous solution/air and polyethylene/air interface are very weak. The L77-C10P mixture shows a very weak repulsion between the two surfactant molecules. This is consistent with the results of surface tension, which indicate that there is no synergism at the air/aqueous solution interface. The area per molecule at the air/aqueous solution interface is between L77 and the individual pyrrolidinone, indicating that there is no significant attractive or repulsive interaction between L77 and pyrrolidinones at the air/aqueous solution interface.

At the interface of polyethylene/aqueous solution, there is an attractive interaction between L77 and pyrrolidinones C4P, CHP, C6P, C2,6P and C8P while the mixture of L77 and C10P has a small positive interaction parameter, indicting weak repulsive interaction. The order of negative β_{SL}^{σ} values is C2,6P>C6P>C8P>CHP>C4P. This is exactly the same order as the decrease in the enhancement of the spreading factor. For C10P, there is no enhancement found in the spreading factor when it is added to L77 aqueous solutions at any mole ratio. The attractive interactions between L77 and pyrrolidinones C4P, CHP, C6P, C2,6P, and C8P are also consistent with the remarkable enhancement of the adsorption of L77 onto powdered polyethylene. The maximum enhancements of adsorption by the pyrrolidinones are in the order C2,6P>C8P>C6P>C4P, which is almost the same as the order of

interactions listed above. Such interactions result in a more packed monolayer at the polyethylene/aqueous solution interface. Perhaps the structural similarity between the branched hydrophobic group in the L77 molecule and the branched hydrocarbon chain in C2,6P molecule accounts for the finding that their interaction is the greatest.

Comparison of values of the mole fractions of L77 and the interaction parameters at the polyethylene/aqueous solution interface, either calculated by use of the nonideal solution treatment or measured directly from adsorption data, showed good agreement between them. This is considered good validation of the nonideal solution treatment for calculating these quantities.

Table B-1. Surface Tension, Contact Angle and Adhesion Tension of L77 on Polyethylene Substrate

(In Phosphate Buffer Solution, pH=7.00, 25 °C)

C (M)	LogC	γ_{LA} (mN/m)	θ	cosθ	γ_{LA}cosθ
1.25×10^{-6}	-5.90	47.3	96.5°	-0.113	-5.35
2.50×10^{-6}	-5.60	42.6	91.6°	-0.028	-1.19
5.00×10^{-6}	-5.30	38.5	85.2°	0.084	3.22
1.00×10^{-5}	-5.00	34.3	77.5°	0.216	7.42
2.00×10^{-5}	-4.70	29.5	68.1°	0.373	11.00
5.00×10^{-5}	-4.30	24.5	46.8°	0.685	16.77
1.00×10^{-4}	-4.00	22.2	19.6°	0.942	20.91
2.00×10^{-4}	-3.70	21.5	9.6°	0.986	21.20
4.00×10^{-4}	-3.40	21.2	4.4°	0.997	21.14
8.00×10^{-4}	-3.10	21.1	0°	1.000	21.10
1.60×10^{-3}	-2.80	21.0	0°	1.000	21.00
3.20×10^{-3}	-2.49	20.9	0°	1.000	20.90

Table B-2. Surface Tension, Contact Angle and Adhesion Tension of C4P on Polyethylene Substrate

(In Phosphate Buffer Solution, pH=7.00, 25 °C)

C (M)	LogC	γ_{LA} (mN/m)	θ	cosθ	γ_{LA}cosθ
4.00×10^{-4}	-3.40	71.8	96.5°	-0.113	-8.13
8.00×10^{-4}	-3.10	71.4	96.1°	-0.106	-7.59
1.60×10^{-3}	-2.80	70.9	95.8°	-0.101	-7.16
3.20×10^{-3}	-2.49	69.7	95.2°	-0.091	-6.32
6.40×10^{-3}	-2.19	68.1	94.8°	-0.084	-5.70
1.28×10^{-2}	-1.89	65.1	93.9°	-0.068	-4.43
2.56×10^{-2}	-1.59	61.2	91.1°	-0.019	-1.17
5.12×10^{-2}	-1.29	56.9	87.5°	0.044	2.48
0.102	-0.99	51.7	82.7°	0.127	6.57
0.250	-0.60	46.1	75.4°	0.252	11.62
0.500	-0.30	41.8	66.6°	0.397	16.60
1.000	0.00	38.9	57.2°	0.542	21.07

Table B-3. Surface Tension, Contact Angle and Adhesion Tension of CHP on Polyethylene Substrate

(In Phosphate Buffer Solution, pH=7.00, 25 °C)

C (M)	LogC	γ_{LA} (mN/m)	θ	cosθ	γ_{LA}cosθ
2.24×10^{-3}	-2.65	65.6	95.3°	-0.092	-6.06
4.48×10^{-3}	-2.35	60.4	95.5°	-0.096	-5.79
8.96×10^{-3}	-2.05	54.2	95.6°	-0.098	-5.29
1.79×10^{-2}	-1.75	48.3	95.1°	-0.089	-4.29
3.58×10^{-2}	-1.45	44.1	90.7°	-0.012	-0.54
7.16×10^{-2}	-1.15	37.7	83.6°	0.111	4.20
1.43×10^{-1}	-0.84	32.8	72.5°	0.301	9.86

Table B-4. Surface Tension, Contact Angle and Adhesion Tension of C6P on Polyethylene Substrate

(In Phosphate Buffer Solution, pH=7.00, 25 °C)

C (M)	LogC	γ_{LA} (mN/m)	θ	cosθ	γ_{LA}cosθ
1.10×10^{-3}	-2.96	63.2	96.2°	-0.108	-6.83
2.20×10^{-3}	-2.66	56.8	96.1°	-0.106	-6.04
4.40×10^{-3}	-2.36	52.6	95.8°	-0.101	-5.32
8.80×10^{-3}	-2.06	47.7	94.2°	-0.073	-3.49
1.76×10^{-2}	-1.75	42.2	89.1°	0.016	0.66
3.52×10^{-2}	-1.45	36.5	79.8°	0.177	6.46
7.04×10^{-2}	-1.15	31.8	70.4°	0.335	10.67

Table B-5. Surface Tension, Contact Angle and Adhesion Tension of C2,6P on Polyethylene Substrate

(In Phosphate Buffer Solution, pH=7.00, 25 °C)

C (M)	LogC	γ_{LA} (mN/m)	θ	cosθ	γ_{LA}cosθ
7.94×10^{-4}	-3.10	52.1	89.6°	0.007	0.36
1.00×10^{-3}	-3.00	50.5	87.6°	0.042	2.11
1.26×10^{-3}	-2.90	48.4	85.3°	0.082	3.97
1.58×10^{-3}	-2.80	46.8	83.1°	0.120	5.62
2.00×10^{-3}	-2.70	45.2	80.5°	0.165	7.46
2.51×10^{-3}	-2.60	43.6	77.4°	0.218	9.51
3.16×10^{-3}	-2.50	41.8	74.2°	0.272	11.38
3.98×10^{-3}	-2.40	40.2	71.3°	0.321	12.89
5.01×10^{-3}	-2.30	38.4	66.9°	0.392	15.07
6.31×10^{-3}	-2.20	36.8	63.1°	0.452	16.65
7.94×10^{-3}	-2.10	35.1	58.2°	0.527	18.50
1.00×10^{-2}	-2.00	33.3	52.4°	0.610	20.32

Table B-6. Surface Tension, Contact Angle and Adhesion Tension of C8P on Polyethylene Substrate

(In Phosphate Buffer Solution, pH=7.00, 25 °C)

C (M)	LogC	γ_{LA} (mN/m)	θ	cosθ	γ_{LA}cosθ
2.82×10^{-4}	-3.55	57.6	93.8°	-0.066	-3.82
3.98×10^{-4}	-3.40	54.5	91.6°	-0.028	-1.52
5.64×10^{-4}	-3.25	50.8	88.4°	0.028	1.42
7.95×10^{-4}	-3.10	47.2	85.7°	0.075	3.54
1.13×10^{-3}	-2.95	43.8	80.6°	0.163	7.15
1.58×10^{-3}	-2.80	40.9	76.3°	0.237	9.69
2.26×10^{-3}	-2.65	37.1	69.2°	0.355	13.17
3.16×10^{-3}	-2.50	33.5	61.6°	0.476	15.93
4.52×10^{-3}	-2.34	29.6	51.5°	0.623	18.43

Table B-7. Surface Tension, Contact Angle and Adhesion Tension of C10P on Polyethylene Substrate

(In Phosphate Buffer Solution, pH=7.00, 25 °C)

C (M)	LogC	γ_{LA} (mN/m)	θ	cosθ	γ_{LA}cosθ
3.12×10^{-5}	-4.51	53.8	96.4°	-0.111	-6.00
5.24×10^{-5}	-4.28	48.6	95.7°	-0.099	-4.83
8.48×10^{-5}	-4.07	44.4	90.8°	-0.014	-0.62
1.24×10^{-4}	-3.91	40.6	84.6°	0.094	3.82
1.87×10^{-4}	-3.73	36.6	76.5°	0.233	8.54
2.80×10^{-4}	-3.55	32.8	74.8°	0.262	8.60
4.20×10^{-4}	-3.38	29.1	72.7°	0.297	8.65

Table B-8. Surface Tension, Contact Angle and Adhesion Tension of Mixtures of L77 and C4P on Polyethylene Substrate (α_{L77} = 0.029, C4P%wt.=87.1%)

(In Phosphate Buffer Solution, pH=7.00, 25 °C)

C (M)	LogC	γ_{LA} (mN/m)	θ	cosθ	γ_{LA}cosθ
1.51×10^{-5}	-4.82	55.1	94.1°	-0.071	-3.94
3.02×10^{-5}	-4.52	49.5	92.6°	-0.045	-2.25
6.04×10^{-5}	-4.22	44.6	88.5°	0.026	1.17
1.21×10^{-4}	-3.92	38.2	83.5°	0.113	4.32
2.42×10^{-4}	-3.62	33.4	77.5°	0.216	7.23
4.84×10^{-4}	-3.32	29.1	69.2°	0.355	10.33
9.68×10^{-4}	-3.01	26.1	58.4°	0.524	13.68
1.94×10^{-3}	-2.71	25.1	47.5°	0.676	16.96
3.88×10^{-3}	-2.41	24.2	34.5°	0.824	19.94

Table B-9. Surface Tension, Contact Angle and Adhesion Tension of Mixtures of L77 and C4P on Polyethylene Substrate

(α_{L77} = 0.110, C4P%wt.=62.0%)

(In Phosphate Buffer Solution, pH=7.00, 25 °C)

C (M)	LogC	γ_{LA} (mN/m)	θ	cosθ	γ_{LA}cosθ
1.12×10^{-5}	-4.95	51.1	92.2°	-0.038	-1.96
2.24×10^{-5}	-4.65	46.9	91.5°	-0.026	-1.23
4.48×10^{-5}	-4.35	42.3	86.3°	0.065	2.73
8.96×10^{-5}	-4.05	36.5	78.2°	0.204	7.46
1.79×10^{-4}	-3.75	31.4	67.9°	0.376	11.81
3.58×10^{-4}	-3.45	26.2	51.6°	0.621	16.27
7.16×10^{-4}	-3.15	24.3	31.2°	0.855	20.79
1.43×10^{-3}	-2.84	23.3	17.4°	0.954	22.23
2.86×10^{-3}	-2.54	23.2	16.6°	0.958	22.23

Table B-10. Surface Tension, Contact Angle and Adhesion Tension of Mixtures of L77 and C4P on Polyethylene Substrate

(α_{L77} = 0.209, C4P%wt.=43.3%)

(In Phosphate Buffer Solution, pH=7.00, 25 °C)

C (M)	LogC	γ_{LA} (mN/m)	θ	cosθ	γ_{LA}cosθ
1.18×10^{-5}	-4.93	46.3	89.7°	0.005	0.24
2.36×10^{-5}	-4.63	41.5	84.3°	0.099	4.12
4.72×10^{-5}	-4.33	36.8	77.7°	0.213	7.84
9.44×10^{-5}	-4.03	32.8	67.8°	0.378	12.39
1.89×10^{-4}	-3.72	28.2	52.4°	0.610	17.21
3.78×10^{-4}	-3.42	24.6	30.8°	0.859	21.13
7.56×10^{-4}	-3.12	23.2	20.3°	0.938	21.76
1.51×10^{-3}	-2.82	22.9	16.8°	0.957	21.92
3.02×10^{-3}	-2.52	22.8	15.6°	0.963	21.96

Table B-11. Surface Tension, Contact Angle and Adhesion Tension of Mixtures of L77 and C4P on Polyethylene Substrate (α_{L77} = 0.313, C4P%wt.=30.7%)

(In Phosphate Buffer Solution, pH=7.00, 25 °C)

C (M)	LogC	γ_{LA} (mN/m)	θ	cosθ	γ_{LA}cosθ
3.43×10^{-6}	-5.46	48.7	94.1°	-0.071	-3.48
6.85×10^{-6}	-5.16	44.8	90.4°	-0.007	0.31
1.37×10^{-5}	-4.86	40.6	84.5°	0.096	3.89
2.74×10^{-5}	-4.56	36.5	78.9°	0.193	7.03
5.48×10^{-5}	-4.26	32.5	69.8°	0.345	11.22
1.10×10^{-4}	-3.96	28.4	58.5°	0.522	14.84
2.19×10^{-4}	-3.66	24.5	39.5°	0.772	18.90
4.38×10^{-4}	-3.36	22.8	25.3°	0.904	20.61
8.76×10^{-4}	-3.06	22.1	22.3°	0.925	20.45
1.95×10^{-3}	-2.71	22.1	21.5°	0.930	20.56

Table B-12. Surface Tension, Contact Angle and Adhesion Tension of Mixtures of L77 and C4P on Polyethylene Substrate (α_{L77} = 0.475, C4P%wt.=18.2%)

(In Phosphate Buffer Solution, pH=7.00, 25 °C)

C (M)	LogC	γ_{LA} (mN/m)	θ	cosθ	γ_{LA}cosθ
2.81×10^{-6}	-5.55	46.2	94.4°	-0.077	-3.54
5.62×10^{-6}	-5.25	42.1	90.2°	-0.003	-0.15
1.12×10^{-5}	-4.95	38.3	83.2°	0.118	4.53
2.24×10^{-5}	-4.65	34.5	76.4°	0.235	8.11
4.48×10^{-5}	-4.35	30.4	66.2°	0.404	12.27
8.96×10^{-5}	-4.05	26.5	52.5°	0.609	16.13
1.81×10^{-4}	-3.74	23.6	30.8°	0.859	20.27
3.62×10^{-4}	-3.44	22.1	19.6°	0.942	20.82
7.24×10^{-4}	-3.14	21.9	12.4°	0.977	21.39
1.44×10^{-3}	-2.84	22.0	5.5°	0.995	21.90

Table B-13. Surface Tension, Contact Angle and Adhesion Tension of Mixtures of L77 and C4P on Polyethylene Substrate

(α_{L77} = 0.611, C4P%wt.=11.4%)

(In Phosphate Buffer Solution, pH=7.00, 25 °C)

C (M)	LogC	γ_{LA} (mN/m)	θ	cosθ	γ_{LA}cosθ
3.30×10^{-6}	-5.48	44.5	90.5°	-0.009	-0.39
6.61×10^{-6}	-5.18	40.4	85.4°	0.080	3.24
1.35×10^{-5}	-4.87	35.8	78.4°	0.201	7.20
2.40×10^{-5}	-4.62	32.1	70.8°	0.329	10.56
4.27×10^{-5}	-4.37	28.6	61.2°	0.482	13.78
8.32×10^{-5}	-4.08	25.7	46.5°	0.688	17.69
1.45×10^{-4}	-3.84	22.5	30.5°	0.862	19.39
2.90×10^{-4}	-3.54	21.7	16.5°	0.959	20.81
5.80×10^{-4}	-3.24	21.5	12.4°	0.997	21.00
1.16×10^{-3}	-2.94	21.4	8.8°	0.988	21.15

Table B-14. Surface Tension, Contact Angle and Adhesion Tension of Mixtures of L77 and C4P on Polyethylene Substrate (α_{L77} = 0.805, C4P%wt=4.7%)

(In Phosphate Buffer Solution, pH=7.00, 25 °C)

C (M)	LogC	γ_{LA} (mN/m)	θ	cosθ	γ_{LA}cosθ
2.10×10^{-6}	-5.68	45.4	93.6°	-0.063	-2.85
4.22×10^{-6}	-5.37	41.1	88.1°	0.033	1.36
8.44×10^{-6}	-5.07	36.5	82.5°	0.131	4.76
1.69×10^{-5}	-4.77	32.4	73.6°	0.282	9.15
3.42×10^{-5}	-4.47	28.3	62.7°	0.459	12.98
6.84×10^{-5}	-4.16	24.6	46.5°	0.688	16.93
1.77×10^{-4}	-3.75	22.1	25.6°	0.902	19.93
3.54×10^{-4}	-3.45	21.9	18.9°	0.946	20.72
7.01×10^{-4}	-3.15	21.7	10.5°	0.983	21.34
1.40×10^{-3}	-2.85	21.4	5.2°	0.996	21.31

Table B-15. Surface Tension, Contact Angle and Adhesion Tension of Mixtures of L77 and CHP on Polyethylene Substrate (α_{L77} = 0.058, CHP%wt.=79.5%)

(In Phosphate Buffer Solution, pH=7.00, 25 °C)

C (M)	LogC	γ_{LA} (mN/m)	θ	cosθ	γ_{LA}cosθ
2.61×10^{-5}	-4.58	48.3	93.6°	-0.063	-3.03
5.22×10^{-5}	-4.28	43.5	88.9°	0.019	0.84
1.04×10^{-4}	-3.98	38.8	83.1°	0.120	4.66
2.08×10^{-4}	-3.68	34.6	75.7°	0.247	8.55
4.16×10^{-4}	-3.38	30.1	64.5°	0.431	12.96
6.16×10^{-4}	-3.21	27.1	54.2°	0.585	15.85
1.03×10^{-3}	-2.99	26.3	42.4°	0.738	19.42
2.06×10^{-3}	-2.69	25.8	37.5°	0.793	20.47
4.12×10^{-3}	-2.39	25.4	34.5°	0.824	20.93

Table B-16. Surface Tension, Contact Angle and Adhesion Tension of Mixtures of L77 and CHP on Polyethylene Substrate (α_{L77} = 0.115, CHP%wt.=64.7%)

(In Phosphate Buffer Solution, pH=7.00, 25 °C)

C (M)	LogC	γ_{LA} (mN/m)	θ	cosθ	γ_{LA}cosθ
1.32×10^{-5}	-4.88	48.4	94.7°	-0.082	-3.97
2.64×10^{-5}	-4.58	43.9	90.5°	-0.009	-0.38
5.28×10^{-5}	-4.28	39.8	82.9°	0.124	4.92
1.03×10^{-4}	-3.99	35.1	73.4°	0.286	10.03
2.06×10^{-4}	-3.69	31.4	59.7°	0.505	15.84
4.12×10^{-4}	-3.39	26.2	44.8°	0.710	18.59
7.22×10^{-4}	-3.14	24.3	26.1°	0.898	21.82
1.44×10^{-3}	-2.84	24.2	21.2°	0.932	22.56
2.88×10^{-3}	-2.54	24.1	15.4°	0.964	23.23

Table B-17. Surface Tension, Contact Angle and Adhesion Tension of Mixtures of L77 and CHP on Polyethylene Substrate (α_{L77} = 0.253, CHP%wt.=41.3%)

(In Phosphate Buffer Solution, pH=7.00, 25 °C)

C (M)	LogC	γ_{LA} (mN/m)	θ	cosθ	γ_{LA}cosθ
1.16×10^{-5}	-4.94	45.8	94.5°	-0.078	-3.59
2.32×10^{-5}	-4.63	41.5	86.4°	0.063	2.61
4.64×10^{-5}	-4.33	36.8	75.4°	0.252	9.28
9.23×10^{-5}	-4.03	32.8	64.8°	0.426	13.97
1.84×10^{-4}	-3.74	28.2	46.9°	0.683	19.27
3.68×10^{-4}	-3.43	24.1	30.8°	0.859	20.70
7.46×10^{-4}	-3.13	23.4	20.8°	0.935	21.87
1.48×10^{-3}	-2.83	23.3	14.8°	0.967	22.53
2.96×10^{-3}	-2.53	23.2	12.4°	0.977	22.66

Table B-18. Surface Tension, Contact Angle and Adhesion Tension of Mixtures of L77 and CHP on Polyethylene Substrate (α_{L77} = 0.407, CHP%wt.=25.8%)

(In Phosphate Buffer Solution, pH=7.00, 25 °C)

C (M)	LogC	γ_{LA} (mN/m)	θ	cosθ	γ_{LA}cosθ
6.23×10^{-6}	-5.21	46.4	95.2°	-0.091	-4.21
1.24×10^{-5}	-4.91	42.2	91.8°	-0.031	-1.33
2.28×10^{-5}	-4.64	38.3	86.4°	0.063	2.40
4.56×10^{-5}	-4.34	33.9	78.9°	0.193	6.53
9.12×10^{-5}	-4.04	29.3	65.8°	0.410	12.01
1.82×10^{-4}	-3.74	25.4	51.3°	0.625	15.88
3.64×10^{-4}	-3.44	23.2	35.4°	0.815	18.91
7.28×10^{-4}	-3.14	22.6	25.3°	0.904	20.43
1.45×10^{-3}	-2.84	22.5	20.5°	0.937	21.08
2.90×10^{-3}	-2.54	22.4	15.4°	0.964	21.60

Table B-19. Surface Tension, Contact Angle and Adhesion Tension of Mixtures of L77 and CHP on Polyethylene Substrate (α_{L77} = 0.581, CHP%wt.=14.7%)

(In Phosphate Buffer Solution, pH=7.00, 25 °C)

C (M)	LogC	γ_{LA} (mN/m)	θ	cosθ	γ_{LA}cosθ
3.42×10^{-6}	-5.47	45.9	95.6°	-0.098	-4.48
6.84×10^{-6}	-5.16	41.8	90.3°	-0.005	-0.22
1.37×10^{-5}	-4.86	37.9	83.2°	0.118	4.49
2.74×10^{-5}	-4.56	33.9	74.4°	0.269	9.12
5.48×10^{-5}	-4.26	28.9	61.6°	0.476	13.75
8.98×10^{-5}	-4.05	26.0	48.8°	0.659	17.13
1.88×10^{-4}	-3.73	22.9	29.5°	0.870	19.93
3.66×10^{-4}	-3.44	22.1	18.3°	0.949	20.98
7.28×10^{-4}	-3.14	22.1	12.1°	0.978	21.61
1.48×10^{-3}	-2.83	22.1	6.2°	0.994	21.97

Table B-20. Surface Tension, Contact Angle and Adhesion Tension of Mixtures of L77 and CHP on Polyethylene Substrate (α_{L77} = 0.694, CHP%wt.=9.5%)

(In Phosphate Buffer Solution, pH=7.00, 25 °C)

C (M)	LogC	γ_{LA} (mN/m)	θ	cosθ	γ_{LA}cosθ
3.11×10^{-6}	-5.51	44.4	93.5°	-0.061	-2.71
6.22×10^{-6}	-5.21	40.2	88.4°	0.028	1.12
1.24×10^{-5}	-4.91	35.8	82.1°	0.137	4.92
2.48×10^{-5}	-4.61	32.1	72.6°	0.299	9.60
4.96×10^{-5}	-4.30	27.6	58.4°	0.524	14.46
1.01×10^{-4}	-4.00	23.7	38.9°	0.778	18.44
2.02×10^{-4}	-3.69	22.2	25.1°	0.906	20.10
4.04×10^{-4}	-3.39	21.7	14.3°	0.969	21.03
8.08×10^{-4}	-3.09	21.5	12.4°	0.977	21.00
1.61×10^{-3}	-2.79	21.4	5.7°	0.995	21.29

Table B-21. Surface Tension, Contact Angle and Adhesion Tension of Mixtures of L77 and CHP on Polyethylene Substrate

(α_{L77} = 0.838, CHP%wt.=4.4%)

(In Phosphate Buffer Solution, pH=7.00, 25 °C)

C (M)	LogC	γ_{LA} (mN/m)	θ	cosθ	γ_{LA}cosθ
1.92×10^{-6}	-5.72	46.1	95.2°	-0.091	-4.18
3.84×10^{-6}	-5.42	41.7	90.3°	-0.005	-0.22
8.54×10^{-6}	-5.07	36.4	82.7°	0.127	4.63
1.71×10^{-5}	-4.77	31.8	73.8°	0.279	8.87
3.44×10^{-5}	-4.46	27.9	61.6°	0.476	13.27
6.88×10^{-5}	-4.16	24.1	45.6°	0.700	16.86
1.79×10^{-4}	-3.75	22.1	23.6°	0.916	20.25
3.58×10^{-4}	-3.45	21.9	17.9°	0.952	20.84
7.16×10^{-4}	-3.15	21.7	10.6°	0.983	21.33
1.43×10^{-3}	-2.84	21.4	6.5°	0.994	21.26

Table B-22. Surface Tension, Contact Angle and Adhesion Tension of Mixtures of L77 and C6P on Polyethylene Substrate (α_{L77} = 0.028, C6P%wt=89.3%)

(In Phosphate Buffer Solution, pH=7.00, 25 °C)

C (M)	LogC	γ_{LA} (mN/m)	θ	cosθ	γ_{LA}cosθ
2.88×10^{-5}	-4.54	55.2	94.8°	-0.084	-4.62
5.76×10^{-5}	-4.24	49.4	94.5°	-0.078	-3.88
1.15×10^{-4}	-3.94	44.8	93.8°	-0.066	-2.97
2.30×10^{-4}	-3.64	38.2	89.6°	0.007	0.27
4.60×10^{-4}	-3.34	34.4	81.9°	0.141	4.85
9.20×10^{-4}	-3.04	29.2	72.4°	0.302	8.83
1.84×10^{-3}	-2.74	26.2	58.6°	0.521	13.65
3.28×10^{-3}	-2.48	25.9	47.5°	0.676	17.50
5.36×10^{-3}	-2.27	25.7	40.2°	0.764	19.63

Table B-23. Surface Tension, Contact Angle and Adhesion Tension of Mixtures of L77 and C6P on Polyethylene Substrate

(α_{L77} = 0.152, C6P%wt=57.4%)

(In Phosphate Buffer Solution, pH=7.00, 25 °C)

C (M)	LogC	γ_{LA} (mN/m)	θ	cosθ	γ_{LA}cosθ
1.01×10^{-5}	-5.00	50.9	94.0°	-0.070	-3.55
2.02×10^{-5}	-4.69	46.8	92.6°	-0.045	-2.12
4.04×10^{-5}	-4.39	42.5	88.4°	0.028	1.19
8.08×10^{-5}	-4.09	36.6	80.5°	0.165	6.04
1.62×10^{-4}	-3.79	31.8	67.9°	0.376	11.96
3.24×10^{-4}	-3.49	26.2	51.3°	0.625	16.38
6.48×10^{-4}	-3.19	24.2	34.5°	0.824	19.94
1.30×10^{-3}	-2.89	23.8	27.6°	0.886	21.09
2.60×10^{-3}	-2.59	23.8	22.2°	0.926	22.04

Table B-24. Surface Tension, Contact Angle and Adhesion Tension of Mixtures of L77 and C6P on Polyethylene Substrate (α_{L77} = 0.243, C6P%wt=42.9%)

(In Phosphate Buffer Solution, pH=7.00, 25 °C)

C (M)	LogC	γ_{LA} (mN/m)	θ	cosθ	γ_{LA}cosθ
1.08×10^{-5}	-4.97	45.8	91.5°	-0.026	-1.20
2.16×10^{-5}	-4.67	41.2	86.1°	0.068	2.80
4.32×10^{-5}	-4.36	36.3	79.8°	0.177	6.43
8.64×10^{-5}	-4.06	31.8	68.5°	0.367	11.65
1.73×10^{-4}	-3.76	27.2	52.4°	0.610	16.60
3.46×10^{-4}	-3.46	24.6	28.2°	0.881	21.68
6.92×10^{-4}	-3.16	23.5	20.5°	0.937	22.01
1.38×10^{-3}	-2.86	23.5	17.2°	0.955	22.45
2.76×10^{-3}	-2.56	23.4	14.5°	0.968	22.65

Table B-25. Surface Tension, Contact Angle and Adhesion Tension of Mixtures of L77 and C6P on Polyethylene Substrate (α_{L77} = 0.417, C6P%wt=25.2%)

(In Phosphate Buffer Solution, pH=7.00, 25 °C)

C (M)	LogC	γ_{LA} (mN/m)	θ	cosθ	γ_{LA}cosθ
3.23×10^{-6}	-5.49	49.1	93.3°	-0.058	-2.83
6.46×10^{-6}	-5.19	44.8	92.2°	-0.038	-1.72
1.29×10^{-5}	-4.89	40.6	87.8°	0.038	1.56
2.58×10^{-5}	-4.59	36.5	79.6°	0.181	6.59
5.16×10^{-5}	-4.29	32.5	69.8°	0.345	11.22
1.03×10^{-4}	-3.99	28.0	56.4°	0.553	15.49
2.06×10^{-4}	-3.69	23.2	36.8°	0.801	18.58
4.12×10^{-4}	-3.39	22.8	23.3°	0.918	20.94
8.24×10^{-4}	-3.08	22.8	22.3°	0.925	21.09
1.64×10^{-3}	-2.79	22.8	20.7°	0.935	21.33

Table B-26. Surface Tension, Contact Angle and Adhesion Tension of Mixtures of L77 and C6P on Polyethylene Substrate (α_{L77} = 0.574, C6P%wt=15.2%)

(In Phosphate Buffer Solution, pH=7.00, 25 °C)

C (M)	LogC	γ_{LA} (mN/m)	θ	cosθ	γ_{LA}cosθ
2.85×10^{-6}	-5.55	47.2	95.6°	-0.098	-4.61
5.70×10^{-6}	-5.24	43.1	90.5°	-0.009	-0.38
1.06×10^{-5}	-4.97	39.3	84.6°	0.094	3.70
2.12×10^{-5}	-4.67	35.1	76.4°	0.235	8.25
4.24×10^{-5}	-4.37	30.8	66.2°	0.404	12.43
8.48×10^{-5}	-4.07	26.5	51.2°	0.627	16.61
1.70×10^{-4}	-3.77	22.8	27.8°	0.885	20.17
3.41×10^{-4}	-3.47	22.7	18.1°	0.951	21.58
6.82×10^{-4}	-3.17	22.6	13.5°	0.972	21.98
1.36×10^{-3}	-2.87	22.6	7.4°	0.992	22.41

Table B-27. Surface Tension, Contact Angle and Adhesion Tension of Mixtures of L77 and C6P on Polyethylene Substrate (α_{L77} = 0.735, C6P%wt=8.0%)

(In Phosphate Buffer Solution, pH=7.00, 25 °C)

C (M)	LogC	γ_{LA} (mN/m)	θ	cosθ	γ_{LA}cosθ
3.05×10^{-6}	-5.52	44.5	92.8°	-0.049	-2.17
6.10×10^{-6}	-5.21	40.2	87.2°	0.049	1.96
1.22×10^{-5}	-4.91	35.7	80.5°	0.165	5.89
2.44×10^{-5}	-4.61	31.2	70.2°	0.339	10.57
4.48×10^{-5}	-4.35	27.3	59.7°	0.505	13.77
8.96×10^{-5}	-4.05	23.4	42.1°	0.742	17.36
1.80×10^{-4}	-3.74	22.5	26.4°	0.896	20.15
3.60×10^{-4}	-3.44	21.9	18.7°	0.947	20.74
7.20×10^{-4}	-3.14	21.8	12.4°	0.977	21.29
1.44×10^{-3}	-2.84	21.8	6.7°	0.993	21.65

Table B-28. Surface Tension, Contact Angle and Adhesion Tension of Mixtures of L77 and C6P on Polyethylene Substrate (α_{L77} = 0.868, C6P%wt=4.5%)

(In Phosphate Buffer Solution, pH=7.00, 25 °C)

C (M)	LogC	γ_{LA} (mN/m)	θ	cosθ	γ_{LA}cosθ
2.02×10^{-6}	-5.69	45.4	93.8°	-0.066	-3.01
4.04×10^{-6}	-5.39	41.1	87.9°	0.037	1.51
8.08×10^{-6}	-5.09	37.0	82.8°	0.125	4.64
1.62×10^{-5}	-4.79	32.6	74.6°	0.266	8.66
3.24×10^{-5}	-4.49	28.4	63.1°	0.452	12.85
6.48×10^{-5}	-4.19	24.5	45.5°	0.701	17.17
1.30×10^{-4}	-3.89	22.0	24.7°	0.909	19.99
2.60×10^{-4}	-3.59	21.8	16.6°	0.958	20.89
5.20×10^{-4}	-3.28	21.7	11.5°	0.980	21.26
1.04×10^{-3}	-2.98	21.6	6.4°	0.994	21.47

Table B-29. Surface Tension, Contact Angle and Adhesion Tension of Mixtures of L77 and C2,6P on Polyethylene Substrate (α_{L77} = 0.025, C2,6P%wt.=91.6%)

(In Phosphate Buffer Solution, pH=7.00, 25 °C)

C (M)	LogC	γ_{LA} (mN/m)	θ	cosθ	γ_{LA}cosθ
9.20×10^{-5}	-4.04	49.9	95.2°	-0.091	-4.52
1.84×10^{-4}	-3.74	45.3	94.4°	-0.077	-3.48
3.68×10^{-4}	-3.43	40.6	88.1°	0.033	1.35
7.36×10^{-4}	-3.13	36.1	79.6°	0.181	6.52
1.47×10^{-3}	-2.83	31.5	67.6°	0.381	12.00
2.94×10^{-3}	-2.53	26.5	50.8°	0.632	16.75

Table B-30. Surface Tension, Contact Angle and Adhesion Tension of Mixtures of L77 and C2,6P on Polyethylene Substrate

(α_{L77} = 0.096, C2,6P%wt.=72.6%)

(In Phosphate Buffer Solution, pH=7.00, 25 °C)

C (M)	LogC	γ_{LA} (mN/m)	θ	cosθ	γ_{LA}cosθ
1.06×10^{-5}	-4.97	50.6	94.1°	-0.071	-3.62
2.12×10^{-5}	-4.67	46.2	89.2°	0.014	0.65
4.24×10^{-5}	-4.37	42.2	82.9°	0.124	5.22
8.48×10^{-5}	-4.07	37.6	75.2°	0.255	9.60
1.70×10^{-4}	-3.77	32.9	63.3°	0.449	14.78
3.40×10^{-4}	-3.47	28.9	49.5°	0.649	18.77
6.80×10^{-4}	-3.17	24.5	30.2°	0.864	21.17
1.36×10^{-3}	-2.87	23.8	24.9°	0.907	21.59
2.72×10^{-3}	-2.57	23.4	19.1°	0.945	22.11

Table B-31. Surface Tension, Contact Angle and Adhesion Tension of Mixtures of L77 and C2,6P on Polyethylene Substrate

(α_{L77} = 0.220, C2,6P%wt.=49.9%)

(In Phosphate Buffer Solution, pH=7.00, 25 °C)

C (M)	LogC	γ_{LA} (mN/m)	θ	cosθ	γ_{LA}cosθ
1.01×10^{-5}	-5.00	47.1	93.8°	-0.066	-3.12
2.02×10^{-5}	-4.69	42.3	87.1°	0.051	2.14
4.04×10^{-5}	-4.39	37.8	79.5°	0.182	6.89
8.08×10^{-5}	-4.09	33.2	68.2°	0.371	12.33
1.62×10^{-4}	-3.79	29.2	53.6°	0.593	17.33
3.24×10^{-4}	-3.49	24.9	39.8°	0.768	19.13
6.48×10^{-4}	-3.19	23.4	28.4°	0.880	20.58
1.30×10^{-3}	-2.89	23.0	18.4°	0.949	21.82
2.60×10^{-3}	-2.59	22.7	14.6°	0.968	21.97

Table B-32. Surface Tension, Contact Angle and Adhesion Tension of Mixtures of L77 and C2,6P on Polyethylene Substrate (α_{L77} = 0.381, C2,6P%wt.=31.4%)

(In Phosphate Buffer Solution, pH=7.00, 25 °C)

C (M)	LogC	γ_{LA} (mN/m)	θ	cosθ	γ_{LA}cosθ
4.42×10^{-6}	-5.35	47.9	94.6°	-0.080	-3.84
8.82×10^{-6}	-5.05	43.5	93.5°	-0.061	-2.66
1.76×10^{-5}	-4.75	39.6	86.5°	0.061	2.42
3.52×10^{-5}	-4.45	35.1	72.3°	0.304	10.67
7.04×10^{-5}	-4.15	30.8	53.6°	0.593	18.28
1.41×10^{-4}	-3.85	26.6	35.8°	0.811	21.57
2.82×10^{-4}	-3.55	22.5	21.8°	0.928	20.89
5.64×10^{-4}	-3.25	22.3	16.2°	0.960	21.41
1.13×10^{-3}	-2.95	22.1	8.8°	0.988	21.84
2.26×10^{-3}	-2.65	22.1	5.9°	0.995	21.98

Table B-33. Surface Tension, Contact Angle and Adhesion Tension of Mixtures of L77 and C2,6P on Polyethylene Substrate (α_{L77} = 0.501, C2,6P%wt.=21.9%)

(In Phosphate Buffer Solution, pH=7.00, 25 °C)

C (M)	LogC	γ_{LA} (mN/m)	θ	cosθ	γ_{LA}cosθ
2.81×10^{-6}	-5.55	47.6	94.6°	-0.080	-3.82
5.62×10^{-6}	-5.25	43.3	94.3°	-0.075	-3.25
1.12×10^{-5}	-4.95	39.2	91.2°	-0.021	-0.82
2.24×10^{-5}	-4.65	34.8	81.6°	0.146	5.08
4.48×10^{-5}	-4.35	30.7	69.5°	0.350	10.75
8.96×10^{-5}	-4.05	26.9	52.4°	0.610	16.41
1.81×10^{-4}	-3.74	23.6	32.3°	0.845	19.95
3.62×10^{-4}	-3.44	22.3	22.6°	0.923	20.59
7.28×10^{-4}	-3.14	22.2	18.2°	0.950	21.09
1.46×10^{-4}	-2.84	22.1	12.4°	0.977	21.58
2.92×10^{-4}	-2.53	22.0	7.6°	0.991	21.81

Table B-34. Surface Tension, Contact Angle and Adhesion Tension of Mixtures of L77 and C2,6P on Polyethylene Substrate (α_{L77} = 0.651, C2,6P%wt.=13.1%)

(In Phosphate Buffer Solution, pH=7.00, 25 °C)

C (M)	LogC	γ_{LA} (mN/m)	θ	cosθ	γ_{LA}cosθ
2.06×10^{-6}	-5.69	47.1	95.4°	-0.094	-4.43
4.11×10^{-6}	-5.39	43.2	93.3°	-0.058	-2.49
8.22×10^{-6}	-5.09	38.6	89.4°	0.010	0.40
1.64×10^{-5}	-4.79	35.1	81.5°	0.148	5.19
3.28×10^{-5}	-4.48	31.1	71.5°	0.317	9.87
6.56×10^{-5}	-4.18	26.4	55.2°	0.571	15.07
1.31×10^{-4}	-3.88	23.3	25.4°	0.903	21.05
2.64×10^{-4}	-3.58	22.2	22.5°	0.924	20.51
5.28×10^{-4}	-3.28	21.9	15.6°	0.963	21.09
1.06×10^{-3}	-2.97	21.8	8.6°	0.989	21.55
2.12×10^{-3}	-2.67	21.9	7.6°	0.991	21.71

Table B-35. Surface Tension, Contact Angle and Adhesion Tension of Mixtures of L77 and C2,6P on Polyethylene Substrate (α_{L77} = 0.825, C2,6P%wt.=5.6%)

(In Phosphate Buffer Solution, pH=7.00, 25 °C)

C (M)	LogC	γ_{LA} (mN/m)	θ	cosθ	γ_{LA}cosθ
1.66×10^{-6}	-5.78	47.2	95.8°	-0.101	-4.77
3.32×10^{-6}	-5.48	42.9	92.1°	-0.037	-1.57
6.64×10^{-6}	-5.18	38.4	86.2°	0.066	2.54
1.33×10^{-5}	-4.88	34.7	78.1°	0.206	7.16
2.66×10^{-5}	-4.58	30.5	66.6°	0.397	12.11
5.32×10^{-5}	-4.27	25.8	48.5°	0.663	17.10
1.06×10^{-4}	-3.97	23.1	30.7°	0.860	19.86
2.12×10^{-4}	-3.67	21.8	23.5°	0.917	19.99
4.24×10^{-4}	-3.37	21.5	18.6°	0.948	20.38
8.48×10^{-4}	-3.07	21.4	14.8°	0.967	20.69
1.70×10^{-3}	-2.77	21.3	9.4°	0.987	21.01
3.40×10^{-3}	-2.47	21.3	6.6°	0.993	21.16

Table B-36. Surface Tension, Contact Angle and Adhesion Tension of Mixtures of L77 and C8P on Polyethylene Substrate (α_{L77} = 0.085, C8P%wt=75.2%)

(In Phosphate Buffer Solution, pH=7.00, 25 °C)

C (M)	LogC	γ_{LA} (mN/m)	θ	cosθ	γ_{LA}cosθ
2.58×10^{-5}	-4.59	53.2	94.3°	-0.075	-3.99
5.16×10^{-5}	-4.29	47.3	93.8°	-0.066	-3.13
1.03×10^{-4}	-3.99	41.5	90.8°	-0.014	-0.58
2.06×10^{-4}	-3.69	36.2	83.7°	0.110	3.97
4.12×10^{-4}	-3.39	31.4	72.3°	0.304	9.55
8.24×10^{-4}	-3.08	26.4	55.7°	0.564	14.88
1.65×10^{-3}	-2.78	25.2	40.5°	0.760	19.16
3.30×10^{-3}	-2.48	24.5	36.1°	0.808	19.80
5.16×10^{-3}	-2.29	24.5	35.4°	0.815	19.97

Table B-37. Surface Tension, Contact Angle and Adhesion Tension of Mixtures of L77 and C8P on Polyethylene Substrate

(α_{L77} = 0.222, C8P%wt=49.7%)

(In Phosphate Buffer Solution, pH=7.00, 25 °C)

C (M)	LogC	γ_{LA} (mN/m)	θ	cosθ	γ_{LA}cosθ
8.60×10^{-6}	-5.07	50.4	93.9°	-0.068	-3.43
1.72×10^{-5}	-4.76	45.2	92.8°	-0.049	-2.21
3.44×10^{-5}	-4.46	40.3	88.2°	0.031	1.27
6.88×10^{-5}	-4.16	35.2	78.8°	0.194	6.84
1.62×10^{-4}	-3.79	29.6	63.3°	0.449	13.30
3.24×10^{-4}	-3.49	26.2	45.7°	0.698	18.30
6.48×10^{-4}	-3.19	24.2	34.1°	0.828	20.04
1.30×10^{-3}	-2.89	23.8	28.3°	0.880	20.96
2.60×10^{-3}	-2.59	23.8	23.9°	0.914	21.76

Table B-38. Surface Tension, Contact Angle and Adhesion Tension of Mixtures of L77 and C8P on Polyethylene Substrate (α_{L77} = 0.375, C8P%wt=31.9%)

(In Phosphate Buffer Solution, pH=7.00, 25 °C)

C (M)	LogC	γ_{LA} (mN/m)	θ	cosθ	γ_{LA}cosθ
6.92×10^{-6}	-5.16	44.9	95.5°	-0.096	-4.30
1.38×10^{-5}	-4.86	39.5	92.1°	-0.037	-1.45
2.76×10^{-5}	-4.56	35.1	83.6°	0.111	3.91
5.52×10^{-5}	-4.26	30.9	72.9°	0.294	9.09
1.10×10^{-4}	-3.96	26.6	57.5°	0.537	14.29
2.20×10^{-4}	-3.66	23.9	38.1°	0.787	18.81
4.40×10^{-4}	-3.36	23.5	20.5°	0.937	22.01
7.94×10^{-4}	-3.10	23.3	17.2°	0.955	22.26
1.38×10^{-3}	-2.86	23.3	14.5°	0.968	22.56

Table B-39. Surface Tension, Contact Angle and Adhesion Tension of Mixtures of L77 and C8P on Polyethylene Substrate (α_{L77} = 0.535, C8P%wt=19.7%)

(In Phosphate Buffer Solution, pH=7.00, 25 °C)

C (M)	LogC	γ_{LA} (mN/m)	θ	cosθ	γ_{LA}cosθ
3.84×10^{-6}	-5.42	46.1	94.1°	-0.071	-3.30
7.68×10^{-6}	-5.11	41.6	92.8°	-0.049	-2.03
1.54×10^{-5}	-4.81	36.8	85.5°	0.078	2.89
3.08×10^{-5}	-4.51	32.1	76.4°	0.235	7.55
5.86×10^{-5}	-4.23	27.6	64.3°	0.434	11.97
9.84×10^{-5}	-4.01	25.1	51.6°	0.621	15.59
1.85×10^{-4}	-3.73	22.8	32.5°	0.843	19.23
3.70×10^{-4}	-3.43	22.3	25.4°	0.903	20.14
7.40×10^{-4}	-3.13	22.2	21.8°	0.928	20.61
1.28×10^{-3}	-2.89	22.2	20.1°	0.939	20.85

Table B-40. Surface Tension, Contact Angle and Adhesion Tension of Mixtures of L77 and C8P on Polyethylene Substrate

(α_{L77} = 0.660, C8P%wt=12.7%)

(In Phosphate Buffer Solution, pH=7.00, 25 °C)

C (M)	LogC	γ_{LA} (mN/m)	θ	cosθ	γ_{LA}cosθ
3.04×10^{-6}	-5.52	45.8	96.6°	-0.115	-5.26
5.88×10^{-6}	-5.23	41.5	91.5°	-0.026	-1.09
1.18×10^{-5}	-4.93	36.9	84.6°	0.094	3.47
2.36×10^{-5}	-4.63	32.6	76.6°	0.232	7.56
4.72×10^{-5}	-4.33	28.3	64.4°	0.432	12.23
9.44×10^{-5}	-4.03	24.5	47.6°	0.674	16.52
1.87×10^{-4}	-3.73	22.8	27.4°	0.888	20.24
3.78×10^{-4}	-3.42	21.9	17.8°	0.952	20.85
7.56×10^{-4}	-3.12	21.8	14.1°	0.970	21.14
1.51×10^{-3}	-2.82	21.8	8.6°	0.989	21.55

Table B-41. Surface Tension, Contact Angle and Adhesion Tension of Mixtures of L77 and C8P on Polyethylene Substrate (α_{L77} = 0.791, C8P%wt=6.9%)

(In Phosphate Buffer Solution, pH=7.00, 25 °C)

C (M)	LogC	γ_{LA} (mN/m)	θ	cosθ	γ_{LA}cosθ
2.92×10^{-6}	-5.53	44.2	94.3°	-0.075	-3.31
5.84×10^{-6}	-5.23	39.9	88.1°	0.033	1.32
1.17×10^{-5}	-4.93	35.4	80.6°	0.163	5.78
2.34×10^{-5}	-4.63	31.0	70.5°	0.334	10.35
4.68×10^{-5}	-4.33	27.0	56.8°	0.548	14.78
9.36×10^{-5}	-4.03	23.0	38.9°	0.778	17.90
1.88×10^{-4}	-3.73	22.3	25.5°	0.903	20.13
3.76×10^{-4}	-3.42	21.7	17.8°	0.952	20.66
7.52×10^{-4}	-3.12	21.7	13.2°	0.974	21.13
1.50×10^{-3}	-2.82	21.7	7.4°	0.992	21.52

Table B-42. Surface Tension, Contact Angle and Adhesion Tension of Mixtures of L77 and C8P on Polyethylene Substrate (α_{L77} = 0.906, C8P%wt=2.8%)

(In Phosphate Buffer Solution, pH=7.00, 25 °C)

C (M)	LogC	γ_{LA} (mN/m)	θ	cosθ	γ_{LA}cosθ
1.95×10^{-6}	-5.71	45.0	95.2°	-0.091	-4.08
3.90×10^{-6}	-5.41	40.6	89.8°	0.003	0.14
7.80×10^{-6}	-5.11	36.6	82.7°	0.127	4.65
1.56×10^{-5}	-4.81	32.1	74.4°	0.269	8.63
3.12×10^{-5}	-4.51	28.0	62.8°	0.457	12.80
6.24×10^{-5}	-4.20	24.2	44.6°	0.712	17.23
1.25×10^{-4}	-3.90	21.9	22.6°	0.923	20.22
2.50×10^{-4}	-3.60	21.7	15.4°	0.964	20.92
5.00×10^{-4}	-3.30	21.6	12.3°	0.977	21.10
1.00×10^{-3}	-3.00	21.6	7.2°	0.992	21.43

Table B-43. Surface Tension, Contact Angle and Adhesion Tension of Mixtures of L77 and C10P on Polyethylene Substrate (α_{L77} = 0.077, C10P%wt=79.4%)

(In Phosphate Buffer Solution, pH=7.00, 25 °C)

C (M)	LogC	γ_{LA} (mN/m)	θ	cosθ	γ_{LA}cosθ
1.61×10^{-5}	-4.79	50.3	95.7°	-0.099	-5.00
2.42×10^{-5}	-4.62	46.8	93.1°	-0.054	-2.53
3.62×10^{-5}	-4.44	42.9	89.0°	0.017	0.75
5.43×10^{-5}	-4.27	39.5	83.1°	0.120	4.75
8.15×10^{-5}	-4.09	35.8	75.8°	0.245	8.78
1.22×10^{-4}	-3.91	32.4	67.1°	0.389	12.61
1.83×10^{-4}	-3.74	28.8	57.5°	0.537	15.47
3.20×10^{-4}	-3.49	25.7	52.2°	0.613	15.75
4.80×10^{-4}	-3.32	25.5	51.2°	0.627	15.98

Table B-44. Surface Tension, Contact Angle and Adhesion Tension of Mixtures of L77 and C10P on Polyethylene Substrate

(α_{L77} = 0.186, C10P%wt=58.4%)

(In Phosphate Buffer Solution, pH=7.00, 25 °C)

C (M)	LogC	γ_{LA} (mN/m)	θ	cosθ	γ_{LA}cosθ
6.60×10^{-6}	-5.18	49.7	96.7°	-0.117	-5.80
1.18×10^{-5}	-4.93	45.2	96.2°	-0.108	-4.88
1.98×10^{-5}	-4.70	41.0	90.5°	-0.009	-0.36
3.34×10^{-5}	-4.48	36.8	84.4°	0.098	3.59
5.12×10^{-5}	-4.29	33.3	76.2°	0.239	7.94
9.00×10^{-5}	-4.05	28.6	64.3°	0.434	12.40
1.66×10^{-4}	-3.78	25.2	50.4°	0.637	16.06
3.30×10^{-4}	-3.48	24.2	44.5°	0.713	17.26
6.31×10^{-4}	-3.20	24.2	43.6°	0.724	17.52

Table B-45. Surface Tension, Contact Angle and Adhesion Tension of Mixtures of L77 and C10P on Polyethylene Substrate (α_{L77} = 0.307, C10P%wt=42.0%)

(In Phosphate Buffer Solution, pH=7.00, 25 °C)

C (M)	LogC	γ_{LA} (mN/m)	θ	cosθ	γ_{LA}cosθ
7.13×10^{-6}	-5.15	45.7	96.5°	-0.113	-5.17
1.43×10^{-5}	-4.84	40.6	90.2°	-0.003	-0.14
2.86×10^{-5}	-4.54	35.3	81.4°	0.150	5.28
5.72×10^{-5}	-4.24	30.6	69.3°	0.353	10.82
1.14×10^{-4}	-3.94	26.2	55.5°	0.566	14.84
1.88×10^{-4}	-3.73	23.6	40.2°	0.764	18.03
3.46×10^{-4}	-3.46	23.5	37.5°	0.793	18.64
5.72×10^{-4}	-3.24	23.4	37.3°	0.795	18.61

Table B-46. Surface Tension, Contact Angle and Adhesion Tension of Mixtures of L77 and C10P on Polyethylene Substrate (α_{L77} = 0.435, C10P%wt=29.5%)

(In Phosphate Buffer Solution, pH=7.00, 25 °C)

C (M)	LogC	γ_{LA} (mN/m)	θ	cosθ	γ_{LA}cosθ
4.01×10^{-6}	-5.40	46.6	96.2°	-0.108	-5.03
8.02×10^{-6}	-5.10	41.9	93.3°	-0.058	-2.41
1.60×10^{-5}	-4.80	37.0	85.4°	0.080	2.97
3.20×10^{-5}	-4.49	32.3	75.6°	0.249	8.03
6.40×10^{-5}	-4.19	27.6	61.8°	0.473	13.04
1.08×10^{-4}	-3.97	24.1	48.7°	0.660	15.91
2.00×10^{-4}	-3.70	23.1	35.4°	0.815	18.83
3.00×10^{-4}	-3.52	23.0	34.1°	0.828	19.05
4.00×10^{-4}	-3.40	22.9	32.8°	0.841	19.25

Table B-47. Surface Tension, Contact Angle and Adhesion Tension of Mixtures of L77 and C10P on Polyethylene Substrate (α_{L77} = 0.575, C10P%wt=19.2%)

(In Phosphate Buffer Solution, pH=7.00, 25 °C)

C (M)	LogC	γ_{LA} (mN/m)	θ	cosθ	γ_{LA}cosθ
3.12×10^{-6}	-5.51	46.1	96.8°	-0.118	-5.46
6.24×10^{-6}	-5.20	41.7	91.8°	-0.031	-1.31
1.25×10^{-5}	-4.90	37.2	84.7°	0.092	3.44
2.50×10^{-5}	-4.60	32.8	75.6°	0.249	8.16
5.00×10^{-5}	-4.30	28.5	63.2°	0.451	12.85
8.00×10^{-5}	-4.10	25.7	52.8°	0.605	15.54
1.60×10^{-4}	-3.80	23.3	34.5°	0.824	19.20
3.20×10^{-4}	-3.49	22.8	30.8°	0.859	19.58
6.40×10^{-4}	-3.19	22.7	29.5°	0.870	19.76

Table B-48. Surface Tension, Contact Angle and Adhesion Tension of Mixtures of L77 and C10P on Polyethylene Substrate (α_{L77} = 0.707, C10P%wt=11.8%)

(In Phosphate Buffer Solution, pH=7.00, 25 °C)

C (M)	LogC	γ_{LA} (mN/m)	θ	cosθ	γ_{LA}cosθ
3.02×10^{-6}	-5.52	44.2	95.6°	-0.098	-4.31
6.04×10^{-6}	-5.22	39.8	89.7°	0.005	0.21
1.21×10^{-5}	-4.92	35.5	82.3°	0.134	4.76
2.42×10^{-5}	-4.62	31.1	72.5°	0.301	9.35
4.84×10^{-5}	-4.32	27.2	60.7°	0.489	13.31
9.68×10^{-5}	-4.01	23.0	40.8°	0.757	17.41
1.94×10^{-4}	-3.71	22.3	27.6°	0.886	19.76
3.88×10^{-4}	-3.41	22.5	25.5°	0.903	20.31
7.76×10^{-4}	-3.11	22.4	24.2°	0.912	20.43

Table B-49. Surface Tension, Contact Angle and Adhesion Tension of Mixtures of L77 and C10P on Polyethylene Substrate

(α_{L77} = 0.867, C10P%wt=4.7%)

(In Phosphate Buffer Solution, pH=7.00, 25 °C)

C (M)	LogC	γ_{LA} (mN/m)	θ	cosθ	γ_{LA}cosθ
2.12×10^{-6}	-5.67	44.8	95.4°	-0.094	-4.22
4.24×10^{-6}	-5.37	40.4	90.5°	-0.009	-0.35
8.48×10^{-6}	-5.07	36.3	83.4°	0.115	4.17
1.70×10^{-5}	-4.77	31.8	74.8°	0.262	8.34
3.40×10^{-5}	-4.47	27.8	62.4°	0.463	12.88
6.80×10^{-5}	-4.17	24.1	45.7°	0.698	16.83
1.20×10^{-4}	-3.92	21.9	24.4°	0.911	19.94
2.40×10^{-4}	-3.62	21.9	20.7°	0.935	20.49
4.80×10^{-4}	-3.32	21.9	18.5°	0.948	20.77

Table B-50. Adsorption of Mixtures of L77 and C4P on the Powdered Polyethylene

Volume of solution = 40.00 mL, Fixed initial α_{L77} = 0.034
Specific area of the polyethylene power, S=0.360 m^2/g

$C_{ini.}$ Total (M)	$C_{ini.}$ L77 (M)	$C_{ini.}$ C4P (M)	Powder (g)	$C_{eq.}$ L77 (M)	Ads. L77 (mol/cm^2)
5.00×10^{-5}	1.70×10^{-6}	4.83×10^{-5}	0.4985	6.50×10^{-8}	3.60×10^{-11}
1.00×10^{-4}	3.40×10^{-6}	9.66×10^{-5}	0.5126	2.25×10^{-7}	6.90×10^{-11}
1.75×10^{-4}	5.95×10^{-6}	1.69×10^{-4}	0.5012	1.25×10^{-6}	1.04×10^{-10}
2.50×10^{-4}	8.50×10^{-6}	2.42×10^{-4}	0.4998	3.33×10^{-6}	1.15×10^{-10}
4.00×10^{-4}	1.36×10^{-5}	3.86×10^{-4}	0.5146	7.48×10^{-6}	1.32×10^{-10}
7.50×10^{-4}	2.55×10^{-5}	7.25×10^{-4}	0.5004	1.84×10^{-5}	1.59×10^{-10}
1.00×10^{-3}	3.40×10^{-5}	9.66×10^{-4}	0.4895	2.62×10^{-5}	1.78×10^{-10}
1.50×10^{-3}	5.10×10^{-5}	1.45×10^{-3}	0.5205	4.18×10^{-5}	1.96×10^{-10}
2.00×10^{-3}	6.80×10^{-5}	1.93×10^{-3}	0.5007	5.82×10^{-5}	2.18×10^{-10}

$C_{eq.}$ C4P (M)	Ads. C4P (mol/cm^2)	$C_{eq.}$ Total (M)	Ads. Total (mol/cm^2)	α_{L77} (eq.) (bulk soln.)	X_{L77} (eq.) (ads. layer)
4.62×10^{-5}	4.60×10^{-11}	4.63×10^{-5}	8.20×10^{-11}	0.001	0.440
9.42×10^{-5}	5.30×10^{-11}	9.44×10^{-5}	1.22×10^{-10}	0.002	0.566
1.66×10^{-4}	6.90×10^{-11}	1.67×10^{-4}	1.73×10^{-10}	0.007	0.603
2.38×10^{-4}	7.60×10^{-11}	2.41×10^{-4}	1.91×10^{-10}	0.014	0.603
3.83×10^{-4}	8.40×10^{-11}	3.90×10^{-4}	2.16×10^{-10}	0.019	0.613
7.21×10^{-4}	8.50×10^{-11}	7.39×10^{-4}	2.43×10^{-10}	0.025	0.653
9.62×10^{-4}	8.60×10^{-11}	9.88×10^{-4}	2.63×10^{-10}	0.026	0.675
1.44×10^{-3}	8.70×10^{-11}	1.49×10^{-3}	2.83×10^{-10}	0.028	0.694
1.93×10^{-3}	8.80×10^{-11}	1.99×10^{-3}	3.06×10^{-10}	0.029	0.712

Table B-51. Adsorption of Mixtures of L77 and C4P on the Powdered Polyethylene

Volume of solution = 40.00 mL, Fixed initial α_{L77} = 0.137
Specific area of the polyethylene power, S=0.360 m^2/g

$C_{ini.}$ Total (M)	$C_{ini.}$ L77 (M)	$C_{ini.}$ C4P (M)	Powder (g)	$C_{eq.}$ L77 (M)	Ads. L77 (mol/cm^2)
2.00×10^{-5}	2.74×10^{-6}	1.73×10^{-5}	0.5012	8.30×10^{-7}	4.20×10^{-11}
5.00×10^{-5}	6.85×10^{-6}	4.32×10^{-5}	0.5223	3.50×10^{-6}	7.10×10^{-11}
7.50×10^{-5}	1.03×10^{-5}	6.47×10^{-5}	0.4986	5.58×10^{-6}	1.05×10^{-10}
1.00×10^{-4}	1.37×10^{-5}	8.63×10^{-5}	0.5004	8.05×10^{-6}	1.25×10^{-10}
1.50×10^{-4}	2.06×10^{-5}	1.29×10^{-4}	0.5125	1.28×10^{-5}	1.69×10^{-10}
2.00×10^{-4}	2.74×10^{-5}	1.73×10^{-4}	0.4896	1.91×10^{-5}	1.89×10^{-10}
2.50×10^{-4}	3.43×10^{-5}	2.16×10^{-4}	0.5200	2.43×10^{-5}	2.13×10^{-10}
3.00×10^{-4}	4.11×10^{-5}	2.59×10^{-4}	0.5147	3.02×10^{-5}	2.34×10^{-10}
3.50×10^{-4}	4.80×10^{-5}	3.02×10^{-4}	0.4873	3.69×10^{-5}	2.51×10^{-10}

$C_{eq.}$ C4P (M)	Ads. C4P (mol/cm^2)	$C_{eq.}$ Total (M)	Ads. Total (mol/cm^2)	α_{L77} (eq.) (bulk soln.)	X_{L77} (eq.) (ads. layer)
1.65×10^{-5}	1.70×10^{-11}	1.73×10^{-5}	5.90×10^{-11}	0.048	0.717
4.21×10^{-5}	2.30×10^{-11}	4.56×10^{-5}	9.40×10^{-11}	0.077	0.761
6.34×10^{-5}	3.10×10^{-11}	6.89×10^{-5}	1.36×10^{-10}	0.081	0.774
8.47×10^{-5}	3.50×10^{-11}	9.28×10^{-5}	1.60×10^{-10}	0.087	0.782
1.27×10^{-4}	4.80×10^{-11}	1.40×10^{-4}	2.17×10^{-10}	0.091	0.780
1.70×10^{-4}	5.50×10^{-11}	1.89×10^{-4}	2.45×10^{-10}	0.101	0.775
2.13×10^{-4}	6.50×10^{-11}	2.37×10^{-4}	2.78×10^{-10}	0.103	0.765
2.55×10^{-4}	7.60×10^{-11}	2.86×10^{-4}	3.10×10^{-10}	0.106	0.757
2.98×10^{-4}	8.40×10^{-11}	3.35×10^{-4}	3.35×10^{-10}	0.110	0.751

Table B-52. Adsorption of Mixtures of L77 and C4P on the Powdered Polyethylene

Volume of solution = 40.00 mL, Fixed initial α_{L77} = 0.243
Specific area of the polyethylene power, S=0.360 m^2/g

$C_{ini.}$ Total (M)	$C_{ini.}$ L77 (M)	$C_{ini.}$ C4P (M)	Powder (g)	$C_{eq.}$ L77 (M)	Ads. L77 (mol/cm^2)
2.00×10^{-5}	4.86×10^{-6}	1.51×10^{-5}	0.4986	2.60×10^{-7}	1.02×10^{-10}
3.00×10^{-5}	7.29×10^{-6}	2.27×10^{-5}	0.4900	6.15×10^{-7}	1.51×10^{-10}
4.00×10^{-5}	9.72×10^{-6}	3.03×10^{-5}	0.5014	1.12×10^{-6}	1.91×10^{-10}
5.00×10^{-5}	1.22×10^{-5}	3.79×10^{-5}	0.5247	1.50×10^{-6}	2.25×10^{-10}
6.00×10^{-5}	1.46×10^{-5}	4.54×10^{-5}	0.4862	3.23×10^{-6}	2.59×10^{-10}
7.50×10^{-5}	1.82×10^{-5}	5.68×10^{-5}	0.4972	5.60×10^{-6}	2.81×10^{-10}
1.00×10^{-4}	2.43×10^{-5}	7.57×10^{-5}	0.5183	1.05×10^{-5}	2.94×10^{-10}
2.00×10^{-4}	4.86×10^{-5}	1.51×10^{-4}	0.5005	3.51×10^{-5}	3.00×10^{-10}
3.00×10^{-4}	7.29×10^{-5}	2.27×10^{-4}	0.5123	5.90×10^{-5}	3.01×10^{-10}

$C_{eq.}$ C4P (M)	Ads. C4P (mol/cm^2)	$C_{eq.}$ Total (M)	Ads. Total (mol/cm^2)	α_{L77} (eq.) (bulk soln.)	X_{L77} (eq.) (ads. layer)
1.17×10^{-5}	7.70×10^{-11}	1.20×10^{-5}	1.79×10^{-10}	0.022	0.571
1.90×10^{-5}	8.40×10^{-11}	1.96×10^{-5}	2.35×10^{-10}	0.031	0.643
2.65×10^{-5}	8.50×10^{-11}	2.76×10^{-5}	2.76×10^{-10}	0.041	0.692
3.38×10^{-5}	8.60×10^{-11}	3.53×10^{-5}	3.11×10^{-10}	0.042	0.724
4.16×10^{-5}	8.70×10^{-11}	4.49×10^{-5}	3.46×10^{-10}	0.072	0.749
5.29×10^{-5}	8.80×10^{-11}	5.85×10^{-5}	3.69×10^{-10}	0.096	0.764
7.16×10^{-5}	8.90×10^{-11}	8.21×10^{-5}	3.83×10^{-10}	0.128	0.772
1.47×10^{-4}	9.00×10^{-11}	1.82×10^{-4}	3.90×10^{-10}	0.193	0.767
2.23×10^{-4}	9.10×10^{-11}	2.82×10^{-4}	3.92×10^{-10}	0.209	0.768

Table B-53. Adsorption of Mixtures of L77 and C4P on the Powdered Polyethylene

Volume of solution = 40.00 mL, Fixed initial α_{L77} = 0.353
Specific area of the polyethylene power, S=0.360 m^2/g

$C_{ini.}$ Total (M)	$C_{ini.}$ L77 (M)	$C_{ini.}$ C4P (M)	Powder (g)	$C_{eq.}$ L77 (M)	Ads. L77 (mol/cm^2)
1.20×10^{-5}	4.24×10^{-6}	7.76×10^{-6}	0.5124	1.40×10^{-7}	8.90×10^{-11}
2.40×10^{-5}	8.50×10^{-6}	1.55×10^{-5}	0.5006	4.00×10^{-7}	1.80×10^{-10}
3.00×10^{-5}	1.06×10^{-5}	1.94×10^{-5}	0.4995	9.00×10^{-7}	2.16×10^{-10}
4.00×10^{-5}	1.41×10^{-5}	2.59×10^{-5}	0.5007	2.50×10^{-6}	2.59×10^{-10}
5.00×10^{-5}	1.77×10^{-5}	3.23×10^{-5}	0.5101	5.20×10^{-6}	2.71×10^{-10}
7.50×10^{-5}	2.65×10^{-5}	4.85×10^{-5}	0.5007	1.38×10^{-5}	2.82×10^{-10}
1.00×10^{-4}	3.53×10^{-5}	6.47×10^{-5}	0.4925	2.27×10^{-5}	2.84×10^{-10}
1.50×10^{-4}	5.30×10^{-5}	9.70×10^{-5}	0.4987	4.01×10^{-5}	2.87×10^{-10}
2.00×10^{-4}	7.10×10^{-5}	1.29×10^{-4}	0.5114	5.74×10^{-5}	2.87×10^{-10}

$C_{eq.}$ C4P (M)	Ads. C4P (mol/cm^2)	$C_{eq.}$ Total (M)	Ads. Total (mol/cm^2)	α_{L77} (eq.) (bulk soln.)	X_{L77} (eq.) (ads. layer)
5.46×10^{-6}	5.00×10^{-11}	5.60×10^{-6}	1.39×10^{-10}	0.024	0.640
1.30×10^{-5}	5.70×10^{-11}	1.34×10^{-5}	2.37×10^{-10}	0.028	0.759
1.67×10^{-5}	6.00×10^{-11}	1.76×10^{-5}	2.76×10^{-10}	0.051	0.782
2.30×10^{-5}	6.30×10^{-11}	2.55×10^{-5}	3.22×10^{-10}	0.097	0.803
2.93×10^{-5}	6.80×10^{-11}	3.45×10^{-5}	3.38×10^{-10}	0.152	0.800
4.53×10^{-5}	7.20×10^{-11}	5.91×10^{-5}	3.53×10^{-10}	0.233	0.797
6.14×10^{-5}	7.60×10^{-11}	8.41×10^{-5}	3.59×10^{-10}	0.270	0.790
9.36×10^{-5}	7.70×10^{-11}	1.34×10^{-4}	3.65×10^{-10}	0.300	0.788
1.26×10^{-4}	8.00×10^{-11}	1.83×10^{-4}	3.68×10^{-10}	0.313	0.781

Table B-54. Adsorption of Mixtures of L77 and C4P on the Powdered Polyethylene

Volume of solution = 40.00 mL, Fixed initial α_{L77} = 0.503
Specific area of the polyethylene power, S=0.360 m^2/g

$C_{ini.}$ Total (M)	$C_{ini.}$ L77 (M)	$C_{ini.}$ C4P (M)	Powder (g)	$C_{eq.}$ L77 (M)	Ads. L77 (mol/cm^2)
1.00×10^{-5}	5.03×10^{-6}	4.97×10^{-6}	0.5006	5.80×10^{-7}	9.90×10^{-11}
1.50×10^{-5}	7.55×10^{-6}	7.45×10^{-6}	0.4987	9.45×10^{-7}	1.47×10^{-10}
2.00×10^{-5}	1.01×10^{-5}	9.90×10^{-6}	0.5142	1.44×10^{-6}	1.86×10^{-10}
2.50×10^{-5}	1.26×10^{-5}	1.24×10^{-5}	0.5000	2.43×10^{-6}	2.25×10^{-10}
5.00×10^{-5}	2.52×10^{-5}	2.48×10^{-5}	0.5045	1.29×10^{-5}	2.71×10^{-10}
7.50×10^{-5}	3.77×10^{-5}	3.73×10^{-5}	0.4975	2.51×10^{-5}	2.83×10^{-10}
1.00×10^{-4}	5.03×10^{-5}	4.97×10^{-5}	0.5125	3.73×10^{-5}	2.81×10^{-10}
1.50×10^{-4}	7.55×10^{-5}	7.45×10^{-5}	0.5004	6.28×10^{-5}	2.85×10^{-10}
2.00×10^{-4}	1.01×10^{-4}	9.90×10^{-5}	0.5015	8.76×10^{-5}	2.87×10^{-10}

$C_{eq.}$ C4P (M)	Ads. C4P (mol/cm^2)	$C_{eq.}$ Total (M)	Ads. Total (mol/cm^2)	α_{L77} (eq.) (bulk soln.)	X_{L77} (eq.) (ads. layer)
4.52×10^{-6}	1.00×10^{-11}	5.10×10^{-6}	1.09×10^{-10}	0.114	0.907
6.78×10^{-6}	1.50×10^{-11}	7.73×10^{-6}	1.62×10^{-10}	0.122	0.907
9.07×10^{-6}	1.90×10^{-11}	1.05×10^{-5}	2.05×10^{-10}	0.137	0.908
1.15×10^{-5}	2.10×10^{-11}	1.39×10^{-5}	2.46×10^{-10}	0.174	0.916
2.38×10^{-5}	2.40×10^{-11}	3.66×10^{-5}	2.95×10^{-10}	0.351	0.920
3.61×10^{-5}	2.70×10^{-11}	6.11×10^{-5}	3.10×10^{-10}	0.410	0.912
4.82×10^{-5}	3.30×10^{-11}	8.55×10^{-5}	3.14×10^{-10}	0.437	0.895
7.29×10^{-5}	3.60×10^{-11}	1.36×10^{-4}	3.21×10^{-10}	0.462	0.888
9.74×10^{-5}	3.90×10^{-11}	1.85×10^{-4}	3.26×10^{-10}	0.473	0.879

Table B-55. Adsorption of Mixtures of L77 and C4P on the Powdered Polyethylene

Volume of solution = 40.00 mL, Fixed initial α_{L77} = 0.634
Specific area of the polyethylene power, S=0.360 m^2/g

$C_{ini.}$ Total (M)	$C_{ini.}$ L77 (M)	$C_{ini.}$ C4P (M)	Powder (g)	$C_{eq.}$ L77 (M)	Ads. L77 (mol/cm^2)
1.00×10^{-5}	6.34×10^{-6}	3.66×10^{-6}	0.4985	1.74×10^{-6}	1.03×10^{-10}
2.00×10^{-5}	1.27×10^{-5}	7.33×10^{-6}	0.5016	4.08×10^{-6}	1.91×10^{-10}
3.00×10^{-5}	1.90×10^{-5}	1.10×10^{-5}	0.5203	8.00×10^{-6}	2.35×10^{-10}
4.00×10^{-5}	2.54×10^{-5}	1.46×10^{-5}	0.5113	1.36×10^{-5}	2.56×10^{-10}
5.00×10^{-5}	3.17×10^{-5}	1.83×10^{-5}	0.5007	1.98×10^{-5}	2.65×10^{-10}
7.50×10^{-5}	4.75×10^{-5}	2.75×10^{-5}	0.4983	3.51×10^{-5}	2.78×10^{-10}
1.00×10^{-4}	6.34×10^{-5}	3.66×10^{-5}	0.4975	5.09×10^{-5}	2.80×10^{-10}
1.50×10^{-4}	9.51×10^{-5}	5.49×10^{-5}	0.5064	8.22×10^{-5}	2.83×10^{-10}
2.00×10^{-4}	1.27×10^{-4}	7.30×10^{-5}	0.5047	1.14×10^{-4}	2.84×10^{-10}

$C_{eq.}$ C4P (M)	Ads. C4P (mol/cm^2)	$C_{eq.}$ Total (M)	Ads. Total (mol/cm^2)	α_{L77} (eq.) (bulk soln.)	X_{L77} (eq.) (ads. layer)
3.41×10^{-6}	6.00×10^{-12}	5.15×10^{-6}	1.08×10^{-10}	0.338	0.948
7.00×10^{-6}	7.00×10^{-12}	1.11×10^{-5}	1.98×10^{-10}	0.368	0.964
1.06×10^{-5}	8.00×10^{-12}	1.86×10^{-5}	2.43×10^{-10}	0.430	0.967
1.42×10^{-5}	1.00×10^{-11}	2.78×10^{-5}	2.66×10^{-10}	0.489	0.963
1.78×10^{-5}	1.10×10^{-11}	3.76×10^{-5}	2.76×10^{-10}	0.526	0.962
2.69×10^{-5}	1.20×10^{-11}	6.20×10^{-5}	2.92×10^{-10}	0.566	0.960
3.60×10^{-5}	1.30×10^{-11}	8.69×10^{-5}	2.96×10^{-10}	0.585	0.956
5.43×10^{-5}	1.40×10^{-11}	1.36×10^{-4}	2.98×10^{-10}	0.602	0.954
7.26×10^{-5}	1.40×10^{-11}	1.86×10^{-4}	2.98×10^{-10}	0.611	0.953

Table B-56. Adsorption of Mixtures of L77 and C4P on the Powdered Polyethylene

Volume of solution = 40.00 mL, Fixed initial α_{L77} = 0.819
Specific area of the polyethylene power, S=0.360 m^2/g

$C_{ini.}$ Total (M)	$C_{ini.}$ L77 (M)	$C_{ini.}$ C4P (M)	Powder (g)	$C_{eq.}$ L77 (M)	Ads. L77 (mol/cm^2)
7.50×10^{-6}	6.14×10^{-6}	1.36×10^{-6}	0.5102	2.25×10^{-6}	8.40×10^{-11}
1.00×10^{-5}	8.19×10^{-6}	1.81×10^{-6}	0.5006	3.09×10^{-6}	1.13×10^{-10}
1.50×10^{-5}	1.23×10^{-5}	2.70×10^{-6}	0.4974	4.74×10^{-6}	1.68×10^{-10}
3.00×10^{-5}	2.46×10^{-5}	5.40×10^{-6}	0.4995	1.43×10^{-5}	2.28×10^{-10}
5.00×10^{-5}	4.10×10^{-5}	9.00×10^{-6}	0.5100	2.90×10^{-5}	2.60×10^{-10}
7.50×10^{-5}	6.14×10^{-5}	1.36×10^{-5}	0.5005	4.93×10^{-5}	2.69×10^{-10}
1.00×10^{-4}	8.19×10^{-5}	1.81×10^{-5}	0.5112	6.95×10^{-5}	2.70×10^{-10}
1.25×10^{-4}	1.02×10^{-4}	2.30×10^{-5}	0.4987	9.01×10^{-5}	2.70×10^{-10}
1.50×10^{-4}	1.23×10^{-4}	2.70×10^{-5}	0.5061	1.10×10^{-4}	2.74×10^{-10}

$C_{eq.}$ C4P (M)	Ads. C4P (mol/cm^2)	$C_{eq.}$ Total (M)	Ads. Total (mol/cm^2)	α_{L77} (eq.) (bulk soln.)	X_{L77} (eq.) (ads. layer)
1.20×10^{-6}	4.00×10^{-12}	3.45×10^{-6}	8.80×10^{-11}	0.654	0.960
1.57×10^{-6}	5.00×10^{-12}	4.66×10^{-6}	1.18×10^{-10}	0.663	0.955
2.42×10^{-6}	5.00×10^{-12}	7.16×10^{-6}	1.73×10^{-10}	0.662	0.963
5.12×10^{-6}	6.00×10^{-12}	1.94×10^{-5}	2.34×10^{-10}	0.736	0.971
8.73×10^{-6}	6.00×10^{-12}	3.77×10^{-5}	2.66×10^{-10}	0.769	0.974
1.32×10^{-5}	7.00×10^{-12}	6.26×10^{-5}	2.76×10^{-10}	0.788	0.973
1.78×10^{-5}	7.00×10^{-12}	8.72×10^{-5}	2.77×10^{-10}	0.796	0.973
2.23×10^{-5}	8.00×10^{-12}	1.12×10^{-4}	2.78×10^{-10}	0.802	0.972
2.68×10^{-5}	8.00×10^{-12}	1.37×10^{-4}	2.82×10^{-10}	0.805	0.972

Table B-57. Adsorption of Mixtures of L77 and CHP on the Powdered Polyethylene

Volume of solution = 40.00 mL, Fixed initial α_{L77} = 0.067
Specific area of the polyethylene power, S=0.360 m^2/g

$C_{ini.}$ Total (M)	$C_{ini.}$ L77 (M)	$C_{ini.}$ CHP (M)	Powder (g)	$C_{eq.}$ L77 (M)	Ads. L77 (mol/cm^2)
2.50×10^{-5}	1.70×10^{-6}	2.33×10^{-5}	0.5102	3.40×10^{-7}	2.80×10^{-11}
5.00×10^{-5}	3.30×10^{-6}	4.67×10^{-5}	0.5008	7.50×10^{-7}	5.80×10^{-11}
7.50×10^{-5}	5.00×10^{-6}	7.00×10^{-5}	0.4975	1.38×10^{-6}	8.20×10^{-11}
1.00×10^{-4}	6.70×10^{-6}	9.33×10^{-5}	0.5113	1.78×10^{-6}	1.07×10^{-10}
1.25×10^{-4}	8.30×10^{-6}	1.17×10^{-4}	0.5006	2.25×10^{-6}	1.36×10^{-10}
2.50×10^{-4}	1.70×10^{-5}	2.33×10^{-4}	0.5012	9.10×10^{-6}	1.70×10^{-10}
5.00×10^{-4}	3.30×10^{-5}	4.67×10^{-4}	0.4984	2.49×10^{-5}	1.91×10^{-10}
7.50×10^{-4}	5.00×10^{-5}	7.00×10^{-4}	0.5022	4.11×10^{-5}	2.04×10^{-10}
1.00×10^{-3}	6.70×10^{-5}	9.33×10^{-4}	0.5117	5.74×10^{-5}	2.08×10^{-10}

$C_{eq.}$ CHP (M)	Ads. CHP (mol/cm^2)	$C_{eq.}$ Total (M)	Ads. Total (mol/cm^2)	α_{L77} (eq.) (bulk soln.)	X_{L77} (eq.) (ads. layer)
2.15×10^{-5}	4.10×10^{-11}	2.18×10^{-5}	6.90×10^{-11}	0.016	0.416
4.41×10^{-5}	5.70×10^{-11}	4.49×10^{-5}	1.15×10^{-10}	0.017	0.505
6.69×10^{-5}	6.90×10^{-11}	6.83×10^{-5}	1.51×10^{-10}	0.020	0.541
8.99×10^{-5}	7.50×10^{-11}	9.16×10^{-5}	1.82×10^{-10}	0.019	0.588
1.13×10^{-4}	7.90×10^{-11}	1.15×10^{-4}	2.15×10^{-10}	0.020	0.633
2.29×10^{-4}	9.00×10^{-11}	2.38×10^{-4}	2.60×10^{-10}	0.038	0.654
4.62×10^{-4}	1.03×10^{-10}	4.87×10^{-4}	2.94×10^{-10}	0.051	0.650
6.95×10^{-4}	1.08×10^{-10}	7.36×10^{-4}	3.12×10^{-10}	0.056	0.654
9.28×10^{-4}	1.15×10^{-10}	9.85×10^{-4}	3.23×10^{-10}	0.058	0.645

Table B-58. Adsorption of Mixtures of L77 and CHP on the Powdered Polyethylene

Volume of solution = 40.00 mL, Fixed initial α_{L77} = 0.136
Specific area of the polyethylene power, S=0.360 m^2/g

$C_{ini.}$ Total (M)	$C_{ini.}$ L77 (M)	$C_{ini.}$ CHP (M)	Powder (g)	$C_{eq.}$ L77 (M)	Ads. L77 (mol/cm^2)
1.25×10^{-5}	1.70×10^{-6}	1.08×10^{-5}	0.4876	2.95×10^{-7}	3.20×10^{-11}
2.50×10^{-5}	3.40×10^{-6}	2.16×10^{-5}	0.4994	7.00×10^{-7}	6.00×10^{-11}
5.00×10^{-5}	6.80×10^{-6}	4.32×10^{-5}	0.5105	1.65×10^{-6}	1.12×10^{-10}
7.50×10^{-5}	1.02×10^{-5}	6.48×10^{-5}	0.5003	2.60×10^{-6}	1.69×10^{-10}
1.00×10^{-4}	1.36×10^{-5}	8.64×10^{-5}	0.5102	4.00×10^{-6}	2.09×10^{-10}
2.00×10^{-4}	2.72×10^{-5}	1.73×10^{-4}	0.5134	1.56×10^{-5}	2.52×10^{-10}
3.00×10^{-4}	4.08×10^{-5}	2.59×10^{-4}	0.5008	2.90×10^{-5}	2.62×10^{-10}
4.00×10^{-4}	5.44×10^{-5}	3.46×10^{-4}	0.4938	4.24×10^{-5}	2.69×10^{-10}
5.00×10^{-4}	6.80×10^{-5}	4.32×10^{-4}	0.5011	5.58×10^{-5}	2.72×10^{-10}

$C_{eq.}$ CHP (M)	Ads. CHP (mol/cm^2)	$C_{eq.}$ Total (M)	Ads. Total (mol/cm^2)	α_{L77} (eq.) (bulk soln.)	X_{L77} (eq.) (ads. layer)
9.54×10^{-6}	2.90×10^{-11}	9.84×10^{-6}	0.61×10^{-11}	0.030	0.527
1.97×10^{-5}	4.30×10^{-11}	2.04×10^{-5}	1.03×10^{-10}	0.034	0.584
4.03×10^{-5}	6.40×10^{-11}	4.20×10^{-5}	1.76×10^{-10}	0.039	0.638
6.15×10^{-5}	7.40×10^{-11}	6.41×10^{-5}	2.43×10^{-10}	0.041	0.694
8.29×10^{-5}	7.70×10^{-11}	8.69×10^{-5}	2.86×10^{-10}	0.046	0.730
1.69×10^{-4}	8.20×10^{-11}	1.85×10^{-4}	3.34×10^{-10}	0.084	0.755
2.55×10^{-4}	8.60×10^{-11}	2.84×10^{-4}	3.48×10^{-10}	0.102	0.753
3.42×10^{-4}	9.10×10^{-11}	3.84×10^{-4}	3.61×10^{-10}	0.110	0.747
4.28×10^{-4}	9.50×10^{-11}	4.84×10^{-4}	3.67×10^{-10}	0.115	0.741

Table B-59. Adsorption of Mixtures of L77 and CHP on the Powdered Polyethylene

Volume of solution = 40.00 mL, Fixed initial α_{L77} = 0.285
Specific area of the polyethylene power, S=0.360 m^2/g

$C_{ini.}$ Total (M)	$C_{ini.}$ L77 (M)	$C_{ini.}$ CHP (M)	Powder (g)	$C_{eq.}$ L77 (M)	Ads. L77 (mol/cm^2)
5.00×10^{-6}	1.43×10^{-6}	3.57×10^{-6}	0.5002	1.85×10^{-7}	2.80×10^{-11}
1.00×10^{-5}	2.85×10^{-6}	7.15×10^{-6}	0.5105	4.25×10^{-7}	5.30×10^{-11}
2.50×10^{-5}	7.10×10^{-6}	1.79×10^{-5}	0.4984	1.18×10^{-6}	1.33×10^{-10}
5.00×10^{-5}	1.43×10^{-5}	3.57×10^{-5}	0.5122	2.58×10^{-6}	2.53×10^{-10}
1.00×10^{-4}	2.85×10^{-5}	7.15×10^{-5}	0.5003	1.59×10^{-5}	2.81×10^{-10}
1.50×10^{-4}	4.30×10^{-5}	1.07×10^{-4}	0.5124	2.94×10^{-5}	2.90×10^{-10}
2.00×10^{-4}	5.70×10^{-5}	1.43×10^{-4}	0.4875	4.39×10^{-5}	3.00×10^{-10}
2.50×10^{-4}	7.10×10^{-5}	1.79×10^{-4}	0.5116	5.71×10^{-5}	3.07×10^{-10}
3.00×10^{-4}	8.55×10^{-5}	2.15×10^{-4}	0.5012	7.14×10^{-5}	3.14×10^{-10}

$C_{eq.}$ CHP (M)	Ads. CHP (mol/cm^2)	$C_{eq.}$ Total (M)	Ads. Total (mol/cm^2)	α_{L77} (eq.) (bulk soln.)	X_{L77} (eq.) (ads. layer)
2.34×10^{-6}	2.70×10^{-11}	2.53×10^{-6}	5.50×10^{-11}	0.073	0.501
5.13×10^{-6}	4.40×10^{-11}	5.55×10^{-6}	9.70×10^{-11}	0.077	0.545
1.53×10^{-5}	5.70×10^{-11}	1.65×10^{-5}	1.90×10^{-10}	0.071	0.700
3.29×10^{-5}	6.20×10^{-11}	3.55×10^{-5}	3.15×10^{-10}	0.073	0.804
6.85×10^{-5}	6.70×10^{-11}	8.43×10^{-5}	3.48×10^{-10}	0.188	0.807
1.04×10^{-4}	7.40×10^{-11}	1.33×10^{-4}	3.64×10^{-10}	0.220	0.798
1.40×10^{-4}	7.90×10^{-11}	1.83×10^{-4}	3.79×10^{-10}	0.239	0.791
1.75×10^{-4}	8.50×10^{-11}	2.32×10^{-4}	3.92×10^{-10}	0.246	0.783
2.11×10^{-4}	8.90×10^{-11}	2.82×10^{-4}	4.03×10^{-10}	0.253	0.780

Table B-60. Adsorption of Mixtures of L77 and CHP on the Powdered Polyethylene

Volume of solution = 40.00 mL, Fixed initial α_{L77} = 0.438
Specific area of the polyethylene power, S=0.360 m^2/g

$C_{ini.}$ Total (M)	$C_{ini.}$ L77 (M)	$C_{ini.}$ CHP (M)	Powder (g)	$C_{eq.}$ L77 (M)	Ads. L77 (mol/cm^2)
5.00×10^{-6}	2.19×10^{-6}	2.81×10^{-6}	0.5124	1.63×10^{-7}	4.40×10^{-11}
1.00×10^{-5}	4.38×10^{-6}	5.62×10^{-6}	0.5006	4.55×10^{-7}	8.70×10^{-11}
1.50×10^{-5}	6.57×10^{-6}	8.43×10^{-6}	0.4989	1.12×10^{-6}	1.21×10^{-10}
2.00×10^{-5}	8.80×10^{-6}	1.12×10^{-5}	0.5016	1.84×10^{-6}	1.53×10^{-10}
2.50×10^{-5}	1.10×10^{-5}	1.40×10^{-5}	0.5004	2.55×10^{-6}	1.87×10^{-10}
5.00×10^{-5}	2.19×10^{-5}	2.81×10^{-5}	0.4997	9.75×10^{-6}	2.70×10^{-10}
1.00×10^{-4}	4.38×10^{-5}	5.62×10^{-5}	0.5016	2.99×10^{-5}	3.08×10^{-10}
1.75×10^{-4}	7.66×10^{-5}	9.84×10^{-5}	0.4986	6.23×10^{-5}	3.21×10^{-10}
2.50×10^{-4}	1.10×10^{-4}	1.40×10^{-4}	0.5105	9.46×10^{-5}	3.24×10^{-10}

$C_{eq.}$ CHP (M)	Ads. CHP (mol/cm^2)	$C_{eq.}$ Total (M)	Ads. Total (mol/cm^2)	α_{L77} (eq.) (bulk soln.)	X_{L77} (eq.) (ads. layer)
2.26×10^{-6}	1.20×10^{-11}	2.42×10^{-6}	0.56×10^{-11}	0.067	0.787
4.87×10^{-6}	1.70×10^{-11}	5.33×10^{-6}	1.04×10^{-10}	0.085	0.840
7.31×10^{-6}	2.50×10^{-11}	8.43×10^{-6}	1.46×10^{-10}	0.133	0.829
9.79×10^{-6}	3.20×10^{-11}	1.16×10^{-5}	1.86×10^{-10}	0.158	0.827
1.24×10^{-5}	3.70×10^{-11}	1.49×10^{-5}	2.24×10^{-10}	0.171	0.834
2.62×10^{-5}	4.20×10^{-11}	3.60×10^{-5}	3.12×10^{-10}	0.271	0.866
5.42×10^{-5}	4.40×10^{-11}	8.41×10^{-5}	3.52×10^{-10}	0.356	0.874
9.62×10^{-5}	4.90×10^{-11}	1.58×10^{-4}	3.70×10^{-10}	0.393	0.867
1.38×10^{-4}	5.10×10^{-11}	2.33×10^{-4}	3.75×10^{-10}	0.407	0.864

Table B-61. Adsorption of Mixtures of L77 and CHP on the Powdered Polyethylene

Volume of solution = 40.00 mL, Fixed initial α_{L77} = 0.602
Specific area of the polyethylene power, S=0.360 m^2/g

$C_{ini.}$ Total (M)	$C_{ini.}$ L77 (M)	$C_{ini.}$ CHP (M)	Powder (g)	$C_{eq.}$ L77 (M)	Ads. L77 (mol/cm^2)
1.25×10^{-5}	7.53×10^{-6}	4.97×10^{-6}	0.4982	9.75×10^{-7}	1.46×10^{-10}
2.50×10^{-5}	1.51×10^{-5}	9.90×10^{-6}	0.5122	4.88×10^{-6}	2.21×10^{-10}
5.00×10^{-5}	3.01×10^{-5}	1.99×10^{-5}	0.5004	1.79×10^{-5}	2.71×10^{-10}
7.50×10^{-5}	4.52×10^{-5}	2.98×10^{-5}	0.5146	3.20×10^{-5}	2.84×10^{-10}
1.00×10^{-4}	6.02×10^{-5}	3.98×10^{-5}	0.4945	4.73×10^{-5}	2.90×10^{-10}
1.25×10^{-4}	7.53×10^{-5}	4.97×10^{-5}	0.4962	6.22×10^{-5}	2.92×10^{-10}
1.50×10^{-4}	9.03×10^{-5}	5.97×10^{-5}	0.5063	7.69×10^{-5}	2.94×10^{-10}
2.00×10^{-4}	1.20×10^{-4}	8.00×10^{-5}	0.5002	1.07×10^{-4}	2.98×10^{-10}
2.50×10^{-4}	1.51×10^{-4}	9.90×10^{-5}	0.5147	1.37×10^{-4}	2.99×10^{-10}

$C_{eq.}$ CHP (M)	Ads. CHP (mol/cm^2)	$C_{eq.}$ Total (M)	Ads. Total (mol/cm^2)	α_{L77} (eq.) (bulk soln.)	X_{L77} (eq.) (ads. layer)
4.67×10^{-6}	7.00×10^{-12}	5.65×10^{-6}	1.53×10^{-10}	0.173	0.956
9.58×10^{-6}	8.00×10^{-12}	1.45×10^{-5}	2.29×10^{-10}	0.337	0.964
1.94×10^{-5}	1.10×10^{-11}	3.73×10^{-5}	2.82×10^{-10}	0.480	0.961
2.93×10^{-5}	1.30×10^{-11}	6.12×10^{-5}	2.97×10^{-10}	0.522	0.956
3.91×10^{-5}	1.60×10^{-11}	8.64×10^{-5}	3.06×10^{-10}	0.547	0.949
4.90×10^{-5}	1.70×10^{-11}	1.11×10^{-4}	3.09×10^{-10}	0.560	0.944
5.88×10^{-5}	1.90×10^{-11}	1.36×10^{-4}	3.13×10^{-10}	0.567	0.939
7.86×10^{-5}	2.20×10^{-11}	1.86×10^{-4}	3.20×10^{-10}	0.577	0.931
9.83×10^{-5}	2.50×10^{-11}	2.35×10^{-4}	3.24×10^{-10}	0.581	0.923

Table B-62. Adsorption of Mixtures of L77 and CHP on the Powdered Polyethylene

Volume of solution = 40.00 mL, Fixed initial α_{L77} = 0.712
Specific area of the polyethylene power, S=0.360 m^2/g

$C_{ini.}$ Total (M)	$C_{ini.}$ L77 (M)	$C_{ini.}$ CHP (M)	Powder (g)	$C_{eq.}$ L77 (M)	Ads. L77 (mol/cm^2)
1.00×10^{-5}	7.12×10^{-6}	2.88×10^{-6}	0.5115	1.75×10^{-6}	1.16×10^{-10}
1.25×10^{-5}	8.90×10^{-6}	3.60×10^{-6}	0.5048	2.35×10^{-6}	1.44×10^{-10}
1.50×10^{-5}	1.07×10^{-5}	4.30×10^{-6}	0.4963	3.11×10^{-6}	1.70×10^{-10}
2.00×10^{-5}	1.42×10^{-5}	5.80×10^{-6}	0.4853	5.32×10^{-6}	2.05×10^{-10}
3.00×10^{-5}	2.14×10^{-5}	8.60×10^{-6}	0.5001	1.06×10^{-5}	2.40×10^{-10}
5.00×10^{-5}	3.56×10^{-5}	1.44×10^{-5}	0.5042	2.34×10^{-5}	2.69×10^{-10}
1.00×10^{-4}	7.12×10^{-5}	2.88×10^{-5}	0.5060	5.84×10^{-5}	2.81×10^{-10}
1.50×10^{-4}	1.07×10^{-4}	4.30×10^{-5}	0.5117	9.38×10^{-5}	2.83×10^{-10}
2.00×10^{-4}	1.42×10^{-4}	5.80×10^{-5}	0.5054	1.29×10^{-4}	2.85×10^{-10}

$C_{eq.}$ CHP (M)	Ads. CHP (mol/cm^2)	$C_{eq.}$ Total (M)	Ads. Total (mol/cm^2)	α_{L77} (eq.) (bulk soln.)	X_{L77} (eq.) (ads. layer)
2.76×10^{-6}	3.00×10^{-12}	4.51×10^{-6}	1.19×10^{-10}	0.388	0.977
3.35×10^{-6}	6.00×10^{-12}	5.70×10^{-6}	1.50×10^{-10}	0.412	0.963
4.05×10^{-6}	6.00×10^{-12}	7.16×10^{-6}	1.76×10^{-10}	0.434	0.965
5.44×10^{-6}	7.00×10^{-12}	1.08×10^{-5}	2.12×10^{-10}	0.494	0.965
8.27×10^{-6}	8.00×10^{-12}	1.89×10^{-5}	2.48×10^{-10}	0.561	0.966
1.40×10^{-5}	9.00×10^{-12}	3.74×10^{-5}	2.78×10^{-10}	0.626	0.968
2.84×10^{-5}	9.00×10^{-12}	8.68×10^{-5}	2.90×10^{-10}	0.673	0.969
4.28×10^{-5}	1.00×10^{-11}	1.37×10^{-4}	2.93×10^{-10}	0.687	0.967
5.71×10^{-5}	1.00×10^{-11}	1.86×10^{-4}	2.95×10^{-10}	0.694	0.966

Table B-63. Adsorption of Mixtures of L77 and CHP on the Powdered Polyethylene

Volume of solution = 40.00 mL, Fixed initial α_{L77} = 0.850
Specific area of the polyethylene power, S=0.360 m^2/g

$C_{ini.}$ Total (M)	$C_{ini.}$ L77 (M)	$C_{ini.}$ CHP (M)	Powder (g)	$C_{eq.}$ L77 (M)	Ads. L77 (mol/cm^2)
1.00×10^{-5}	8.50×10^{-6}	1.50×10^{-6}	0.5018	2.88×10^{-6}	1.25×10^{-10}
1.50×10^{-5}	1.28×10^{-5}	2.20×10^{-6}	0.5104	4.65×10^{-6}	1.76×10^{-10}
2.00×10^{-5}	1.70×10^{-5}	3.00×10^{-6}	0.4994	7.55×10^{-6}	2.10×10^{-10}
3.00×10^{-5}	2.55×10^{-5}	4.50×10^{-6}	0.5113	1.45×10^{-5}	2.40×10^{-10}
5.00×10^{-5}	4.25×10^{-5}	7.50×10^{-6}	0.5107	3.06×10^{-5}	2.59×10^{-10}
7.50×10^{-5}	6.37×10^{-5}	1.13×10^{-5}	0.4962	5.18×10^{-5}	2.68×10^{-10}
1.00×10^{-4}	8.50×10^{-5}	1.50×10^{-5}	0.5055	7.26×10^{-5}	2.73×10^{-10}
1.25×10^{-4}	1.06×10^{-4}	1.90×10^{-5}	0.5024	9.38×10^{-5}	2.75×10^{-10}
1.50×10^{-4}	1.28×10^{-4}	2.20×10^{-5}	0.5007	1.15×10^{-4}	2.78×10^{-10}

$C_{eq.}$ CHP (M)	Ads. CHP (mol/cm^2)	$C_{eq.}$ Total (M)	Ads. Total (mol/cm^2)	α_{L77} (eq.) (bulk soln.)	X_{L77} (eq.) (ads. layer)
1.50×10^{-6}	0.00	4.38×10^{-6}	1.25×10^{-10}	0.658	1.000
2.20×10^{-6}	1.10×10^{-12}	6.85×10^{-6}	1.77×10^{-10}	0.679	0.994
2.93×10^{-6}	1.70×10^{-12}	1.05×10^{-5}	2.12×10^{-10}	0.721	0.992
4.40×10^{-6}	2.20×10^{-12}	1.89×10^{-5}	2.42×10^{-10}	0.767	0.991
7.38×10^{-6}	2.70×10^{-12}	3.80×10^{-5}	2.62×10^{-10}	0.806	0.990
1.11×10^{-5}	3.40×10^{-12}	6.29×10^{-5}	2.71×10^{-10}	0.824	0.988
1.48×10^{-5}	3.80×10^{-12}	8.74×10^{-5}	2.76×10^{-10}	0.830	0.986
1.86×10^{-5}	4.40×10^{-12}	1.12×10^{-4}	2.80×10^{-10}	0.835	0.984
2.23×10^{-5}	5.00×10^{-12}	1.37×10^{-4}	2.83×10^{-10}	0.838	0.982

Table B-64. Adsorption of Mixtures of L77 and C6P on the Powdered Polyethylene

Volume of solution = 40.00 mL, Fixed initial α_{L77} = 0.039
Specific area of the polyethylene power, S=0.360 m^2/g

$C_{ini.}$ Total (M)	$C_{ini.}$ L77 (M)	$C_{ini.}$ C6P (M)	Powder (g)	$C_{eq.}$ L77 (M)	Ads. L77 (mol/cm^2)
1.00×10^{-5}	3.90×10^{-7}	9.61×10^{-6}	0.5121	1.00×10^{-8}	8.00×10^{-12}
1.60×10^{-5}	6.00×10^{-7}	1.54×10^{-5}	0.5003	6.15×10^{-8}	1.20×10^{-11}
2.50×10^{-5}	1.00×10^{-6}	2.40×10^{-5}	0.5106	1.63×10^{-7}	1.80×10^{-11}
5.00×10^{-5}	1.95×10^{-6}	4.81×10^{-5}	0.4945	5.25×10^{-7}	3.20×10^{-11}
1.00×10^{-4}	3.90×10^{-6}	9.61×10^{-5}	0.5001	5.50×10^{-7}	7.40×10^{-11}
2.00×10^{-4}	8.00×10^{-6}	1.92×10^{-4}	0.4965	2.45×10^{-6}	1.20×10^{-10}
4.00×10^{-4}	1.60×10^{-5}	3.84×10^{-4}	0.5117	8.00×10^{-6}	1.65×10^{-10}
6.00×10^{-4}	2.30×10^{-5}	5.77×10^{-4}	0.5078	1.48×10^{-5}	1.89×10^{-10}
8.00×10^{-4}	3.10×10^{-5}	7.69×10^{-4}	0.4990	2.18×10^{-5}	2.10×10^{-10}

$C_{eq.}$ C6P (M)	Ads. C6P (mol/cm^2)	$C_{eq.}$ Total (M)	Ads. Total (mol/cm^2)	α_{L77} (eq.) (bulk soln.)	X_{L77} (eq.) (ads. layer)
5.76×10^{-6}	8.40×10^{-11}	5.77×10^{-6}	9.20×10^{-11}	0.002	0.090
1.06×10^{-5}	1.07×10^{-10}	1.06×10^{-5}	1.19×10^{-10}	0.006	0.105
1.81×10^{-5}	1.29×10^{-10}	1.83×10^{-5}	1.47×10^{-10}	0.009	0.121
4.14×10^{-5}	1.49×10^{-10}	4.19×10^{-5}	1.81×10^{-10}	0.013	0.176
8.93×10^{-5}	1.52×10^{-10}	8.98×10^{-5}	2.27×10^{-10}	0.006	0.328
1.85×10^{-4}	1.54×10^{-10}	1.88×10^{-4}	2.74×10^{-10}	0.013	0.437
3.77×10^{-4}	1.54×10^{-10}	3.85×10^{-4}	3.19×10^{-10}	0.021	0.517
5.69×10^{-4}	1.61×10^{-10}	5.84×10^{-4}	3.50×10^{-10}	0.025	0.539
7.61×10^{-4}	1.65×10^{-10}	7.83×10^{-4}	3.75×10^{-10}	0.028	0.561

Table B-65. Adsorption of Mixtures of L77 and C6P on the Powdered Polyethylene

Volume of solution = 40.00 mL, Fixed initial α_{L77} = 0.172
Specific area of the polyethylene power, S=0.360 m^2/g

$C_{ini.}$ Total (M)	$C_{ini.}$ L77 (M)	$C_{ini.}$ C6P (M)	Powder (g)	$C_{eq.}$ L77 (M)	Ads. L77 (mol/cm^2)
2.50×10^{-6}	4.30×10^{-7}	2.07×10^{-6}	0.5007	2.75×10^{-8}	9.00×10^{-12}
5.00×10^{-6}	8.60×10^{-7}	4.14×10^{-6}	0.4956	7.50×10^{-8}	1.80×10^{-11}
1.25×10^{-5}	2.10×10^{-6}	1.04×10^{-5}	0.5124	2.55×10^{-7}	4.10×10^{-11}
2.50×10^{-5}	4.30×10^{-6}	2.07×10^{-5}	0.4963	7.00×10^{-7}	8.10×10^{-11}
5.00×10^{-5}	8.60×10^{-6}	4.14×10^{-5}	0.5050	1.55×10^{-6}	1.55×10^{-10}
7.50×10^{-5}	1.29×10^{-5}	6.21×10^{-5}	0.5003	2.03×10^{-6}	2.42×10^{-10}
1.50×10^{-4}	2.60×10^{-5}	1.24×10^{-4}	0.4985	1.35×10^{-5}	2.74×10^{-10}
3.00×10^{-4}	5.20×10^{-5}	2.48×10^{-4}	0.5046	3.89×10^{-5}	2.79×10^{-10}
5.00×10^{-4}	8.60×10^{-5}	4.14×10^{-4}	0.5107	7.31×10^{-5}	2.82×10^{-10}

$C_{eq.}$ C6P (M)	Ads. C6P (mol/cm^2)	$C_{eq.}$ Total (M)	Ads. Total (mol/cm^2)	α_{L77} (eq.) (bulk soln.)	X_{L77} (eq.) (ads. layer)
6.55×10^{-7}	3.10×10^{-11}	6.83×10^{-7}	4.00×10^{-11}	0.040	0.221
1.93×10^{-6}	5.00×10^{-11}	2.00×10^{-6}	6.80×10^{-11}	0.037	0.262
6.68×10^{-6}	8.00×10^{-11}	6.93×10^{-6}	1.21×10^{-10}	0.037	0.340
1.64×10^{-5}	9.60×10^{-11}	1.71×10^{-5}	1.77×10^{-10}	0.041	0.456
3.68×10^{-5}	1.01×10^{-10}	3.84×10^{-5}	2.56×10^{-10}	0.040	0.605
5.74×10^{-5}	1.04×10^{-10}	5.94×10^{-5}	3.46×10^{-10}	0.034	0.698
1.19×10^{-4}	1.08×10^{-10}	1.33×10^{-4}	3.82×10^{-10}	0.102	0.717
2.43×10^{-4}	1.11×10^{-10}	2.82×10^{-4}	3.90×10^{-10}	0.138	0.715
4.09×10^{-4}	1.13×10^{-10}	4.82×10^{-4}	3.95×10^{-10}	0.152	0.713

Table B-66. Adsorption of Mixtures of L77 and C6P on the Powdered Polyethylene

Volume of solution = 40.00 mL, Fixed initial α_{L77} = 0.269
Specific area of the polyethylene power, S=0.360 m^2/g

$C_{ini.}$ Total (M)	$C_{ini.}$ L77 (M)	$C_{ini.}$ C6P (M)	Powder (g)	$C_{eq.}$ L77 (M)	Ads. L77 (mol/cm^2)
5.00×10^{-6}	1.35×10^{-6}	3.65×10^{-6}	0.4992	4.50×10^{-8}	2.90×10^{-11}
1.00×10^{-5}	2.69×10^{-6}	7.31×10^{-6}	0.4985	1.14×10^{-7}	5.70×10^{-11}
1.50×10^{-5}	4.00×10^{-6}	1.10×10^{-5}	0.5042	2.10×10^{-7}	8.40×10^{-11}
2.50×10^{-5}	6.70×10^{-6}	1.83×10^{-5}	0.5107	3.75×10^{-7}	1.38×10^{-10}
5.00×10^{-5}	1.35×10^{-5}	3.65×10^{-5}	0.5004	2.15×10^{-6}	2.51×10^{-10}
1.00×10^{-4}	2.69×10^{-5}	7.31×10^{-5}	0.4946	1.33×10^{-5}	3.06×10^{-10}
2.00×10^{-4}	5.40×10^{-5}	1.46×10^{-4}	0.5085	3.89×10^{-5}	3.26×10^{-10}
3.00×10^{-4}	8.10×10^{-5}	2.19×10^{-4}	0.5134	6.53×10^{-5}	3.33×10^{-10}
4.00×10^{-4}	1.08×10^{-4}	2.92×10^{-4}	0.5008	9.24×10^{-5}	3.37×10^{-10}

$C_{eq.}$ C6P (M)	Ads. C6P (mol/cm^2)	$C_{eq.}$ Total (M)	Ads. Total (mol/cm^2)	α_{L77} (eq.) (bulk soln.)	X_{L77} (eq.) (ads. layer)
1.29×10^{-6}	5.30×10^{-11}	1.32×10^{-6}	8.20×10^{-11}	0.034	0.354
4.19×10^{-6}	7.00×10^{-11}	4.30×10^{-6}	1.27×10^{-10}	0.027	0.452
7.39×10^{-6}	7.90×10^{-11}	7.60×10^{-6}	1.63×10^{-10}	0.028	0.517
1.45×10^{-5}	8.20×10^{-11}	1.49×10^{-5}	2.20×10^{-10}	0.025	0.627
3.28×10^{-5}	8.40×10^{-11}	3.49×10^{-5}	3.35×10^{-10}	0.062	0.748
6.92×10^{-5}	8.70×10^{-11}	8.25×10^{-5}	3.93×10^{-10}	0.161	0.779
1.42×10^{-4}	8.50×10^{-11}	1.81×10^{-4}	4.11×10^{-10}	0.215	0.793
2.15×10^{-4}	8.50×10^{-11}	2.81×10^{-4}	4.18×10^{-10}	0.233	0.796
2.88×10^{-4}	8.80×10^{-11}	3.81×10^{-4}	4.25×10^{-10}	0.243	0.793

Table B-67. Adsorption of Mixtures of L77 and C6P on the Powdered Polyethylene

Volume of solution = 40.00 mL, Fixed initial α_{L77} = 0.441
Specific area of the polyethylene power, S=0.360 m^2/g

$C_{ini.}$ Total (M)	$C_{ini.}$ L77 (M)	$C_{ini.}$ C6P (M)	Powder (g)	$C_{eq.}$ L77 (M)	Ads. L77 (mol/cm^2)
5.00×10^{-6}	2.20×10^{-6}	2.80×10^{-6}	0.4895	6.25×10^{-8}	4.90×10^{-11}
1.00×10^{-5}	4.41×10^{-6}	5.59×10^{-6}	0.5120	2.60×10^{-7}	9.00×10^{-11}
2.00×10^{-5}	8.82×10^{-6}	1.12×10^{-5}	0.5202	7.20×10^{-7}	1.73×10^{-10}
3.00×10^{-5}	1.32×10^{-5}	1.68×10^{-5}	0.4975	3.16×10^{-6}	2.25×10^{-10}
4.00×10^{-5}	1.76×10^{-5}	2.24×10^{-5}	0.5107	6.09×10^{-6}	2.51×10^{-10}
8.00×10^{-5}	3.53×10^{-5}	4.47×10^{-5}	0.5003	2.29×10^{-5}	2.74×10^{-10}
1.50×10^{-4}	6.61×10^{-5}	8.39×10^{-5}	0.5114	5.27×10^{-5}	2.93×10^{-10}
2.25×10^{-4}	9.90×10^{-5}	1.26×10^{-4}	0.4967	8.56×10^{-5}	3.05×10^{-10}
3.00×10^{-4}	1.32×10^{-4}	1.68×10^{-4}	0.5005	1.18×10^{-4}	3.17×10^{-10}

$C_{eq.}$ C6P (M)	Ads. C6P (mol/cm^2)	$C_{eq.}$ Total (M)	Ads. Total (mol/cm^2)	α_{L77} (eq.) (bulk soln.)	X_{L77} (eq.) (ads. layer)
2.00×10^{-6}	1.80×10^{-11}	2.06×10^{-6}	6.70×10^{-11}	0.030	0.730
4.28×10^{-6}	2.80×10^{-11}	4.54×10^{-6}	1.19×10^{-10}	0.057	0.760
9.64×10^{-6}	3.30×10^{-11}	1.04×10^{-5}	2.06×10^{-10}	0.070	0.840
1.50×10^{-5}	4.00×10^{-11}	1.81×10^{-5}	2.65×10^{-10}	0.174	0.849
2.03×10^{-5}	4.40×10^{-11}	2.64×10^{-5}	2.96×10^{-10}	0.231	0.850
4.25×10^{-5}	5.00×10^{-11}	6.54×10^{-5}	3.24×10^{-10}	0.351	0.847
8.15×10^{-5}	5.00×10^{-11}	1.34×10^{-4}	3.44×10^{-10}	0.392	0.854
1.23×10^{-4}	5.50×10^{-11}	2.09×10^{-4}	3.60×10^{-10}	0.410	0.848
1.65×10^{-4}	5.40×10^{-11}	2.83×10^{-4}	3.72×10^{-10}	0.417	0.854

Table B-68. Adsorption of Mixtures of L77 and C6P on the Powdered Polyethylene

Volume of solution = 40.00 mL, Fixed initial α_{L77} = 0.595
Specific area of the polyethylene power, S=0.360 m^2/g

$C_{ini.}$ Total (M)	$C_{ini.}$ L77 (M)	$C_{ini.}$ C6P (M)	Powder (g)	$C_{eq.}$ L77 (M)	Ads. L77 (mol/cm^2)
5.00×10^{-6}	2.97×10^{-6}	2.03×10^{-6}	0.5122	4.25×10^{-7}	5.50×10^{-11}
1.00×10^{-5}	5.95×10^{-6}	4.05×10^{-6}	0.5034	9.25×10^{-7}	1.11×10^{-10}
1.50×10^{-5}	8.92×10^{-6}	6.08×10^{-6}	0.4954	1.58×10^{-6}	1.65×10^{-10}
2.00×10^{-5}	1.19×10^{-5}	8.10×10^{-6}	0.4967	3.08×10^{-6}	1.97×10^{-10}
4.00×10^{-5}	2.38×10^{-5}	1.62×10^{-5}	0.5002	1.23×10^{-5}	2.57×10^{-10}
7.00×10^{-5}	4.16×10^{-5}	2.84×10^{-5}	0.4981	2.93×10^{-5}	2.75×10^{-10}
1.00×10^{-4}	5.95×10^{-5}	4.05×10^{-5}	0.5164	4.64×10^{-5}	2.83×10^{-10}
1.75×10^{-4}	1.04×10^{-4}	7.10×10^{-5}	0.5124	9.07×10^{-5}	2.91×10^{-10}
2.50×10^{-4}	1.49×10^{-4}	1.01×10^{-4}	0.5202	1.35×10^{-4}	2.96×10^{-10}

$C_{eq.}$ C6P (M)	Ads. C6P (mol/cm^2)	$C_{eq.}$ Total (M)	Ads. Total (mol/cm^2)	α_{L77} (eq.) (bulk soln.)	X_{L77} (eq.) (ads. layer)
1.63×10^{-6}	9.00×10^{-12}	2.06×10^{-6}	6.40×10^{-11}	0.207	0.867
3.24×10^{-6}	1.80×10^{-11}	4.17×10^{-6}	1.29×10^{-10}	0.222	0.862
5.18×10^{-6}	2.00×10^{-11}	6.76×10^{-6}	1.85×10^{-10}	0.233	0.892
7.16×10^{-6}	2.10×10^{-11}	1.02×10^{-5}	2.18×10^{-10}	0.300	0.904
1.52×10^{-5}	2.20×10^{-11}	2.75×10^{-5}	2.78×10^{-10}	0.446	0.922
2.73×10^{-5}	2.40×10^{-11}	5.66×10^{-5}	2.99×10^{-10}	0.518	0.921
3.94×10^{-5}	2.40×10^{-11}	8.57×10^{-5}	3.07×10^{-10}	0.541	0.921
6.97×10^{-5}	2.60×10^{-11}	1.60×10^{-4}	3.17×10^{-10}	0.566	0.917
1.00×10^{-4}	2.70×10^{-11}	2.35×10^{-4}	3.23×10^{-10}	0.574	0.916

Table B-69. Adsorption of Mixtures of L77 and C6P on the Powdered Polyethylene

Volume of solution = 40.00 mL, Fixed initial α_{L77} = 0.751
Specific area of the polyethylene power, S=0.360 m^2/g

$C_{ini.}$ Total (M)	$C_{ini.}$ L77 (M)	$C_{ini.}$ C6P (M)	Powder (g)	$C_{eq.}$ L77 (M)	Ads. L77 (mol/cm^2)
5.00×10^{-6}	3.75×10^{-6}	1.25×10^{-6}	0.5042	1.18×10^{-6}	5.70×10^{-11}
1.00×10^{-5}	7.51×10^{-6}	2.49×10^{-6}	0.4987	1.99×10^{-6}	1.23×10^{-10}
1.50×10^{-5}	1.13×10^{-5}	3.70×10^{-6}	0.5007	3.59×10^{-6}	1.70×10^{-10}
3.00×10^{-5}	2.25×10^{-5}	7.50×10^{-6}	0.4965	1.21×10^{-5}	2.33×10^{-10}
4.00×10^{-5}	3.00×10^{-5}	1.00×10^{-5}	0.5101	1.85×10^{-5}	2.52×10^{-10}
7.00×10^{-5}	5.26×10^{-5}	1.74×10^{-5}	0.5020	4.02×10^{-5}	2.73×10^{-10}
1.20×10^{-4}	9.01×10^{-5}	2.99×10^{-5}	0.5124	7.72×10^{-5}	2.81×10^{-10}
1.50×10^{-4}	1.13×10^{-4}	3.70×10^{-5}	0.4954	1.00×10^{-4}	2.82×10^{-10}
2.00×10^{-4}	1.50×10^{-4}	5.00×10^{-5}	0.5113	1.37×10^{-4}	2.85×10^{-10}

$C_{eq.}$ C6P (M)	Ads. C6P (mol/cm^2)	$C_{eq.}$ Total (M)	Ads. Total (mol/cm^2)	α_{L77} (eq.) (bulk soln.)	X_{L77} (eq.) (ads. layer)
9.90×10^{-7}	6.00×10^{-12}	2.17×10^{-6}	6.20×10^{-11}	0.544	0.910
2.21×10^{-6}	6.00×10^{-12}	4.20×10^{-6}	1.29×10^{-10}	0.473	0.952
3.45×10^{-6}	7.00×10^{-12}	7.04×10^{-6}	1.77×10^{-10}	0.510	0.964
7.17×10^{-6}	7.00×10^{-12}	1.93×10^{-5}	2.40×10^{-10}	0.629	0.972
9.63×10^{-6}	7.00×10^{-12}	2.81×10^{-5}	2.59×10^{-10}	0.658	0.972
1.71×10^{-5}	8.00×10^{-12}	5.73×10^{-5}	2.81×10^{-10}	0.702	0.972
2.95×10^{-5}	8.00×10^{-12}	1.07×10^{-4}	2.89×10^{-10}	0.723	0.971
3.70×10^{-5}	9.00×10^{-12}	1.37×10^{-4}	2.91×10^{-10}	0.730	0.969
4.94×10^{-5}	9.00×10^{-12}	1.86×10^{-4}	2.94×10^{-10}	0.735	0.970

Table B-70. Adsorption of Mixtures of L77 and C6P on the Powdered Polyethylene

Volume of solution = 40.00 mL, Fixed initial α_{L77} = 0.877
Specific area of the polyethylene power, S=0.360 m^2/g

$C_{ini.}$ Total (M)	$C_{ini.}$ L77 (M)	$C_{ini.}$ C6P (M)	Powder (g)	$C_{eq.}$ L77 (M)	Ads. L77 (mol/cm^2)
2.50×10^{-6}	2.19×10^{-6}	3.10×10^{-7}	0.5104	8.38×10^{-7}	2.90×10^{-11}
5.00×10^{-6}	4.39×10^{-6}	6.10×10^{-7}	0.5025	1.76×10^{-6}	5.80×10^{-11}
1.00×10^{-5}	8.77×10^{-6}	1.23×10^{-6}	0.5042	3.47×10^{-6}	1.17×10^{-10}
2.00×10^{-5}	1.75×10^{-5}	2.50×10^{-6}	0.4946	8.47×10^{-6}	2.04×10^{-10}
4.00×10^{-5}	3.51×10^{-5}	4.90×10^{-6}	0.5057	2.35×10^{-5}	2.53×10^{-10}
6.00×10^{-5}	5.26×10^{-5}	7.40×10^{-6}	0.5010	4.05×10^{-5}	2.68×10^{-10}
8.00×10^{-5}	7.02×10^{-5}	9.80×10^{-6}	0.4895	5.81×10^{-5}	2.74×10^{-10}
1.20×10^{-4}	1.05×10^{-4}	1.50×10^{-5}	0.4974	9.28×10^{-5}	2.78×10^{-10}
1.60×10^{-4}	1.40×10^{-4}	2.00×10^{-5}	0.5019	1.28×10^{-4}	2.80×10^{-10}

$C_{eq.}$ C6P (M)	Ads. C6P (mol/cm^2)	$C_{eq.}$ Total (M)	Ads. Total (mol/cm^2)	α_{L77} (eq.) (bulk soln.)	X_{L77} (eq.) (ads. layer)
2.23×10^{-7}	2.00×10^{-12}	1.06×10^{-6}	3.10×10^{-11}	0.790	0.941
5.00×10^{-7}	3.00×10^{-12}	2.26×10^{-6}	6.10×10^{-11}	0.779	0.958
1.10×10^{-6}	3.00×10^{-12}	4.57×10^{-6}	1.20×10^{-10}	0.760	0.976
2.32×10^{-6}	3.00×10^{-12}	1.08×10^{-5}	2.07×10^{-10}	0.785	0.984
4.76×10^{-6}	4.00×10^{-12}	2.83×10^{-5}	2.57×10^{-10}	0.832	0.986
7.20×10^{-6}	4.00×10^{-12}	4.77×10^{-5}	2.72×10^{-10}	0.849	0.986
9.65×10^{-6}	4.00×10^{-12}	6.78×10^{-5}	2.78×10^{-10}	0.858	0.984
1.45×10^{-5}	5.00×10^{-12}	1.07×10^{-4}	2.83×10^{-10}	0.864	0.983
1.95×10^{-5}	5.00×10^{-12}	1.47×10^{-4}	2.85×10^{-10}	0.868	0.982

Table B-71. Adsorption of Mixtures of L77 and C2,6P on the Powdered Polyethylene

Volume of solution = 40.00 mL, Fixed initial α_{L77} = 0.036
Specific area of the polyethylene power, S=0.360 m^2/g

$C_{ini.}$ Total (M)	$C_{ini.}$ L77 (M)	$C_{ini.}$ C2,6P (M)	Powder (g)	$C_{eq.}$ L77 (M)	Ads. L77 (mol/cm^2)
1.00×10^{-5}	3.60×10^{-7}	9.64×10^{-6}	0.5102	4.00×10^{-8}	7.00×10^{-12}
1.50×10^{-5}	5.00×10^{-7}	1.45×10^{-5}	0.4991	8.75×10^{-8}	1.00×10^{-11}
2.50×10^{-5}	9.00×10^{-7}	2.41×10^{-5}	0.5005	8.75×10^{-8}	1.80×10^{-11}
5.00×10^{-5}	1.80×10^{-6}	4.82×10^{-5}	0.5008	1.30×10^{-7}	3.70×10^{-11}
1.00×10^{-4}	3.60×10^{-6}	9.64×10^{-5}	0.5124	2.50×10^{-7}	7.30×10^{-11}
2.00×10^{-4}	7.20×10^{-6}	1.93×10^{-4}	0.4984	1.85×10^{-6}	1.19×10^{-10}
4.00×10^{-4}	1.44×10^{-5}	3.86×10^{-4}	0.4895	6.80×10^{-6}	1.73×10^{-10}
6.00×10^{-4}	2.20×10^{-5}	5.78×10^{-4}	0.5040	1.30×10^{-5}	1.90×10^{-10}
8.00×10^{-4}	2.90×10^{-5}	7.71×10^{-4}	0.5015	2.00×10^{-5}	1.96×10^{-10}

$C_{eq.}$ C2,6P (M)	Ads. C2,6P (mol/cm^2)	$C_{eq.}$ Total (M)	Ads. Total (mol/cm^2)	α_{L77} (eq.) (bulk soln.)	X_{L77} (eq.) (ads. layer)
7.04×10^{-6}	5.70×10^{-11}	7.08×10^{-6}	6.40×10^{-11}	0.006	0.110
1.07×10^{-5}	8.50×10^{-11}	1.07×10^{-5}	9.50×10^{-11}	0.008	0.106
1.93×10^{-5}	1.07×10^{-10}	1.94×10^{-5}	1.25×10^{-10}	0.005	0.145
4.28×10^{-5}	1.20×10^{-10}	4.29×10^{-5}	1.57×10^{-10}	0.003	0.236
9.05×10^{-5}	1.27×10^{-10}	9.08×10^{-5}	2.00×10^{-10}	0.003	0.363
1.87×10^{-4}	1.31×10^{-10}	1.89×10^{-4}	2.50×10^{-10}	0.010	0.477
3.80×10^{-4}	1.34×10^{-10}	3.86×10^{-4}	3.07×10^{-10}	0.018	0.562
5.72×10^{-4}	1.39×10^{-10}	5.85×10^{-4}	3.29×10^{-10}	0.022	0.578
7.65×10^{-4}	1.41×10^{-10}	7.85×10^{-4}	3.36×10^{-10}	0.025	0.582

Table B-72. Adsorption of Mixtures of L77 and C2,6P on the Powdered Polyethylene

Volume of solution = 40.00 mL, Fixed initial α_{L77} = 0.115
Specific area of the polyethylene power, S=0.360 m^2/g

$C_{ini.}$ Total (M)	$C_{ini.}$ L77 (M)	$C_{ini.}$ C2,6P (M)	Powder (g)	$C_{eq.}$ L77 (M)	Ads. L77 (mol/cm^2)
2.50×10^{-6}	2.90×10^{-7}	2.21×10^{-6}	0.5104	7.50×10^{-9}	6.00×10^{-12}
5.00×10^{-6}	5.70×10^{-7}	4.43×10^{-6}	0.4976	1.50×10^{-8}	1.30×10^{-11}
1.00×10^{-5}	1.15×10^{-6}	8.85×10^{-6}	0.5004	6.25×10^{-8}	2.40×10^{-11}
2.00×10^{-5}	2.30×10^{-6}	1.77×10^{-5}	0.4984	9.50×10^{-8}	4.90×10^{-11}
4.00×10^{-5}	4.60×10^{-6}	3.54×10^{-5}	0.4956	2.50×10^{-7}	9.80×10^{-11}
7.50×10^{-5}	8.63×10^{-6}	6.64×10^{-5}	0.5112	1.00×10^{-6}	1.66×10^{-10}
1.50×10^{-4}	1.73×10^{-5}	1.33×10^{-4}	0.5004	7.05×10^{-6}	2.26×10^{-10}
3.00×10^{-4}	3.45×10^{-5}	2.66×10^{-4}	0.4988	2.39×10^{-5}	2.36×10^{-10}
5.00×10^{-4}	5.75×10^{-5}	4.43×10^{-4}	0.5002	4.68×10^{-5}	2.38×10^{-10}

$C_{eq.}$ C2,6P (M)	Ads. C2,6P (mol/cm^2)	$C_{eq.}$ Total (M)	Ads. Total (mol/cm^2)	α_{L77} (eq.) (bulk soln.)	X_{L77} (eq.) (ads. layer)
7.98×10^{-7}	3.10×10^{-11}	8.06×10^{-7}	3.70×10^{-11}	0.009	0.165
2.14×10^{-6}	5.10×10^{-11}	2.15×10^{-6}	6.40×10^{-11}	0.007	0.197
5.43×10^{-6}	7.60×10^{-11}	5.49×10^{-6}	1.00×10^{-10}	0.011	0.241
1.34×10^{-5}	9.60×10^{-11}	1.35×10^{-5}	1.45×10^{-10}	0.007	0.339
3.08×10^{-5}	1.03×10^{-10}	3.11×10^{-5}	2.01×10^{-10}	0.008	0.486
6.16×10^{-5}	1.04×10^{-10}	6.26×10^{-5}	2.70×10^{-10}	0.016	0.614
1.28×10^{-4}	1.08×10^{-10}	1.35×10^{-4}	3.34×10^{-10}	0.052	0.678
2.60×10^{-4}	1.14×10^{-10}	2.84×10^{-4}	3.50×10^{-10}	0.084	0.674
4.37×10^{-4}	1.20×10^{-10}	4.84×10^{-4}	3.58×10^{-10}	0.097	0.665

Table B-73. Adsorption of Mixtures of L77 and C2,6P on the Powdered Polyethylene

Volume of solution = 40.00 mL, Fixed initial α_{L77} = 0.246
Specific area of the polyethylene power, S=0.360 m^2/g

$C_{ini.}$ Total (M)	$C_{ini.}$ L77 (M)	$C_{ini.}$ C2,6P (M)	Powder (g)	$C_{eq.}$ L77 (M)	Ads. L77 (mol/cm^2)
4.00×10^{-6}	9.80×10^{-7}	3.02×10^{-6}	0.4992	2.90×10^{-8}	2.10×10^{-11}
6.00×10^{-6}	1.48×10^{-6}	4.52×10^{-6}	0.4985	6.60×10^{-8}	3.10×10^{-11}
1.00×10^{-5}	2.46×10^{-6}	7.54×10^{-6}	0.5042	7.50×10^{-8}	5.30×10^{-11}
2.00×10^{-5}	4.90×10^{-6}	1.51×10^{-5}	0.5107	1.70×10^{-7}	1.03×10^{-10}
4.00×10^{-5}	9.80×10^{-6}	3.02×10^{-5}	0.5004	1.34×10^{-6}	1.89×10^{-10}
8.00×10^{-5}	1.97×10^{-5}	6.03×10^{-5}	0.4946	8.56×10^{-6}	2.50×10^{-10}
1.50×10^{-4}	3.70×10^{-5}	1.13×10^{-4}	0.5085	2.44×10^{-5}	2.74×10^{-10}
2.50×10^{-4}	6.10×10^{-5}	1.89×10^{-4}	0.5134	4.85×10^{-5}	2.81×10^{-10}
3.50×10^{-4}	8.60×10^{-5}	2.64×10^{-4}	0.5008	7.32×10^{-5}	2.87×10^{-10}

$C_{eq.}$ C2,6P (M)	Ads. C2,6P (mol/cm^2)	$C_{eq.}$ Total (M)	Ads. Total (mol/cm^2)	α_{L77} (eq.) (bulk soln.)	X_{L77} (eq.) (ads. layer)
8.99×10^{-7}	4.70×10^{-11}	9.28×10^{-7}	6.80×10^{-11}	0.031	0.311
1.90×10^{-6}	5.90×10^{-11}	1.97×10^{-6}	9.00×10^{-11}	0.034	0.349
4.52×10^{-6}	6.70×10^{-11}	4.60×10^{-6}	1.19×10^{-10}	0.016	0.441
1.16×10^{-5}	7.70×10^{-11}	1.17×10^{-5}	1.80×10^{-10}	0.014	0.574
2.59×10^{-5}	9.50×10^{-11}	2.72×10^{-5}	2.84×10^{-10}	0.049	0.664
5.59×10^{-5}	1.00×10^{-10}	6.45×10^{-5}	3.50×10^{-10}	0.133	0.714
1.08×10^{-4}	1.02×10^{-10}	1.32×10^{-4}	3.76×10^{-10}	0.183	0.729
1.84×10^{-4}	1.03×10^{-10}	2.32×10^{-4}	3.85×10^{-10}	0.209	0.731
2.59×10^{-4}	1.07×10^{-10}	3.32×10^{-4}	3.94×10^{-10}	0.220	0.729

Table B-74. Adsorption of Mixtures of L77 and C2,6P on the Powdered Polyethylene

Volume of solution = 40.00 mL, Fixed initial α_{L77} = 0.415
Specific area of the polyethylene power, S=0.360 m^2/g

$C_{ini.}$ Total (M)	$C_{ini.}$ L77 (M)	$C_{ini.}$ C2,6P (M)	Powder (g)	$C_{eq.}$ L77 (M)	Ads. L77 (mol/cm^2)
5.00×10^{-6}	2.08×10^{-6}	2.92×10^{-6}	0.5045	3.15×10^{-7}	3.90×10^{-11}
1.00×10^{-5}	4.15×10^{-6}	5.85×10^{-6}	0.5143	4.75×10^{-7}	7.90×10^{-11}
2.00×10^{-5}	8.30×10^{-6}	1.17×10^{-5}	0.5074	1.25×10^{-6}	1.54×10^{-10}
2.50×10^{-5}	1.04×10^{-5}	1.46×10^{-5}	0.4898	2.25×10^{-6}	1.84×10^{-10}
5.00×10^{-5}	2.08×10^{-5}	2.92×10^{-5}	0.4745	9.40×10^{-6}	2.66×10^{-10}
1.00×10^{-4}	4.15×10^{-5}	5.85×10^{-5}	0.5007	2.66×10^{-5}	3.31×10^{-10}
1.50×10^{-4}	6.23×10^{-5}	8.78×10^{-5}	0.5023	4.64×10^{-5}	3.52×10^{-10}
2.00×10^{-4}	8.30×10^{-5}	1.17×10^{-4}	0.4984	6.69×10^{-5}	3.59×10^{-10}
2.50×10^{-4}	1.04×10^{-4}	1.46×10^{-4}	0.5015	8.71×10^{-5}	3.69×10^{-10}

$C_{eq.}$ C2,6P (M)	Ads. C2,6P (mol/cm^2)	$C_{eq.}$ Total (M)	Ads. Total (mol/cm^2)	α_{L77} (eq.) (bulk soln.)	X_{L77} (eq.) (ads. layer)
1.34×10^{-6}	3.50×10^{-11}	1.66×10^{-6}	7.40×10^{-11}	0.190	0.526
2.88×10^{-6}	6.40×10^{-11}	3.35×10^{-6}	1.43×10^{-10}	0.142	0.553
7.85×10^{-6}	8.40×10^{-11}	9.10×10^{-6}	2.38×10^{-10}	0.137	0.647
1.08×10^{-5}	8.60×10^{-11}	1.31×10^{-5}	2.70×10^{-10}	0.172	0.681
2.53×10^{-5}	9.20×10^{-11}	3.47×10^{-5}	3.58×10^{-10}	0.271	0.742
5.42×10^{-5}	9.50×10^{-11}	8.08×10^{-5}	4.26×10^{-10}	0.329	0.776
8.33×10^{-5}	9.80×10^{-11}	1.30×10^{-4}	4.50×10^{-10}	0.358	0.781
1.12×10^{-4}	1.03×10^{-10}	1.79×10^{-4}	4.63×10^{-10}	0.373	0.777
1.42×10^{-4}	1.03×10^{-10}	2.29×10^{-4}	4.72×10^{-10}	0.381	0.782

Table B-75. Adsorption of Mixtures of L77 and C2,6P on the Powdered Polyethylene

Volume of solution = 40.00 mL, Fixed initial α_{L77} = 0.530
Specific area of the polyethylene power, S=0.360 m^2/g

$C_{ini.}$ Total (M)	$C_{ini.}$ L77 (M)	$C_{ini.}$ C2,6P (M)	Powder (g)	$C_{eq.}$ L77 (M)	Ads. L77 (mol/cm^2)
5.00×10^{-6}	2.65×10^{-6}	2.35×10^{-6}	0.4995	1.00×10^{-7}	5.70×10^{-11}
1.00×10^{-5}	5.30×10^{-6}	4.70×10^{-6}	0.5005	2.00×10^{-7}	1.13×10^{-10}
1.50×10^{-5}	7.95×10^{-6}	7.05×10^{-6}	0.4954	8.50×10^{-7}	1.59×10^{-10}
2.00×10^{-5}	1.06×10^{-5}	9.40×10^{-6}	0.5021	1.78×10^{-6}	1.95×10^{-10}
4.00×10^{-5}	2.12×10^{-5}	1.88×10^{-5}	0.5105	8.15×10^{-6}	2.84×10^{-10}
7.00×10^{-5}	3.71×10^{-5}	3.29×10^{-5}	0.5047	2.20×10^{-5}	3.32×10^{-10}
1.00×10^{-4}	5.30×10^{-5}	4.70×10^{-5}	0.4987	3.74×10^{-5}	3.48×10^{-10}
1.75×10^{-4}	9.28×10^{-5}	8.23×10^{-5}	0.5014	7.65×10^{-5}	3.61×10^{-10}
2.50×10^{-4}	1.32×10^{-4}	1.18×10^{-4}	0.5003	1.16×10^{-4}	3.65×10^{-10}

$C_{eq.}$ C2,6P (M)	Ads. C2,6P (mol/cm^2)	$C_{eq.}$ Total (M)	Ads. Total (mol/cm^2)	α_{L77} (eq.) (bulk soln.)	X_{L77} (eq.) (ads. layer)
1.96×10^{-6}	9.00×10^{-12}	2.06×10^{-6}	6.50×10^{-11}	0.049	0.867
3.89×10^{-6}	1.80×10^{-11}	4.09×10^{-6}	1.31×10^{-10}	0.049	0.863
5.83×10^{-6}	2.70×10^{-11}	6.68×10^{-6}	1.87×10^{-10}	0.127	0.854
7.89×10^{-6}	3.30×10^{-11}	9.67×10^{-6}	2.29×10^{-10}	0.184	0.854
1.69×10^{-5}	4.10×10^{-11}	2.51×10^{-5}	3.25×10^{-10}	0.325	0.873
3.07×10^{-5}	4.80×10^{-11}	5.27×10^{-5}	3.80×10^{-10}	0.417	0.875
4.47×10^{-5}	5.00×10^{-11}	8.21×10^{-5}	3.98×10^{-10}	0.455	0.873
7.98×10^{-5}	5.50×10^{-11}	1.56×10^{-4}	4.17×10^{-10}	0.489	0.867
1.15×10^{-4}	6.20×10^{-11}	2.31×10^{-4}	4.27×10^{-10}	0.503	0.856

Table B-76. Adsorption of Mixtures of L77 and C2,6P on the Powdered Polyethylene

Volume of solution = 40.00 mL, Fixed initial α_{L77} = 0.672
Specific area of the polyethylene power, S=0.360 m^2/g

$C_{ini.}$ Total (M)	$C_{ini.}$ L77 (M)	$C_{ini.}$ C2,6P (M)	Powder (g)	$C_{eq.}$ L77 (M)	Ads. L77 (mol/cm^2)
5.00×10^{-6}	3.36×10^{-6}	1.64×10^{-6}	0.4956	8.10×10^{-7}	5.70×10^{-11}
1.00×10^{-5}	6.72×10^{-6}	3.28×10^{-6}	0.4875	1.45×10^{-6}	1.20×10^{-10}
1.50×10^{-5}	1.01×10^{-5}	4.90×10^{-6}	0.5124	2.56×10^{-6}	1.63×10^{-10}
2.50×10^{-5}	1.68×10^{-5}	8.20×10^{-6}	0.5002	6.40×10^{-6}	2.31×10^{-10}
4.00×10^{-5}	2.69×10^{-5}	1.31×10^{-5}	0.5135	1.43×10^{-5}	2.72×10^{-10}
7.00×10^{-5}	4.70×10^{-5}	2.30×10^{-5}	0.4985	3.34×10^{-5}	3.03×10^{-10}
1.20×10^{-4}	8.06×10^{-5}	3.94×10^{-5}	0.5013	6.59×10^{-5}	3.26×10^{-10}
1.50×10^{-4}	1.01×10^{-4}	4.90×10^{-5}	0.5006	8.57×10^{-5}	3.35×10^{-10}
2.00×10^{-4}	1.34×10^{-4}	6.60×10^{-5}	0.5002	1.19×10^{-4}	3.42×10^{-10}

$C_{eq.}$ C2,6P (M)	Ads. C2,6P (mol/cm^2)	$C_{eq.}$ Total (M)	Ads. Total (mol/cm^2)	α_{L77} (eq.) (bulk soln.)	X_{L77} (eq.) (ads. layer)
1.26×10^{-6}	9.00×10^{-12}	2.07×10^{-6}	6.60×10^{-11}	0.391	0.870
2.57×10^{-6}	1.60×10^{-11}	4.02×10^{-6}	1.36×10^{-10}	0.360	0.882
3.88×10^{-6}	2.30×10^{-11}	6.44×10^{-6}	1.86×10^{-10}	0.397	0.879
6.95×10^{-6}	2.80×10^{-11}	1.33×10^{-5}	2.59×10^{-10}	0.479	0.893
1.18×10^{-5}	2.90×10^{-11}	2.61×10^{-5}	3.01×10^{-10}	0.549	0.904
2.16×10^{-5}	3.00×10^{-11}	5.50×10^{-5}	3.33×10^{-10}	0.608	0.909
3.80×10^{-5}	3.10×10^{-11}	1.04×10^{-4}	3.57×10^{-10}	0.635	0.914
4.78×10^{-5}	3.20×10^{-11}	1.34×10^{-4}	3.67×10^{-10}	0.642	0.914
6.41×10^{-5}	3.30×10^{-11}	1.83×10^{-4}	3.75×10^{-10}	0.650	0.912

Table B-77. Adsorption of Mixtures of L77 and C2,6P on the Powdered Polyethylene

Volume of solution = 40.00 mL, Fixed initial α_{L77} = 0.836
Specific area of the polyethylene power, S=0.360 m^2/g

$C_{ini.}$ Total (M)	$C_{ini.}$ L77 (M)	$C_{ini.}$ C2,6P (M)	Powder (g)	$C_{eq.}$ L77 (M)	Ads. L77 (mol/cm^2)
2.50×10^{-6}	2.09×10^{-6}	4.10×10^{-7}	0.5018	9.85×10^{-7}	2.40×10^{-11}
5.00×10^{-6}	4.18×10^{-6}	8.20×10^{-7}	0.4986	1.48×10^{-6}	6.00×10^{-11}
1.00×10^{-5}	8.36×10^{-6}	1.64×10^{-6}	0.4994	2.84×10^{-6}	1.23×10^{-10}
2.00×10^{-5}	1.67×10^{-5}	3.30×10^{-6}	0.5020	7.40×10^{-6}	2.06×10^{-10}
4.00×10^{-5}	3.34×10^{-5}	6.56×10^{-6}	0.5042	2.19×10^{-5}	2.55×10^{-10}
6.00×10^{-5}	5.02×10^{-5}	9.80×10^{-6}	0.4927	3.81×10^{-5}	2.73×10^{-10}
8.00×10^{-5}	6.69×10^{-5}	1.31×10^{-5}	0.5102	5.38×10^{-5}	2.84×10^{-10}
1.20×10^{-4}	1.00×10^{-4}	2.00×10^{-5}	0.5050	8.68×10^{-5}	2.98×10^{-10}
1.60×10^{-4}	1.34×10^{-4}	2.60×10^{-5}	0.5066	1.20×10^{-4}	3.07×10^{-10}

$C_{eq.}$ C2,6P (M)	Ads. C2,6P (mol/cm^2)	$C_{eq.}$ Total (M)	Ads. Total (mol/cm^2)	α_{L77} (eq.) (bulk soln.)	X_{L77} (eq.) (ads. layer)
3.17×10^{-7}	2.00×10^{-12}	1.30×10^{-6}	2.60×10^{-11}	0.757	0.922
6.84×10^{-7}	3.00×10^{-12}	2.16×10^{-6}	6.30×10^{-11}	0.684	0.952
1.43×10^{-6}	5.00×10^{-12}	4.26×10^{-6}	1.28×10^{-10}	0.665	0.963
2.96×10^{-6}	7.00×10^{-12}	1.04×10^{-5}	2.13×10^{-10}	0.714	0.967
6.15×10^{-6}	9.00×10^{-12}	2.80×10^{-5}	2.64×10^{-10}	0.781	0.966
9.41×10^{-6}	1.00×10^{-11}	4.75×10^{-5}	2.83×10^{-10}	0.802	0.966
1.27×10^{-5}	1.00×10^{-11}	6.65×10^{-5}	2.94×10^{-10}	0.809	0.967
1.92×10^{-5}	1.00×10^{-11}	1.06×10^{-4}	3.08×10^{-10}	0.819	0.967
2.57×10^{-5}	1.10×10^{-11}	1.46×10^{-4}	3.18×10^{-10}	0.823	0.966

Table B-78. Adsorption of Mixtures of L77 and C8P on the Powdered Polyethylene

Volume of solution = 40.00 mL, Fixed initial α_{L77} = 0.094
Specific area of the polyethylene power, S=0.360 m^2/g

$C_{ini.}$ Total (M)	$C_{ini.}$ L77 (M)	$C_{ini.}$ C8P (M)	Powder (g)	$C_{eq.}$ L77 (M)	Ads. L77 (mol/cm^2)
1.00×10^{-5}	9.40×10^{-7}	9.06×10^{-6}	0.4976	3.50×10^{-8}	2.00×10^{-11}
2.50×10^{-5}	2.30×10^{-6}	2.27×10^{-5}	0.5026	1.10×10^{-7}	5.00×10^{-11}
5.00×10^{-5}	4.70×10^{-6}	4.53×10^{-5}	0.4884	5.75×10^{-7}	9.40×10^{-11}
7.50×10^{-5}	7.00×10^{-6}	6.80×10^{-5}	0.4981	1.45×10^{-6}	1.25×10^{-10}
1.25×10^{-4}	1.20×10^{-5}	1.13×10^{-4}	0.5103	4.65×10^{-6}	1.55×10^{-10}
2.50×10^{-4}	2.30×10^{-5}	2.27×10^{-4}	0.4946	1.54×10^{-5}	1.82×10^{-10}
5.00×10^{-4}	4.70×10^{-5}	4.53×10^{-4}	0.5041	3.79×10^{-5}	2.01×10^{-10}
7.50×10^{-4}	7.00×10^{-5}	6.80×10^{-4}	0.5125	6.06×10^{-5}	2.14×10^{-10}
1.00×10^{-3}	9.40×10^{-5}	9.06×10^{-4}	0.5014	8.37×10^{-5}	2.28×10^{-10}

$C_{eq.}$ C8P (M)	Ads. C8P (mol/cm^2)	$C_{eq.}$ Total (M)	Ads. Total (mol/cm^2)	α_{L77} (eq.) (bulk soln.)	X_{L77} (eq.) (ads. layer)
5.96×10^{-6}	6.90×10^{-11}	6.00×10^{-6}	8.90×10^{-11}	0.006	0.226
1.72×10^{-5}	1.20×10^{-10}	1.73×10^{-5}	1.70×10^{-10}	0.006	0.292
3.92×10^{-5}	1.39×10^{-10}	3.98×10^{-5}	2.33×10^{-10}	0.014	0.402
6.13×10^{-5}	1.48×10^{-10}	6.28×10^{-5}	2.73×10^{-10}	0.023	0.457
1.06×10^{-4}	1.60×10^{-10}	1.11×10^{-4}	3.15×10^{-10}	0.042	0.491
2.19×10^{-4}	1.72×10^{-10}	2.34×10^{-4}	3.54×10^{-10}	0.066	0.513
4.44×10^{-4}	1.90×10^{-10}	4.82×10^{-4}	3.91×10^{-10}	0.079	0.514
6.70×10^{-4}	2.03×10^{-10}	7.31×10^{-4}	4.17×10^{-10}	0.083	0.513
8.96×10^{-4}	2.11×10^{-10}	9.80×10^{-4}	4.39×10^{-10}	0.085	0.520

Table B-79. Adsorption of Mixtures of L77 and C8P on the Powdered Polyethylene

Volume of solution = 40.00 mL, Fixed initial α_{L77} = 0.244
Specific area of the polyethylene power, S=0.360 m^2/g

$C_{ini.}$ Total (M)	$C_{ini.}$ L77 (M)	$C_{ini.}$ C8P (M)	Powder (g)	$C_{eq.}$ L77 (M)	Ads. L77 (mol/cm^2)
2.50×10^{-6}	6.10×10^{-7}	1.89×10^{-6}	0.5102	4.75×10^{-7}	3.00×10^{-12}
5.00×10^{-6}	1.22×10^{-6}	3.78×10^{-6}	0.4965	1.85×10^{-7}	2.30×10^{-11}
1.00×10^{-5}	2.44×10^{-6}	7.56×10^{-6}	0.4987	4.50×10^{-8}	5.30×10^{-11}
2.00×10^{-5}	4.90×10^{-6}	1.51×10^{-5}	0.5033	3.00×10^{-8}	1.07×10^{-10}
4.00×10^{-5}	9.80×10^{-6}	3.02×10^{-5}	0.5112	2.14×10^{-6}	1.66×10^{-10}
7.50×10^{-5}	1.83×10^{-5}	5.67×10^{-5}	0.5004	8.45×10^{-6}	2.19×10^{-10}
1.25×10^{-4}	3.05×10^{-5}	9.45×10^{-5}	0.5101	1.91×10^{-5}	2.48×10^{-10}
2.50×10^{-4}	6.10×10^{-5}	1.89×10^{-4}	0.5005	4.83×10^{-5}	2.81×10^{-10}
4.00×10^{-4}	9.80×10^{-5}	3.02×10^{-4}	0.5008	8.42×10^{-5}	2.98×10^{-10}

$C_{eq.}$ C8P (M)	Ads. C8P (mol/cm^2)	$C_{eq.}$ Total (M)	Ads. Total (mol/cm^2)	α_{L77} (eq.) (bulk soln.)	X_{L77} (eq.) (ads. layer)
9.75×10^{-7}	2.00×10^{-11}	1.45×10^{-6}	2.30×10^{-11}	0.327	0.129
2.32×10^{-6}	3.30×10^{-11}	2.50×10^{-6}	5.60×10^{-11}	0.074	0.414
5.01×10^{-6}	5.70×10^{-11}	5.06×10^{-6}	1.10×10^{-10}	0.009	0.484
1.19×10^{-5}	7.10×10^{-11}	1.20×10^{-5}	1.78×10^{-10}	0.003	0.602
2.64×10^{-5}	8.30×10^{-11}	2.86×10^{-5}	2.49×10^{-10}	0.075	0.666
5.23×10^{-5}	9.90×10^{-11}	6.07×10^{-5}	3.18×10^{-10}	0.139	0.689
8.94×10^{-5}	1.11×10^{-10}	1.09×10^{-4}	3.59×10^{-10}	0.176	0.690
1.83×10^{-4}	1.40×10^{-10}	2.31×10^{-4}	4.21×10^{-10}	0.209	0.668
2.95×10^{-4}	1.68×10^{-10}	3.79×10^{-4}	4.66×10^{-10}	0.222	0.640

Table B-80. Adsorption of Mixtures of L77 and C8P on the Powdered Polyethylene

Volume of solution = 40.00 mL, Fixed initial α_{L77} = 0.401
Specific area of the polyethylene power, S=0.360 m^2/g

$C_{ini.}$ Total (M)	$C_{ini.}$ L77 (M)	$C_{ini.}$ C8P (M)	Powder (g)	$C_{eq.}$ L77 (M)	Ads. L77 (mol/cm^2)
5.00×10^{-6}	2.00×10^{-6}	3.00×10^{-6}	0.5124	1.50×10^{-7}	4.00×10^{-11}
1.00×10^{-5}	4.01×10^{-6}	5.99×10^{-6}	0.5006	1.85×10^{-7}	8.50×10^{-11}
1.50×10^{-5}	6.02×10^{-6}	8.98×10^{-6}	0.5213	3.15×10^{-7}	1.21×10^{-10}
2.00×10^{-5}	8.00×10^{-6}	1.20×10^{-5}	0.4986	1.17×10^{-6}	1.53×10^{-10}
3.00×10^{-5}	1.20×10^{-5}	1.80×10^{-5}	0.5122	2.48×10^{-6}	2.07×10^{-10}
5.00×10^{-5}	2.00×10^{-5}	3.00×10^{-5}	0.5201	7.18×10^{-6}	2.75×10^{-10}
1.00×10^{-4}	4.01×10^{-5}	5.99×10^{-5}	0.4994	2.60×10^{-5}	3.14×10^{-10}
2.00×10^{-4}	8.00×10^{-5}	1.20×10^{-4}	0.4937	6.49×10^{-5}	3.44×10^{-10}
3.00×10^{-4}	1.20×10^{-4}	1.80×10^{-4}	0.5038	1.04×10^{-4}	3.54×10^{-10}

$C_{eq.}$ C8P (M)	Ads. C8P (mol/cm^2)	$C_{eq.}$ Total (M)	Ads. Total (mol/cm^2)	α_{L77} (eq.) (bulk soln.)	X_{L77} (eq.) (ads. layer)
1.48×10^{-6}	3.30×10^{-11}	1.63×10^{-6}	7.30×10^{-11}	0.092	0.550
3.19×10^{-6}	6.20×10^{-11}	3.38×10^{-6}	1.47×10^{-10}	0.055	0.577
5.29×10^{-6}	7.90×10^{-11}	5.60×10^{-6}	2.00×10^{-10}	0.056	0.606
7.71×10^{-6}	9.50×10^{-11}	8.88×10^{-6}	2.48×10^{-10}	0.132	0.616
1.32×10^{-5}	1.04×10^{-10}	1.57×10^{-5}	3.11×10^{-10}	0.158	0.666
2.47×10^{-5}	1.12×10^{-10}	3.19×10^{-5}	3.87×10^{-10}	0.225	0.710
5.45×10^{-5}	1.20×10^{-10}	8.05×10^{-5}	4.34×10^{-10}	0.323	0.723
1.14×10^{-4}	1.27×10^{-10}	1.79×10^{-4}	4.71×10^{-10}	0.363	0.730
1.74×10^{-4}	1.34×10^{-10}	2.78×10^{-4}	4.88×10^{-10}	0.375	0.725

Table B-81. Adsorptions of Mixture of L77 and C8P on the Powdered Polyethylene

Volume of solution = 40.00 mL, Fixed initial α_{L77} = 0.551
Specific area of the polyethylene power, S=0.360 m^2/g

$C_{ini.}$ Total (M)	$C_{ini.}$ L77 (M)	$C_{ini.}$ C8P (M)	Powder (g)	$C_{eq.}$ L77 (M)	Ads. L77 (mol/cm^2)
5.00×10^{-6}	2.75×10^{-6}	2.25×10^{-6}	0.5143	3.88×10^{-7}	5.10×10^{-11}
1.00×10^{-5}	5.51×10^{-6}	4.49×10^{-6}	0.5062	4.85×10^{-7}	1.10×10^{-10}
1.50×10^{-5}	8.26×10^{-6}	6.74×10^{-6}	0.4992	1.22×10^{-6}	1.57×10^{-10}
2.50×10^{-5}	1.38×10^{-5}	1.12×10^{-5}	0.4985	4.15×10^{-6}	2.15×10^{-10}
4.00×10^{-5}	2.20×10^{-5}	1.80×10^{-5}	0.5017	1.10×10^{-5}	2.45×10^{-10}
8.00×10^{-5}	4.41×10^{-5}	3.59×10^{-5}	0.5020	3.17×10^{-5}	2.73×10^{-10}
1.50×10^{-4}	8.26×10^{-5}	6.74×10^{-5}	0.5015	6.93×10^{-5}	2.96×10^{-10}
2.25×10^{-4}	1.24×10^{-4}	1.01×10^{-4}	0.5012	1.10×10^{-4}	3.14×10^{-10}
3.00×10^{-4}	1.65×10^{-4}	1.35×10^{-4}	0.5007	1.50×10^{-4}	3.32×10^{-10}

$C_{eq.}$ C8P (M)	Ads. C8P (mol/cm^2)	$C_{eq.}$ Total (M)	Ads. Total (mol/cm^2)	α_{L77} (eq.) (bulk soln.)	X_{L77} (eq.) (ads. layer)
1.45×10^{-6}	1.70×10^{-11}	1.84×10^{-6}	6.80×10^{-11}	0.211	0.749
3.18×10^{-6}	2.90×10^{-11}	3.67×10^{-6}	1.39×10^{-10}	0.132	0.793
5.19×10^{-6}	3.40×10^{-11}	6.41×10^{-6}	1.91×10^{-10}	0.190	0.820
9.44×10^{-6}	4.00×10^{-11}	1.36×10^{-5}	2.55×10^{-10}	0.305	0.843
1.59×10^{-5}	4.50×10^{-11}	2.69×10^{-5}	2.90×10^{-10}	0.408	0.845
3.34×10^{-5}	5.50×10^{-11}	6.52×10^{-5}	3.28×10^{-10}	0.487	0.832
6.43×10^{-5}	6.90×10^{-11}	1.34×10^{-4}	3.65×10^{-10}	0.519	0.812
9.74×10^{-5}	8.00×10^{-11}	2.07×10^{-4}	3.94×10^{-10}	0.530	0.796
1.31×10^{-4}	9.10×10^{-11}	2.81×10^{-4}	4.23×10^{-10}	0.535	0.785

Table B-82. Adsorption of Mixtures of L77 and C8P on the Powdered Polyethylene

Volume of solution = 40.00 mL, Fixed initial α_{L77} = 0.672
Specific area of the polyethylene power, S=0.360 m^2/g

$C_{ini.}$ Total (M)	$C_{ini.}$ L77 (M)	$C_{ini.}$ C8P (M)	Powder (g)	$C_{eq.}$ L77 (M)	Ads. L77 (mol/cm^2)
5.00×10^{-6}	3.36×10^{-6}	1.64×10^{-6}	0.5204	8.10×10^{-7}	5.40×10^{-11}
1.00×10^{-5}	6.72×10^{-6}	3.28×10^{-6}	0.5167	1.45×10^{-6}	1.13×10^{-10}
1.50×10^{-5}	1.01×10^{-5}	4.90×10^{-6}	0.5016	2.73×10^{-6}	1.63×10^{-10}
2.00×10^{-5}	1.34×10^{-5}	6.56×10^{-6}	0.4988	4.62×10^{-6}	1.97×10^{-10}
4.00×10^{-5}	2.69×10^{-5}	1.31×10^{-5}	0.4993	1.56×10^{-5}	2.51×10^{-10}
7.00×10^{-5}	4.70×10^{-5}	2.30×10^{-5}	0.5107	3.44×10^{-5}	2.74×10^{-10}
1.00×10^{-4}	6.72×10^{-5}	3.28×10^{-5}	0.5011	5.44×10^{-5}	2.84×10^{-10}
1.75×10^{-4}	1.18×10^{-4}	5.70×10^{-5}	0.5024	1.04×10^{-4}	3.00×10^{-10}
2.50×10^{-4}	1.68×10^{-4}	8.20×10^{-5}	0.5006	1.54×10^{-4}	3.09×10^{-10}

$C_{eq.}$ C8P (M)	Ads. C8P (mol/cm^2)	$C_{eq.}$ Total (M)	Ads. Total (mol/cm^2)	α_{L77} (eq.) (bulk soln.)	X_{L77} (eq.) (ads. layer)
1.25×10^{-6}	8.00×10^{-12}	2.06×10^{-6}	6.30×10^{-11}	0.394	0.867
2.47×10^{-6}	1.70×10^{-11}	3.92×10^{-6}	1.30×10^{-10}	0.369	0.867
4.03×10^{-6}	2.00×10^{-11}	6.76×10^{-6}	1.83×10^{-10}	0.404	0.892
5.62×10^{-6}	2.10×10^{-11}	1.02×10^{-5}	2.18×10^{-10}	0.451	0.904
1.19×10^{-5}	2.70×10^{-11}	2.75×10^{-5}	2.78×10^{-10}	0.567	0.902
2.14×10^{-5}	3.40×10^{-11}	5.58×10^{-5}	3.08×10^{-10}	0.617	0.890
3.10×10^{-5}	4.00×10^{-11}	8.54×10^{-5}	3.24×10^{-10}	0.637	0.876
5.52×10^{-5}	4.90×10^{-11}	1.59×10^{-4}	3.49×10^{-10}	0.653	0.860
7.95×10^{-5}	5.60×10^{-11}	2.34×10^{-4}	3.65×10^{-10}	0.660	0.847

Table B-83. Adsorption of Mixtures of L77 and C8P on the Powdered Polyethylene

Volume of solution = 40.00 mL, Fixed initial α_{L77} = 0.799
Specific area of the polyethylene power, S=0.360 m^2/g

$C_{ini.}$ Total (M)	$C_{ini.}$ L77 (M)	$C_{ini.}$ C8P (M)	Powder (g)	$C_{eq.}$ L77 (M)	Ads. L77 (mol/cm^2)
5.00×10^{-6}	4.00×10^{-6}	1.00×10^{-6}	0.5205	1.42×10^{-6}	5.50×10^{-11}
1.00×10^{-5}	7.99×10^{-6}	2.01×10^{-6}	0.5144	2.47×10^{-6}	1.19×10^{-10}
1.50×10^{-5}	1.20×10^{-5}	3.00×10^{-6}	0.5038	4.31×10^{-6}	1.69×10^{-10}
2.50×10^{-5}	2.00×10^{-5}	5.00×10^{-6}	0.4987	9.83×10^{-6}	2.26×10^{-10}
4.00×10^{-5}	3.20×10^{-5}	8.00×10^{-6}	0.5104	2.04×10^{-5}	2.51×10^{-10}
6.00×10^{-5}	4.79×10^{-5}	1.21×10^{-5}	0.5030	3.61×10^{-5}	2.61×10^{-10}
1.00×10^{-4}	7.99×10^{-5}	2.01×10^{-5}	0.5014	6.76×10^{-5}	2.74×10^{-10}
1.50×10^{-4}	1.20×10^{-4}	3.00×10^{-5}	0.5105	1.07×10^{-4}	2.85×10^{-10}
2.00×10^{-4}	1.60×10^{-4}	4.00×10^{-5}	0.5006	1.46×10^{-4}	2.96×10^{-10}

$C_{eq.}$ C8P (M)	Ads. C8P (mol/cm^2)	$C_{eq.}$ Total (M)	Ads. Total (mol/cm^2)	α_{L77} (eq.) (bulk soln.)	X_{L77} (eq.) (ads. layer)
7.50×10^{-7}	5.00×10^{-12}	2.17×10^{-6}	6.00×10^{-11}	0.654	0.910
1.66×10^{-6}	8.00×10^{-12}	4.13×10^{-6}	1.27×10^{-10}	0.598	0.940
2.55×10^{-6}	1.00×10^{-11}	6.86×10^{-6}	1.80×10^{-10}	0.628	0.943
4.39×10^{-6}	1.40×10^{-11}	1.42×10^{-5}	2.40×10^{-10}	0.691	0.941
7.16×10^{-6}	1.90×10^{-11}	2.76×10^{-5}	2.70×10^{-10}	0.740	0.929
1.10×10^{-5}	2.30×10^{-11}	4.72×10^{-5}	2.84×10^{-10}	0.766	0.920
1.89×10^{-5}	2.60×10^{-11}	8.65×10^{-5}	3.00×10^{-10}	0.781	0.913
2.88×10^{-5}	2.90×10^{-11}	1.36×10^{-4}	3.13×10^{-10}	0.787	0.908
3.88×10^{-5}	3.10×10^{-11}	1.85×10^{-4}	3.27×10^{-10}	0.791	0.905

Table B-84. Adsorption of Mixtures of L77 and C8P on the Powdered Polyethylene

Volume of solution = 40.00 mL, Fixed initial α_{L77} = 0.908
Specific area of the polyethylene power, S=0.360 m^2/g

$C_{ini.}$ Total (M)	$C_{ini.}$ L77 (M)	$C_{ini.}$ C8P (M)	Powder (g)	$C_{eq.}$ L77 (M)	Ads. L77 (mol/cm^2)
3.00×10^{-6}	2.72×10^{-6}	2.80×10^{-7}	0.5116	1.37×10^{-6}	2.90×10^{-11}
6.25×10^{-6}	5.68×10^{-6}	5.70×10^{-7}	0.5042	2.25×10^{-6}	7.50×10^{-11}
1.00×10^{-5}	9.08×10^{-6}	9.20×10^{-7}	0.4975	3.53×10^{-6}	1.24×10^{-10}
1.88×10^{-5}	1.71×10^{-5}	1.70×10^{-6}	0.4881	8.25×10^{-6}	2.01×10^{-10}
3.75×10^{-5}	3.41×10^{-5}	3.40×10^{-6}	0.5027	2.29×10^{-5}	2.47×10^{-10}
6.25×10^{-5}	5.68×10^{-5}	5.70×10^{-6}	0.4995	4.49×10^{-5}	2.64×10^{-10}
1.00×10^{-4}	9.08×10^{-5}	9.20×10^{-6}	0.5112	7.83×10^{-5}	2.73×10^{-10}
1.25×10^{-4}	1.14×10^{-4}	1.10×10^{-5}	0.5035	1.01×10^{-4}	2.76×10^{-10}
1.50×10^{-4}	1.36×10^{-4}	1.40×10^{-5}	0.5020	1.24×10^{-4}	2.79×10^{-10}

$C_{eq.}$ C8P (M)	Ads. C8P (mol/cm^2)	$C_{eq.}$ Total (M)	Ads. Total (mol/cm^2)	α_{L77} (eq.) (bulk soln.)	X_{L77} (eq.) (ads. layer)
1.91×10^{-7}	2.00×10^{-12}	1.56×10^{-6}	3.10×10^{-11}	0.878	0.941
4.60×10^{-7}	3.00×10^{-12}	2.71×10^{-6}	7.80×10^{-11}	0.830	0.968
7.88×10^{-7}	3.00×10^{-12}	4.32×10^{-6}	1.27×10^{-10}	0.818	0.977
1.47×10^{-6}	6.00×10^{-12}	9.71×10^{-6}	2.07×10^{-10}	0.849	0.971
3.05×10^{-6}	9.00×10^{-12}	2.59×10^{-5}	2.56×10^{-10}	0.883	0.965
5.22×10^{-6}	1.20×10^{-11}	5.01×10^{-5}	2.76×10^{-10}	0.896	0.957
8.53×10^{-6}	1.50×10^{-11}	8.68×10^{-5}	2.87×10^{-10}	0.902	0.949
1.07×10^{-5}	1.70×10^{-11}	1.12×10^{-4}	2.93×10^{-10}	0.904	0.943
1.29×10^{-5}	2.00×10^{-11}	1.36×10^{-4}	2.99×10^{-10}	0.906	0.933

Table B-85. Adsorption of Mixtures of L77 and C10P on the Powdered Polyethylene

Volume of solution = 40.00 mL, Fixed initial α_{L77} = 0.064
Specific area of the polyethylene power, S=0.360 m^2/g

$C_{ini.}$ Total (M)	$C_{ini.}$ L77 (M)	$C_{ini.}$ C10P (M)	Powder (g)	$C_{eq.}$ L77 (M)	Ads. L77 (mol/cm^2)
1.00×10^{-5}	6.40×10^{-7}	9.36×10^{-6}	0.5122	1.10×10^{-7}	1.10×10^{-11}
2.50×10^{-5}	1.60×10^{-6}	2.34×10^{-5}	0.5031	8.20×10^{-7}	1.70×10^{-11}
5.00×10^{-5}	3.20×10^{-6}	4.68×10^{-5}	0.5045	2.17×10^{-6}	2.30×10^{-11}
7.50×10^{-5}	4.80×10^{-6}	7.02×10^{-5}	0.4984	3.52×10^{-6}	2.90×10^{-11}
1.00×10^{-4}	6.40×10^{-6}	9.36×10^{-5}	0.5105	4.87×10^{-6}	3.30×10^{-11}
2.00×10^{-4}	1.30×10^{-5}	1.87×10^{-4}	0.5014	1.10×10^{-5}	3.90×10^{-11}
3.00×10^{-4}	1.90×10^{-5}	2.81×10^{-4}	0.5006	1.72×10^{-5}	4.50×10^{-11}
4.00×10^{-4}	2.60×10^{-5}	3.74×10^{-4}	0.5112	2.33×10^{-5}	5.00×10^{-11}
5.00×10^{-4}	3.20×10^{-5}	4.68×10^{-4}	0.5020	2.92×10^{-5}	6.20×10^{-11}

$C_{eq.}$ C10P (M)	Ads. C10P (mol/cm^2)	$C_{eq.}$ Total (M)	Ads. Total (mol/cm^2)	α_{L77} (eq.) (bulk soln.)	X_{L77} (eq.) (ads. layer)
8.98×10^{-6}	8.00×10^{-12}	9.09×10^{-6}	1.90×10^{-11}	0.012	0.579
2.16×10^{-5}	4.00×10^{-11}	2.24×10^{-5}	5.70×10^{-11}	0.037	0.303
4.22×10^{-5}	1.02×10^{-10}	4.43×10^{-5}	1.25×10^{-10}	0.049	0.182
6.11×10^{-5}	2.04×10^{-10}	6.46×10^{-5}	2.33×10^{-10}	0.055	0.123
7.51×10^{-5}	4.03×10^{-10}	8.00×10^{-5}	4.36×10^{-10}	0.061	0.076
1.35×10^{-4}	1.15×10^{-9}	1.46×10^{-4}	1.19×10^{-9}	0.075	0.033
2.00×10^{-4}	1.80×10^{-9}	2.17×10^{-4}	1.84×10^{-9}	0.079	0.024
2.71×10^{-4}	2.26×10^{-9}	2.94×10^{-4}	2.31×10^{-9}	0.079	0.022
3.51×10^{-4}	2.60×10^{-9}	3.80×10^{-4}	2.66×10^{-9}	0.077	0.023

Table B-86. Adsorption of Mixtures of L77 and C10P on the Powdered Polyethylene

Volume of solution = 40.00 mL, Fixed initial α_{L77} = 0.158
Specific area of the polyethylene power, S=0.360 m^2/g

$C_{ini.}$ Total (M)	$C_{ini.}$ L77 (M)	$C_{ini.}$ C10P (M)	Powder (g)	$C_{eq.}$ L77 (M)	Ads. L77 (mol/cm^2)
1.00×10^{-5}	1.58×10^{-6}	8.42×10^{-6}	0.5246	9.78×10^{-7}	1.30×10^{-11}
2.50×10^{-5}	3.90×10^{-6}	2.11×10^{-5}	0.5108	3.04×10^{-6}	2.00×10^{-11}
5.00×10^{-5}	7.90×10^{-6}	4.21×10^{-5}	0.4954	6.77×10^{-6}	2.50×10^{-11}
7.50×10^{-5}	1.19×10^{-5}	6.31×10^{-5}	0.5023	1.02×10^{-5}	3.60×10^{-11}
1.00×10^{-4}	1.58×10^{-5}	8.42×10^{-5}	0.5044	1.40×10^{-5}	4.00×10^{-11}
1.50×10^{-4}	2.40×10^{-5}	1.26×10^{-4}	0.5031	2.15×10^{-5}	4.90×10^{-11}
2.00×10^{-4}	3.20×10^{-5}	1.68×10^{-4}	0.5012	2.87×10^{-5}	6.40×10^{-11}
3.00×10^{-4}	4.70×10^{-5}	2.53×10^{-4}	0.5009	4.41×10^{-5}	7.40×10^{-11}
5.00×10^{-4}	7.90×10^{-5}	4.21×10^{-4}	0.5010	7.52×10^{-5}	8.40×10^{-11}

$C_{eq.}$ C10P (M)	Ads. C10P (mol/cm^2)	$C_{eq.}$ Total (M)	Ads. Total (mol/cm^2)	α_{L77} (eq.) (bulk soln.)	X_{L77} (eq.) (ads. layer)
8.04×10^{-6}	8.00×10^{-12}	9.02×10^{-6}	2.10×10^{-11}	0.108	0.610
1.93×10^{-5}	3.90×10^{-11}	2.23×10^{-5}	5.90×10^{-11}	0.136	0.338
3.75×10^{-5}	1.04×10^{-10}	4.43×10^{-5}	1.29×10^{-10}	0.153	0.196
5.35×10^{-5}	2.13×10^{-10}	6.37×10^{-5}	2.49×10^{-10}	0.160	0.146
6.57×10^{-5}	4.08×10^{-10}	7.97×10^{-5}	4.48×10^{-10}	0.175	0.090
9.21×10^{-5}	7.56×10^{-10}	1.14×10^{-4}	8.05×10^{-10}	0.189	0.061
1.17×10^{-4}	1.13×10^{-9}	1.46×10^{-4}	1.20×10^{-9}	0.197	0.053
1.81×10^{-4}	1.58×10^{-9}	2.25×10^{-4}	1.65×10^{-9}	0.196	0.045
3.32×10^{-4}	1.98×10^{-9}	4.07×10^{-4}	2.06×10^{-9}	0.185	0.041

Table B-87. Adsorption of Mixtures of L77 and C10P on the Powdered Polyethylene

Volume of solution = 40.00 mL, Fixed initial α_{L77} = 0.271
Specific area of the polyethylene power, S=0.360 m^2/g

$C_{ini.}$ Total (M)	$C_{ini.}$ L77 (M)	$C_{ini.}$ C10P (M)	Powder (g)	$C_{eq.}$ L77 (M)	Ads. L77 (mol/cm^2)
7.50×10^{-6}	2.03×10^{-6}	5.47×10^{-6}	0.5109	3.58×10^{-7}	3.60×10^{-11}
1.50×10^{-5}	4.10×10^{-6}	1.09×10^{-5}	0.5065	1.24×10^{-6}	6.20×10^{-11}
2.50×10^{-5}	6.80×10^{-6}	1.82×10^{-5}	0.4977	3.40×10^{-6}	7.50×10^{-11}
5.00×10^{-5}	1.36×10^{-5}	3.64×10^{-5}	0.5021	9.65×10^{-6}	8.60×10^{-11}
1.00×10^{-4}	2.71×10^{-5}	7.29×10^{-5}	0.4995	2.36×10^{-5}	7.80×10^{-11}
1.50×10^{-4}	4.10×10^{-5}	1.09×10^{-4}	0.5122	3.67×10^{-5}	8.50×10^{-11}
2.00×10^{-4}	5.40×10^{-5}	1.46×10^{-4}	0.5017	5.01×10^{-5}	9.20×10^{-11}
3.00×10^{-4}	8.10×10^{-5}	2.19×10^{-4}	0.5005	7.69×10^{-5}	9.90×10^{-11}
5.00×10^{-4}	1.36×10^{-4}	3.64×10^{-4}	0.5032	1.31×10^{-4}	1.01×10^{-10}

$C_{eq.}$ C10P (M)	Ads. C10P (mol/cm^2)	$C_{eq.}$ Total (M)	Ads. Total (mol/cm^2)	α_{L77} (eq.) (bulk soln.)	X_{L77} (eq.) (ads. layer)
4.64×10^{-6}	1.80×10^{-11}	5.00×10^{-6}	5.40×10^{-11}	0.072	0.669
9.50×10^{-6}	3.10×10^{-11}	1.07×10^{-5}	9.30×10^{-11}	0.115	0.663
1.54×10^{-5}	6.40×10^{-11}	1.88×10^{-5}	1.39×10^{-10}	0.181	0.540
2.88×10^{-5}	1.69×10^{-10}	3.85×10^{-5}	2.55×10^{-10}	0.251	0.338
5.74×10^{-5}	3.46×10^{-10}	8.09×10^{-5}	4.24×10^{-10}	0.291	0.185
8.90×10^{-5}	4.41×10^{-10}	1.26×10^{-4}	5.26×10^{-10}	0.292	0.162
1.20×10^{-4}	5.70×10^{-10}	1.70×10^{-4}	6.62×10^{-10}	0.294	0.139
1.80×10^{-4}	8.60×10^{-10}	2.57×10^{-4}	9.59×10^{-10}	0.299	0.103
2.96×10^{-4}	1.50×10^{-9}	4.27×10^{-4}	1.60×10^{-9}	0.307	0.063

Table B-88. Adsorption of Mixtures of L77 and C10P on the Powdered Polyethylene

Volume of solution = 40.00 mL, Fixed initial α_{L77} = 0.401
Specific area of the polyethylene power, S=0.360 m^2/g

$C_{ini.}$ Total (M)	$C_{ini.}$ L77 (M)	$C_{ini.}$ C10P (M)	Powder (g)	$C_{eq.}$ L77 (M)	Ads. L77 (mol/cm^2)
7.50×10^{-6}	3.01×10^{-6}	4.49×10^{-6}	0.5202	8.45×10^{-7}	4.60×10^{-11}
1.50×10^{-5}	6.02×10^{-6}	8.98×10^{-6}	0.5148	2.94×10^{-6}	6.60×10^{-11}
2.50×10^{-5}	1.00×10^{-5}	1.50×10^{-5}	0.5033	6.40×10^{-6}	8.00×10^{-11}
5.00×10^{-5}	2.00×10^{-5}	3.00×10^{-5}	0.5111	1.62×10^{-5}	8.50×10^{-11}
1.00×10^{-4}	4.01×10^{-5}	5.99×10^{-5}	0.4985	3.61×10^{-5}	9.00×10^{-11}
1.50×10^{-4}	6.02×10^{-5}	8.98×10^{-5}	0.5042	5.57×10^{-5}	9.80×10^{-11}
2.00×10^{-4}	8.08×10^{-5}	1.20×10^{-4}	0.5015	7.53×10^{-5}	1.09×10^{-10}
3.00×10^{-4}	1.20×10^{-4}	1.80×10^{-4}	0.5020	1.15×10^{-4}	1.15×10^{-10}
4.00×10^{-4}	1.60×10^{-4}	2.40×10^{-4}	0.5038	1.55×10^{-4}	1.22×10^{-10}

$C_{eq.}$ C10P (M)	Ads. C10P (mol/cm^2)	$C_{eq.}$ Total (M)	Ads. Total (mol/cm^2)	α_{L77} (eq.) (bulk soln.)	X_{L77} (eq.) (ads. layer)
3.92×10^{-6}	1.20×10^{-11}	4.77×10^{-6}	5.80×10^{-11}	0.178	0.789
7.55×10^{-6}	3.10×10^{-11}	1.05×10^{-5}	9.70×10^{-11}	0.280	0.682
1.21×10^{-5}	6.30×10^{-11}	1.85×10^{-5}	1.43×10^{-10}	0.346	0.558
2.36×10^{-5}	1.39×10^{-10}	3.97×10^{-5}	2.24×10^{-10}	0.407	0.379
4.69×10^{-5}	2.91×10^{-10}	8.29×10^{-5}	3.81×10^{-10}	0.435	0.236
7.20×10^{-5}	3.93×10^{-10}	1.28×10^{-4}	4.91×10^{-10}	0.436	0.199
9.72×10^{-5}	5.00×10^{-10}	1.73×10^{-4}	6.09×10^{-10}	0.436	0.178
1.48×10^{-4}	6.92×10^{-10}	2.64×10^{-4}	8.07×10^{-10}	0.437	0.143
2.02×10^{-4}	8.38×10^{-10}	3.56×10^{-4}	9.60×10^{-10}	0.434	0.127

Table B-89. Adsorption of Mixtures of L77 and C10P on the Powdered Polyethylene

Volume of solution = 40.00 mL, Fixed initial α_{L77} = 0.554
Specific area of the polyethylene power, S=0.360 m^2/g

$C_{ini.}$ Total (M)	$C_{ini.}$ L77 (M)	$C_{ini.}$ C10P (M)	Powder (g)	$C_{eq.}$ L77 (M)	Ads. L77 (mol/cm^2)
7.50×10^{-6}	4.16×10^{-6}	3.34×10^{-6}	0.5124	1.99×10^{-6}	4.70×10^{-11}
1.00×10^{-5}	5.54×10^{-6}	4.46×10^{-6}	0.5226	2.72×10^{-6}	6.00×10^{-11}
1.50×10^{-5}	8.31×10^{-6}	6.69×10^{-6}	0.4975	4.69×10^{-6}	8.10×10^{-11}
2.00×10^{-5}	1.11×10^{-5}	8.90×10^{-6}	0.5027	6.43×10^{-6}	1.03×10^{-10}
3.00×10^{-5}	1.66×10^{-5}	1.34×10^{-5}	0.4896	1.13×10^{-5}	1.20×10^{-10}
5.00×10^{-5}	2.77×10^{-5}	2.23×10^{-5}	0.5103	2.13×10^{-5}	1.40×10^{-10}
1.00×10^{-4}	5.54×10^{-5}	4.46×10^{-5}	0.5012	4.80×10^{-5}	1.64×10^{-10}
2.00×10^{-4}	1.11×10^{-4}	8.90×10^{-5}	0.5009	1.02×10^{-4}	1.87×10^{-10}
3.00×10^{-4}	1.66×10^{-4}	1.34×10^{-4}	0.5004	1.57×10^{-4}	2.04×10^{-10}

$C_{eq.}$ C10P (M)	Ads. C10P (mol/cm^2)	$C_{eq.}$ Total (M)	Ads. Total (mol/cm^2)	α_{L77} (eq.) (bulk soln.)	X_{L77} (eq.) (ads. layer)
2.93×10^{-6}	9.00×10^{-12}	4.92×10^{-6}	5.60×10^{-11}	0.405	0.838
3.53×10^{-6}	2.00×10^{-11}	6.25×10^{-6}	8.00×10^{-11}	0.435	0.751
4.85×10^{-6}	4.10×10^{-11}	9.54×10^{-6}	1.22×10^{-10}	0.491	0.664
6.27×10^{-6}	5.90×10^{-11}	1.27×10^{-5}	1.62×10^{-10}	0.506	0.637
9.33×10^{-6}	9.20×10^{-11}	2.07×10^{-5}	2.12×10^{-10}	0.549	0.566
1.65×10^{-5}	1.27×10^{-10}	3.77×10^{-5}	2.67×10^{-10}	0.564	0.523
3.62×10^{-5}	1.86×10^{-10}	8.42×10^{-5}	3.50×10^{-10}	0.570	0.468
7.68×10^{-5}	2.75×10^{-10}	1.79×10^{-4}	4.62×10^{-10}	0.571	0.406
1.18×10^{-4}	3.61×10^{-10}	2.75×10^{-4}	5.65×10^{-10}	0.572	0.361

Table B-90. Adsorption of Mixtures of L77 and C10P on the Powdered Polyethylene

Volume of solution = 40.00 mL, Fixed initial α_{L77} = 0.690
Specific area of the polyethylene power, S=0.360 m^2/g

$C_{ini.}$ Total (M)	$C_{ini.}$ L77 (M)	$C_{ini.}$ C10P (M)	Powder (g)	$C_{eq.}$ L77 (M)	Ads. L77 (mol/cm^2)
7.50×10^{-6}	5.17×10^{-6}	2.33×10^{-6}	0.5014	2.76×10^{-6}	5.30×10^{-11}
1.00×10^{-5}	6.90×10^{-6}	3.10×10^{-6}	0.4995	3.83×10^{-6}	6.80×10^{-11}
1.50×10^{-5}	1.04×10^{-5}	4.60×10^{-6}	0.4964	5.98×10^{-6}	9.80×10^{-11}
2.00×10^{-5}	1.38×10^{-5}	6.20×10^{-6}	0.5145	8.40×10^{-6}	1.17×10^{-10}
3.00×10^{-5}	2.07×10^{-5}	9.30×10^{-6}	0.5088	1.42×10^{-5}	1.43×10^{-10}
5.00×10^{-5}	3.45×10^{-5}	1.55×10^{-5}	0.4975	2.68×10^{-5}	1.71×10^{-10}
1.00×10^{-4}	6.90×10^{-5}	3.10×10^{-5}	0.5024	5.99×10^{-5}	2.02×10^{-10}
1.50×10^{-4}	1.04×10^{-4}	4.60×10^{-5}	0.5120	9.30×10^{-5}	2.28×10^{-10}
2.00×10^{-4}	1.38×10^{-4}	6.20×10^{-5}	0.5013	1.27×10^{-4}	2.48×10^{-10}

$C_{eq.}$ C10P (M)	Ads. C10P (mol/cm^2)	$C_{eq.}$ Total (M)	Ads. Total (mol/cm^2)	α_{L77} (eq.) (bulk soln.)	X_{L77} (eq.) (ads. layer)
1.91×10^{-6}	9.00×10^{-12}	4.67×10^{-6}	6.20×10^{-11}	0.592	0.852
2.17×10^{-6}	2.10×10^{-11}	5.99×10^{-6}	8.90×10^{-11}	0.639	0.767
2.81×10^{-6}	4.10×10^{-11}	8.79×10^{-6}	1.39×10^{-10}	0.680	0.704
3.55×10^{-6}	5.70×10^{-11}	1.20×10^{-5}	1.74×10^{-10}	0.703	0.671
6.00×10^{-6}	7.20×10^{-11}	2.02×10^{-5}	2.15×10^{-10}	0.702	0.665
1.14×10^{-5}	9.10×10^{-11}	3.82×10^{-5}	2.62×10^{-10}	0.701	0.653
2.51×10^{-5}	1.30×10^{-10}	8.50×10^{-5}	3.32×10^{-10}	0.704	0.608
3.87×10^{-5}	1.70×10^{-10}	1.32×10^{-4}	3.98×10^{-10}	0.706	0.574
5.27×10^{-5}	2.07×10^{-10}	1.79×10^{-4}	4.55×10^{-10}	0.707	0.546

Table B-91. Adsorption of Mixtures of L77 and C10P on the Powdered Polyethylene

Volume of solution = 40.00 mL, Fixed initial α_{L77} = 0.855
Specific area of the polyethylene power, S=0.360 m^2/g

$C_{ini.}$ Total (M)	$C_{ini.}$ L77 (M)	$C_{ini.}$ C10P (M)	Powder (g)	$C_{eq.}$ L77 (M)	Ads. L77 (mol/cm^2)
7.50×10^{-6}	6.41×10^{-6}	1.09×10^{-6}	0.4963	3.24×10^{-6}	7.10×10^{-11}
1.00×10^{-5}	8.55×10^{-6}	1.45×10^{-6}	0.5141	4.40×10^{-6}	9.00×10^{-11}
1.50×10^{-5}	1.28×10^{-5}	2.20×10^{-6}	0.4888	7.30×10^{-6}	1.26×10^{-10}
2.00×10^{-5}	1.71×10^{-5}	2.90×10^{-6}	0.5056	1.07×10^{-5}	1.41×10^{-10}
3.00×10^{-5}	2.57×10^{-5}	4.30×10^{-6}	0.4972	1.81×10^{-5}	1.69×10^{-10}
5.00×10^{-5}	4.28×10^{-5}	7.20×10^{-6}	0.5021	3.36×10^{-5}	2.03×10^{-10}
1.00×10^{-4}	8.55×10^{-5}	1.45×10^{-5}	0.5004	7.49×10^{-5}	2.35×10^{-10}
1.50×10^{-4}	1.28×10^{-4}	2.20×10^{-5}	0.5018	1.17×10^{-4}	2.47×10^{-10}
2.00×10^{-4}	1.71×10^{-4}	2.90×10^{-5}	0.5033	1.59×10^{-4}	2.55×10^{-10}

$C_{eq.}$ C10P (M)	Ads. C10P (mol/cm^2)	$C_{eq.}$ Total (M)	Ads. Total (mol/cm^2)	α_{L77} (eq.) (bulk soln.)	X_{L77} (eq.) (ads. layer)
8.49×10^{-7}	5.00×10^{-12}	4.09×10^{-6}	7.60×10^{-11}	0.792	0.930
1.02×10^{-6}	9.00×10^{-12}	5.42×10^{-6}	9.90×10^{-11}	0.813	0.905
1.34×10^{-6}	1.90×10^{-11}	8.64×10^{-6}	1.45×10^{-10}	0.845	0.868
1.29×10^{-6}	3.50×10^{-11}	1.20×10^{-5}	1.76×10^{-10}	0.893	0.799
2.11×10^{-6}	5.00×10^{-11}	2.02×10^{-5}	2.19×10^{-10}	0.895	0.771
4.43×10^{-6}	6.30×10^{-11}	3.80×10^{-5}	2.66×10^{-10}	0.884	0.765
1.11×10^{-5}	7.50×10^{-11}	8.60×10^{-5}	3.10×10^{-10}	0.871	0.758
1.79×10^{-5}	8.50×10^{-11}	1.35×10^{-4}	3.32×10^{-10}	0.867	0.745
2.48×10^{-5}	9.30×10^{-11}	1.84×10^{-4}	3.48×10^{-10}	0.865	0.733

Figure B-1. Surface Tension of L77, C4P and Their Mixtures at Air/Aqueous Solution Interface

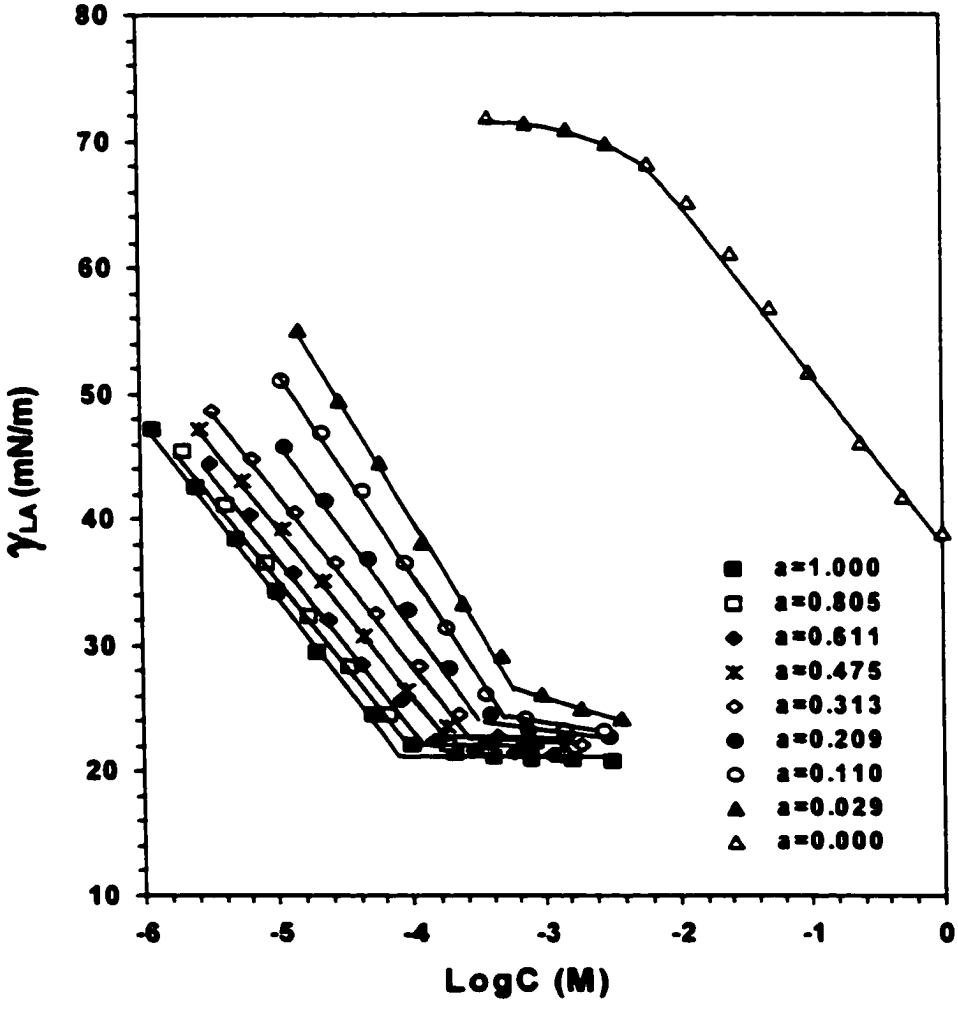

Figure B-2. Surface Tension of L77, CHP and Their Mixtures at Air/Aqueous Solution Interface

Phosphate Buffer Solution, pH=7.00, 25 °C
(a: mole fraction of L77 in the solution phase)

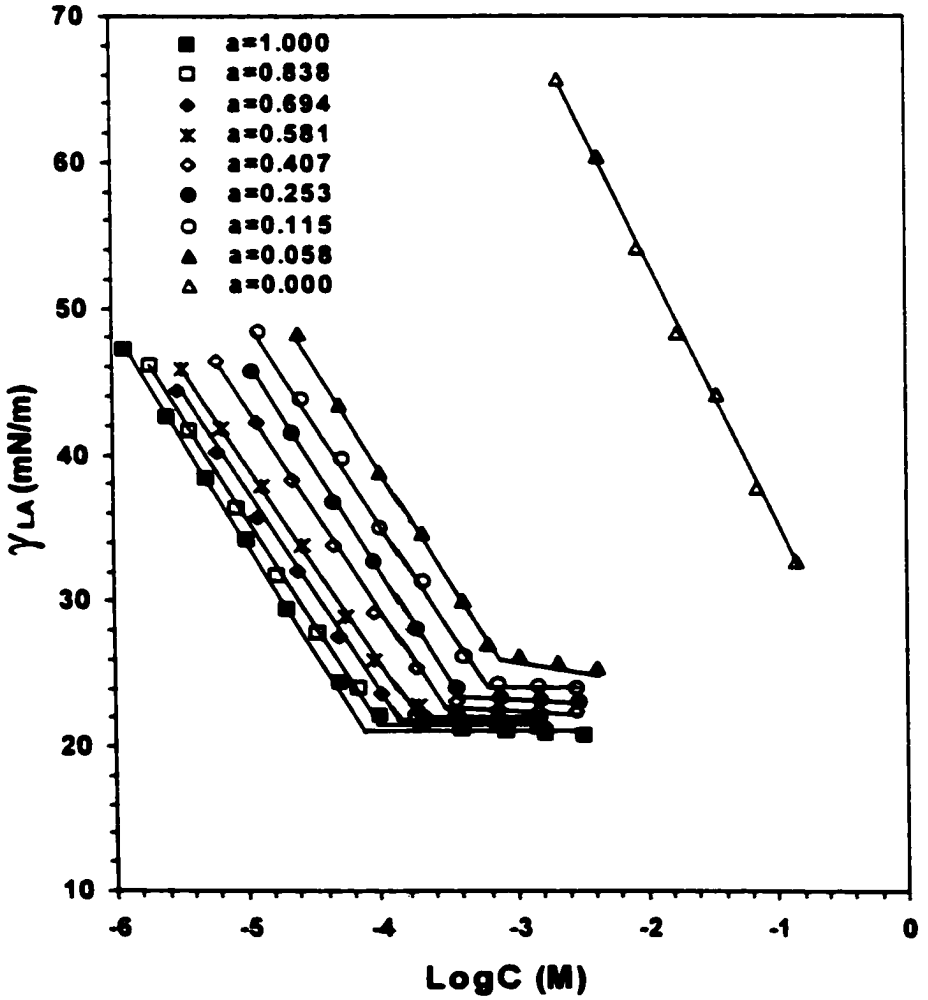

Figure B-3. Surface Tension of L77, C6P and Their Mixtures at Air/Aqueous Solution Interface

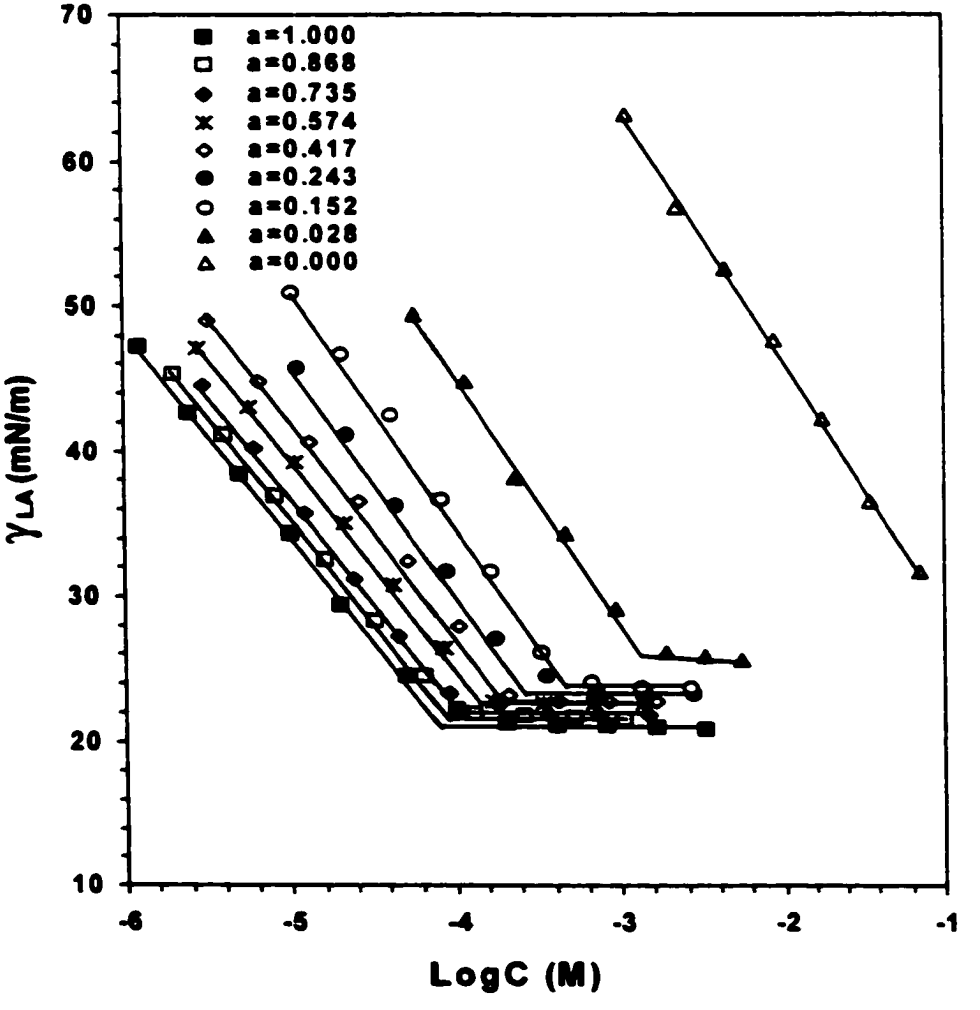

Figure B-4. Surface Tension of L77, C2,6P and Their Mixtures at Air/Aqueous Solution Interface

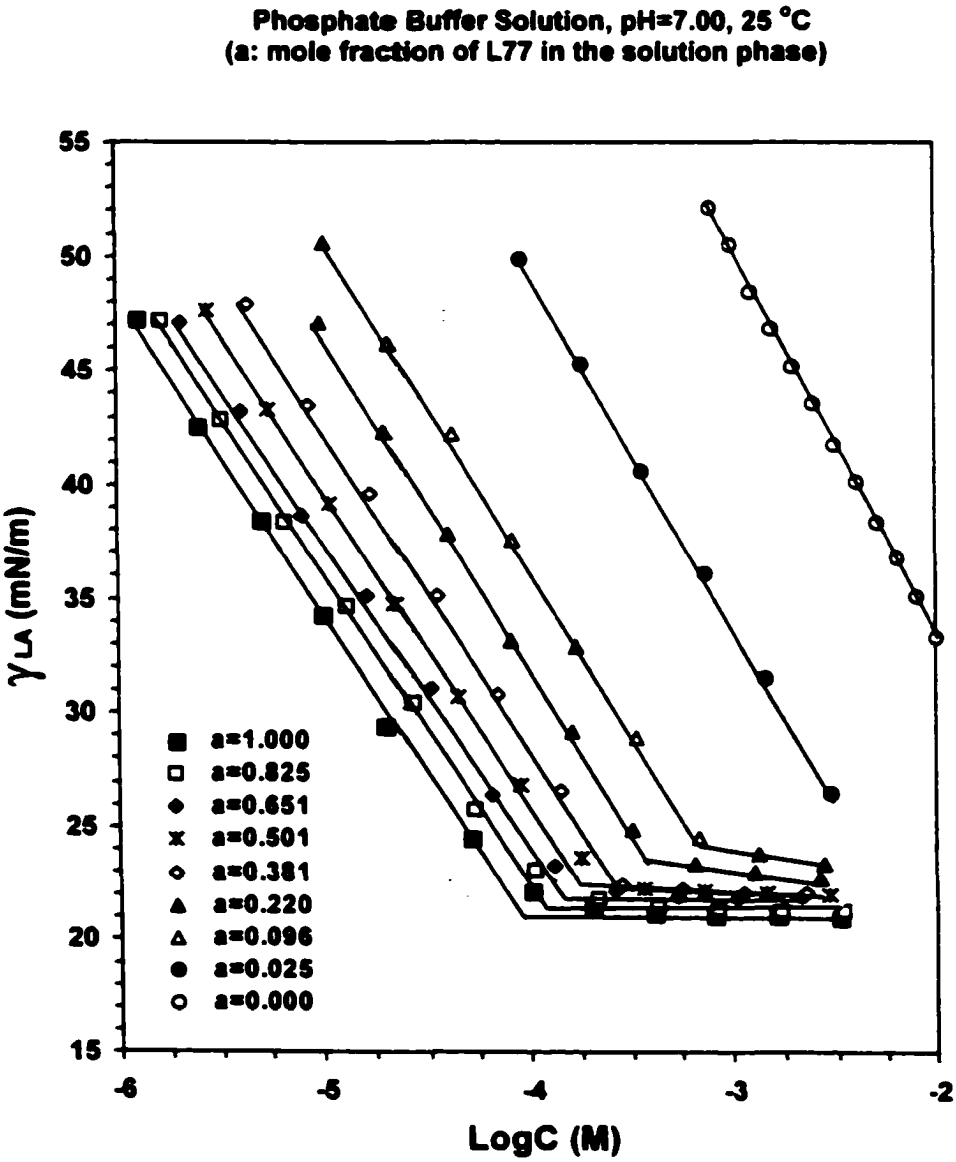

Figure B-5. Surface Tension of L77, C8P and Their Mixtures at Air/Aqueous Solution Interface

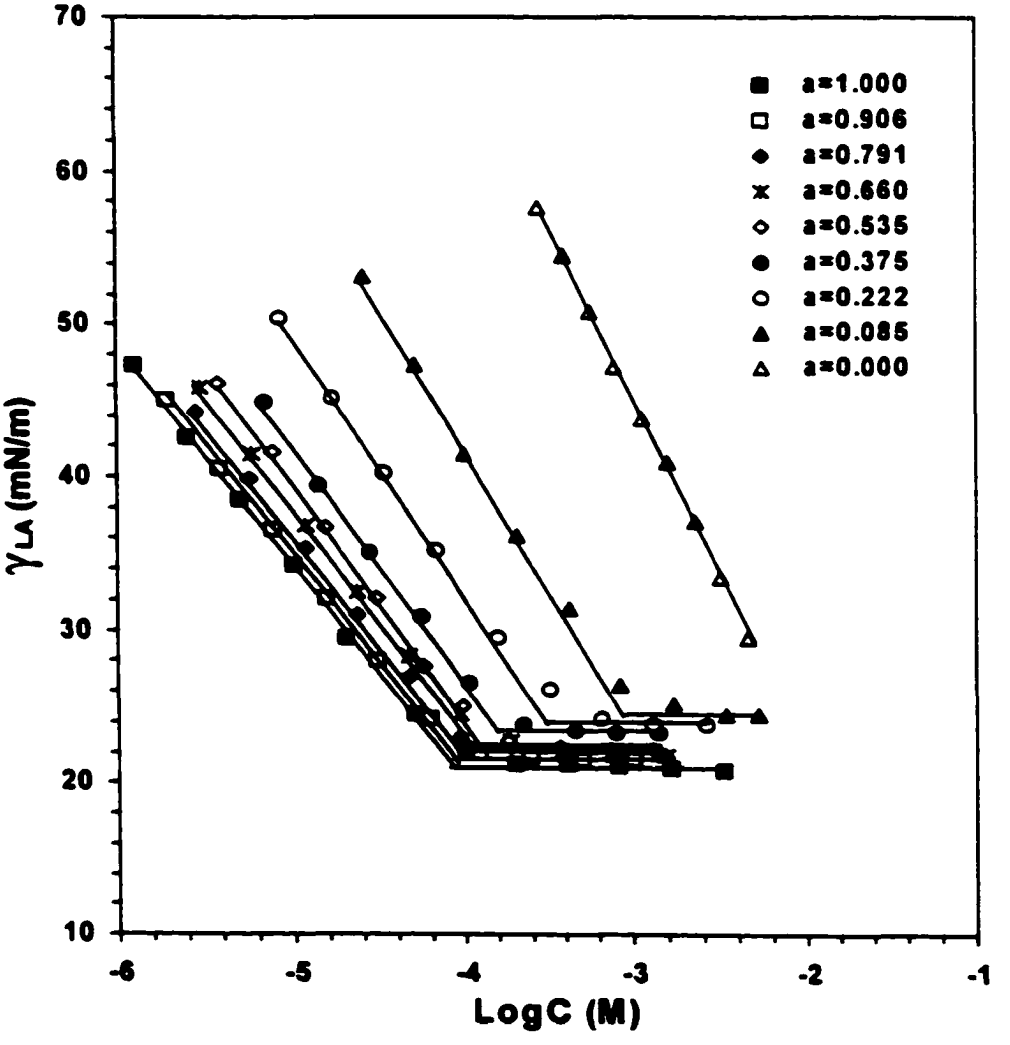

Figure B-6. Surface Tension of L77, C10P and Their Mixtures at Air/Aqueous Solution Interface

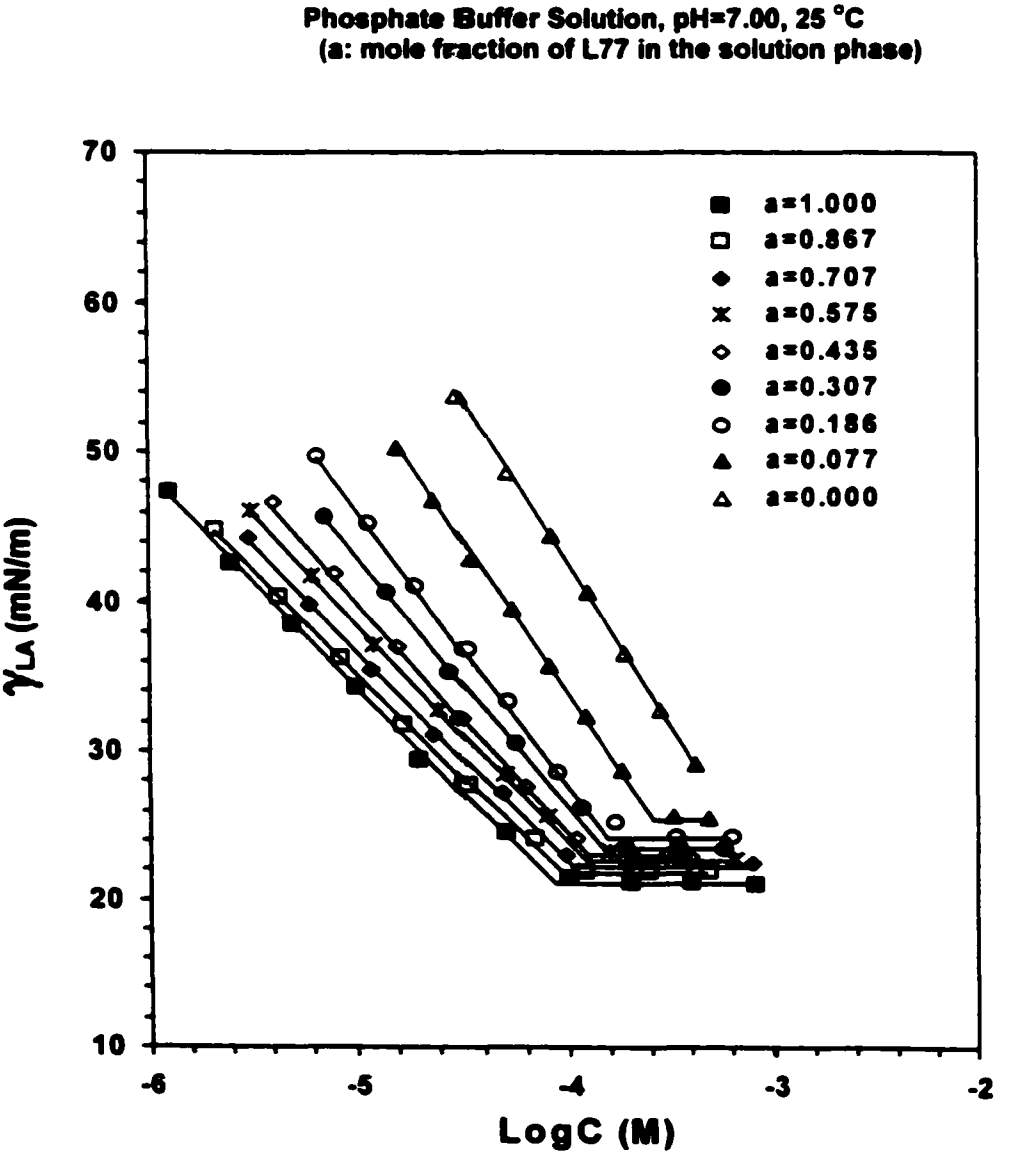

Figure B-7. Adhesion Tension of L77, C4P and Their Mixtures on Polyethylene Substrate

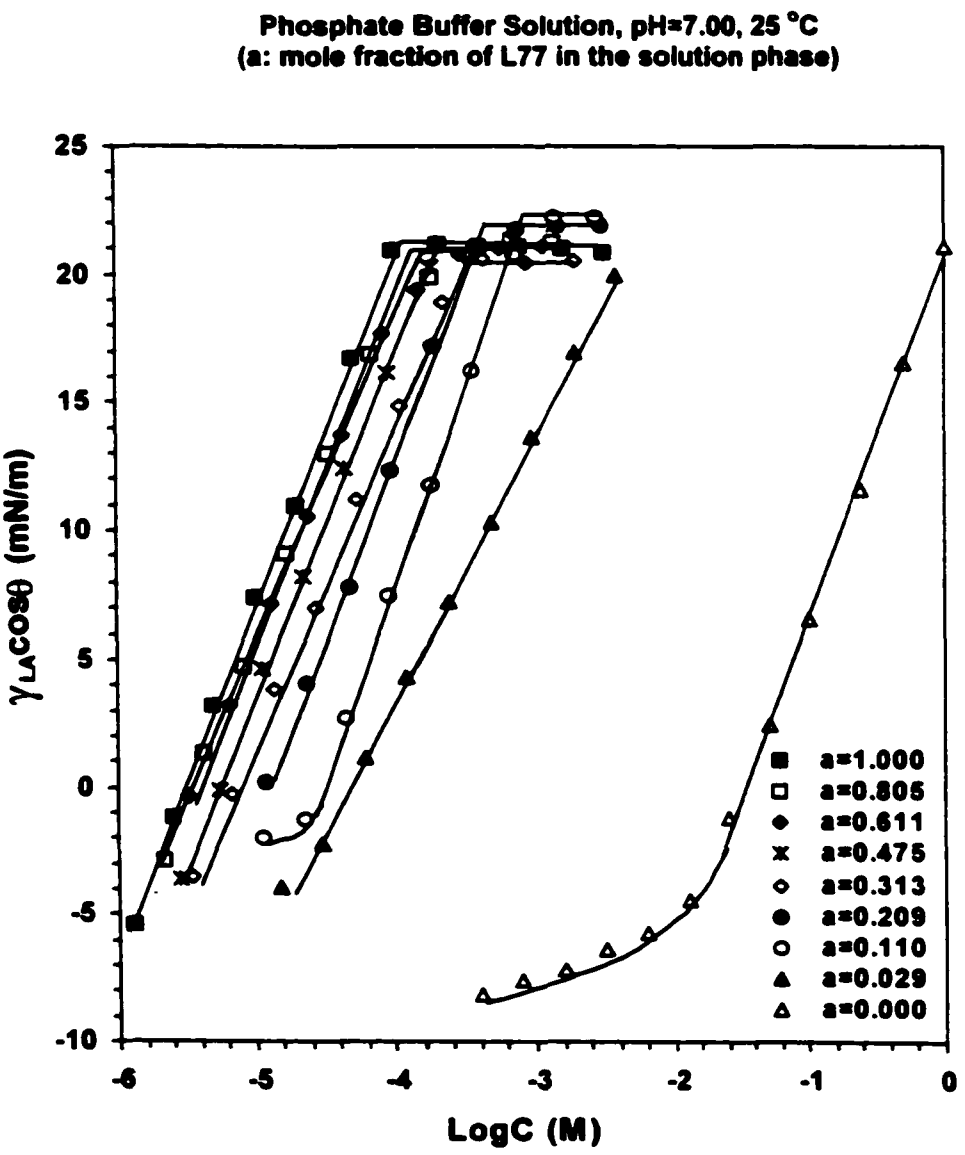

Figure B-8. Adhesion Tension of L77, CHP and Their Mixtures on Polyethylene Substrate

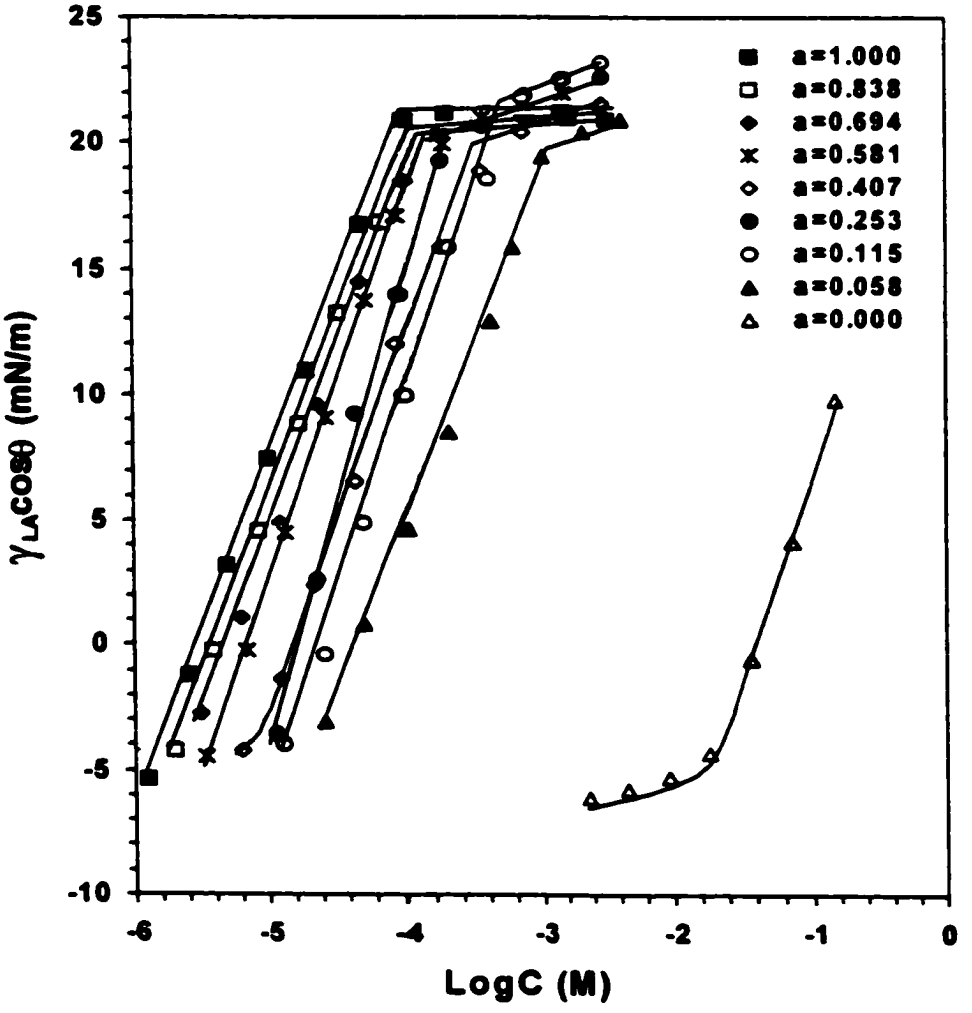

Figure B-9. Adhesion Tension of L77, C6P and Their Mixtures on Polyethylene Substrate

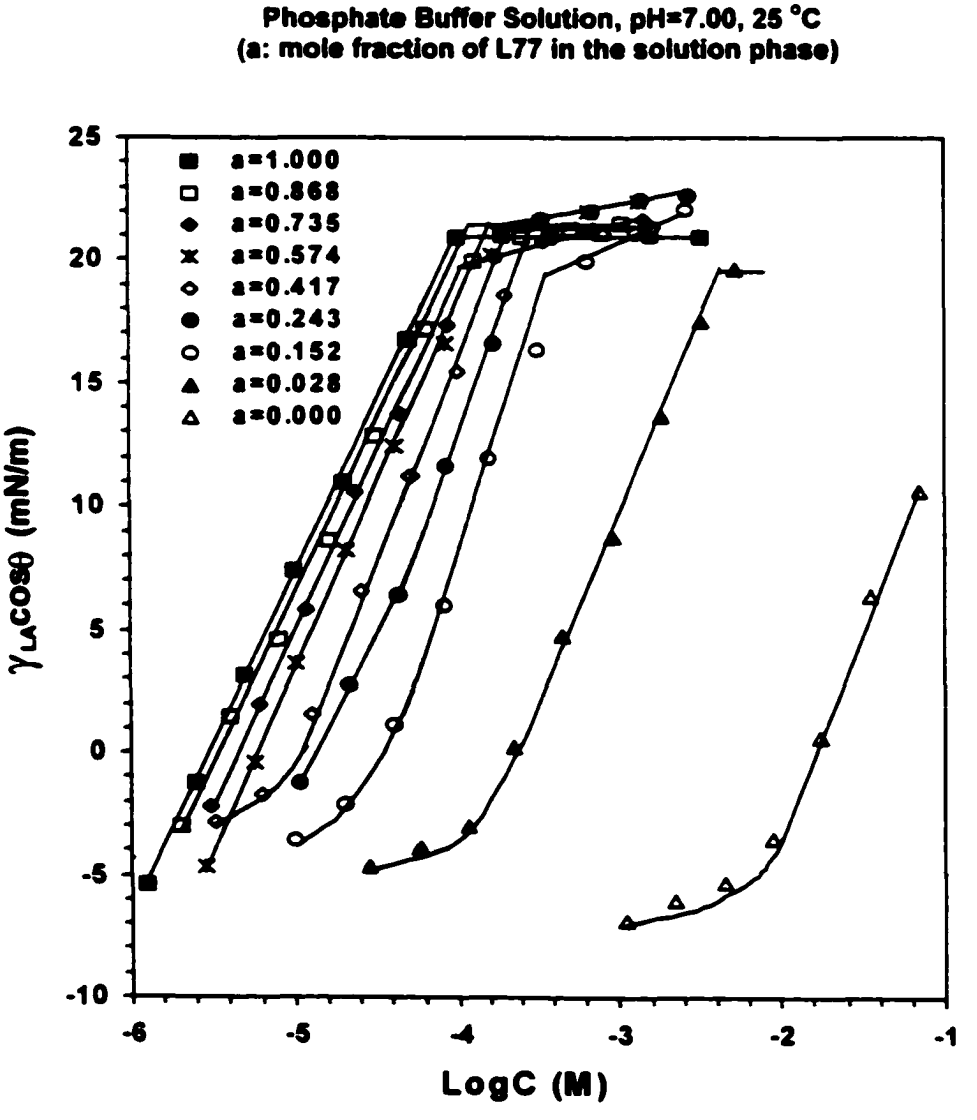

Figure B-10. Adhesion Tension of L77, C2,6P and Their Mixtures on Polyethylene Substrate

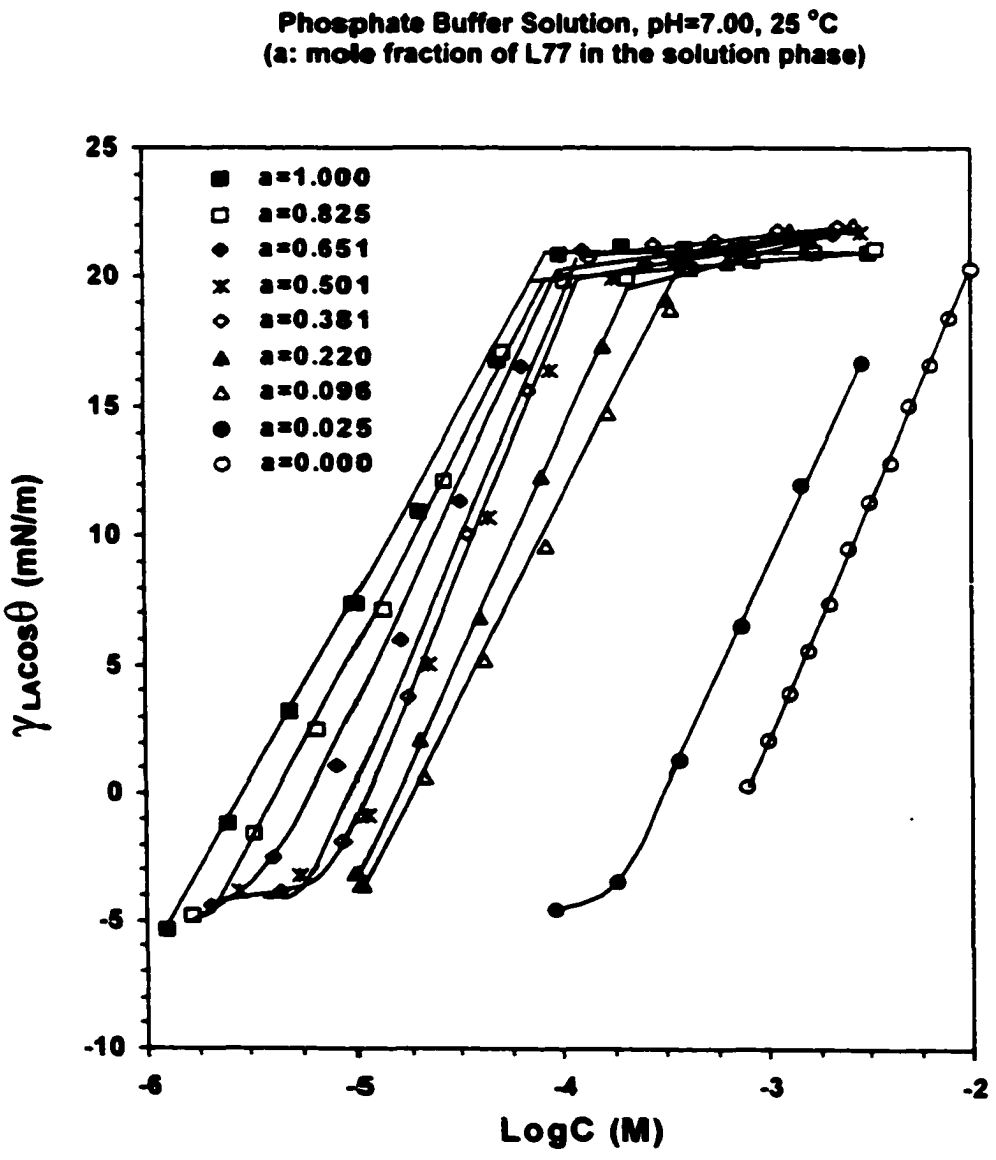

Figure B-11. Adhesion Tension of L77, C8P and Their Mixtures on Polyethylene Substrate

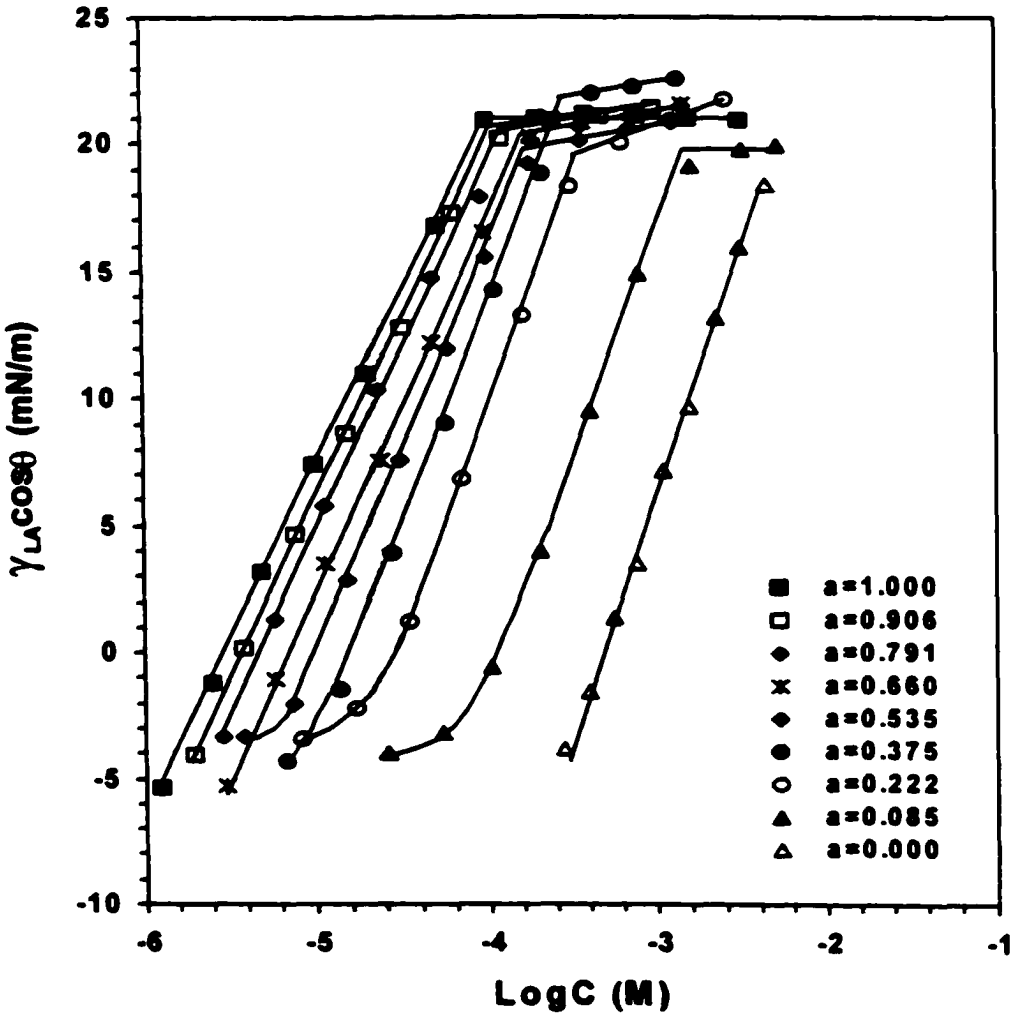

Figure B-12. Adhesion Tension of L77, C10P and Their Mixtures on Polyethylene Substrate

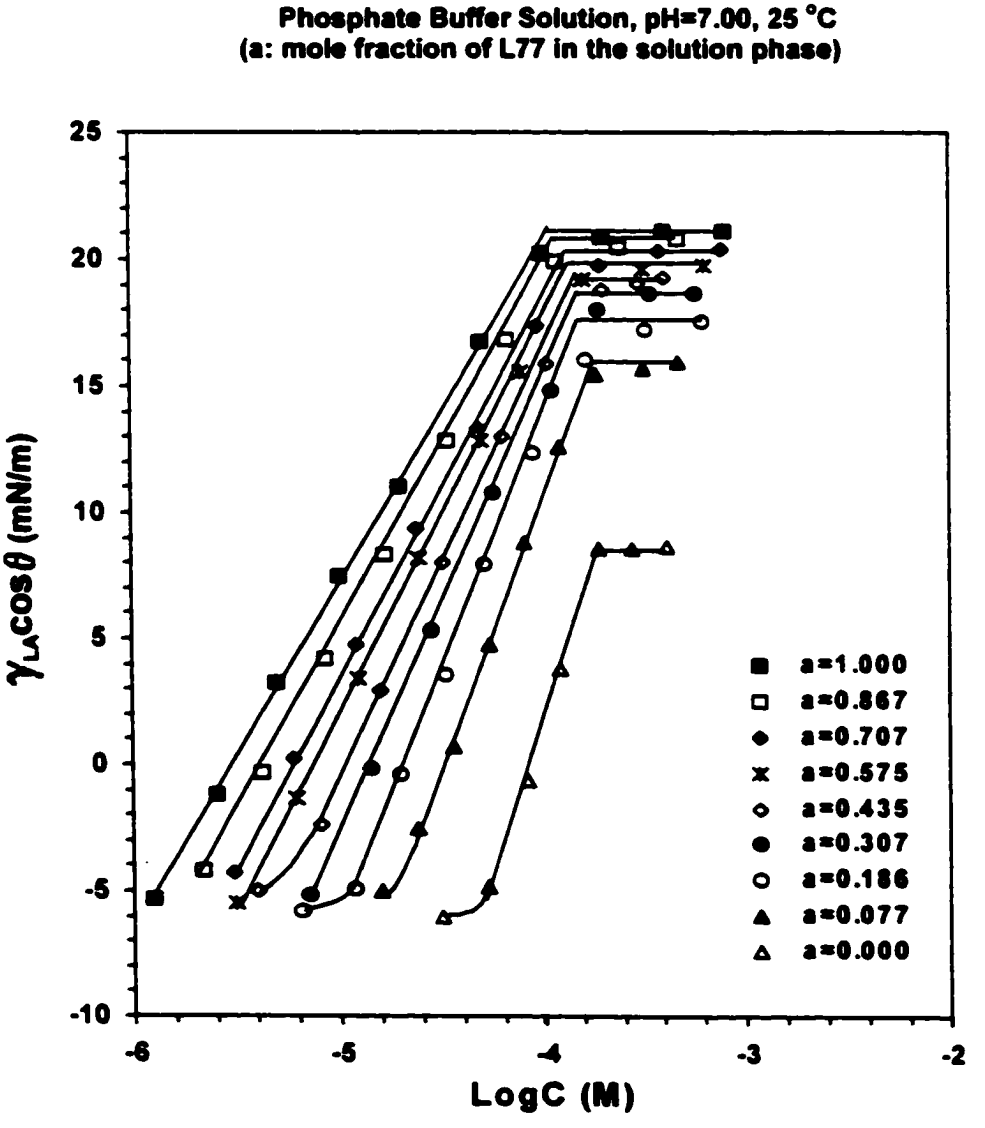

Figure B-13. Adsorption Isotherms of L77, C4P and Their Mixtures onto Powdered Polyethylene

(Fixed initial α_{L77}=0.034)

(In Phosphate Buffer Solution, pH=7.00)

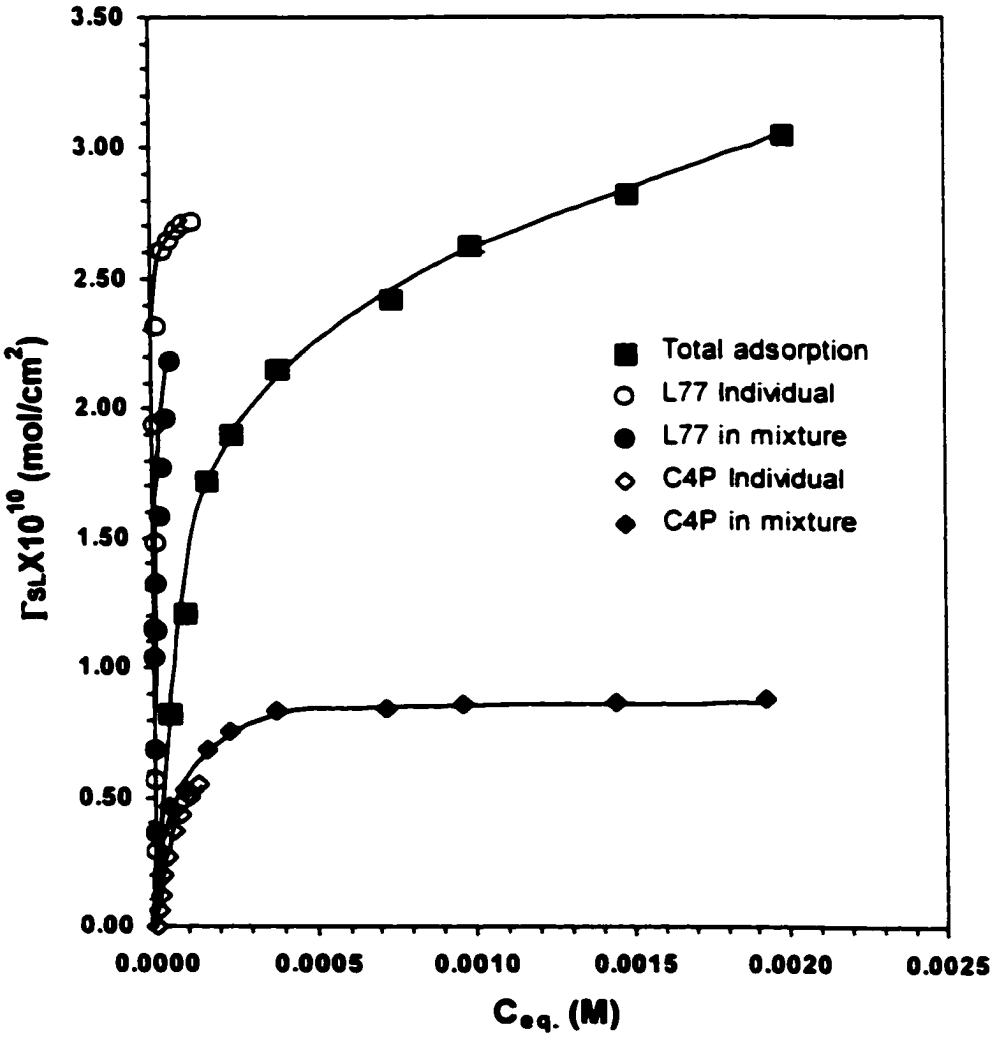

Figure B-14. Adsorption Isotherms of L77, C4P and Their Mixtures onto Powdered Polyethylene

(Fixed initial α_{L77}=0.137)

(In Phosphate Buffer Solution, pH=7.00)

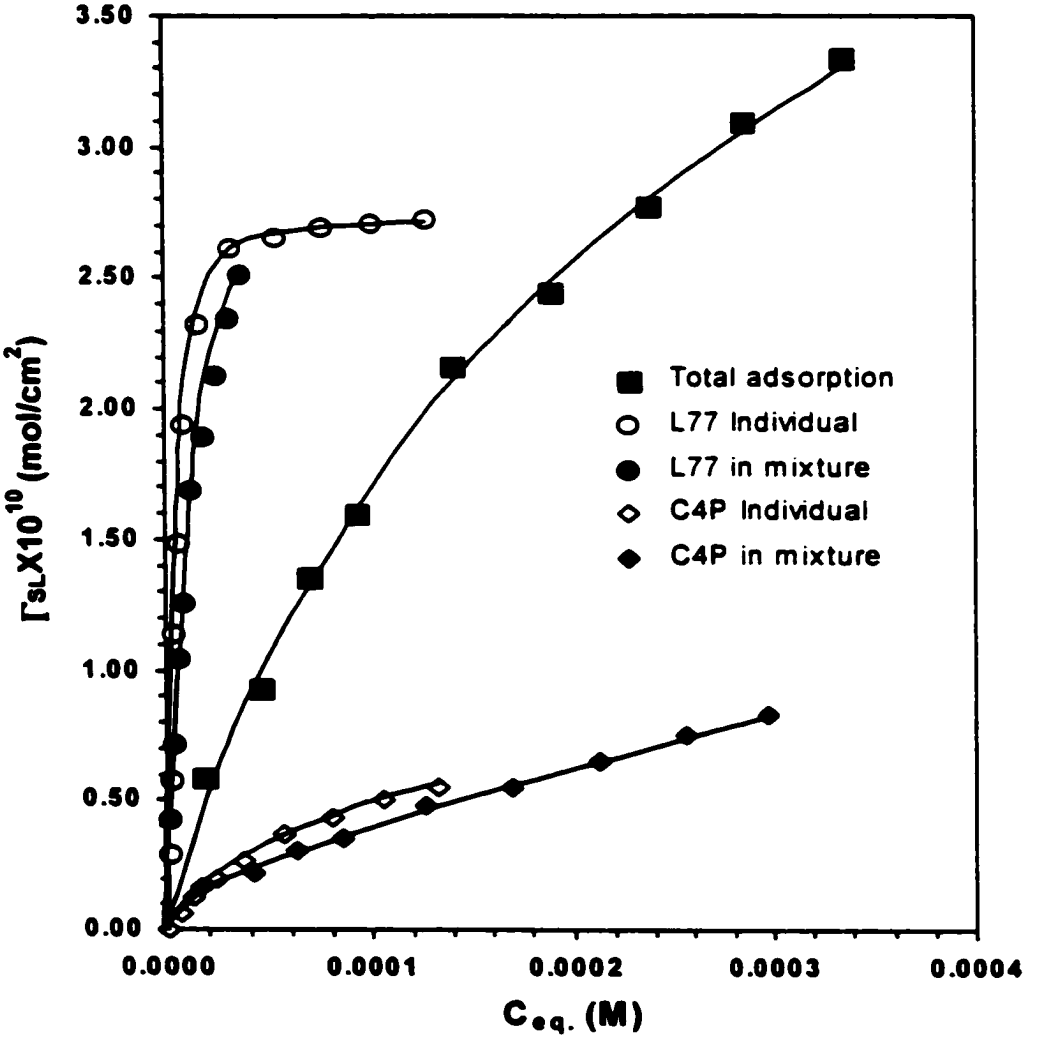

Figure B-15. Adsorption Isotherms of L77, C4P and Their Mixtures onto Powdered Polyethylene

(Fixed initial α_{L77}=0.243)

(In Phosphate Buffer Solution, pH=7.00)

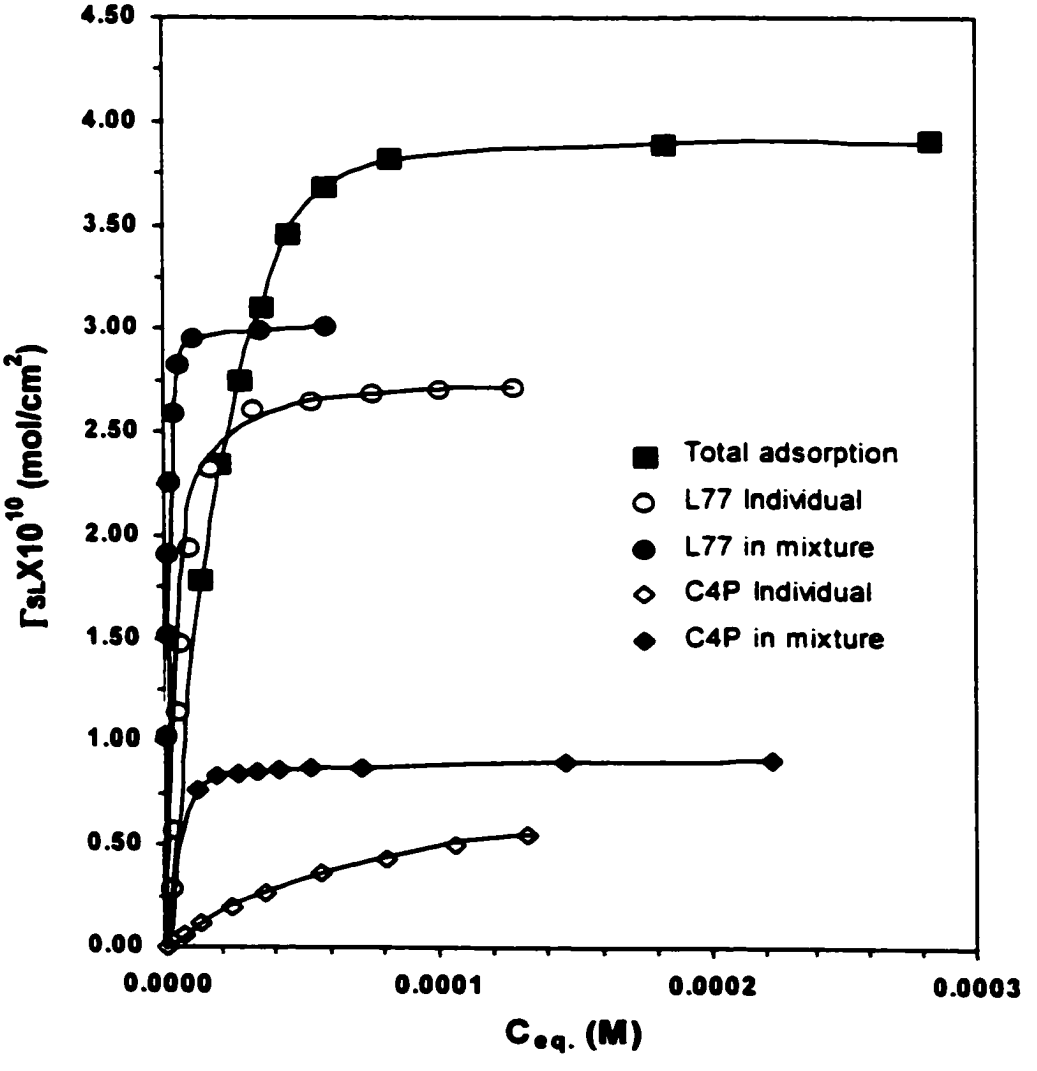

Figure B-16. Adsorption Isotherms of L77, C4P and Their Mixtures onto Powdered Polyethylene

(Fixed initial α_{L77}=0.353)

(In Phosphate Buffer Solution, pH=7.00)

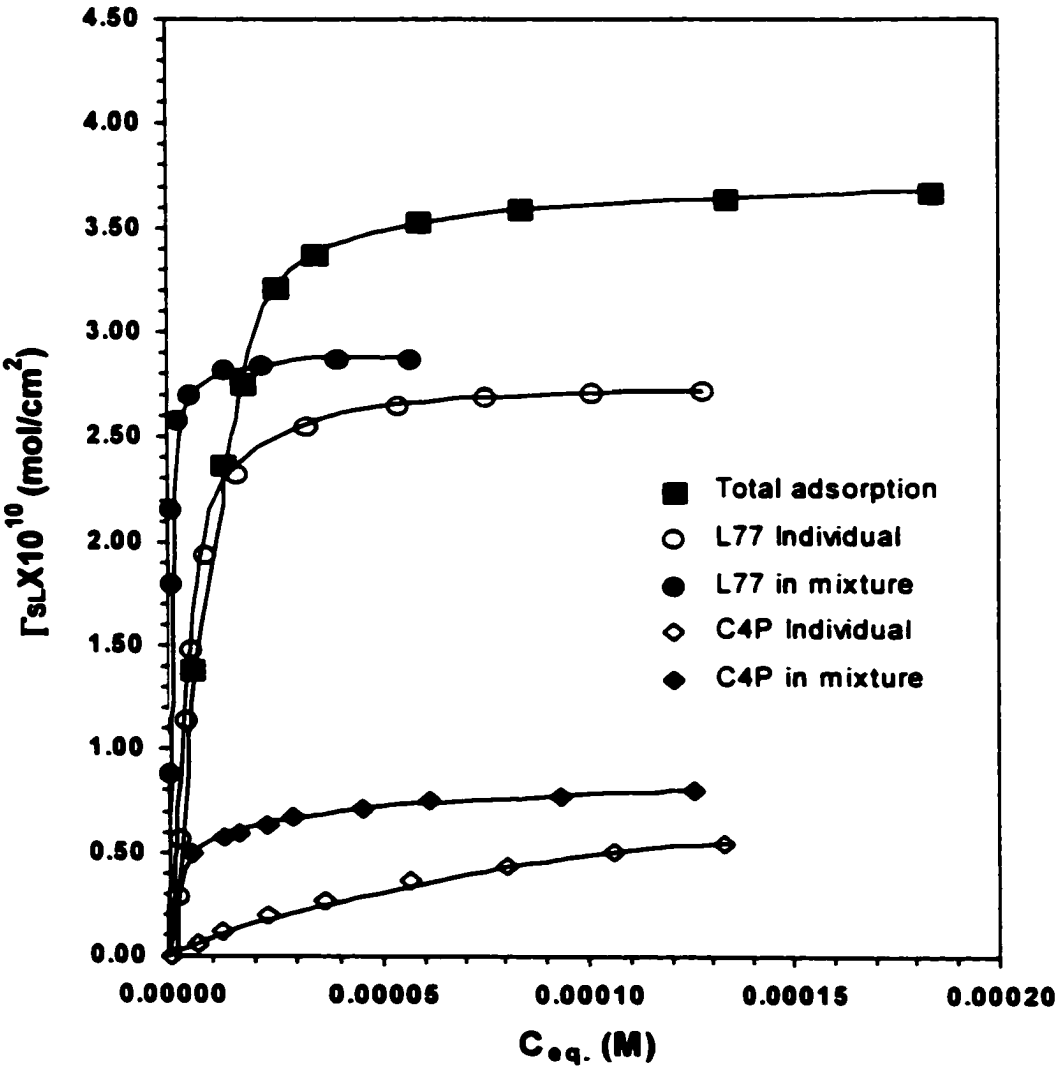

Figure B-17. Adsorption Isotherms of L77, C4P and Their Mixtures onto Powdered Polyethylene

(Fixed initial α_{L77}=0.503)

(In Phosphate Buffer Solution, pH=7.00)

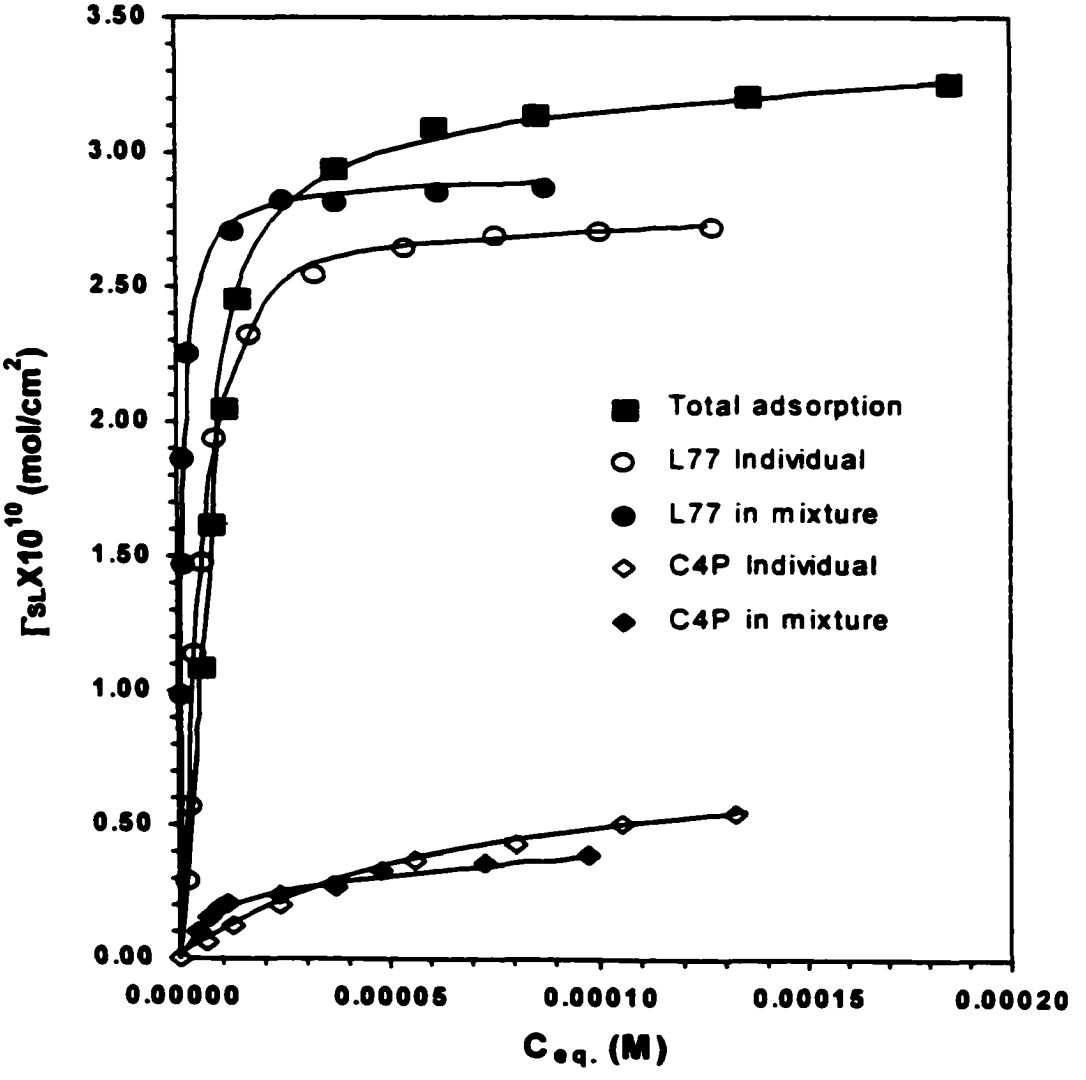

Figure B-18. Adsorption Isotherms of L77, C4P and Their Mixtures onto Powdered Polyethylene

(Fixed initial α_{L77}=0.634)

(In Phosphate Buffer Solution, pH=7.00)

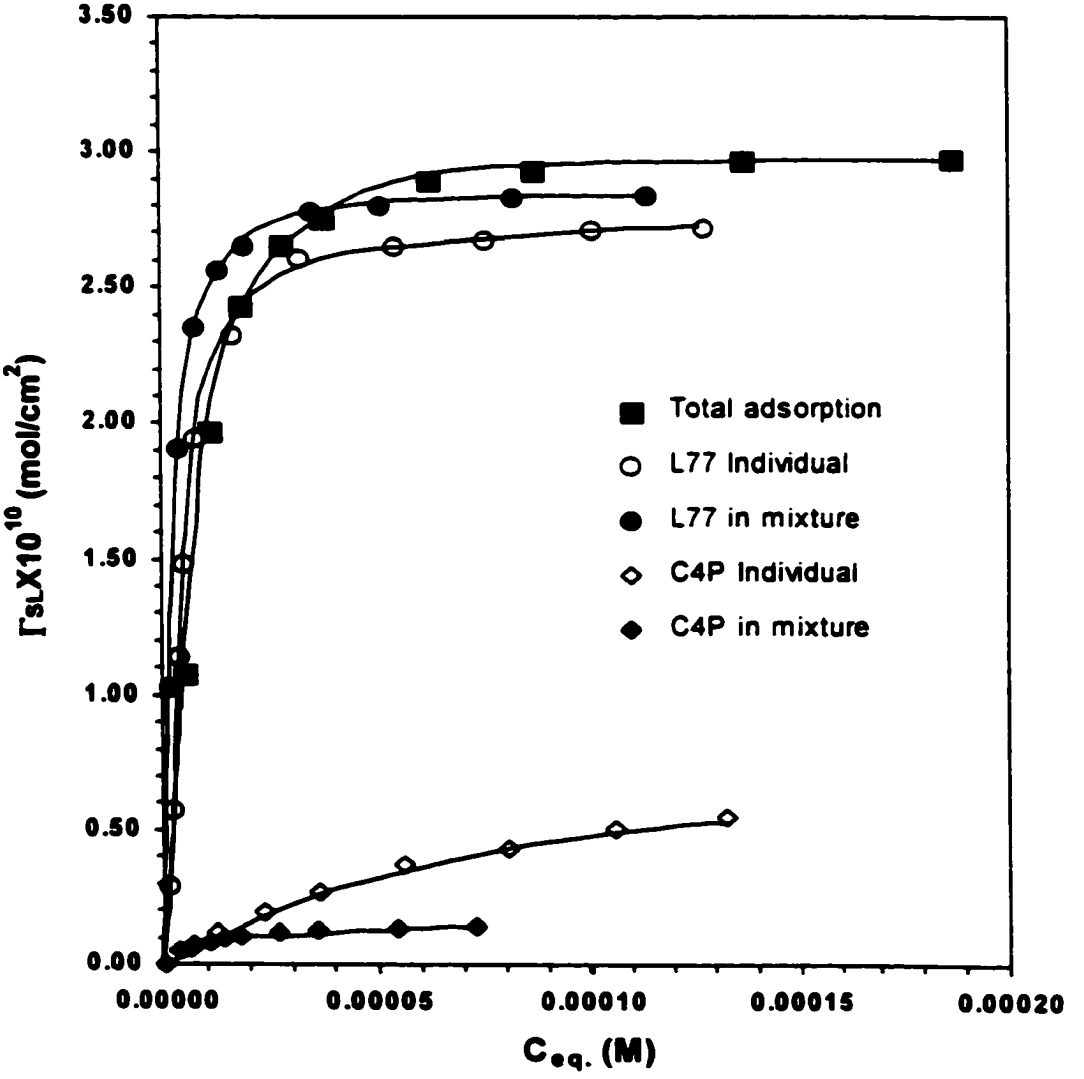

Figure B-19. Adsorption Isotherms of L77, C4P and Their Mixtures onto Powdered Polyethylene

(Fixed initial α_{L77}=0.819)

(In Phosphate Buffer Solution, pH=7.00)

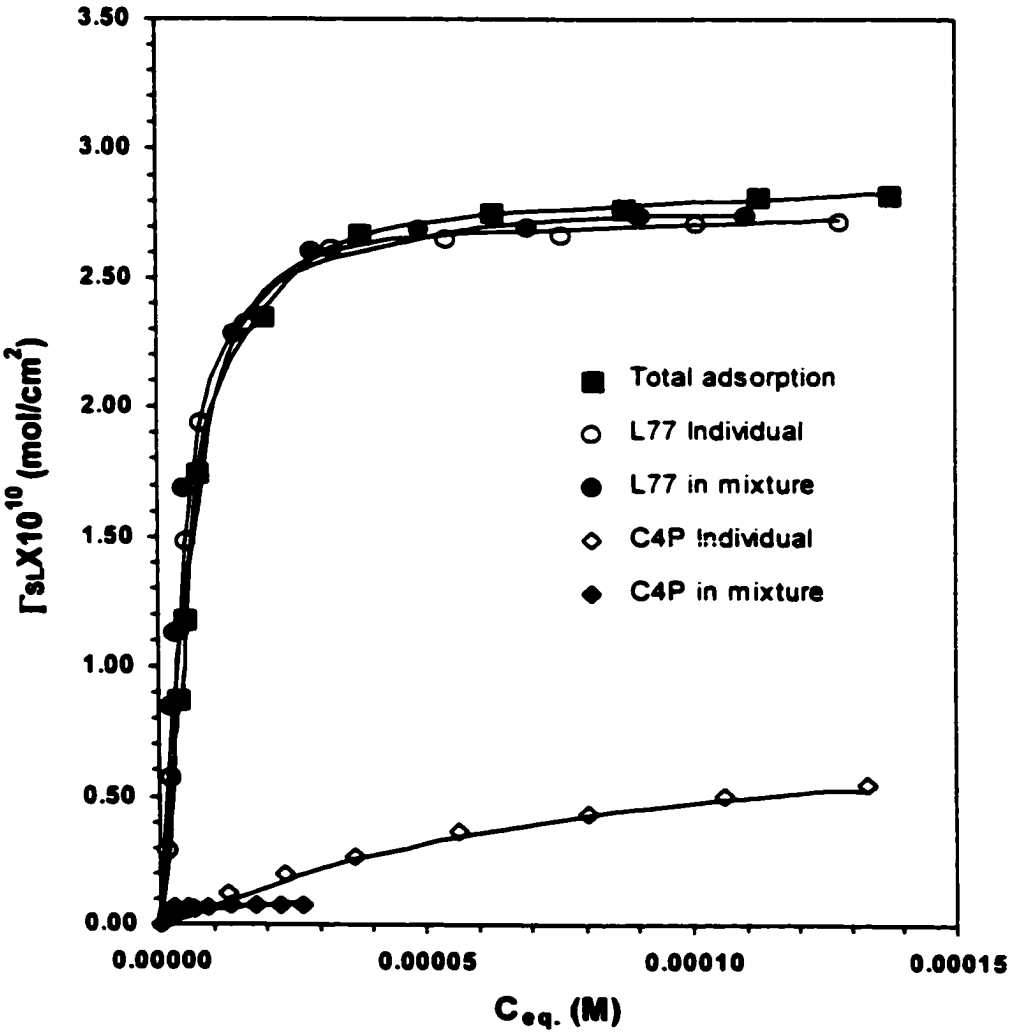

Figure B-20. Adsorption Isotherms of L77, CHP and Their Mixtures onto Powdered Polyethylene

(Fixed initial α_{L77}=0.067)

(In Phosphate Buffer Solution, pH=7.00)

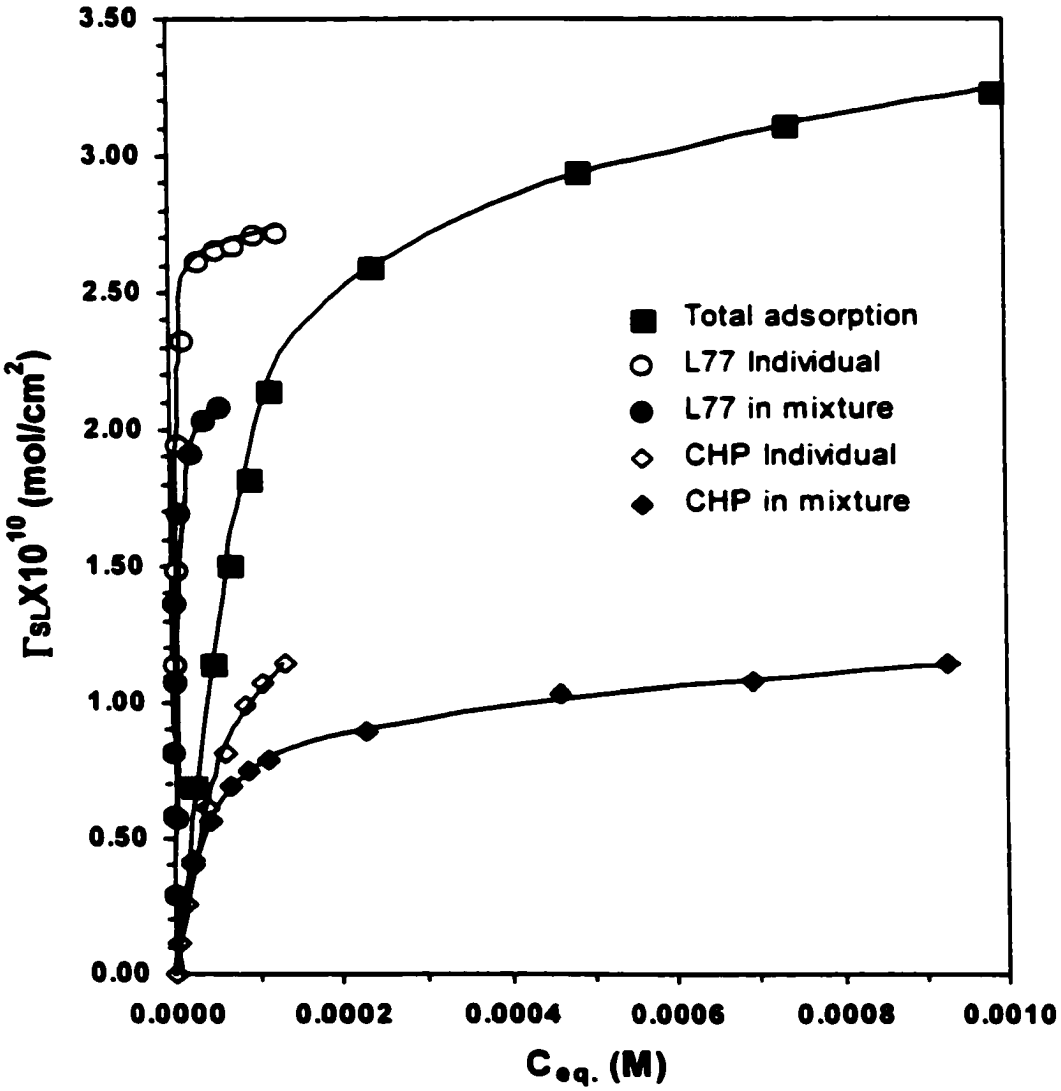

Figure B-21. Adsorption Isotherms of L77, CHP and Their Mixtures onto Powdered Polyethylene

(Fixed initial α_{L77}=0.136)

(In Phosphate Buffer Solution, pH=7.00)

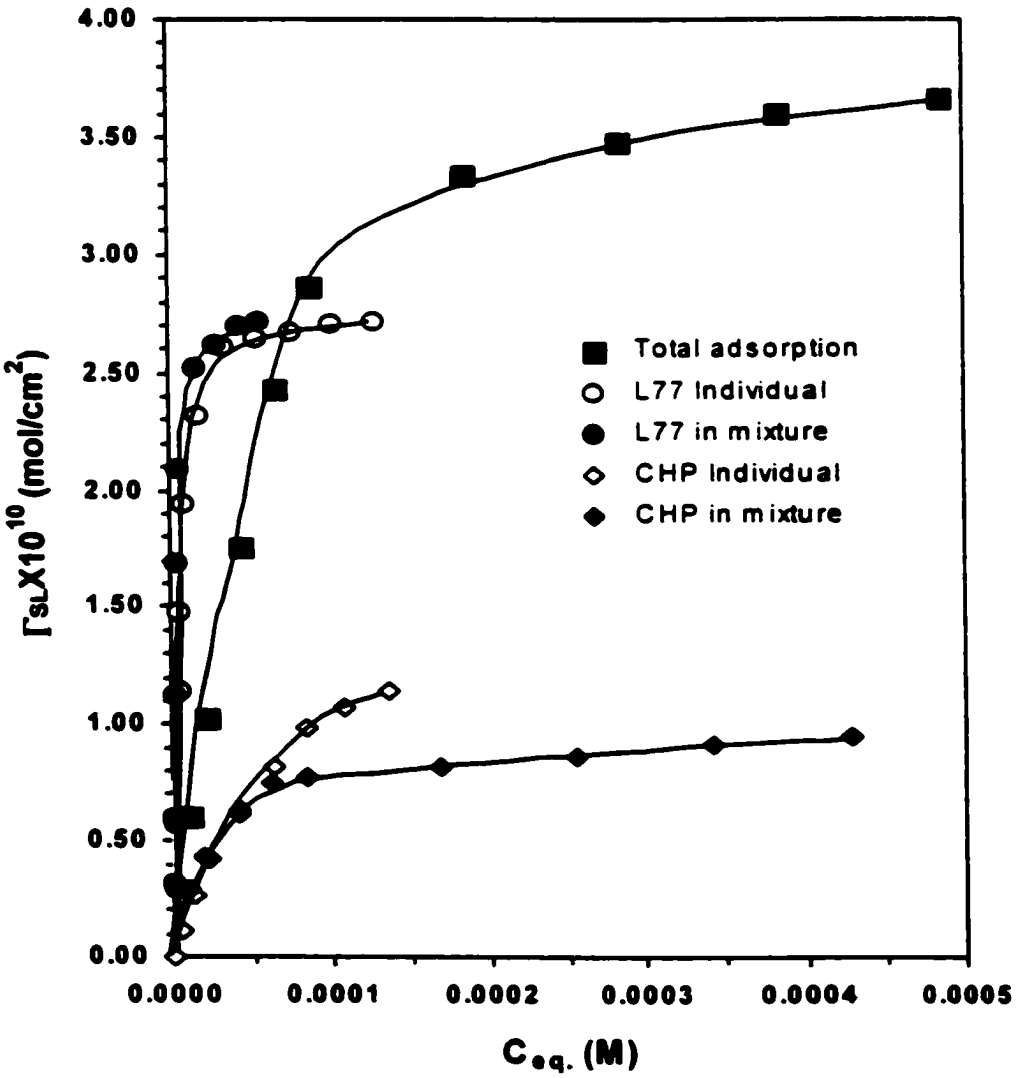

Figure B-22. Adsorption Isotherms of L77, CHP and Their Mixtures onto Powdered Polyethylene

(Fixed initial α_{L77}=0.285)

(In Phosphate Buffer Solution, pH=7.00)

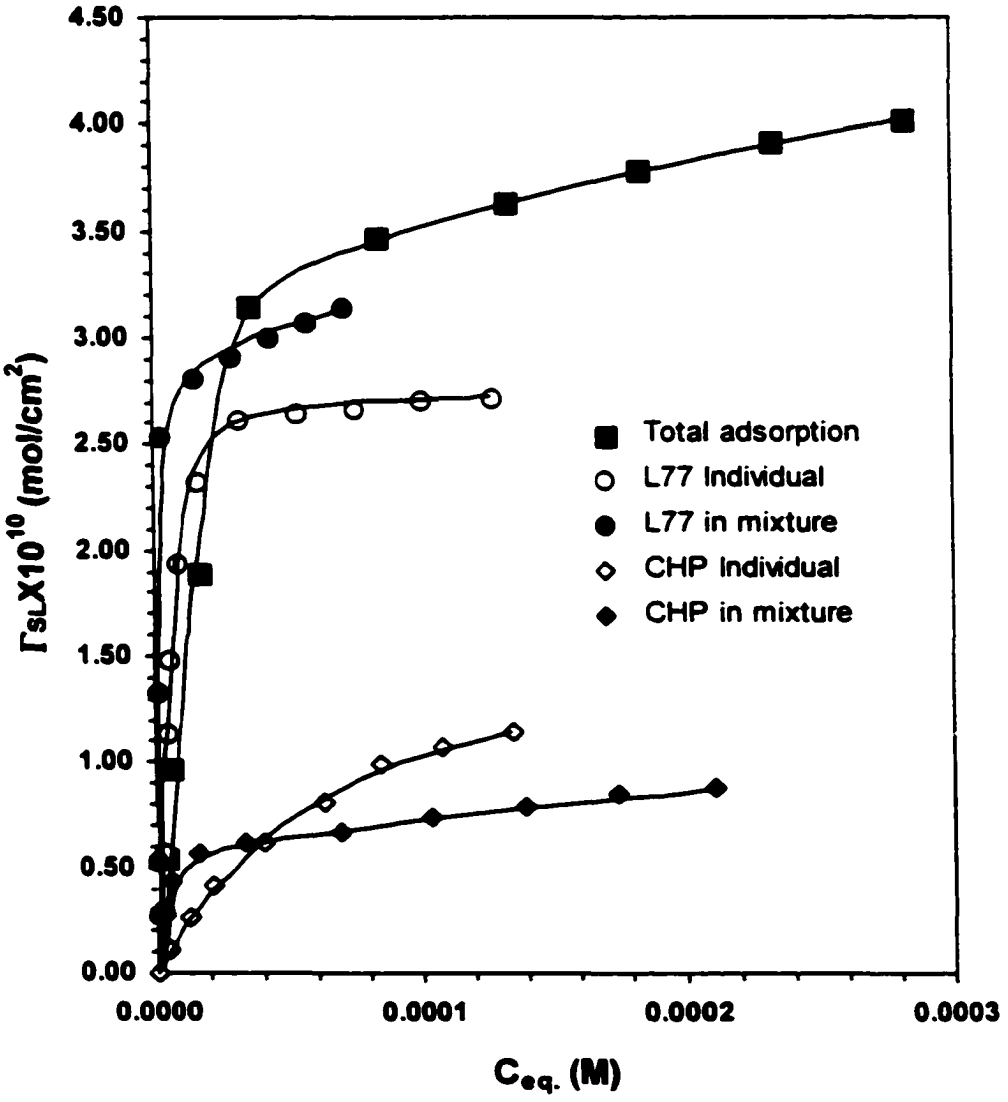

Figure B-23. Adsorption Isotherms of L77, CHP and Their Mixtures onto Powdered Polyethylene

(Fixed initial α_{L77}=0.438)

(In Phosphate Buffer Solution, pH=7.00)

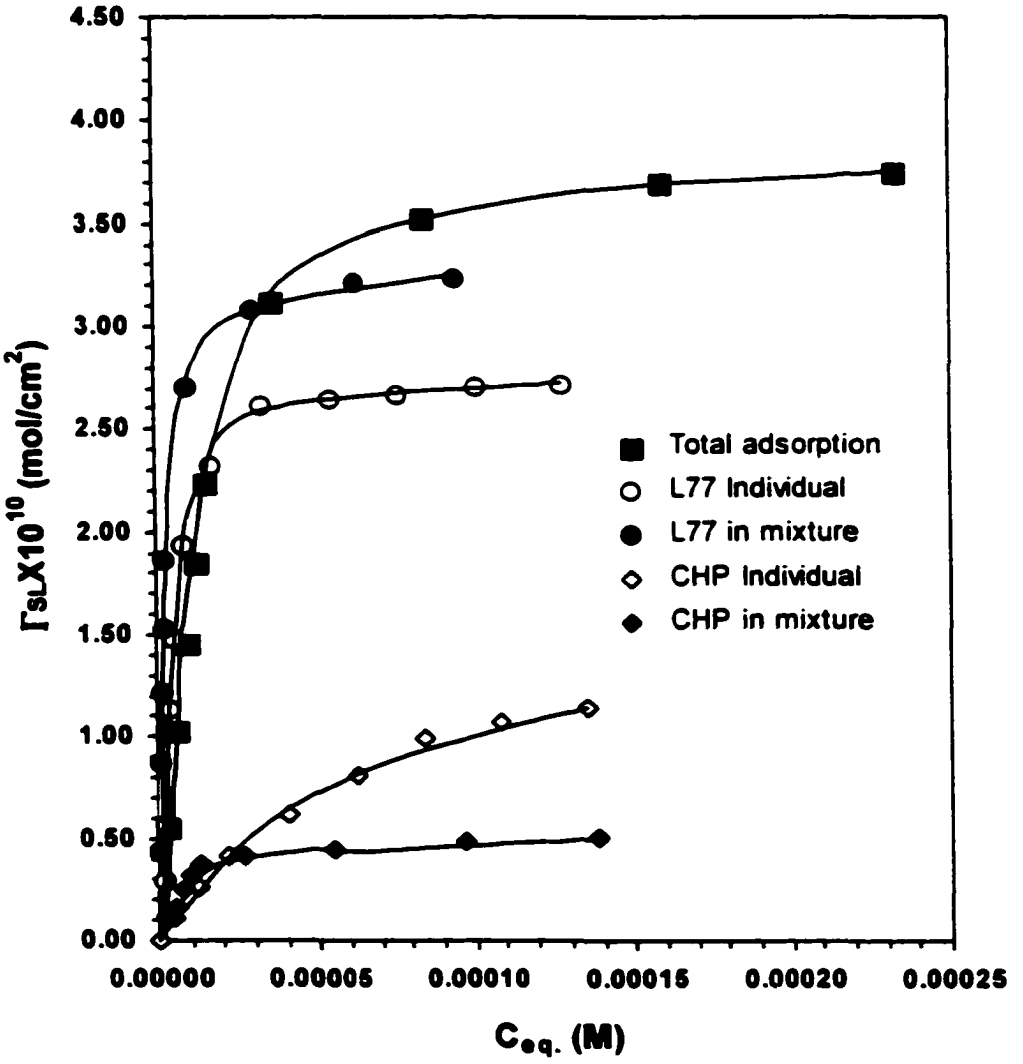

Figure B-24. Adsorption Isotherms of L77, CHP and Their Mixtures onto Powdered Polyethylene

(Fixed initial α_{L77}=0.602)

(In Phosphate Buffer Solution, pH=7.00)

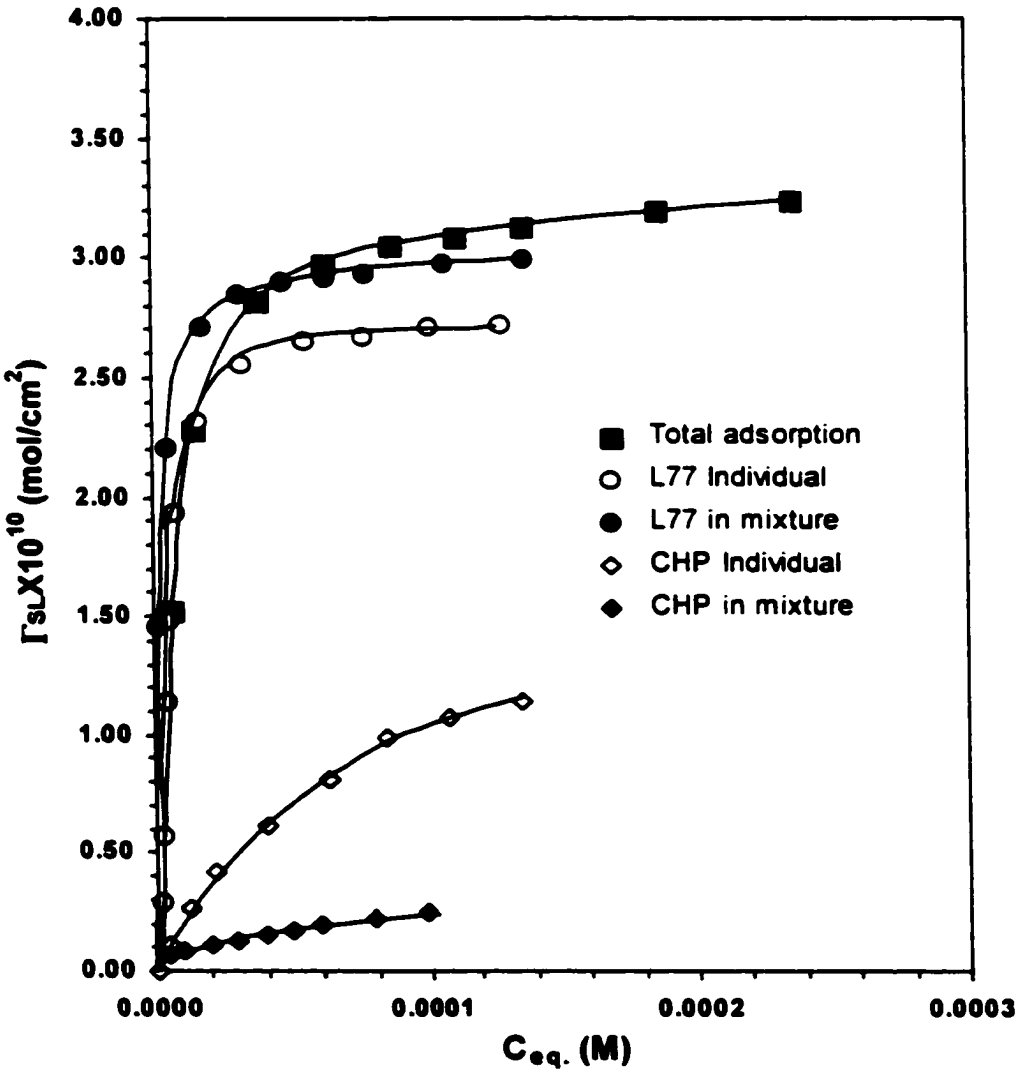

Figure B-25. Adsorption Isotherms of L77, CHP and Their Mixtures onto Powdered Polyethylene

(Fixed initial α_{L77}=0.712)

(In Phosphate Buffer Solution, pH=7.00)

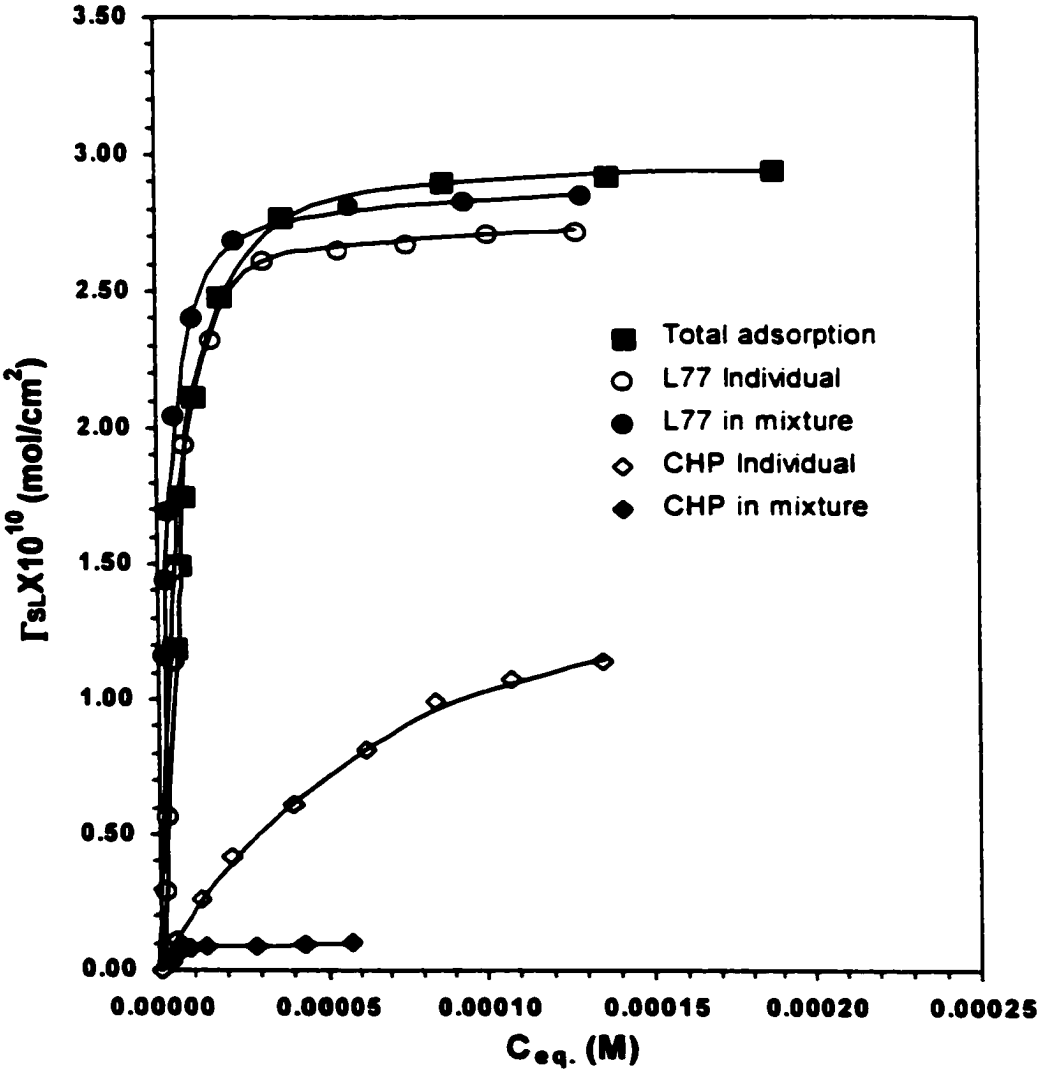

Figure B-26. Adsorption Isotherms of L77, CHP and Their Mixtures onto Powdered Polyethylene

(Fixed initial α_{L77}=0.850)

(In Phosphate Buffer Solution, pH=7.00)

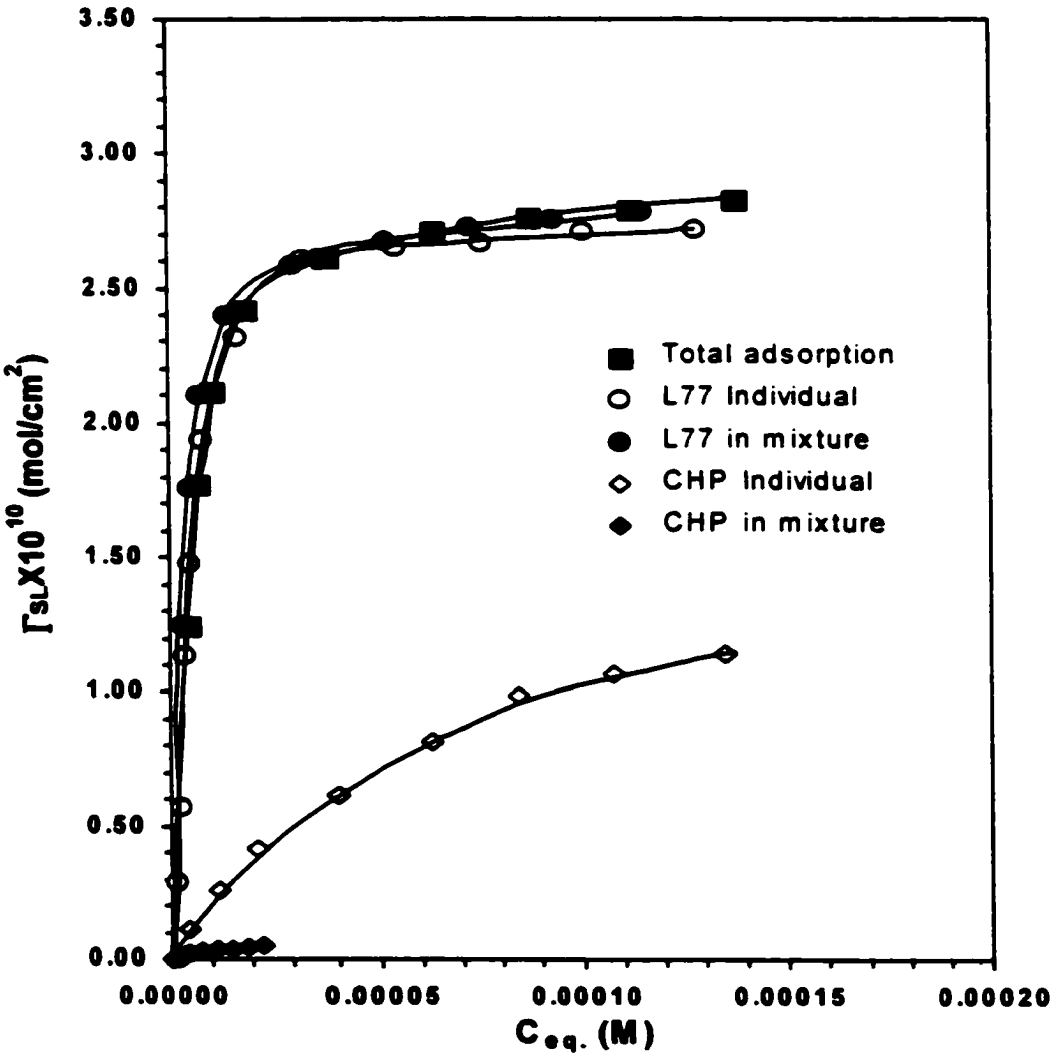

Figure B-27. Adsorption Isotherms of L77, C6P and Their Mixtures onto Powdered Polyethylene

(Fixed initial α_{L77}=0.039)

(In Phosphate Buffer Solution, pH=7.00)

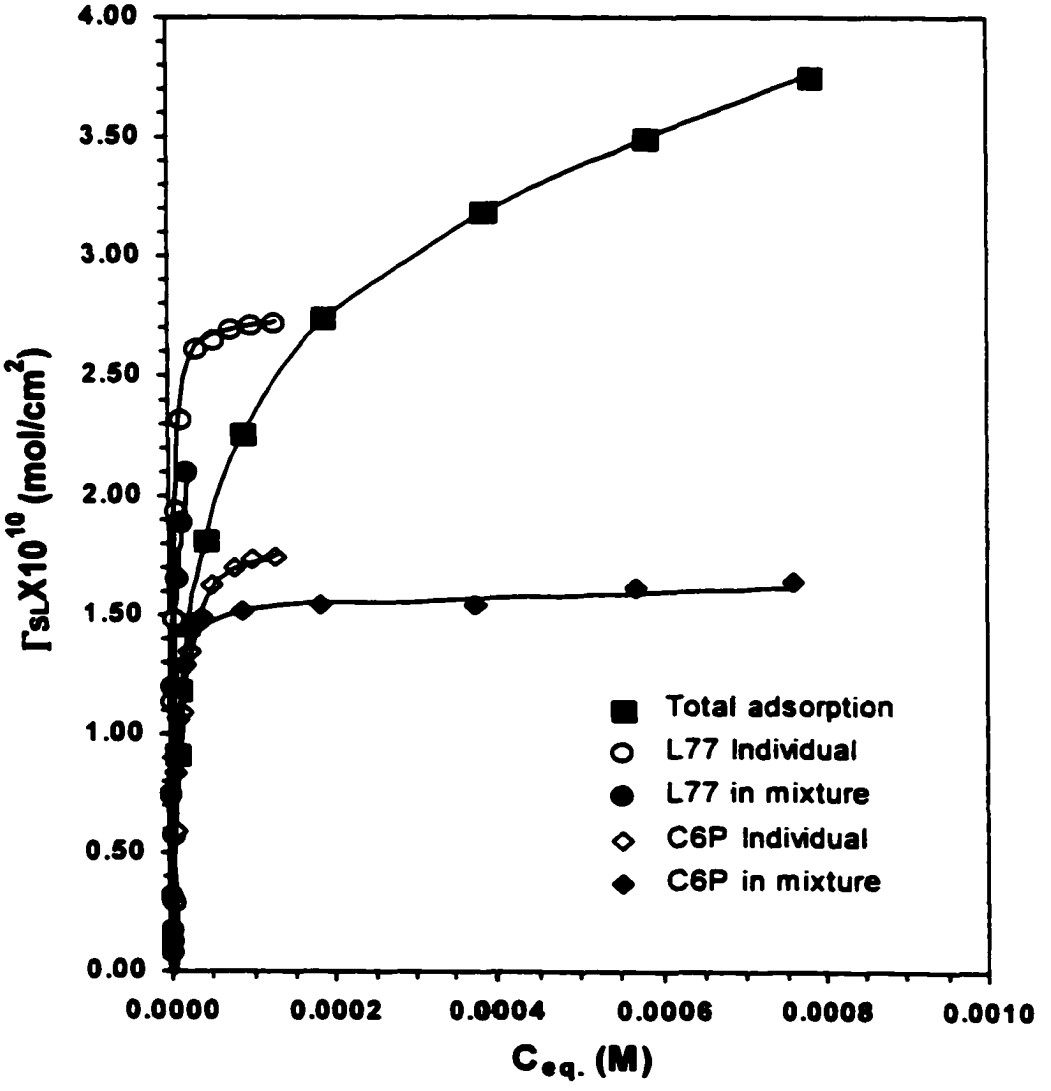

Figure B-28. Adsorption Isotherms of L77, C6P and Their Mixtures onto Powdered Polyethylene

(Fixed initial α_{L77}=0.172)

(In Phosphate Buffer Solution, pH=7.00)

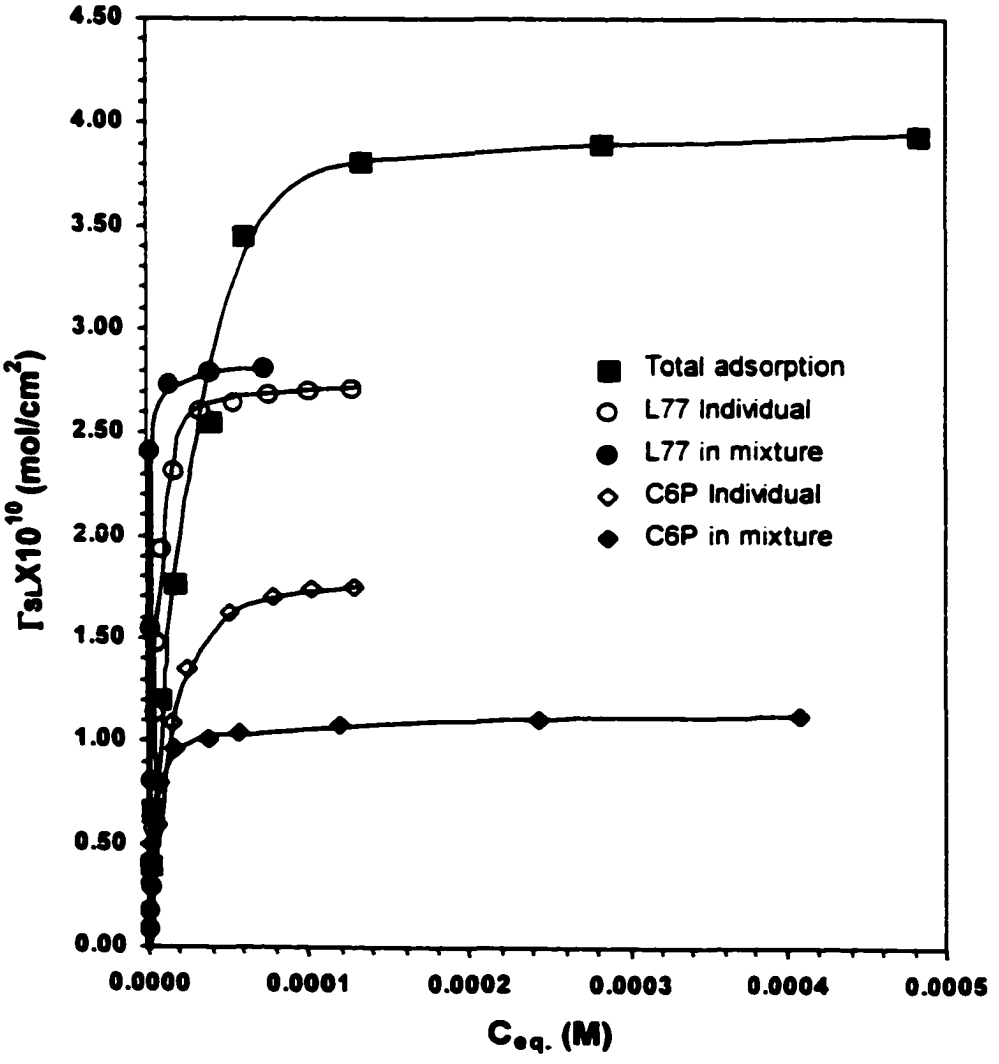

Figure B-29. Adsorption Isotherms of L77, C6P and Their Mixtures onto Powdered Polyethylene

(Fixed initial α_{L77}=0.269)

(In Phosphate Buffer Solution, pH=7.00)

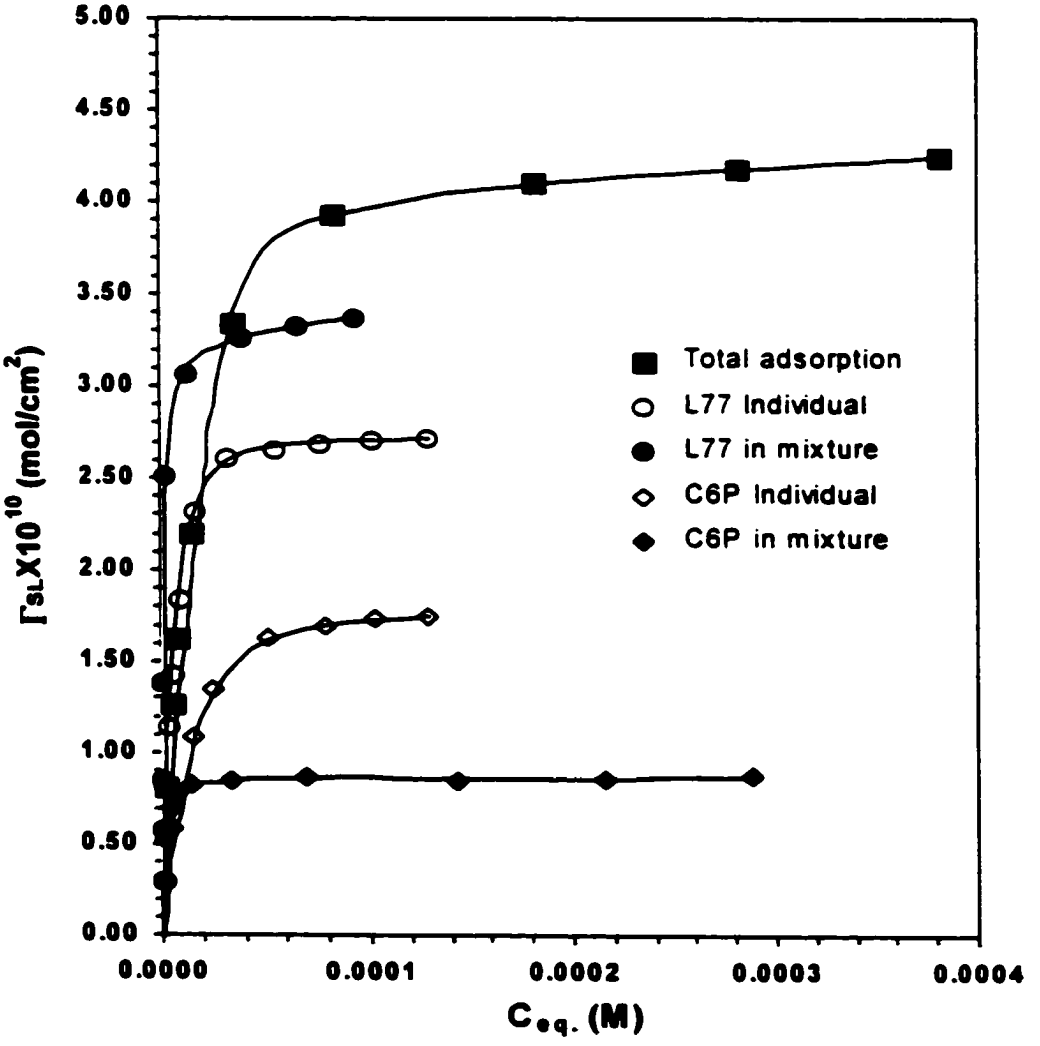

Figure B-30. Adsorption Isotherms of L77, C6P and Their Mixtures onto Powdered Polyethylene

(Fixed initial α_{L77}=0.441)

(In Phosphate Buffer Solution, pH=7.00)

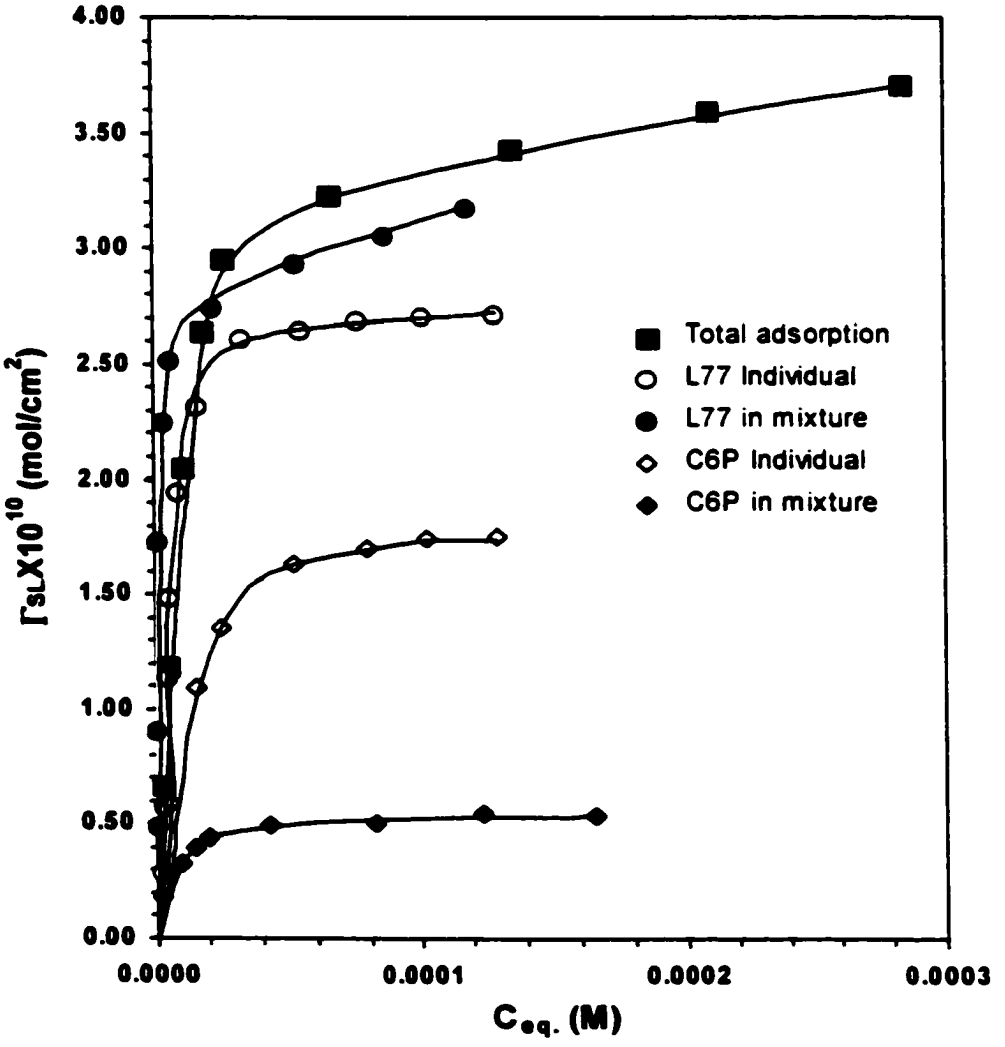

Figure B-31. Adsorption Isotherms of L77, C6P and Their Mixtures onto Powdered Polyethylene

(Fixed initial α_{L77}=0.595)

(In Phosphate Buffer Solution, pH=7.00)

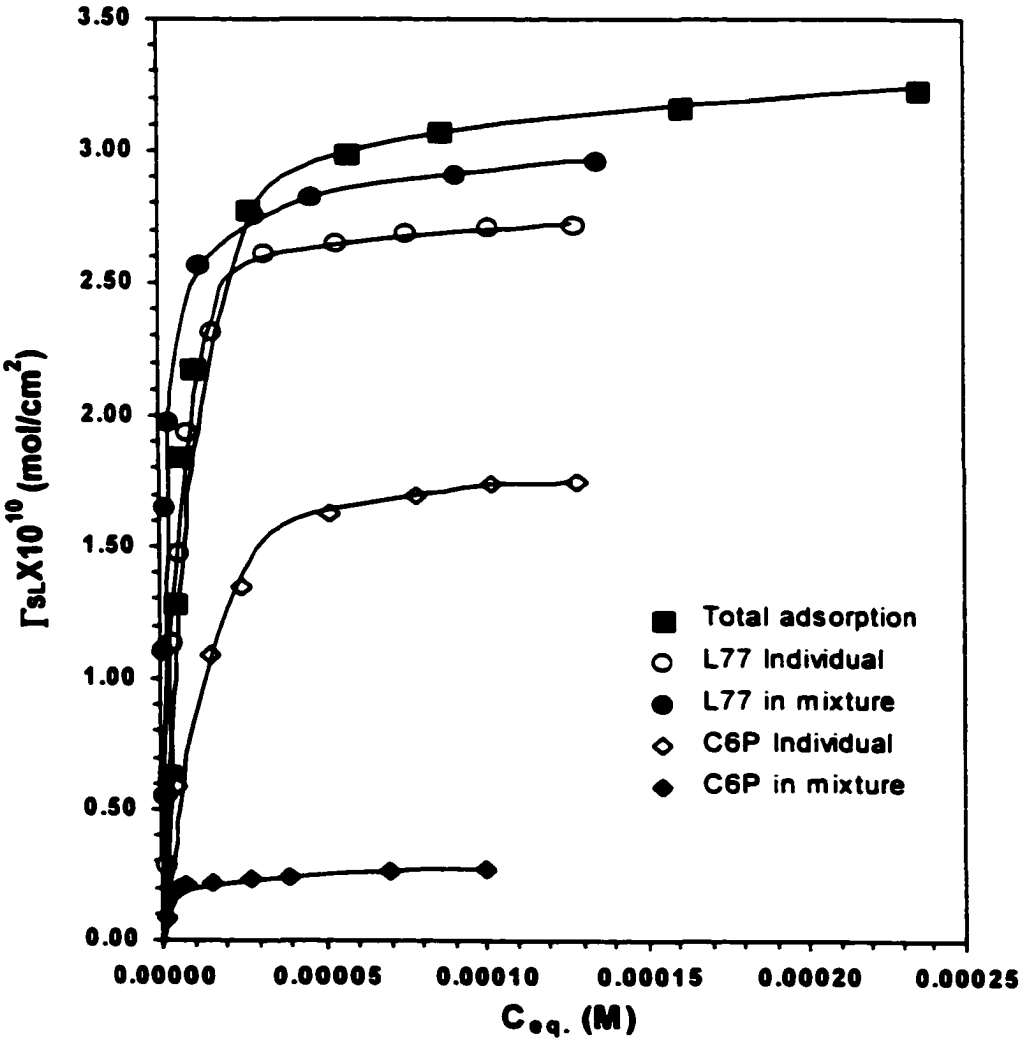

Figure B-32. Adsorption Isotherms of L77, C6P and Their Mixtures onto Powdered Polyethylene

(Fixed initial α_{L77}=0.751)

(In Phosphate Buffer Solution, pH=7.00)

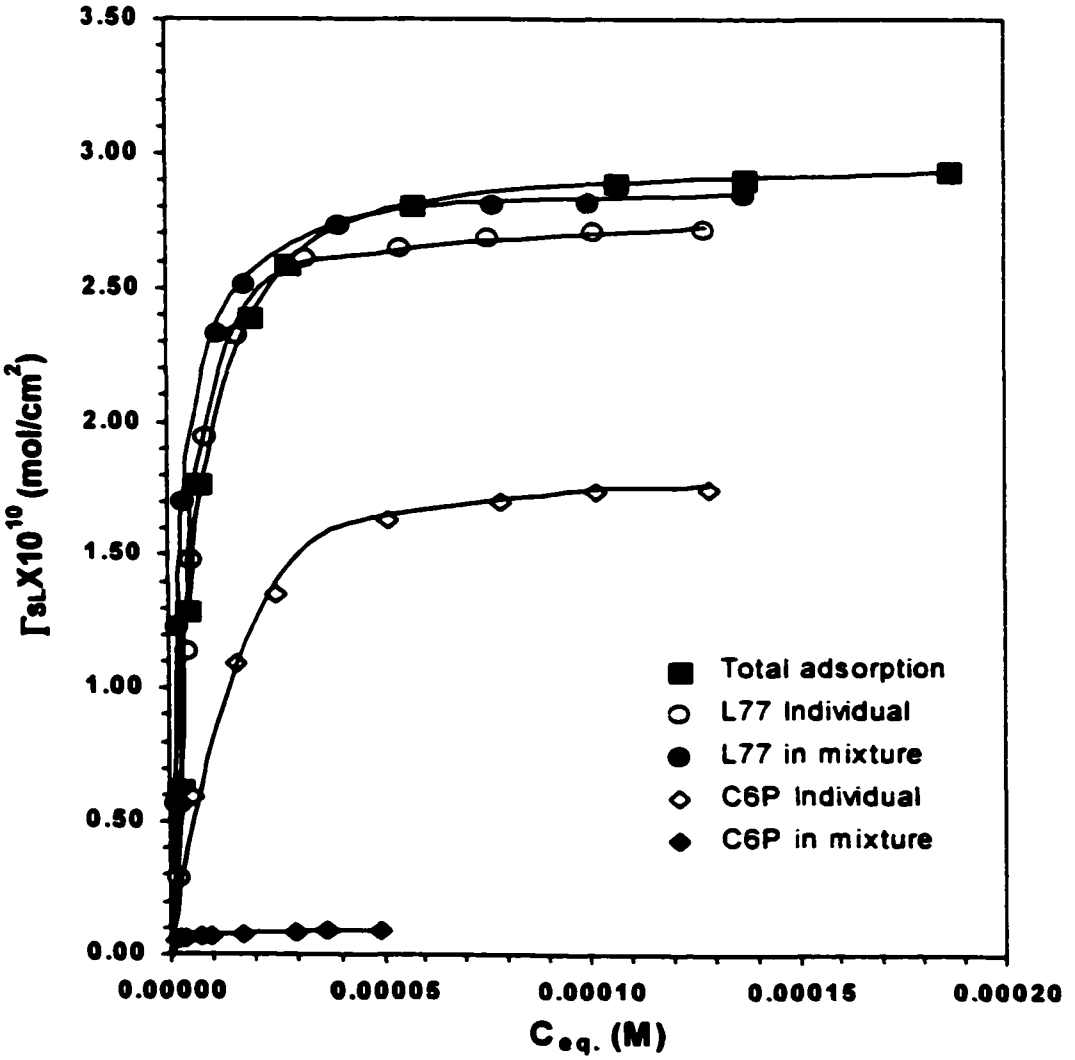

Figure B-33. Adsorption Isotherms of L77, C6P and Their Mixtures onto Powdered Polyethylene

(Fixed initial α_{L77}=0.877)

(In Phosphate Buffer Solution, pH=7.00)

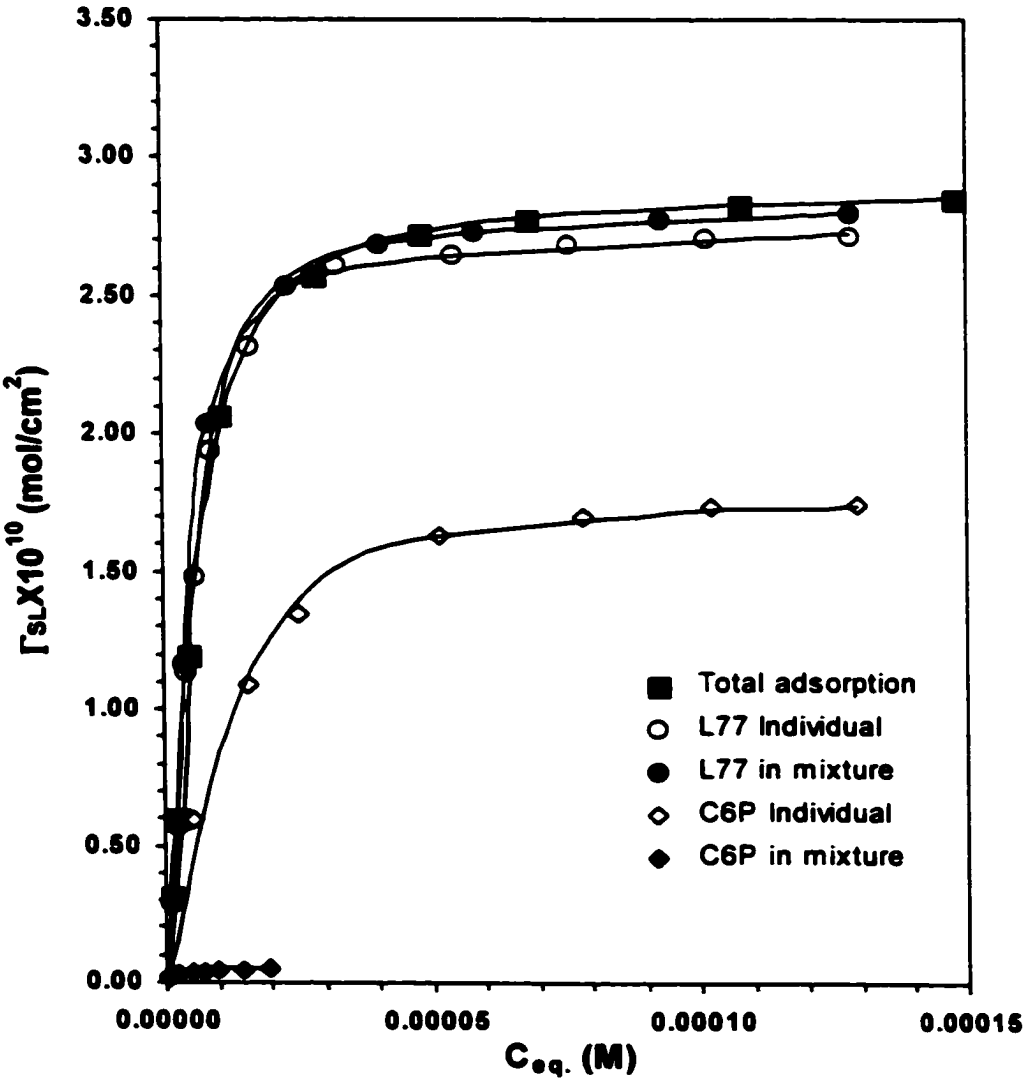

Figure B-34. Adsorption Isotherms of L77, C2,6P and Their Mixtures onto Powdered Polyethylene

(Fixed initial α_{L77}=0.036)

(In Phosphate Buffer Solution, pH=7.00)

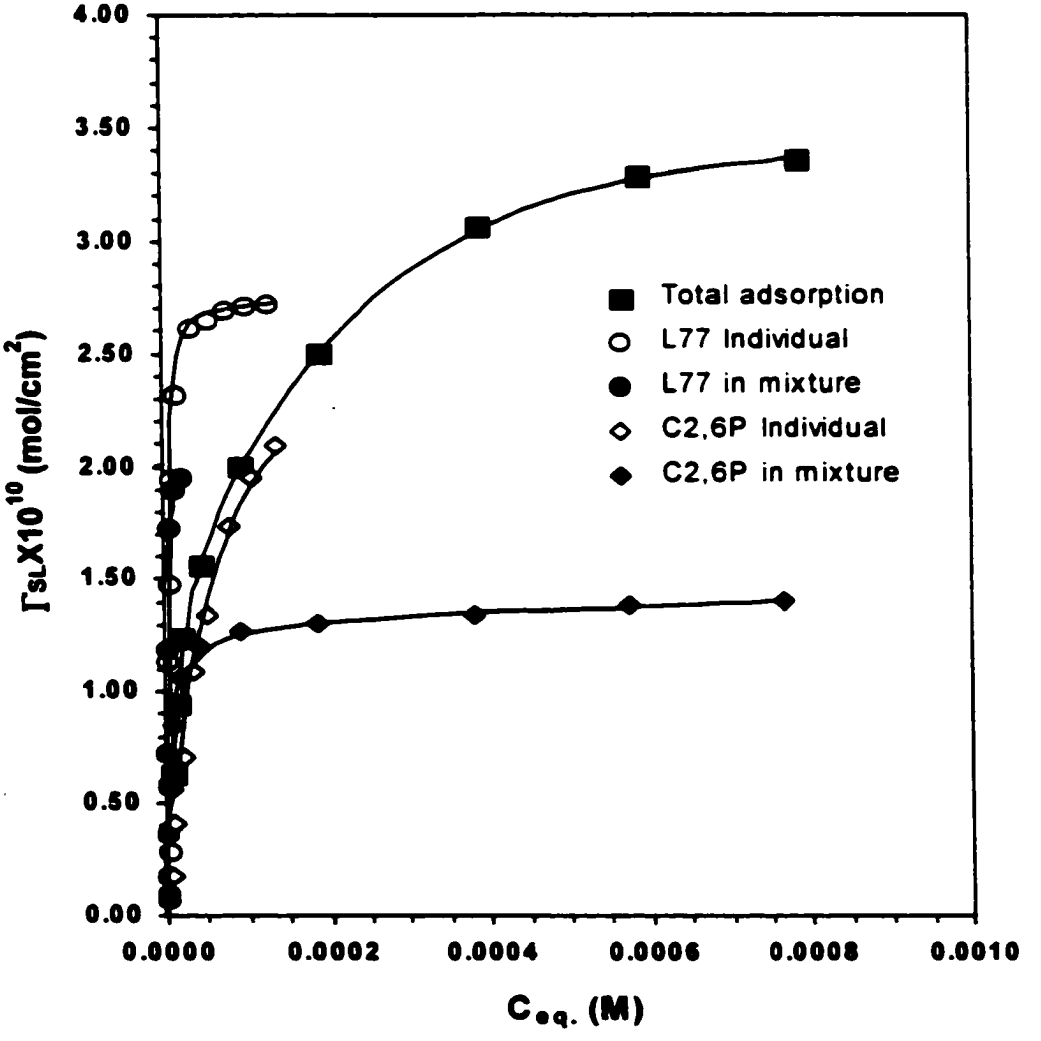

Figure B-35. Adsorption Isotherms of L77, C2,6P and Their Mixtures onto Powdered Polyethylene

(Fixed initial α_{L77}=0.115)

(In Phosphate Buffer Solution, pH=7.00)

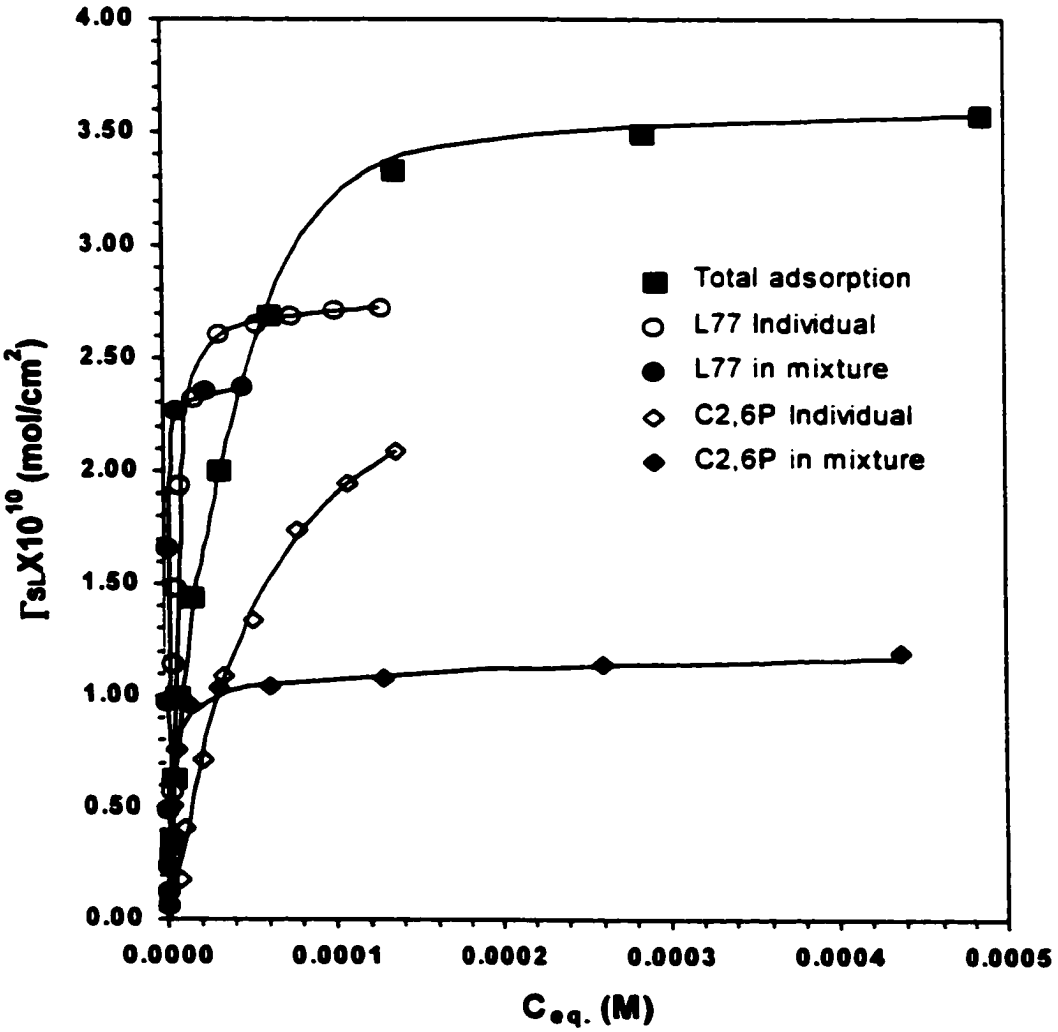

Figure B-36. Adsorption Isotherms of L77, C2,6P and Their Mixtures onto Powdered Polyethylene

(Fixed initial α_{L77}=0.246)

(In Phosphate Buffer Solution, pH=7.00)

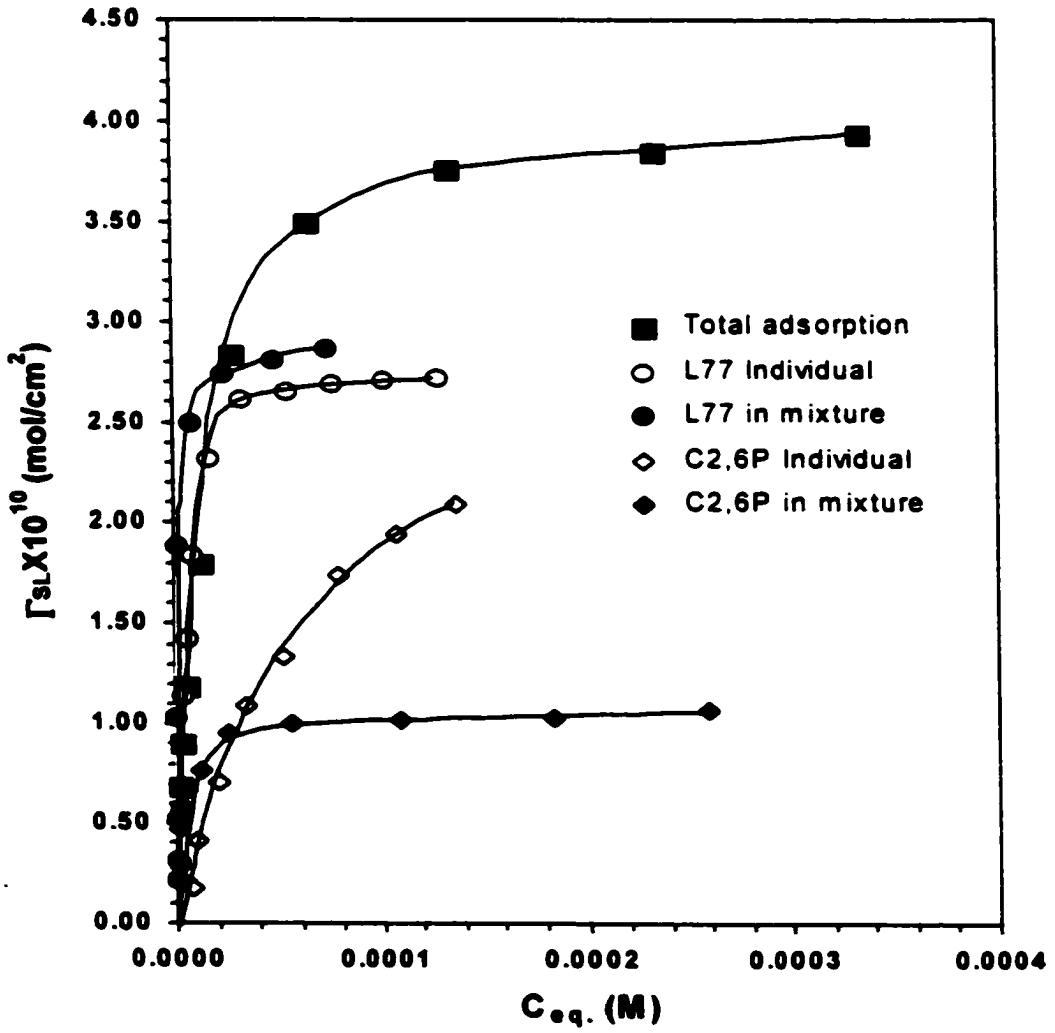

Figure B-37. Adsorption Isotherms of L77, C2,6P and Their Mixtures onto Powdered Polyethylene

(Fixed initial α_{L77}=0.415)

(In Phosphate Buffer Solution, pH=7.00)

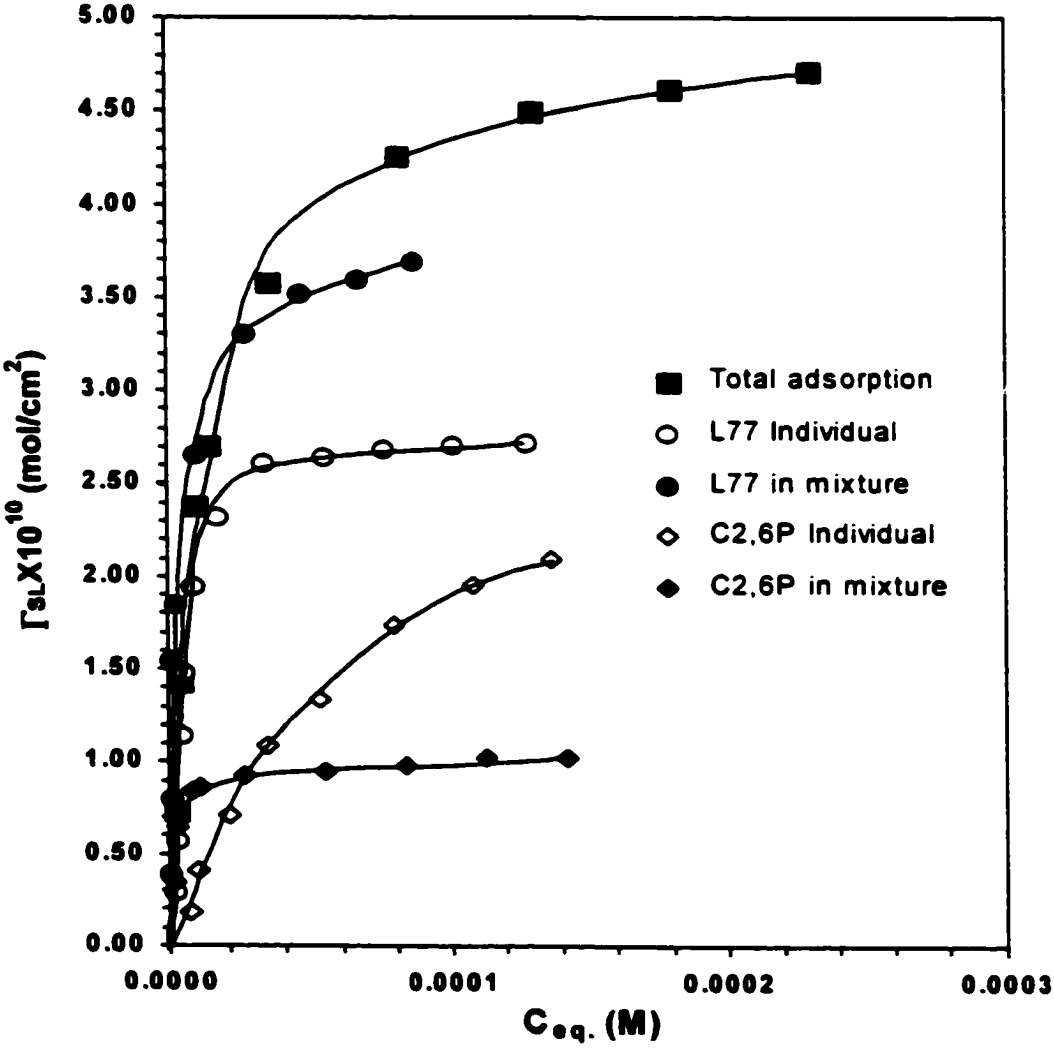

Figure B-38. Adsorption Isotherms of L77, C2,6P and Their Mixtures onto Powdered Polyethylene

(Fixed initial α_{L77}=0.530)

(In Phosphate Buffer Solution, pH=7.00)

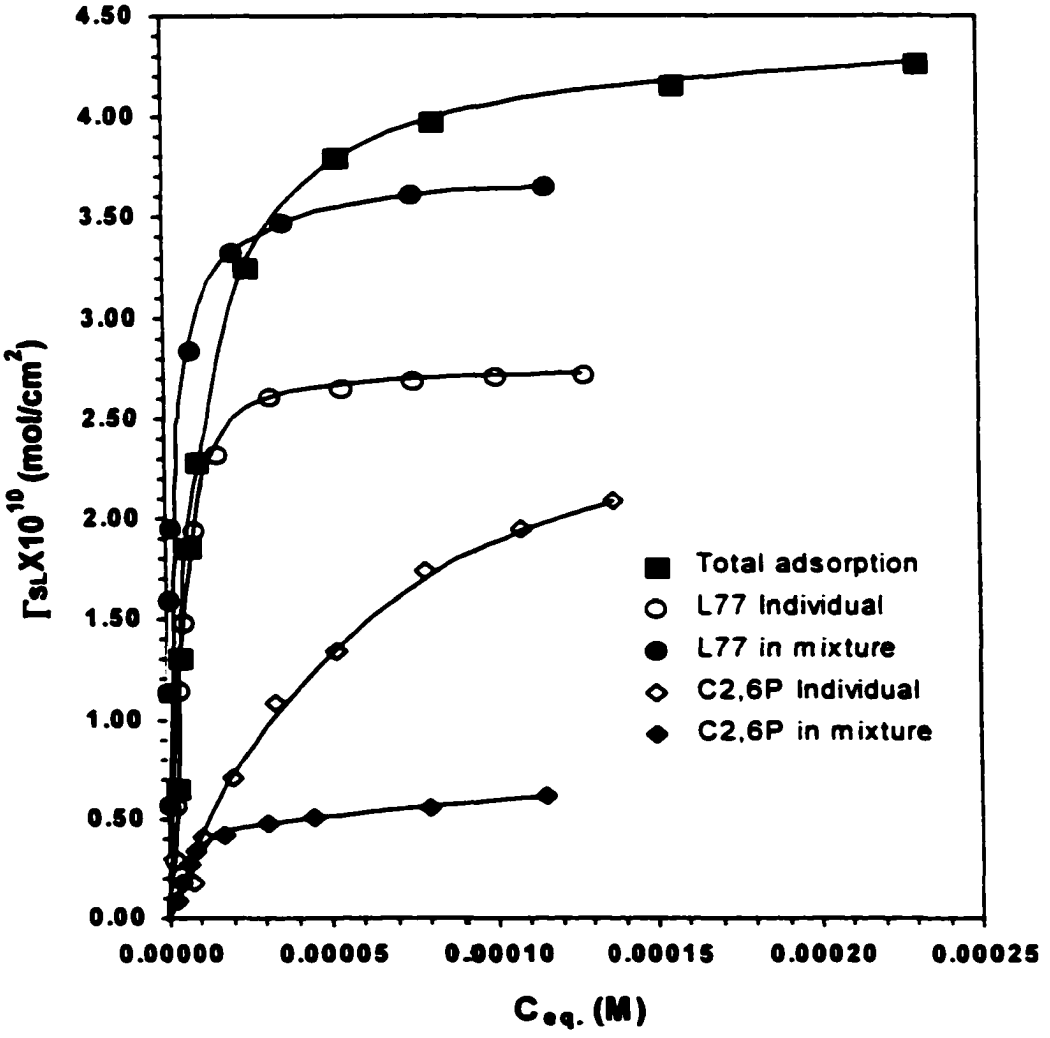

Figure B-39. Adsorption Isotherms of L77, C2,6P and Their Mixtures onto Powdered Polyethylene

(Fixed initial α_{L77}=0.672)

(In Phosphate Buffer Solution, pH=7.00)

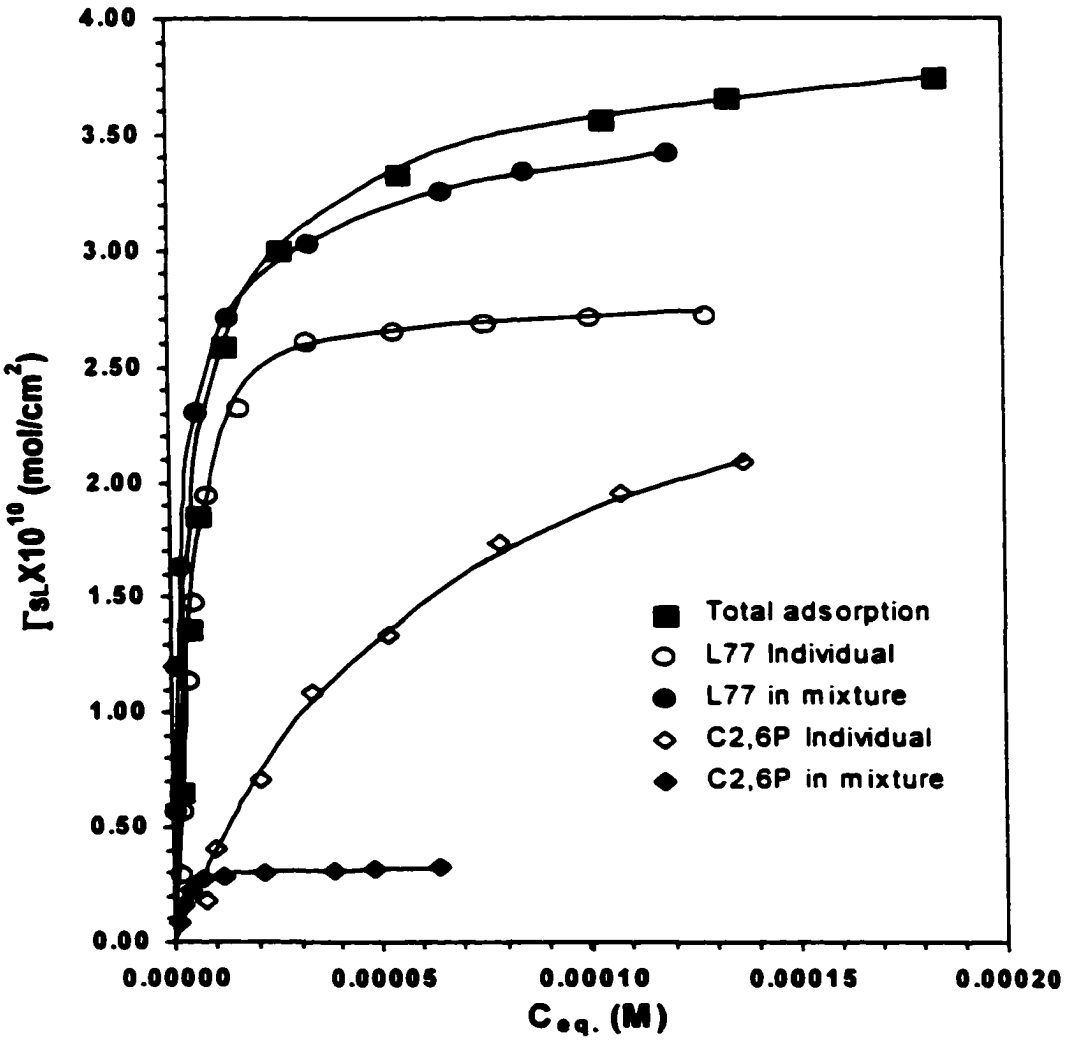

Figure B-40. Adsorption Isotherms of L77, C2,6P and Their Mixtures onto Powdered Polyethylene

(Fixed initial α_{L77}=0.836)

(In Phosphate Buffer Solution, pH=7.00)

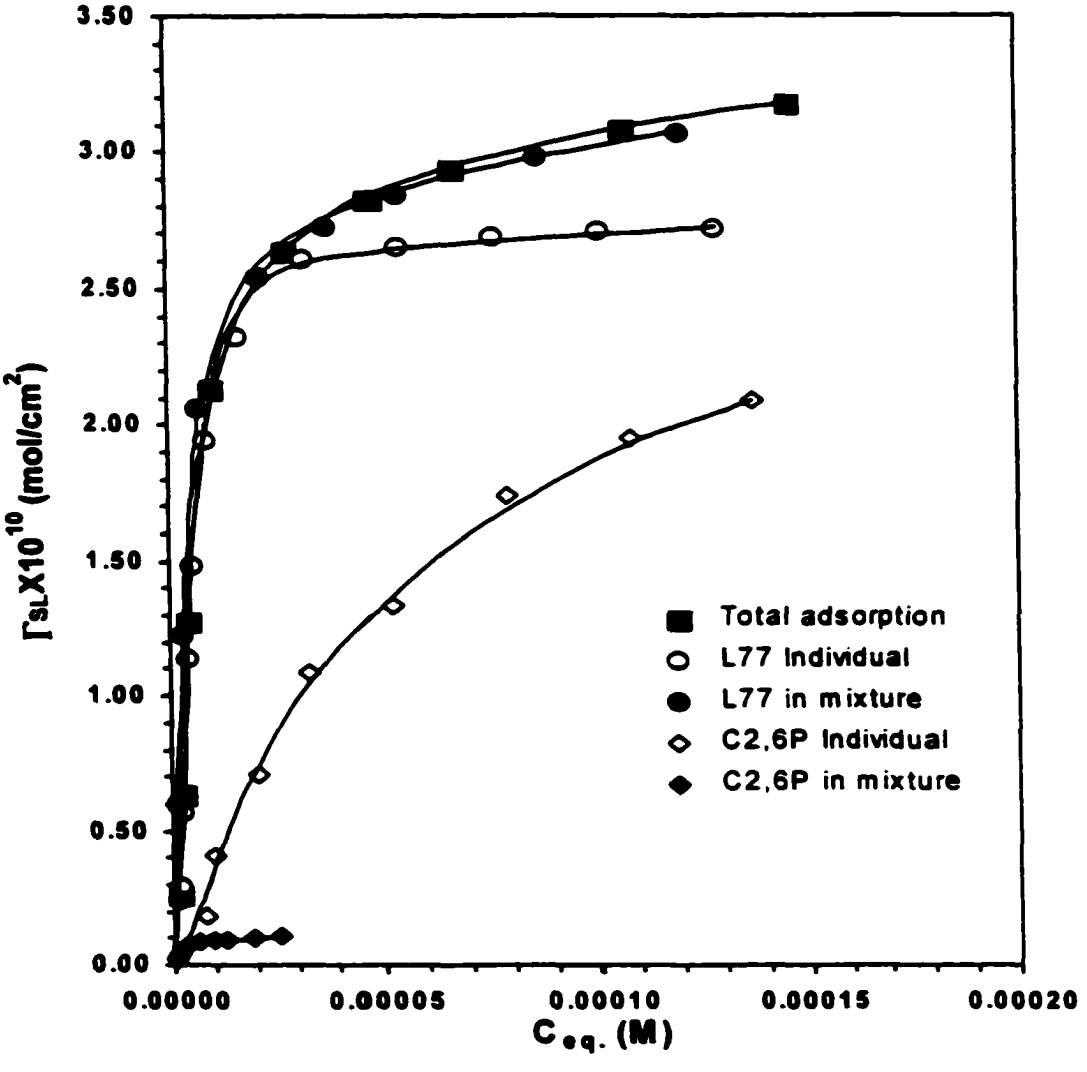

Figure B-41. Adsorption Isotherms of L77, C8P and Their Mixtures onto Powdered Polyethylene

(Fixed initial α_{L77}=0.094)

(In Phosphate Buffer Solution, pH=7.00)

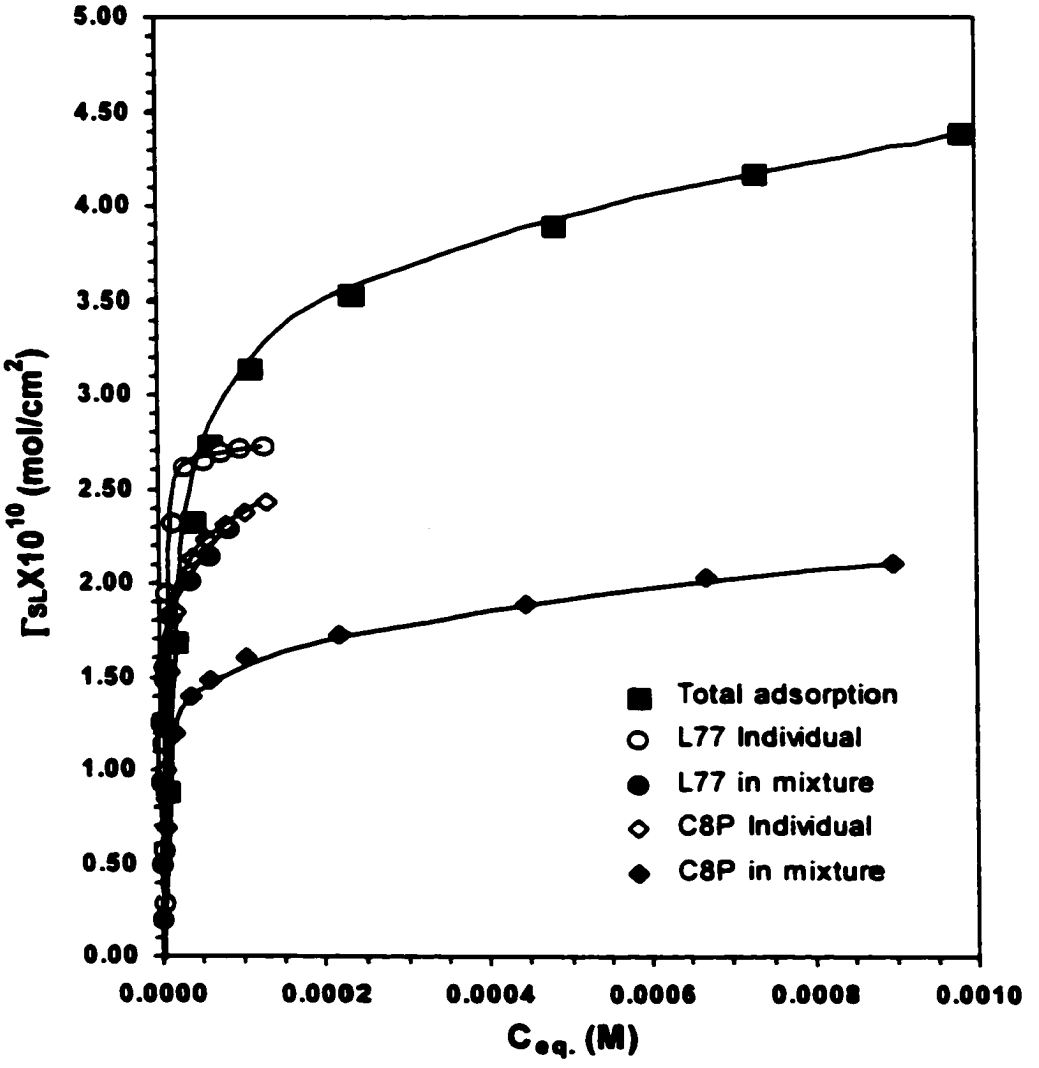

Figure B-42. Adsorption Isotherms of L77, C8P and Their Mixtures onto Powdered Polyethylene

(Fixed initial α_{L77}=0.244)

(In Phosphate Buffer Solution, pH=7.00)

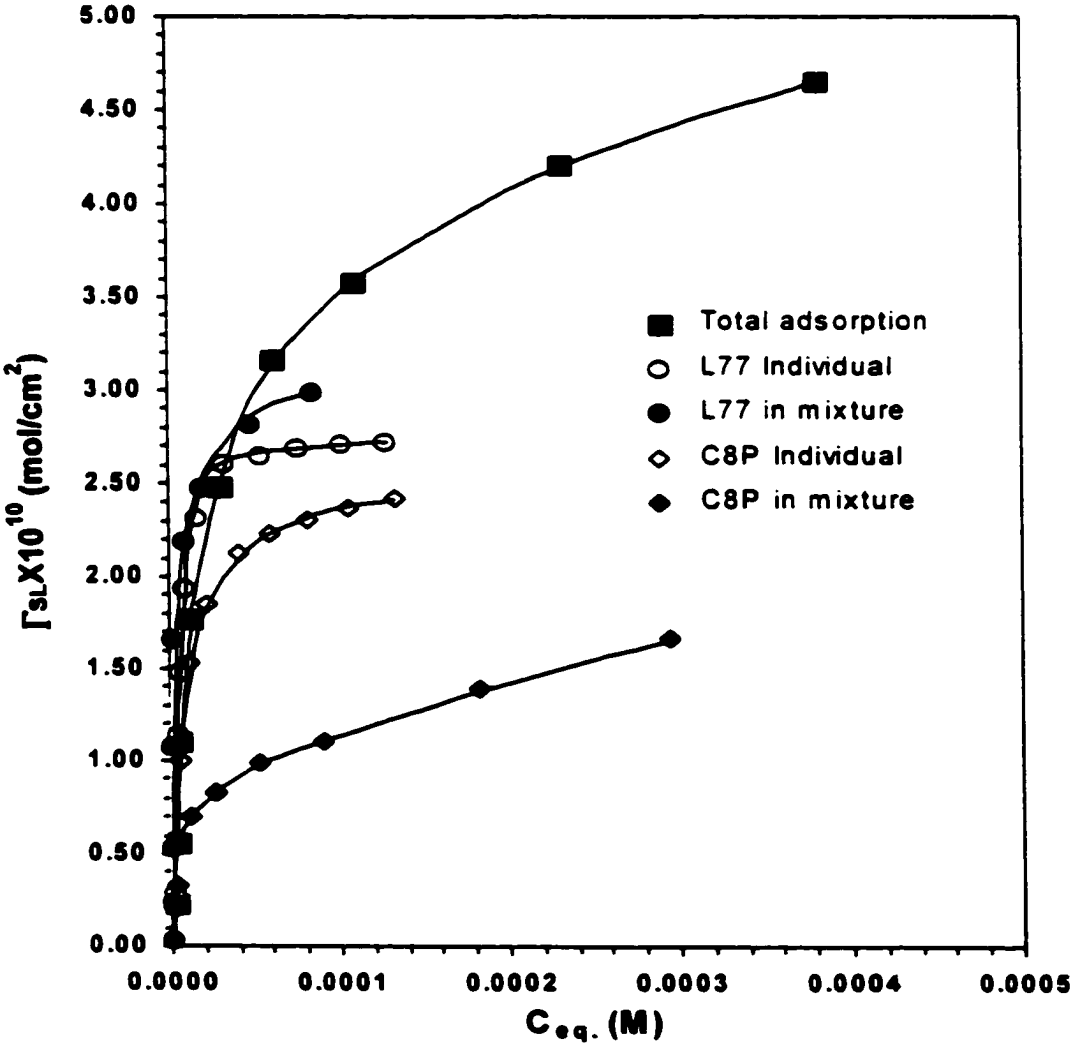

Figure B-43. Adsorption Isotherms of L77, C8P and Their Mixtures onto Powdered Polyethylene

(Fixed initial α_{L77}=0.401)

(In Phosphate Buffer Solution, pH=7.00)

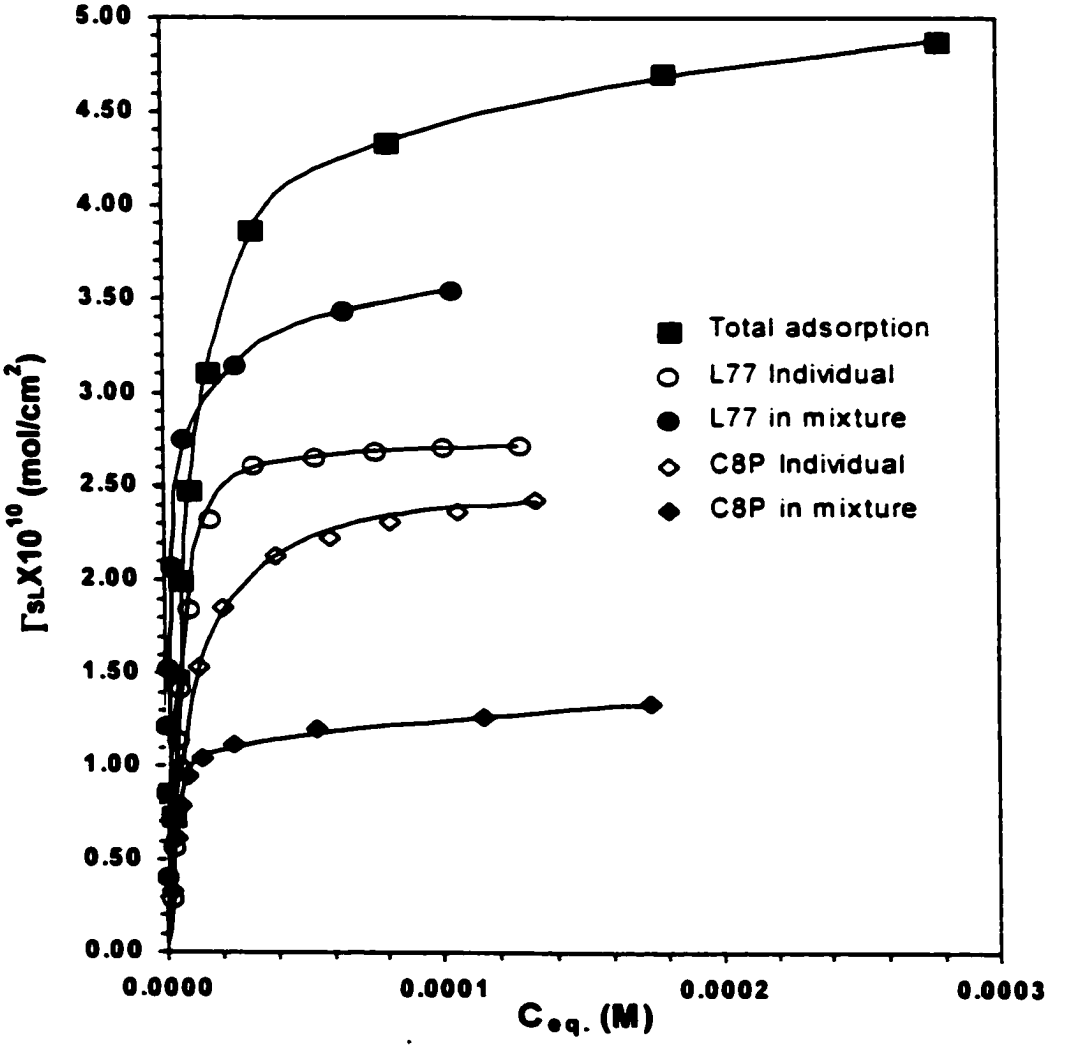

Figure B-44. Adsorption Isotherms of L77, C8P and Their Mixtures onto Powdered Polyethylene

(Fixed initial α_{L77}=0.551)

(In Phosphate Buffer Solution, pH=7.00)

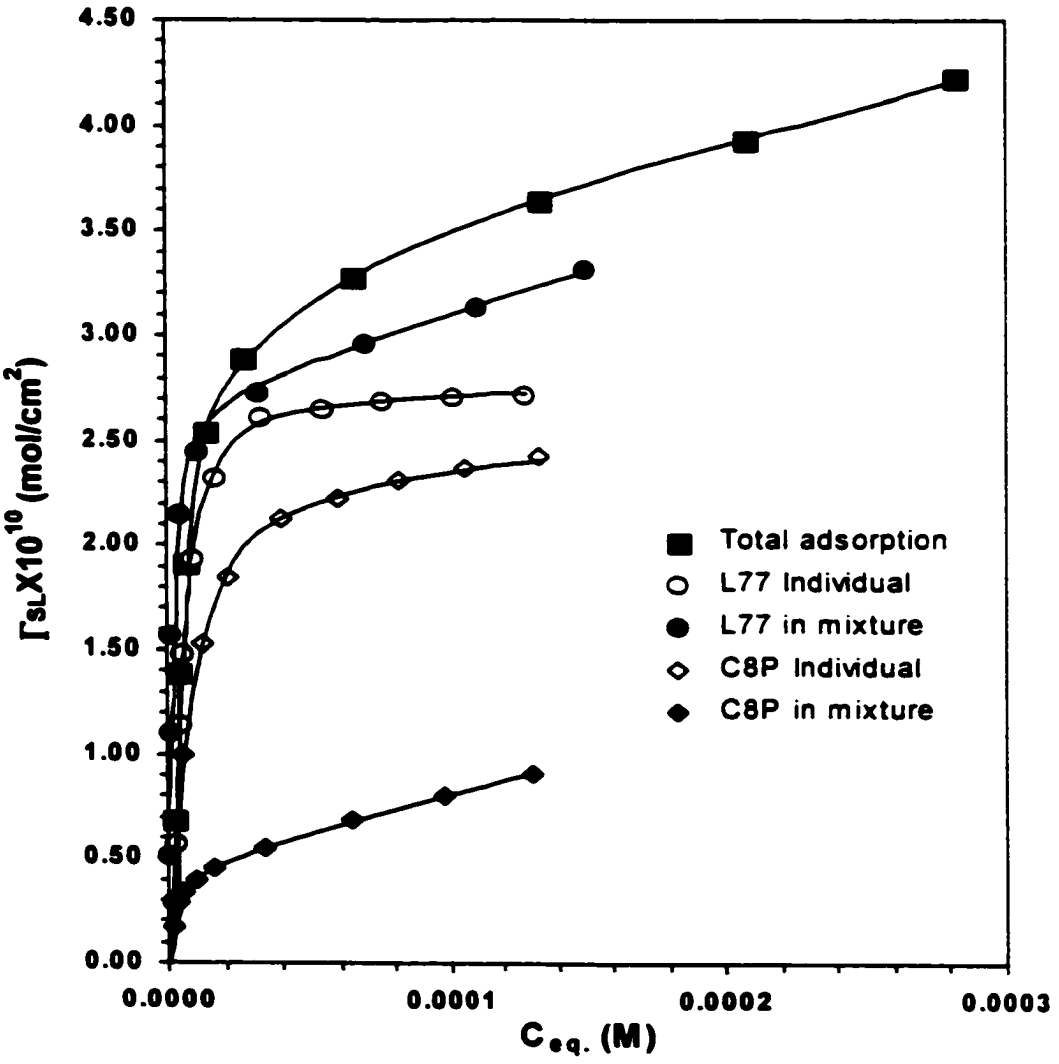

Figure B-45. Adsorption Isotherms of L77, C8P and Their Mixtures onto Powdered Polyethylene

(Fixed initial α_{L77}=0.672)

(In Phosphate Buffer Solution, pH=7.00)

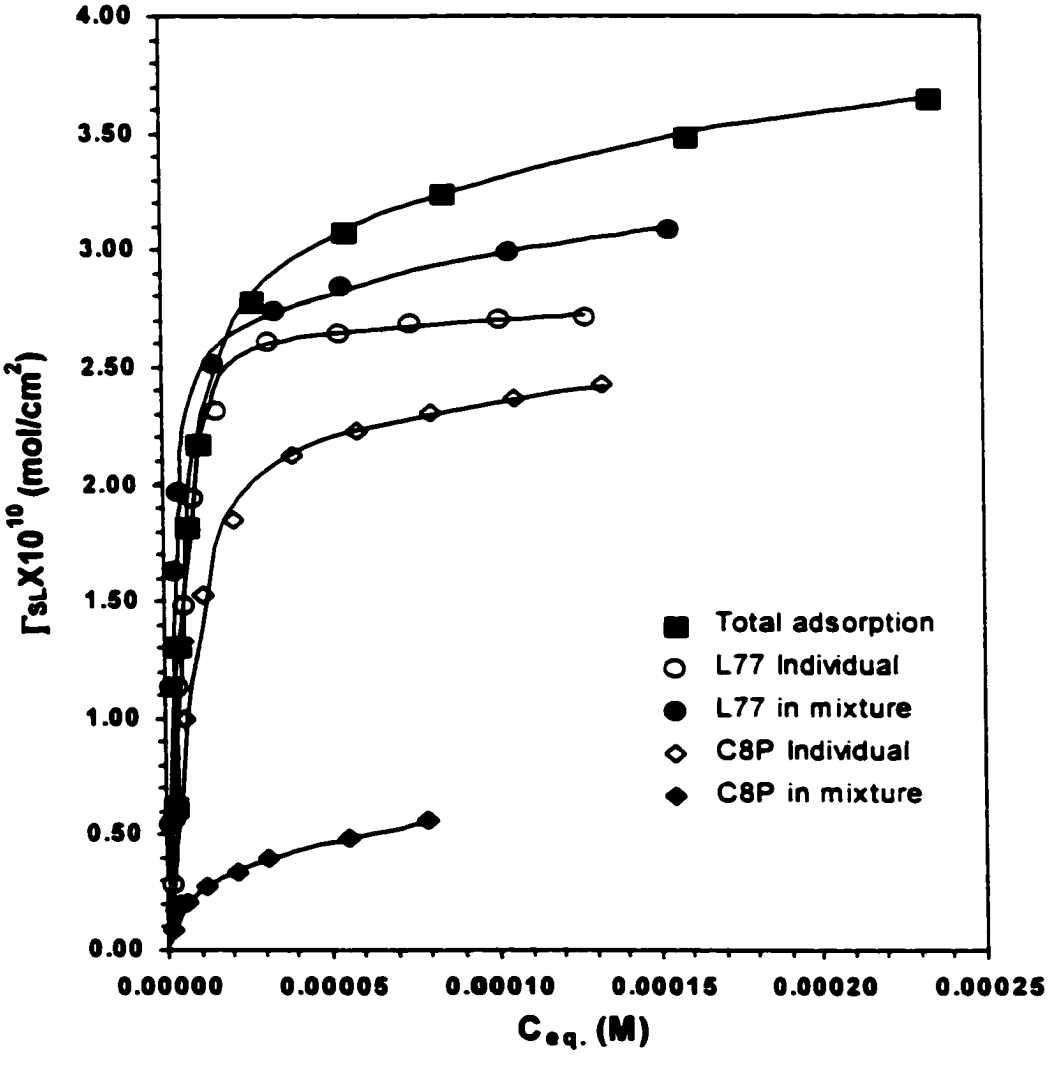

Figure B-46. Adsorption Isotherms of L77, C8P and Their Mixtures onto Powdered Polyethylene

(Fixed initial α_{L77}=0.799)

(In Phosphate Buffer Solution, pH=7.00)

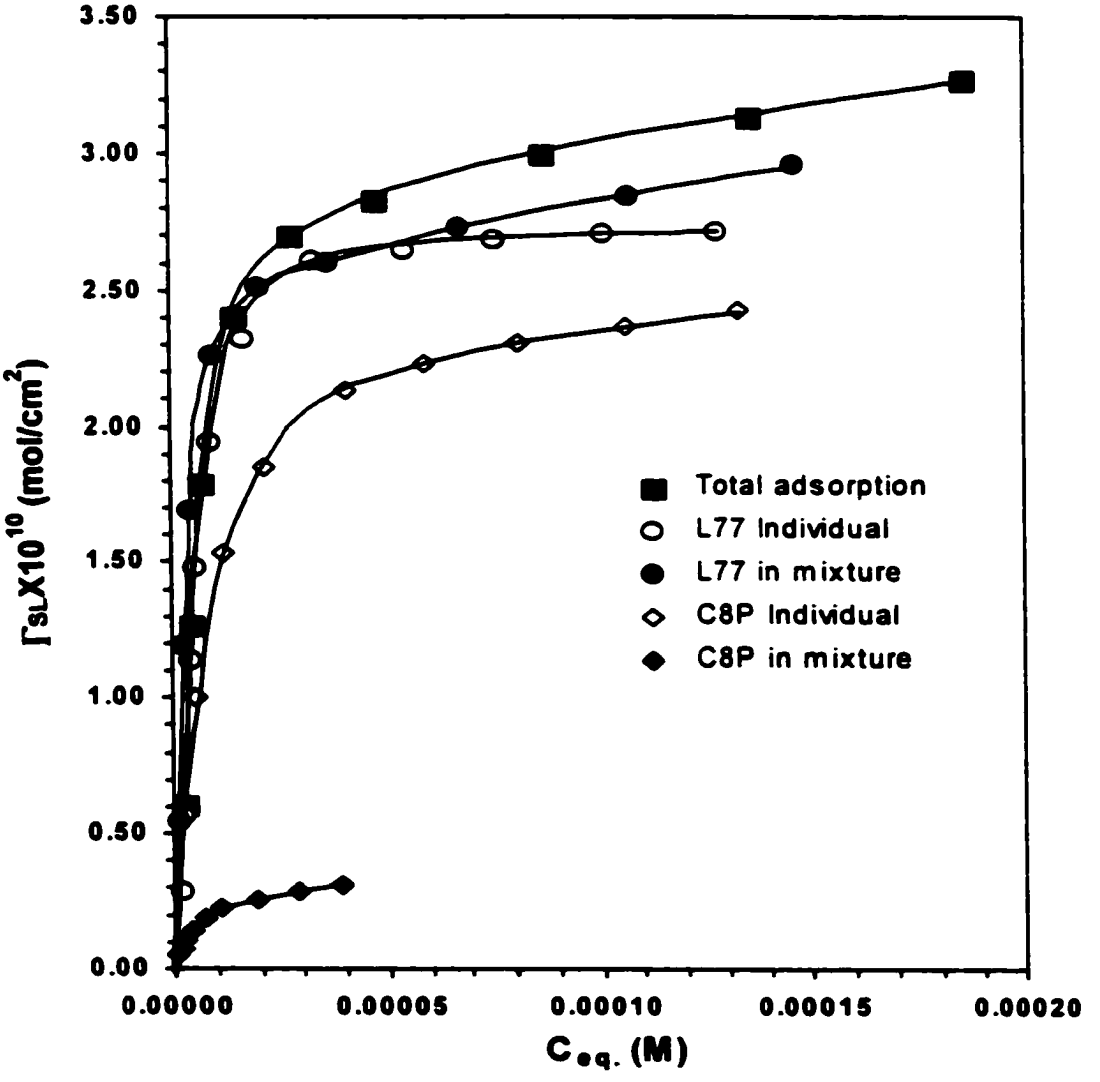

Figure B-47. Adsorption Isotherms of L77, C8P and Their Mixtures onto Powdered Polyethylene

(Fixed initial α_{L77}=0.908)

(In Phosphate Buffer Solution, pH=7.00)

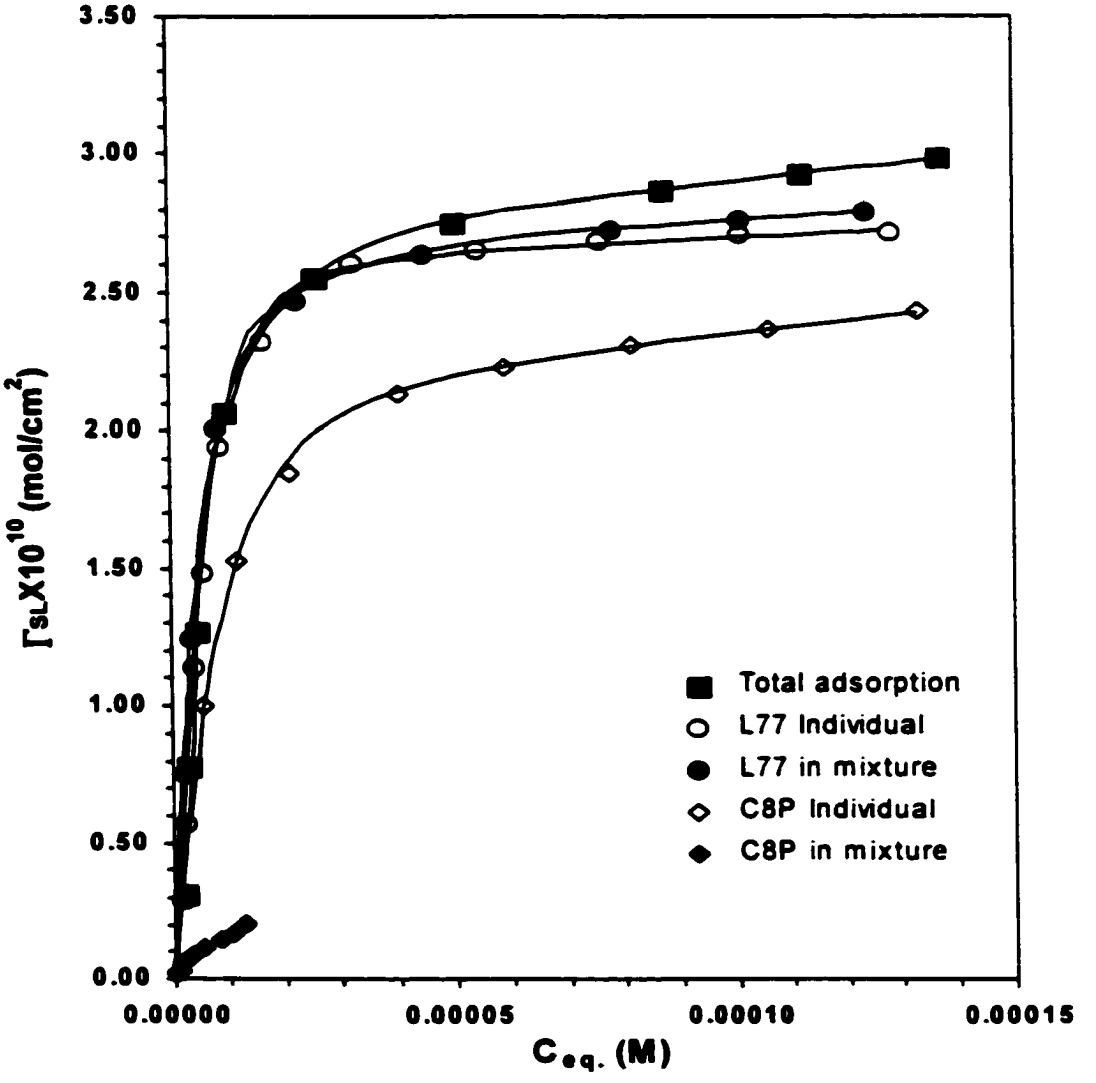

Figure B-48. Adsorption Isotherms of L77, C10P and Their Mixtures onto Powdered Polyethylene

(Fixed initial α_{L77}=0.064)

(In Phosphate Buffer Solution, pH=7.00)

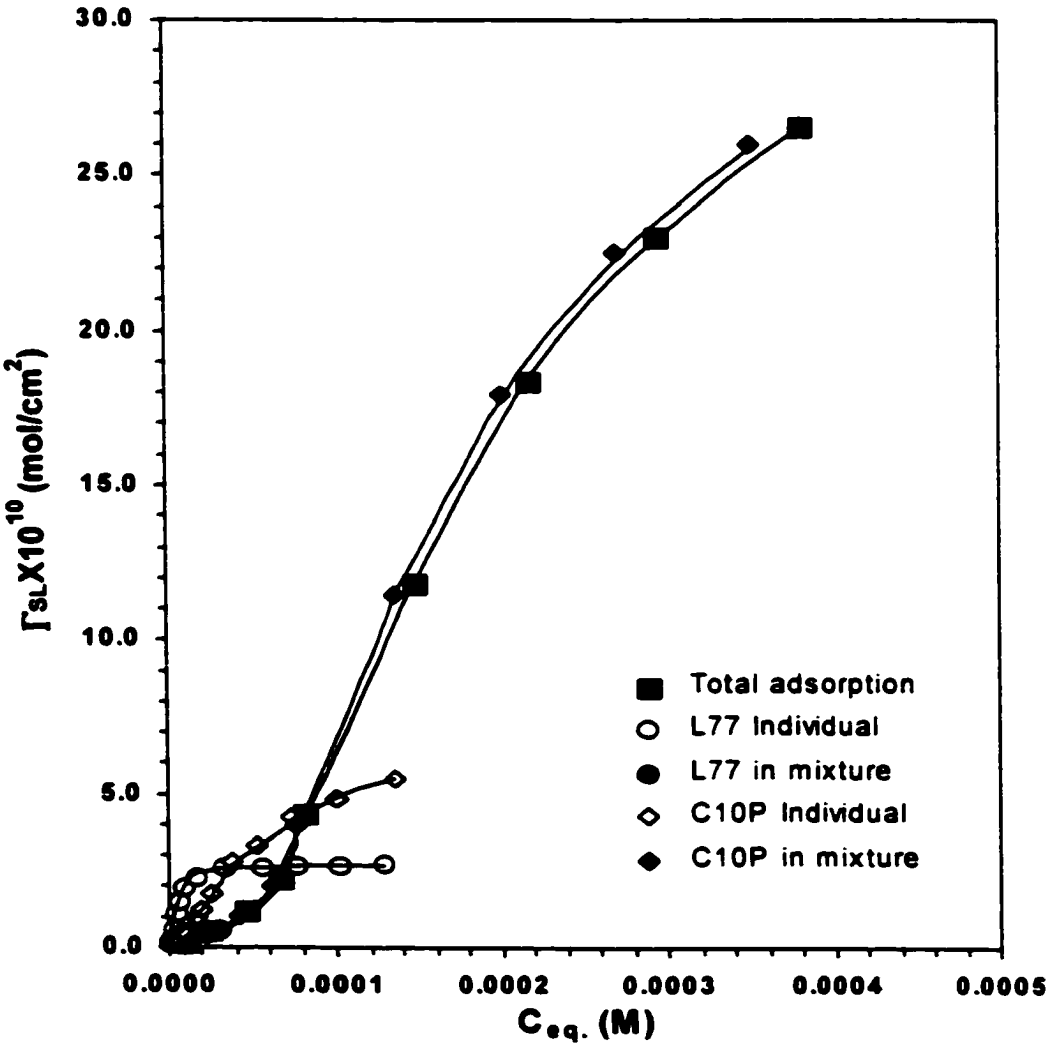

Figure B-49. Adsorption Isotherms of L77, C10P and Their Mixtures onto Powdered Polyethylene

(Fixed initial α_{L77}=0.158)

(In Phosphate Buffer Solution, pH=7.00)

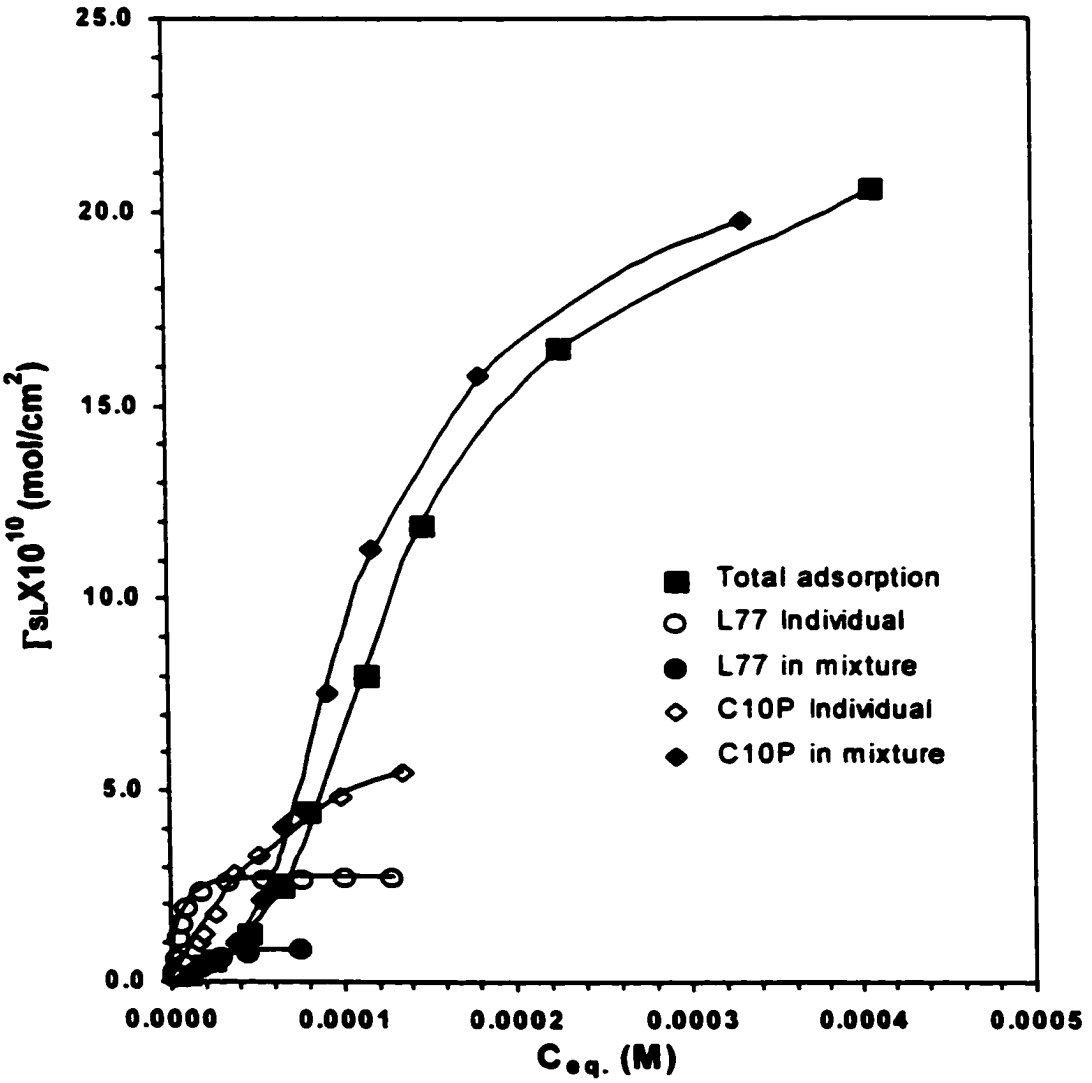

Figure B-50. Adsorption Isotherms of L77, C10P and Their Mixtures onto Powdered Polyethylene

(Fixed initial α_{L77}=0.271)

(In Phosphate Buffer Solution, pH=7.00)

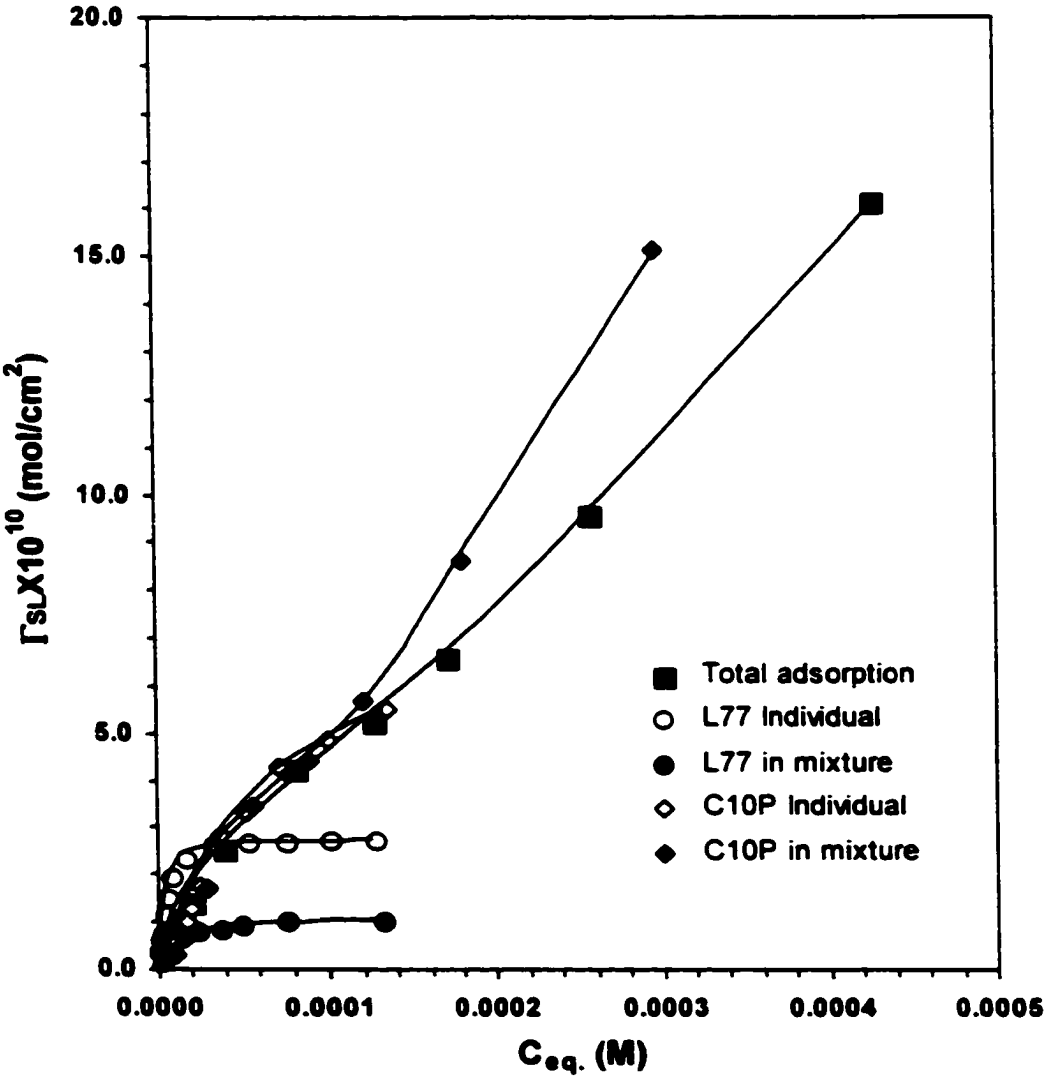

Figure B-51. Adsorption Isotherms of L77, C10P and Their Mixtures onto Powdered Polyethylene

(Fixed initial α_{L77}=0.401)

(In Phosphate Buffer Solution, pH=7.00)

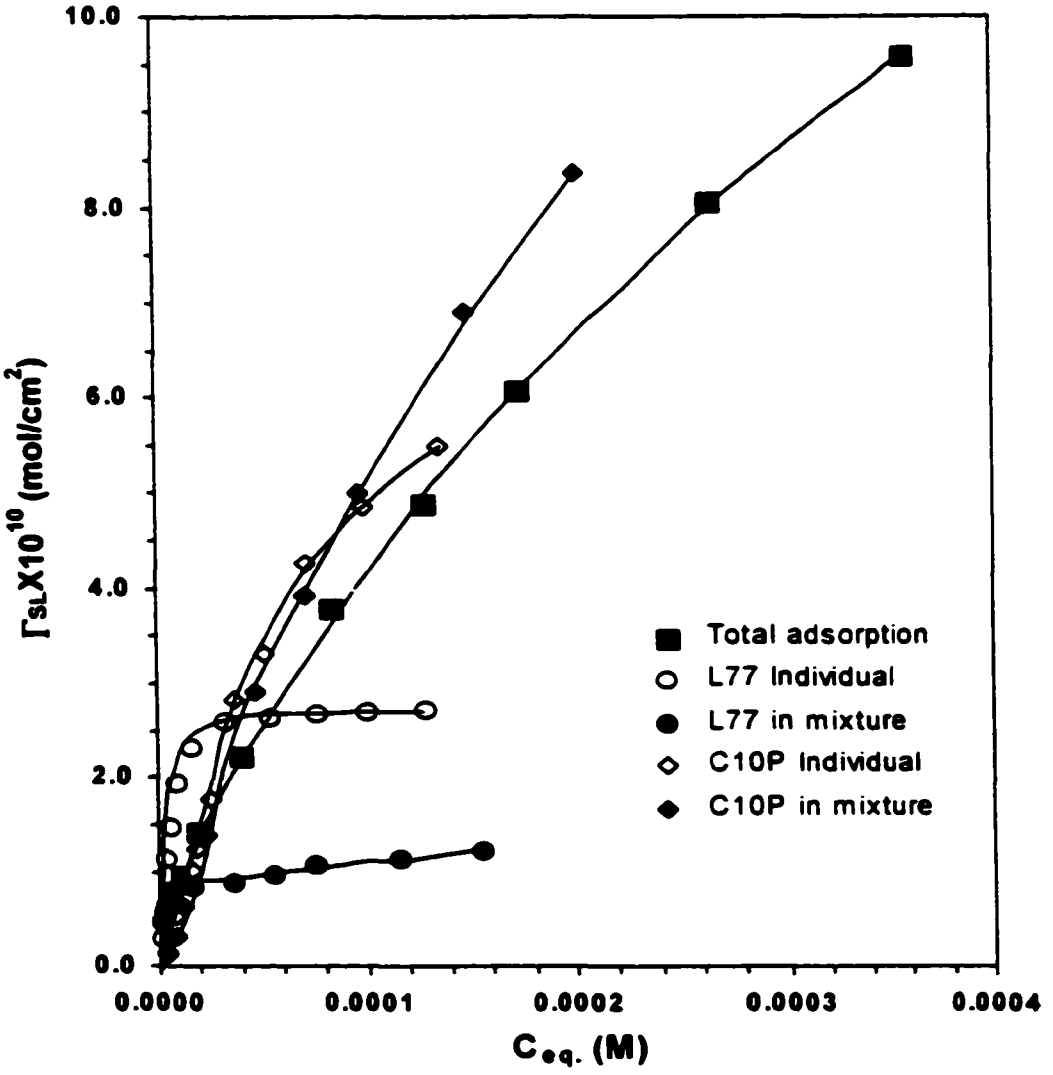

Figure B-52. Adsorption Isotherms of L77, C10P and Their Mixtures onto Powdered Polyethylene

(Fixed initial α_{L77}=0.554)

(In Phosphate Buffer Solution, pH=7.00)

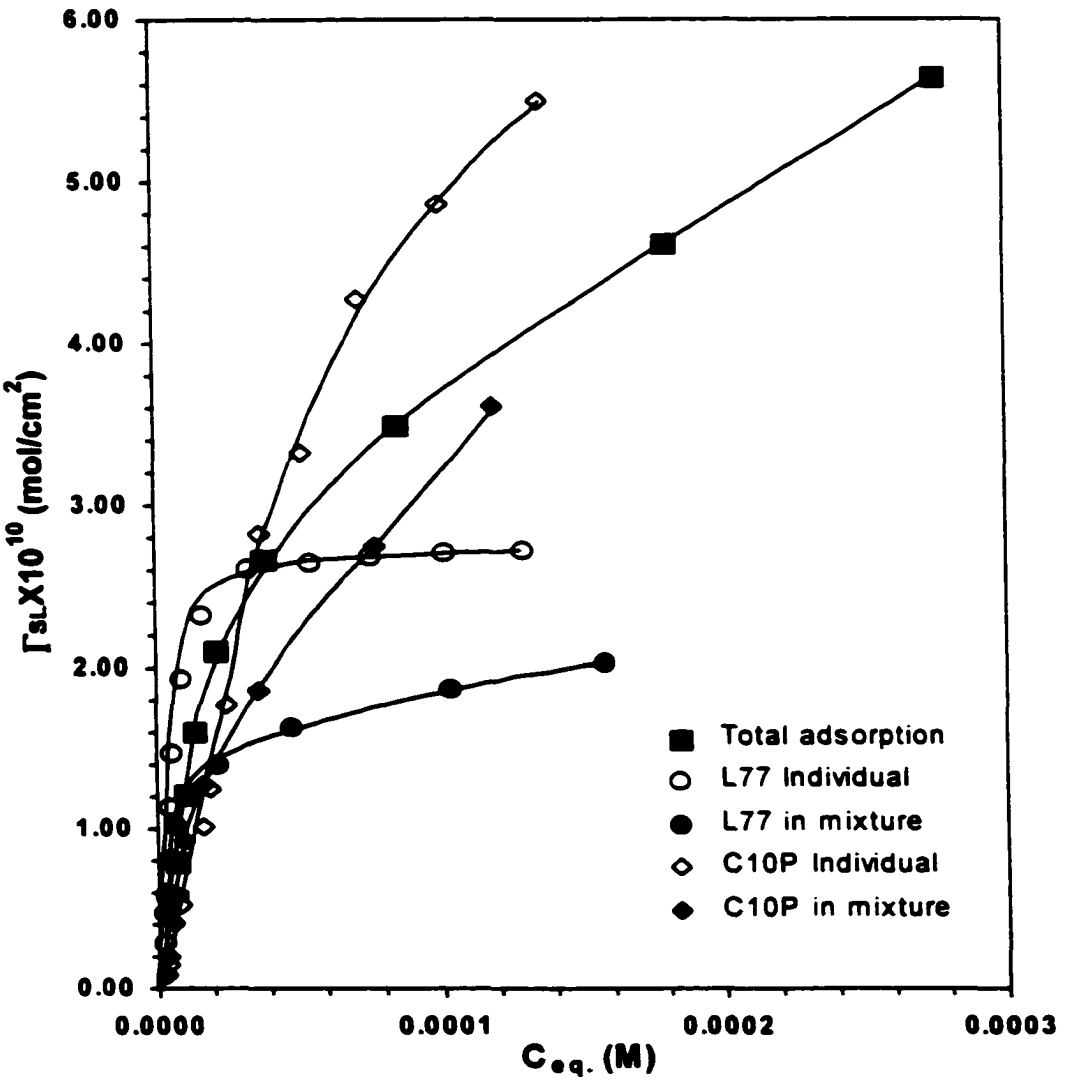

Figure B-53. Adsorption Isotherms of L77, C10P and Their Mixtures onto Powdered Polyethylene

(Fixed initial α_{L77}=0.690)

(In Phosphate Buffer Solution, pH=7.00)

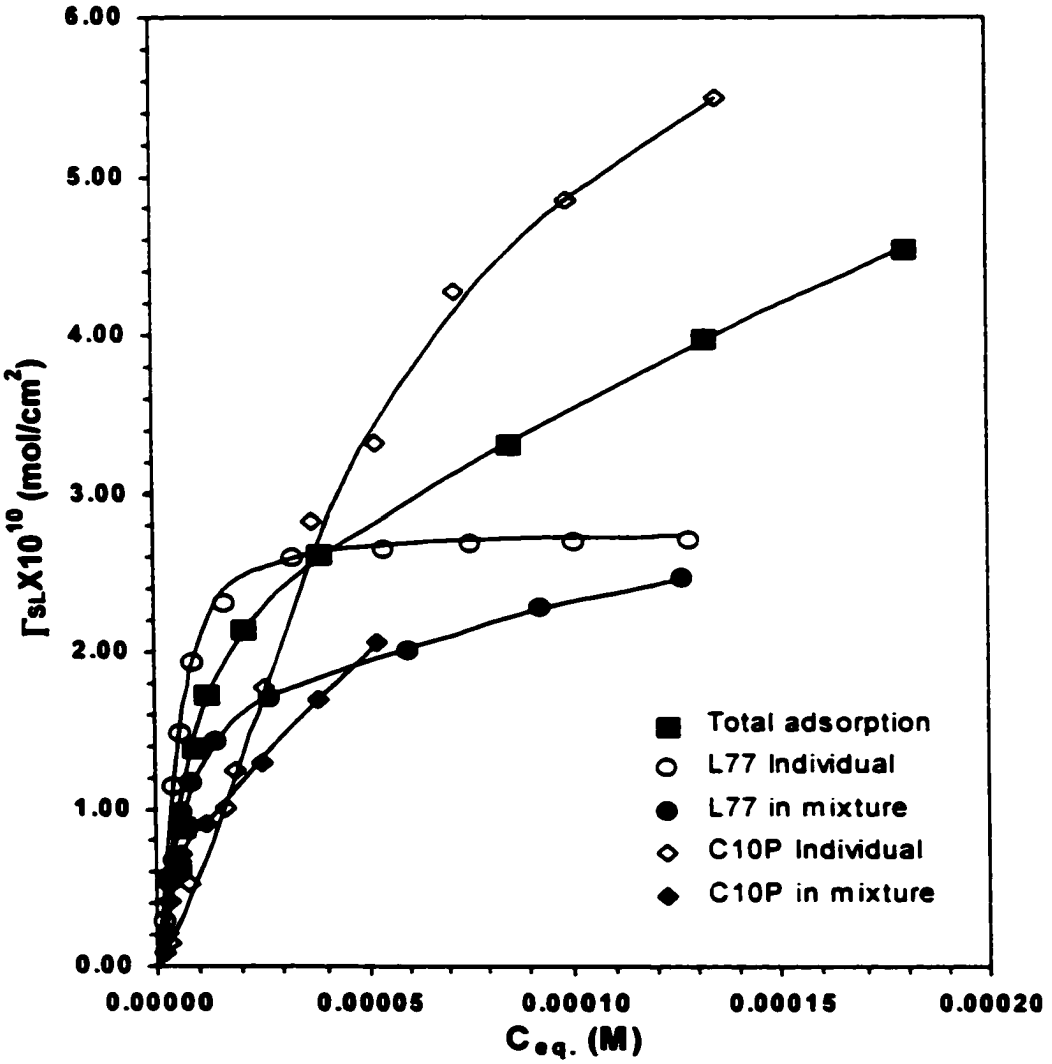

Figure B-54. Adsorption Isotherms of L77, C10P and Their Mixtures onto Powdered Polyethylene

(Fixed initial α_{L77}=0.855)

(In Phosphate Buffer Solution, pH=7.00)

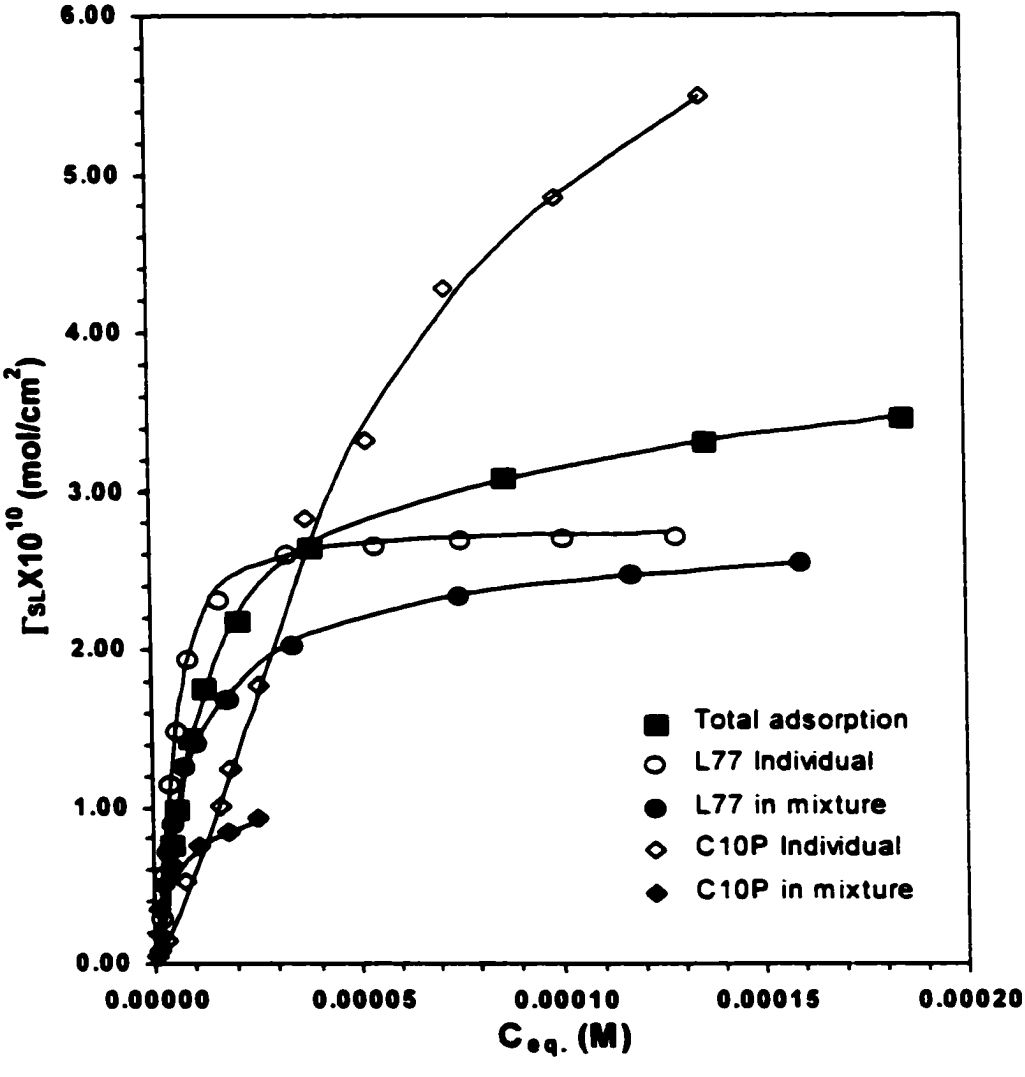

Figure B-55. Plots of $\Gamma_{SL,Total}$ vs. LnC for L77, C4P and Their Mixtures

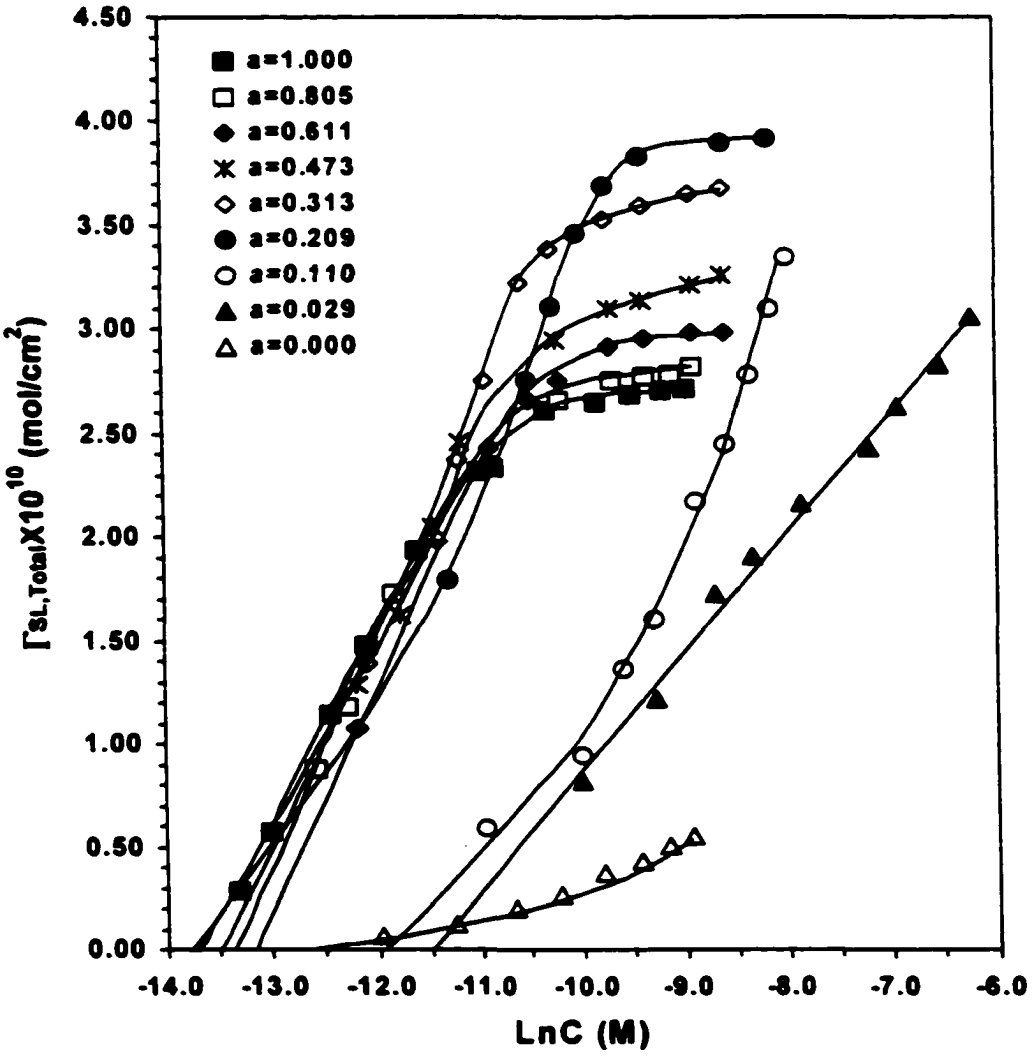

Figure B-56. Plots of $\Gamma_{SL,Total}$ vs. LnC for L77, CHP and Their Mixtures

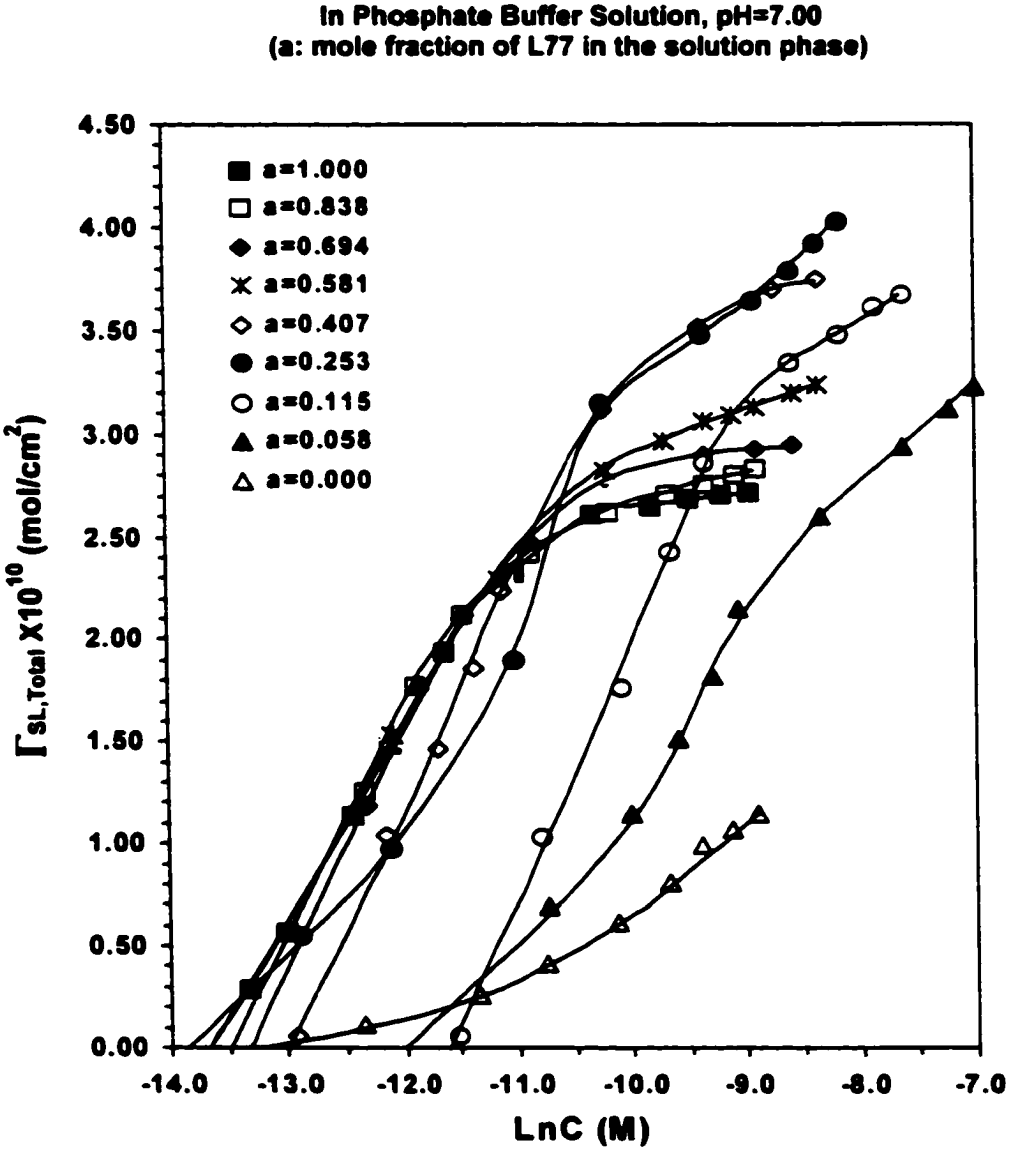

Figure B-57. Plots of $\Gamma_{SL,Total}$ vs. LnC for L77, C6P and Their Mixtures

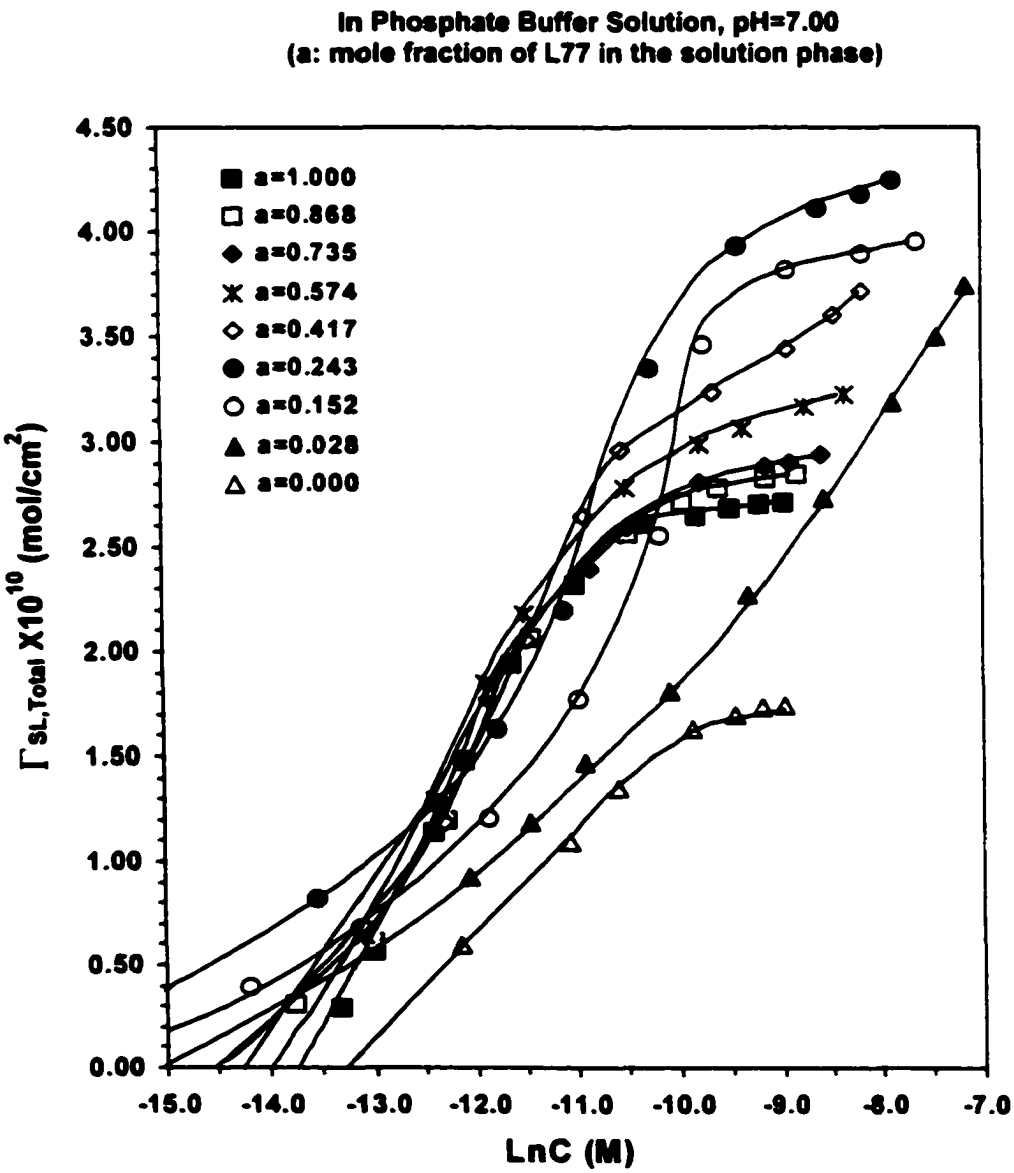

Figure B-58. Plots of $\Gamma_{SL,Total}$ vs. LnC for L77, C2,6P and Their Mixtures

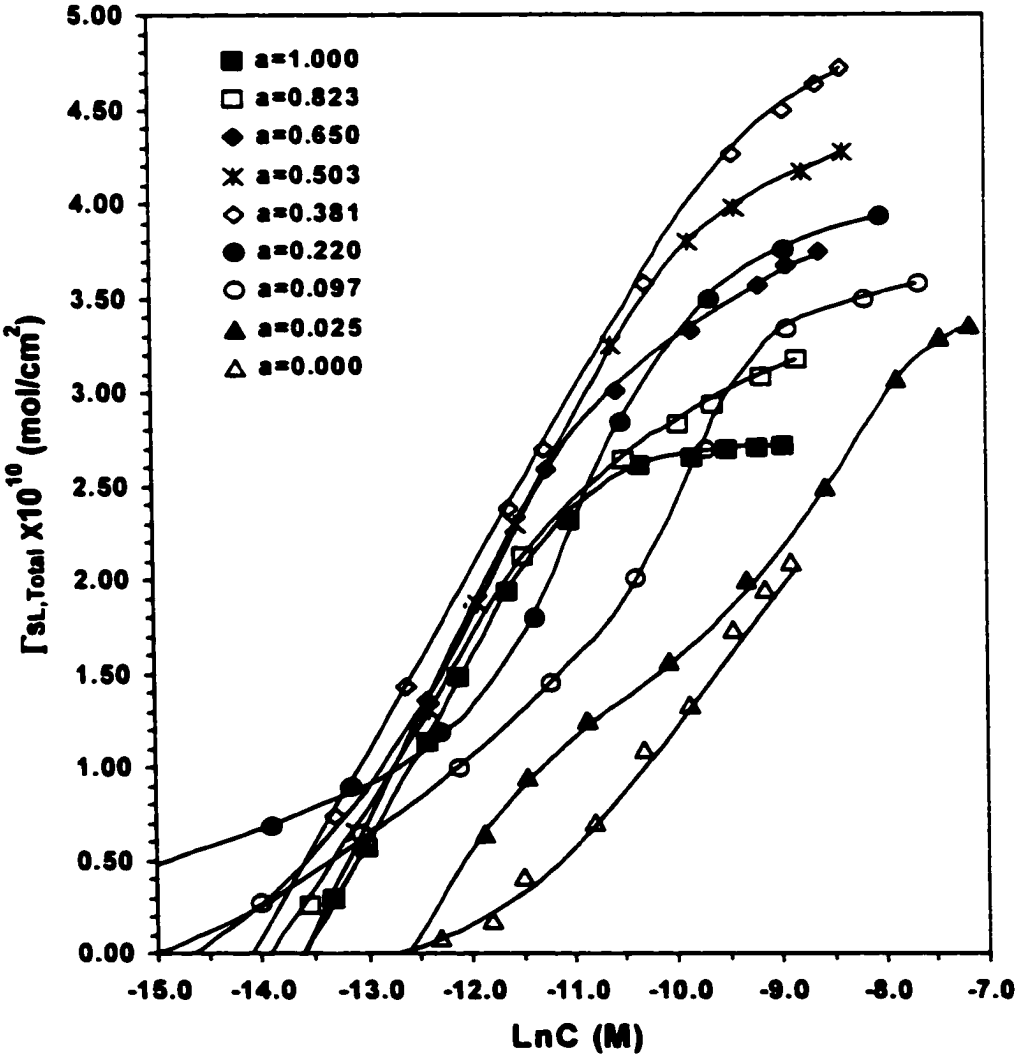

Figure B-59. Plots of $\Gamma_{SL,Total}$ vs. LnC for L77, C8P and Their Mixtures

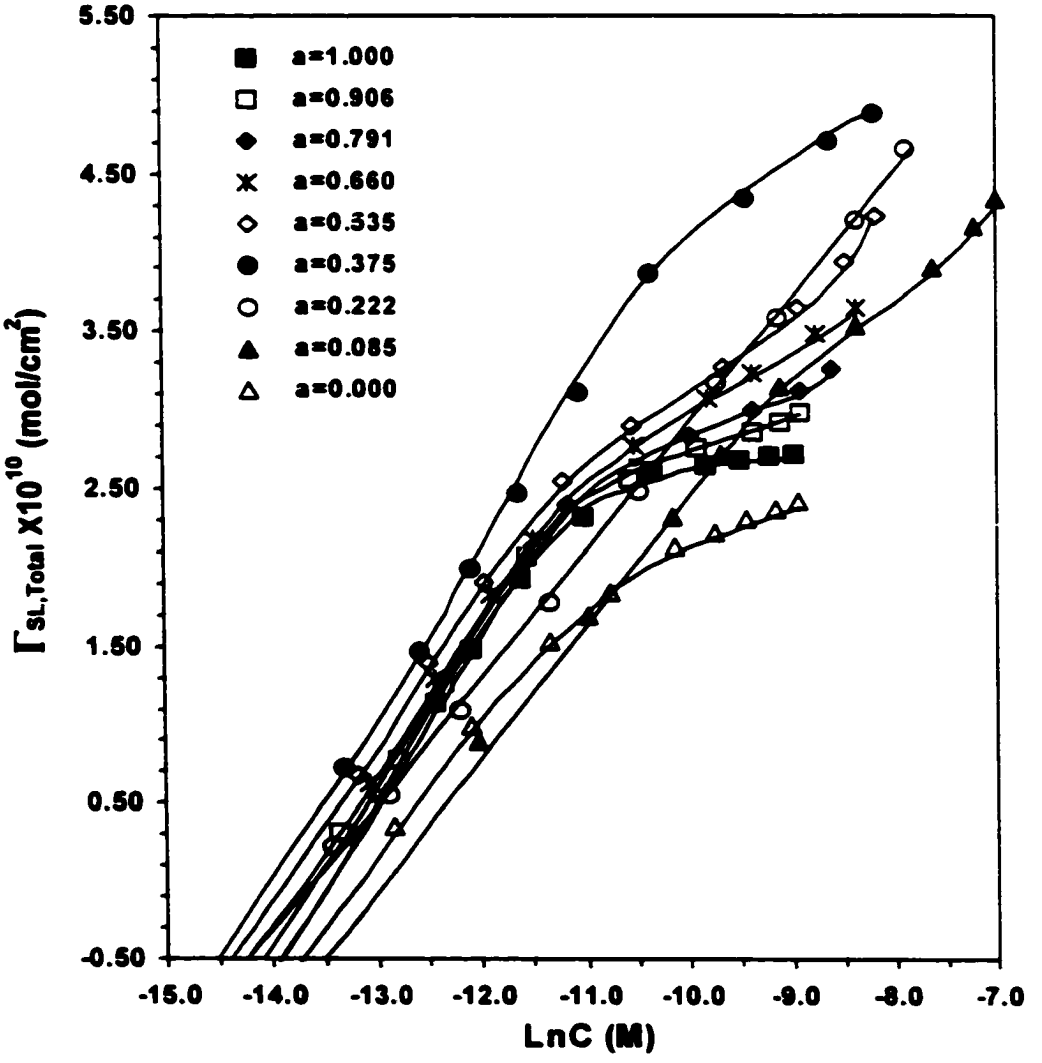

Figure B-60. Plots of $\Gamma_{SL,Total}$ vs. LnC for L77, C10P and Their Mixtures

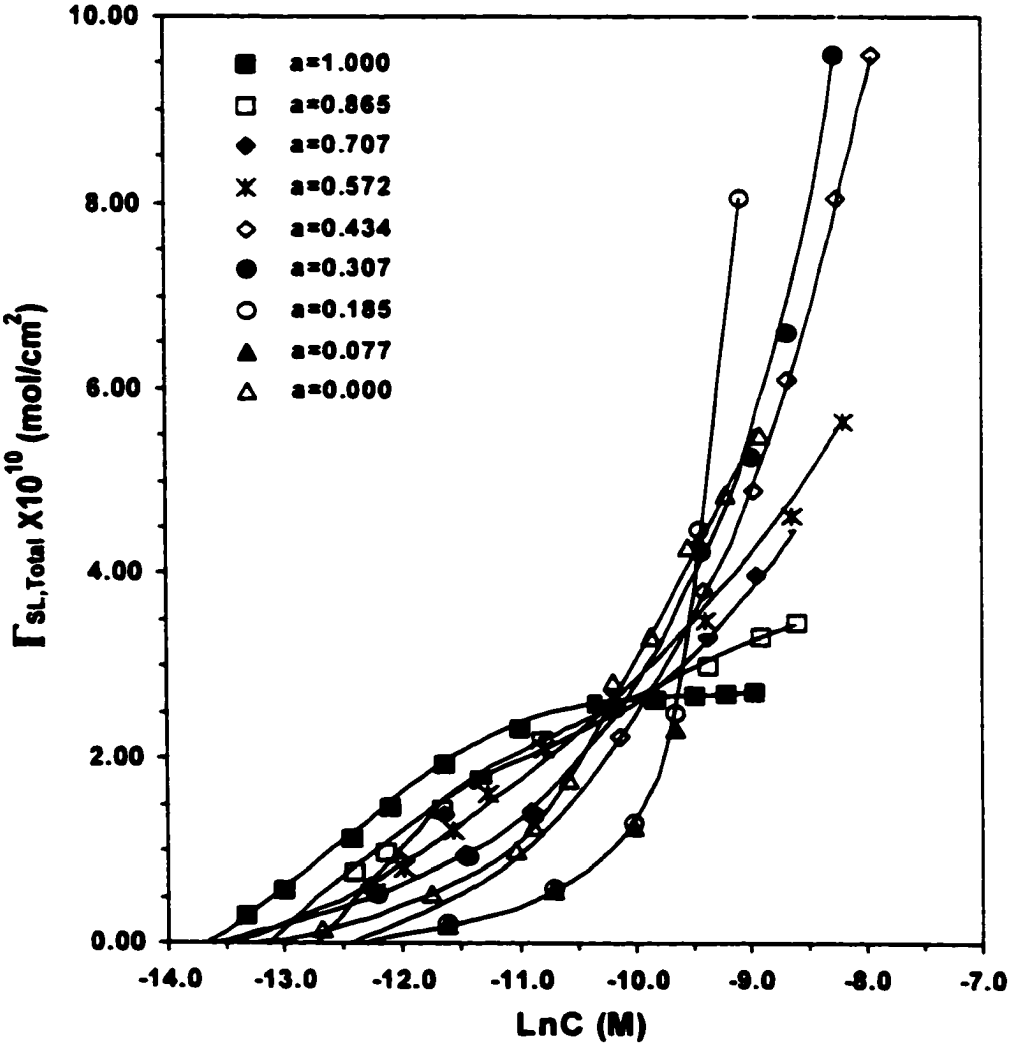

Figure B-61. Plots of π_{SL} vs. LnC for L77, C4P and Their Mixtures

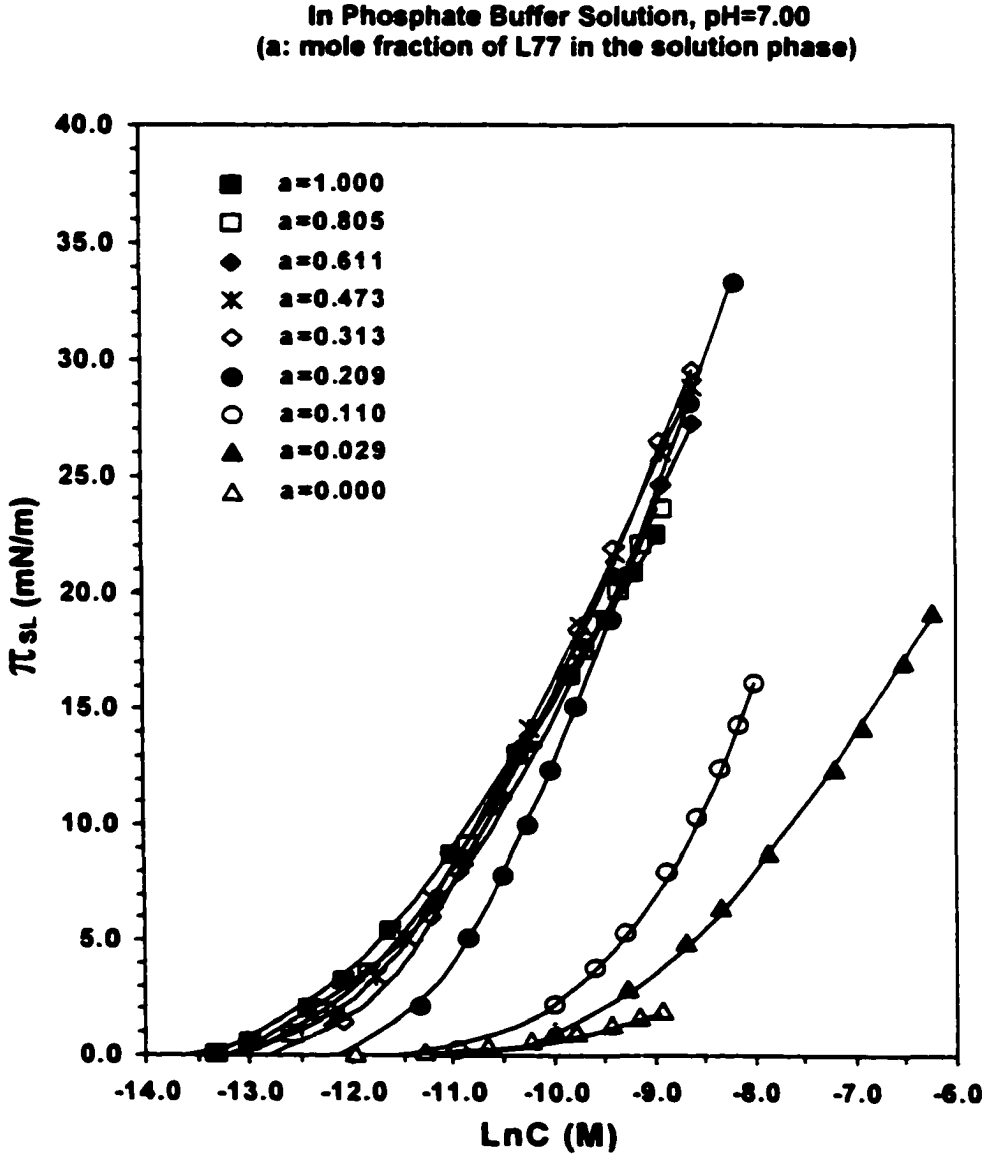

Figure B-62. Plots of π_{SL} vs. LnC for L77, CHP and Their Mixtures

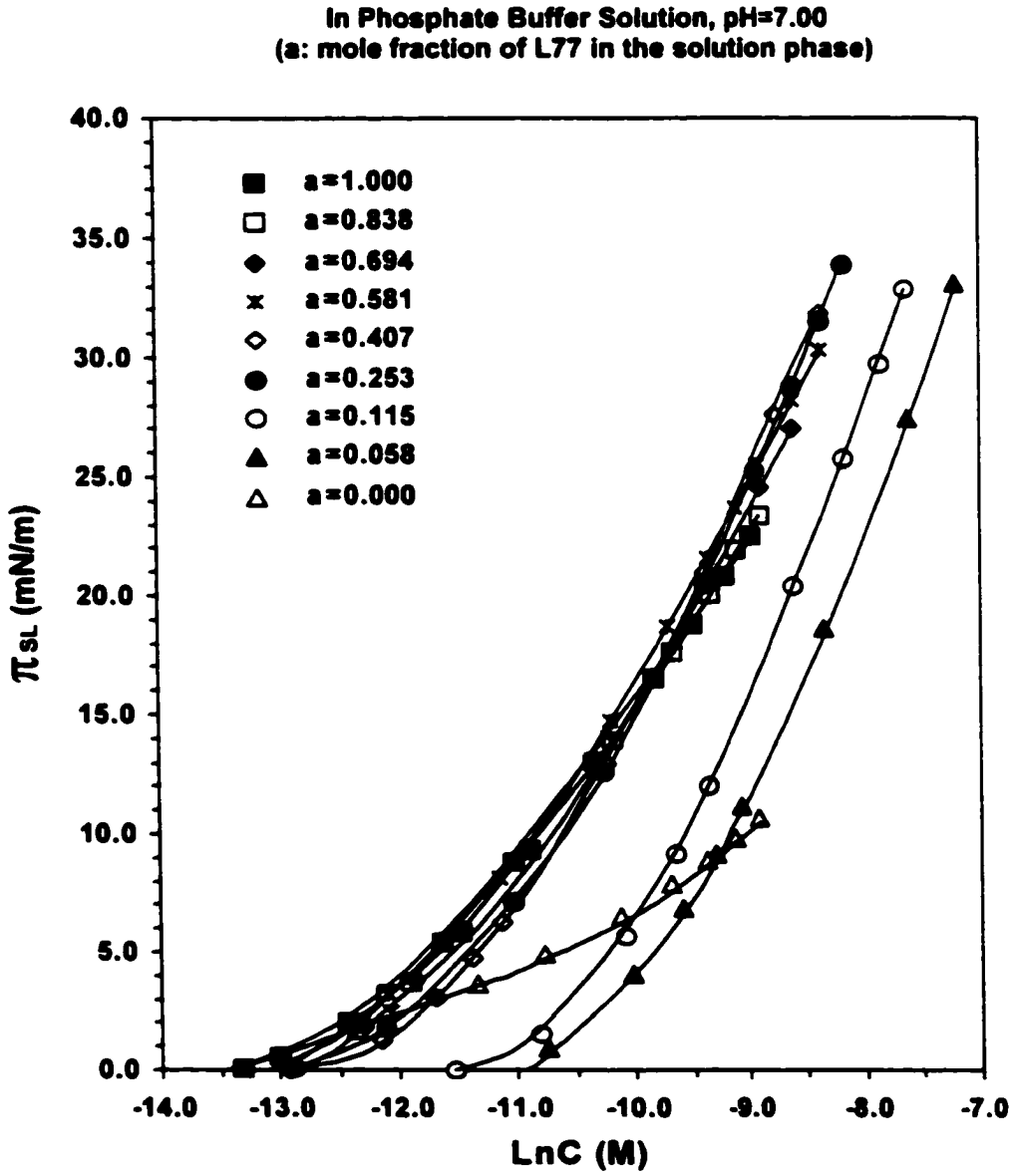

Figure B-63. Plots of π_{SL} vs. LnC for L77, C6P and Their Mixtures

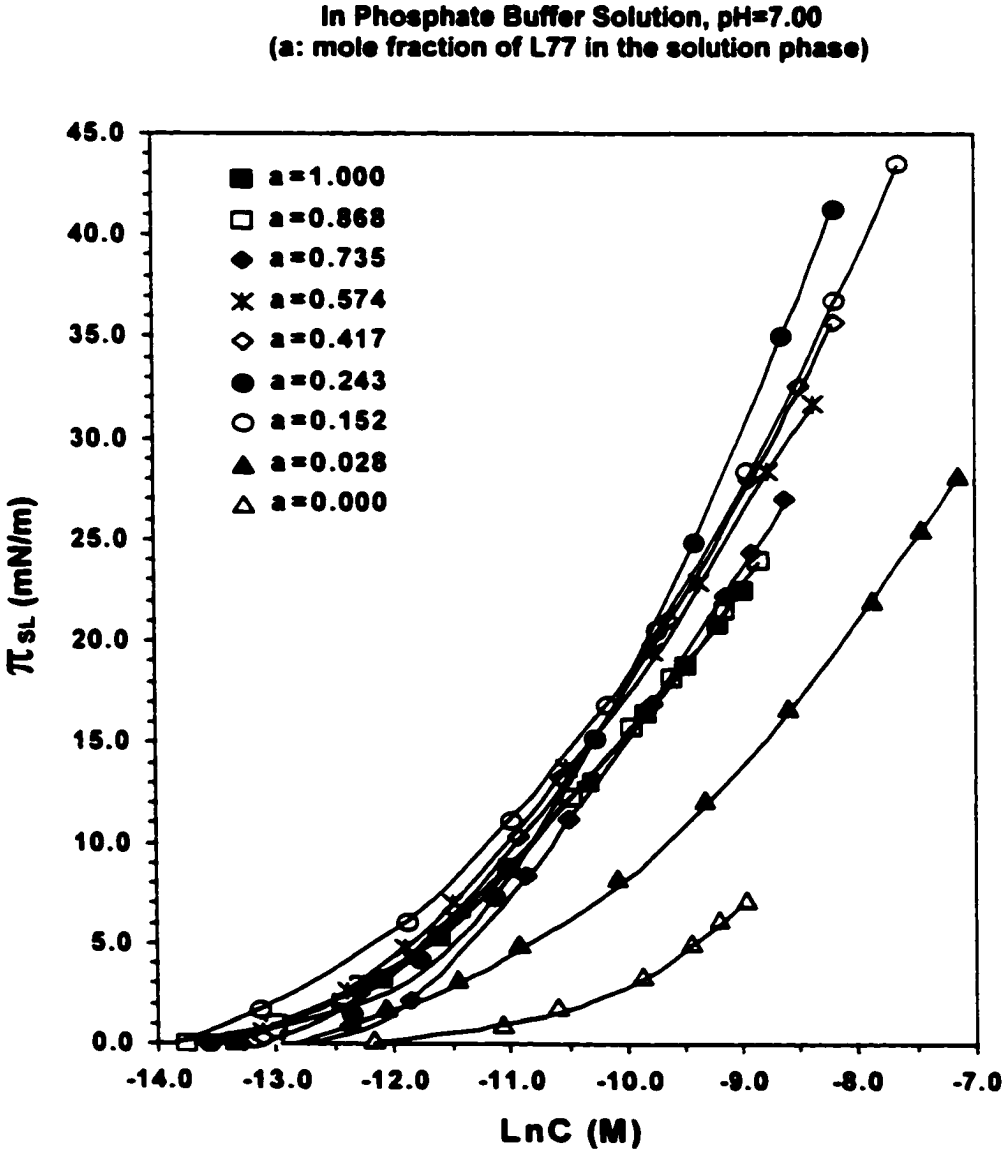

Figure B-64. Plots of π_{SL} vs. LnC for L77, C2,6P and Their Mixtures

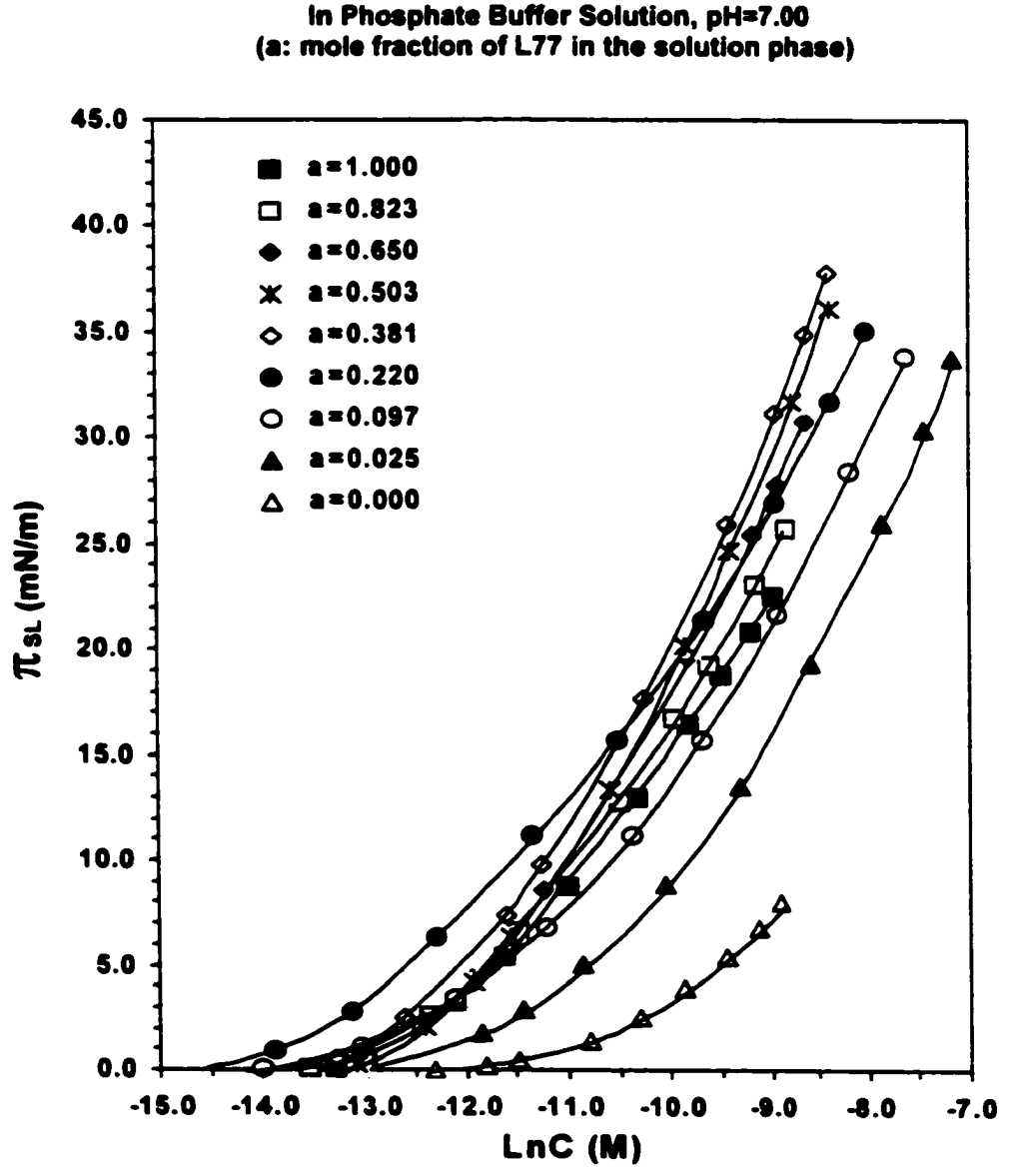

Figure B-65. Plots of π_{SL} vs. LnC for L77, C8P and Their Mixtures

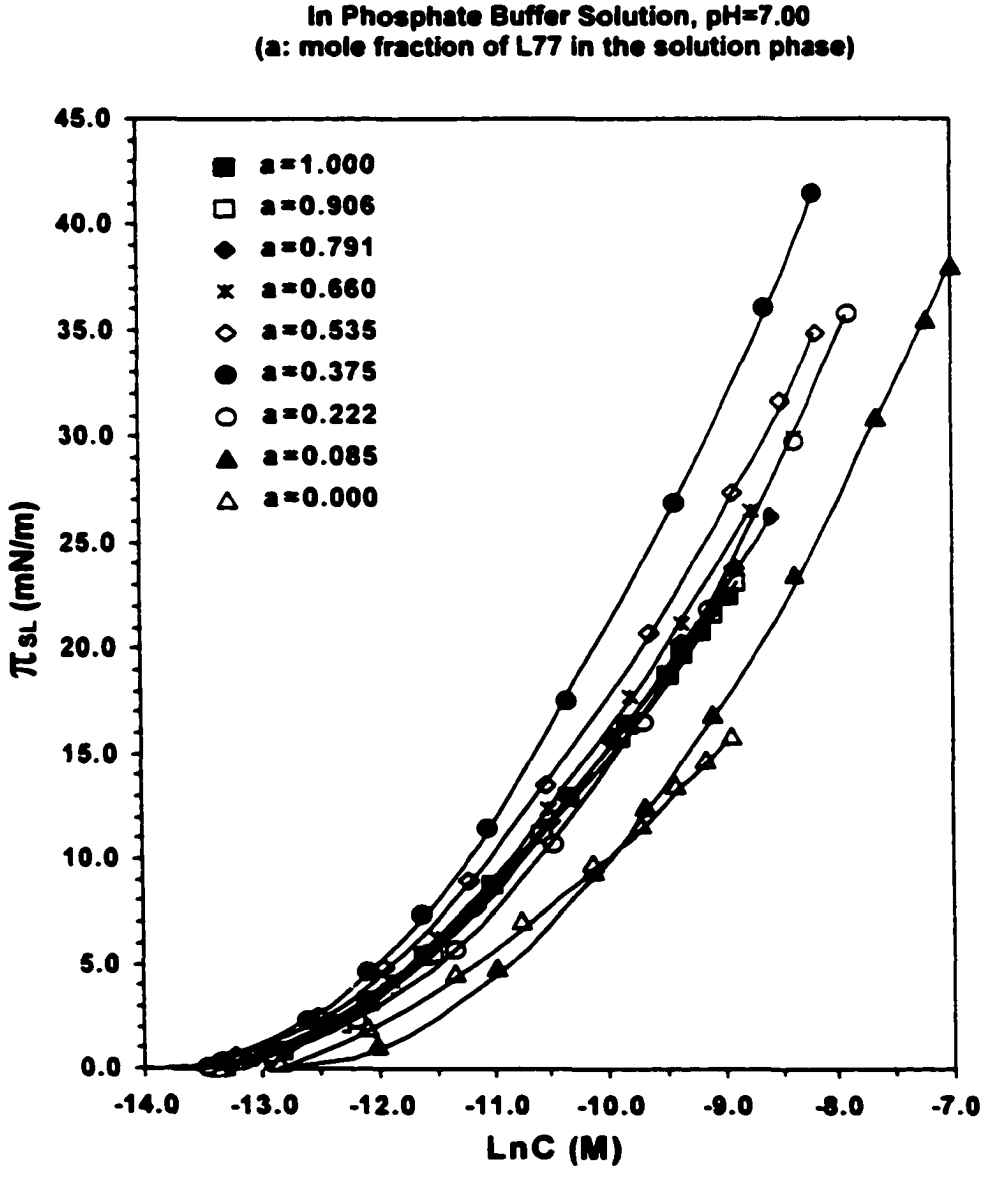

Figure B-66. Plots of π_{SL} vs. LnC for L77, C10P and Their Mixtures

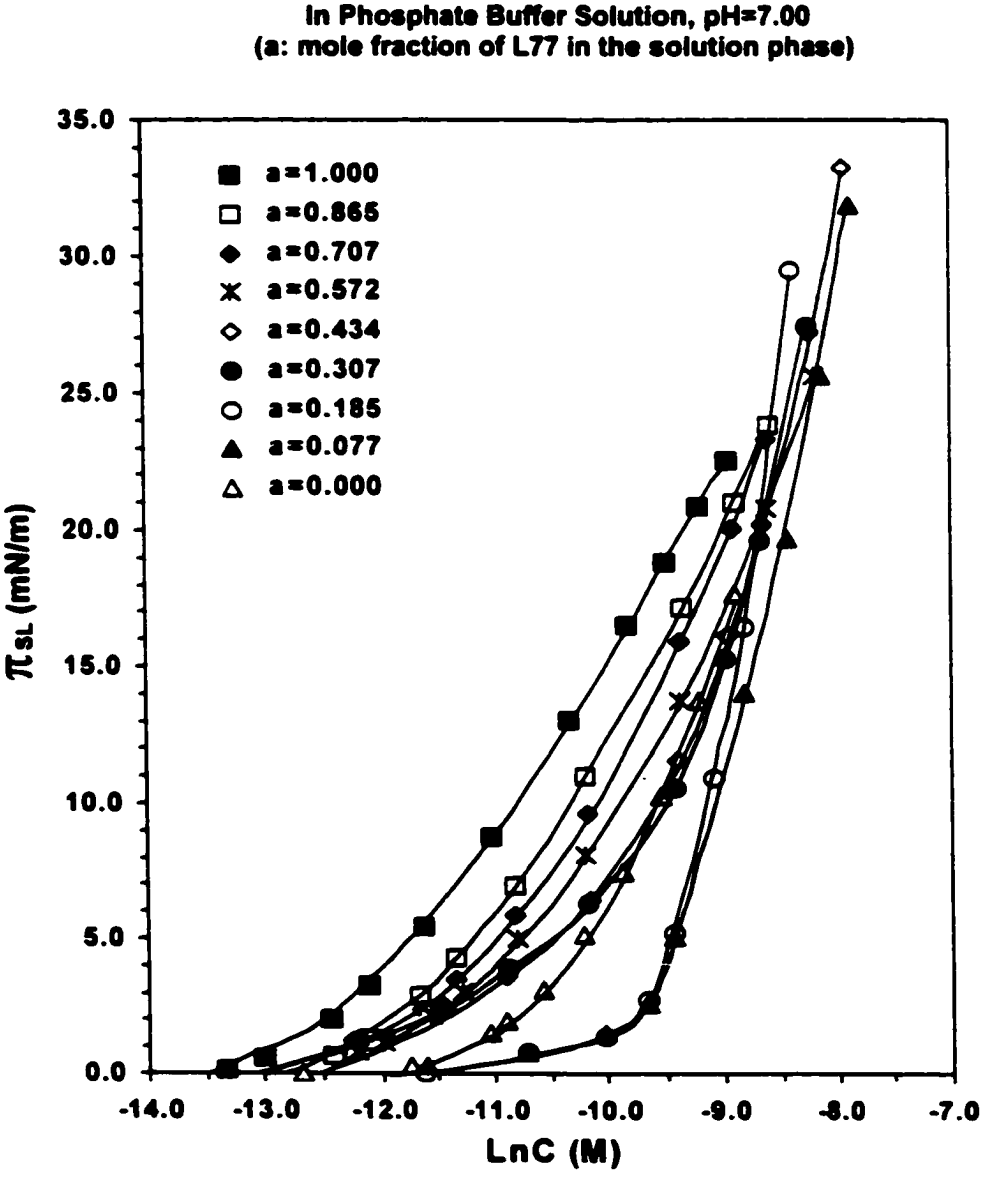

Appendix I

Analysis of Experimental Errors

1. $\Delta|\Gamma_{LA}|_{Max}$: $\Gamma_{LA} = -\frac{1}{nRT}\left(\frac{d\gamma_{LA}}{d\ln C}\right)_T$

$$\Delta|\Gamma_{LA}|_{max} = \left|\frac{\partial\Gamma_{LA}}{\partial T}\right|\cdot\Delta T + \left|\frac{\partial\Gamma_{LA}}{\partial\gamma_{LA}}\right|\cdot\Delta\gamma_{LA} + \left|\frac{\partial\Gamma_{LA}}{\partial C}\right|\cdot\Delta C$$

$$= \left|\frac{1}{nRT^2}\cdot\frac{d\gamma_{LA}}{d\ln C}\right|\cdot\Delta T + \left|\frac{1}{nRT}\cdot\frac{d^2\gamma_{LA}}{(d\ln C)^2}\right|\cdot\left|\left(\frac{d\gamma_{LA}}{d\ln C}\right)^{-1}\right|\cdot\Delta\gamma_{LA} + \left|\frac{1}{nRT}\cdot\frac{d^2\gamma_{LA}}{(d\ln C)^2}\right|\cdot\frac{1}{C}\cdot\Delta C$$

$$= \frac{1}{nRT}\left[\frac{1}{T}\left|\frac{d\gamma_{LA}}{d\ln C}\right|\cdot\Delta T + \left|\frac{d^2\gamma_{LA}}{(d\ln C)^2}\right|\cdot\left|\frac{d\gamma_{LA}}{d\ln C}\right|^{-1}\cdot\Delta\gamma_{LA} + \left|\frac{d^2\gamma_{LA}}{(d\ln C)^2}\right|\cdot\frac{\Delta C}{C}\right]$$

Where: $R = 8.3143\times10^7\ erg\cdot K^{-1}\cdot mol^{-1}$, $T = 298.2\ K$;

n=1 for nonionic surfactants

$$\left(\frac{d\gamma_{LA}}{d\ln C}\right)_T = 14.5; \qquad \frac{d^2\gamma_{LA}}{(d\ln C)^2} = 0.5; \qquad \frac{\Delta C}{C} = 2\times10^{-2}$$

$$\Delta T = 0.5K; \qquad \Delta\gamma_{LA} = 0.5mN/m$$

$$\Delta|\Gamma|_{max} = \frac{1}{8.3143\times10^7\times298.2}\left[\frac{14.5}{298}\times0.5 + 0.5\times\frac{0.5}{14.5} + 0.5\times2\times10^{-2}\right]$$

$$= \frac{1}{2.48\times10^{10}}(0.024 + 0.017 + 0.01) = 2.06\times10^{-12}(mol/cm^2)$$

$$\frac{\Delta|\Gamma_{LA}|_{max}}{\Gamma_{LA}}\times100\% = \frac{2.06\times10^{-12}}{2.52\times10^{-10}}\times100\% = 0.817\%$$

2. $\Delta|\Gamma_{SL}|_{Max}$: $$\Gamma_{SL} = \frac{(C_{ini} - C_{Eq})\cdot V}{W}$$

(1) UV Absorbance Measurements: ABS = εbC

$$\Gamma_{SL} = \frac{(ABS_{ini} - ABS_{Eq})}{\varepsilon \cdot W \cdot b}$$

$$|\ln \Gamma_{SL}| = |\ln(ABS_{ini} - ABS_{eq})| + |\ln V| + |\ln \varepsilon| + |\ln W| + |\ln b|$$

$$\frac{\Delta\Gamma_{SL}}{\Gamma_{SL}} = \frac{\Delta ABS_{ini} + \Delta ABS_{eq}}{|ABS_{ini} - ABS_{eq}|} + \frac{\Delta V}{V} + \frac{\Delta\varepsilon}{\varepsilon} + \frac{\Delta W}{W} + \frac{\Delta b}{b}$$

Where $\Delta ABS_{ini.} = \Delta ABS_{eq.} = 0.002$; $ABS_{ini} = 1.465$; $ABS_{eq} = 0.848$

$\Delta V = 0.05$ml; $V = 40.00$ml; $\Delta\varepsilon = 55\ M^{-1}\cdot cm^{-1}$

$\varepsilon = 6125\ M^{-1}\cdot cm^{-1}$; $\Delta W = 0.0001$ g; $W = 0.5000$ g; $\Delta b = 0$

$$\frac{\Delta\Gamma_{SL}}{\Gamma_{SL}} \times 100\% = \left\{\frac{0.002 + 0.002}{1.465 - 0.848} + \frac{0.05}{40.0} + \frac{55}{6125} + \frac{0.0001}{0.5000}\right\} \times 100\% = 1.49\%$$

(2) Two Phases Titration:

$$C_{ini} = \frac{C \times V_1}{V_0}; \qquad C_{eq} = \frac{C \times V_2}{V_0};$$

$$\Gamma_{SL} = \left(\frac{CV_1}{V_0} - \frac{CV_2}{V_0}\right)\cdot\frac{V}{W} = \frac{C}{V_0}\cdot\frac{V}{W}\cdot(V_1 - V_2)$$

$$\frac{\Delta\Gamma_{SL}}{\Gamma_{SL}} = \frac{\Delta V_1 + \Delta V_2}{V_1 - V_2} + \frac{\Delta C}{C} + \frac{\Delta V_0}{V_0} + \frac{\Delta V}{V} + \frac{\Delta W}{W}$$

Where $\Delta V_1=\Delta V_2=0.10$ ml; $V_1=32.45$ ml, $V_2=18.20$ml

$\Delta V_0=0.02$ml, $V_0=20.00$ ml; $\Delta V=0.05$ml, $V=40.00$ml

$\Delta W=0.0001$ g, $W=0.5000$ g; $\Delta C=0$

$$\frac{\Delta\Gamma_{SL}}{\Gamma_{SL}} \times 100\% = \left(\frac{0.10+0.10}{32.45-18.20} + \frac{0.02}{20.00} + \frac{0.02}{40.00} + \frac{0.0001}{0.5000}\right) \times 100\% = 1.42\%$$

Total: $$\frac{\Delta|\Gamma_{SL}|_{max}}{\Gamma_{SL}} \times 100\% = 1.49\% + 1.42\% = 2.91\%$$

When $\Gamma_{SL} = 2.72\times10^{-10}$ mol/cm^2

$\Delta|\Gamma_{SL}|_{max} = 7.9\times10^{-12}$ mol/cm^2

3. $\Delta|\Gamma_{SA}|_{Max}$: $$\Gamma_{SA} = \Gamma_{SL} - \frac{1}{nRT}\frac{d(\gamma_{LA}\cos\theta)}{d\ln C}$$

$$\Delta|\Gamma_{SA}|_{max} = \Delta|\Gamma_{SL}|_{max} + \frac{1}{nRT} \times \Delta\left|\frac{d(\gamma_{LA}\cos\theta)}{d\ln C}\right|_{max}$$

$$= 7.9\times10^{-12} + \frac{1}{8.3143\times10^{7}\times298.2} \times 0.1$$

$$= 1.2\times10^{-11}(mol/cm^2).$$

Appendix II

Fitted Polynomial Functions for the Curves of Γ_{SL} vs. LnC

1. L77-C4P System

α_{L77}=1.000 y=-9.757-2.690x-0.145x^2, α_{L77}=0.805 y=-12.618-3.229x-0.174x^2

α_{L77}=0.611 y=-14.500-3.820x-0.280x^2, α_{L77}=0.473 y=-12.377-3.470x-0.193x^2

α_{L77}=0.313 y=-16.961-4.561x -0.252x^2, α_{L77}=0.209 y=-19.592-5.454x -0.316x^2

α_{L77}=0.110 y=26.321+4.229x+0.169x^2, α_{L77}=0.029 y=4.874+0.128x -0.028x^2

α_{L77}=0.000 y=5.461+0.837x+0.032x^2

2. L77-CHP System

α_{L77}=0.838 y=-10.094-2.948x-0.159x^2, α_{L77}=0.694 y=-12.270-3.307x-0.179x^2

α_{L77}=0.581 y=-4.673-1.901x-0.115x^2, α_{L77}=0.407 y=-4.747-2.228x-0.144x^2

α_{L77}=0.253 y=3.645-0.578x -0.065x^2, α_{L77}=0.115 y=-3.817-2.270x-0.168x^2

α_{L77}=0.058 y=2.998-0.521x -0.069x^2, α_{L77}=0.000 y=10.597+1.593x+0.060x^2

3. L77-C6P System

α_{L77}=0.868 y=-2.490-1.372x-0.086x^2, α_{L77}=0.735 y=-7.590-2.365x -0.133x^2

α_{L77}=0.574 y=-6.364-2.215x-0.128x^2, α_{L77}=0.417 y=-2.283-1.578x-0.104x^2

α_{L77}=0.243 y=6.980+0.109x-0.027x^2, α_{L77}=0.152 y=10.144+0.837x+0.0095x^2

α_{L77}=0.028 y=9.865-1.022x-0.0225x^2, α_{L77}=0.000 y=-2.312-1.070x-0.0684x^2

4. L77-C2,6P System

α_{L77}=0.823 y=−3.047−1.570x−0.0982x^2, α_{L77}=0.650 y=−4.258−1.988x−0.123x^2

α_{L77}=0.503 y=−1.787−1.709x−0.117x^2, α_{L77}=0.381 y=3.498−0.768x−0.0738x^2

α_{L77}=0.220 y=8.584+0.510x−0.0054x^2, α_{L77}=0.097 y=9.716+0.880x+0.0141x^2

α_{L77}=0.025 y=9.542+1.013x+0.0225x^2, α_{L77}=0.000 y=16.064+2.252x+0.0773x^2

5. L77-C8P System

α_{L77}=0.906 y=−6.906−2.246x−0.128x^2, α_{L77}=0.791 y=−5.927−2.314x−0.125x^2

α_{L77}=0.660 y=−1.251−1.340x−0.0911x^2, α_{L77}=0.535 y=3.247−0.574x−0.0578x^2

α_{L77}=0.375 y=4.464−0.555x−0.0621x^2, α_{L77}=0.222 y=12.288+1.064x+0.0122x^2

α_{L77}=0.085 y=6.150+0.0194x−0.035x^2, α_{L77}=0.000 y=−4.757−1.724x−0.103x^2

6. L77-C10P System

α_{L77}=0.865 y=0.775−1.017x−0.0822x^2, α_{L77}=0.707 y=17.042+1.801x+0.039x^2

α_{L77}=0.572 y=25.412+3.267x+0.102x^2, α_{L77}=0.434 y=83.43+14.118x+0.602x^2

α_{L77}=0.307 y=28.568+3.857x+0.128 x^2, α_{L77}=0.185 y=255.8+46.172x+2.079x^2

α_{L77}=0.077 y=378.46+70.035x+3.231x^2, α_{L77}=0.000 y=62.489+9.799x+0.385x^2

BIBLIOGRAPHY

[1] Nuttall, W. H. Fifth Report on Colloids, etc. *Brit. Assoc. Adv. Sci.* **1923**, pp.38–47

[2] Sluhan, C. A. *J. Chem. Education* **1943**, 20, pp.38–40.

[3] Ackley, R. R. *Ann. N.Y. Acad. Sci.* **1946**, 46, pp.511–529.

[4] Paice, E. S. *J. Textile Inst.* **1949**, 40, pp. 876–90.

[5] Mcworter, C. G. The Use of Adjuvants, in Adjuvants for Herbicides, Weed Science Society of America, Champaign, IL, **1982**, pp.1–8

[6] Gomez H. C. *Grasas Aceites (Seville)* **1983**, 34(4), pp.253–259.

[7] Tadros, T. F. *Adv. Colloid Interface Sci.* **1993**, 46 pp.1–47.

[8] Rosen, M. J.; Dahanayake, M. Industrial Utilization of Surfactants Principles and Practice AOCS Press, Champaign, IL, **2001**, pp.105–119

[9] Behems, R. W. *Weeds* **1964**, 12, pp.255–258

[10] Smith, L. W., Foy, C. L. and Bayer, D. E. *Weed Res.* **1966**, 6, pp.233–242

[11] Beresford, J.; Smith, F. M. Dispersion Powders Liquids, 2nd Ed. **1973**, pp. 383–409.

[12] Hanske, Peter. *Adhaesion* **1974**, 18(8), p.232, pp. 234–238.

[13] O'Lenick, A. J., Jr.; Smith, W. C. *Soap, Cosmet., Chem. Spec.* **1988**, 64(10), p.36, pp.40–42, p.107.

[14] Gaskin, R. E.; Stevens, P. J. G. *Pestic. Sci.* **1993**, 38, 103–110

[15] Knoche, M. *Weed Res.* **1994**, 34, 221–227

[16] Hawkyard, C. J.; Lavasani, M. R. Babaei; Singh, P. A Comparison of Manual and Automated Test Methods for Wettability, Pap. World Conf. Text. Inst., 80th , **2000**, pp.34–45.

[17] Marmur, A., Lelah, M. D. *J. Colloid Interface Sci.* **1980**, 78, 262–270

[18] Brenner, R. E., Jr., Teletzke, G. F., Scriven, L. E., Davis, H. T. *J. Chem. Phys.*, **1984**, 80, 589–601

[19] Sharma, A., Ruckenstein, E. *J. Colloid Interface Sci.*, **1986**, 111, 8–14

[20] Garoff, S., Sirota, E. B., Sinha, S. K., Stanley, H. B. *J. Chem. Phys.*, **1989**, 90, 7505–7512

[21] Rosen, M. J. "*Surfactant and Interfacial Phenomena*", 2nd ed, John Wiley and Sons, New York, **1989**, pp.240–275

[22] Kung,W. C., Scriven, L. E., Davis, H. T. *Chem. Phys.*, **1990**, 149, 141–148

[23] Tiberg, F., Cazabat, A. M. *Langmuir*, **1992**, 8, 2547–2555

[24] Adamson, A. W.; Gast, A. P. "*Physical Chemistry of Surfaces*" 6th ed, John Wiley and Sons, New York, **1997**, pp.465–484

[25] Zhu, S.; Miller, W. G.; Scriven, L. E.; Davis, H. T. *Colloid and Surf A: Physicochemical and Engineering Aspects* **1994**, 90(1), 63-78

[26] Lin, Z.; Hill, R. M.; Davis, H. T; Ward, M. D. *Langmuir*, **1994**, 10(11), 4060–4068

[27] Stoebe, T.; Lin, Z.; Hill, R. M.; Ward, M. D.; Davis, H. T. *Langmuir*, **1996**, 12(2), 337–344

[28] Svitova, T.; Hoffmann, H.; Hill, R. M. *Langmuir*, **1996**, 12(7), 1712–1721.

[29] Stoebe, T.; Lin, Z.; Hill, R. M.; Ward, M. D.; Davis, H. T. *Langmuir*, **1997**, 13(26), 7282–7286

[30] Churaev, N. V.; Starov, V. M. *Colloid J.*, **1998**, 60(6), 790–793

[31] Svitova, T.; Hill, R. M.; Smirnova, Yu.; Stuermer, A.; Yakubov, G. *Langmuir*, **1998**, 14(18), 5023–5031

[32] Stoebe, T.; Hill, R. M.; Ward, M. D.; Scriven, L. E., Davis, H. T. In Silicon Surfactants: Surfactant-Enhanced Spreading, Hill, R. M., Ed.; *Surfactant Science Series* 86; Marcel Dekker, New York, **1999**, pp.275–312

[33] Wagner, R.; Wu, Y.; Berlepsch, H. V.; Zastrow, H.; Weiland, B.; Perepelittchenko, L. *Appl. Organomet. Chem.* ,**1999**, 13(11), 845–855

[34] Churaev, N. V.; Esipova, N. E.; Hill, R. M.; Sobolev, V. D.; Starov, V. M.; Zorin, Z. M. *Langmuir*, **2001**, 17(5), 1338–1348

[35] Churaev, N. V.; Ershov, A. P.; Esipova, N. E.; Hill, R. M.; Sobolev, V. D.; Zorin, Z. M. *Langmuir*, **2001**, 17(5), 1349-1356

[36] Rosen, Milton J.; Song, L. D. *Langmuir*, **1996**, 12(20), 4945–4949

[37] Rosen, Milton J.; Wu, Y. F. *Langmuir*, **2001**, 17(23), 7296–7305

[38] Tiberg, F.; Cazabat, A.M. *Langmuir*, **1994**, 10(7), 2301–2306

[39] Valignat, M. P.; Cazabat, A. M.; Tiberg, F. *Ber. Bunsen-Ges. Phys. Chem.*, **1994**, 98(3), 424–428

[40] He, M.; Lin, Z.; Scriven, L. E.; Davis, H. T.; Snow, S. A. *J. Phys. Chem.* **1994**, 98(24), 6148–6157

[41] Tiberg, F.; Cazabat, A. M. *Europhys. Lett.*, **1994**, 25(3), 205–210

[42] Goddard, E. D.; Ananthapadmanabhan, K. P.; Chandar, P. *Langmuir*, **1995**, 11(4), 1415–1422

[43] Nikolov, A. D.; Wasan, D. T.; Koczo, K. *ASTM Spec. Tech. Publ.*, **1998**, STP 1347(Pesticide Formulations and Application Sysmems: Vol. 18, pp.131–139.

[44] Kunieda, H.; Taoka, H.; Iwanaga, T.; Harashima, A. *Langmuir*, **1998**, 14(18), 5113–5120.

[45] Nikolov, A.; Wasan, D.; Koczo, K.; Policello, G. *Spreading mechanisms of "superwetter" on hydrophobic surfaces* in Book of Abstracts, 216th ACS National Meeting, **1998,** August 23–27, Boston

[46] Venzmer, J.; Wilkowski, S.P. *Organic superspreading surfactant blends vs: Trisiloxane surfactants - mechanisms of spreading and wetting,* 216th ACS National Meeting, **1998,** August 23–27

[47] Victor M. S., Serguei R. K., Manuel G. V. *J. Colloid and Inter. Sci,* **2000,** 227(1), 185–190

[48] Kabalnov, A. *Langmuir,* **2000**, 16(6), 2595–2603

[49] Kabalnov, A. *Eur. Phys. J. E.*, **2000**, 2(3), 255–264

[50] Nikolov, A. D.; Wasan, D. T.; Chengara, A.; Koczo, K.; Policello, G. A.; Kolossvary, I. *Adv. in Colloid and Inter. Sci.*, **2002**, 96(1-3), 325–338

[51] Wu, Y. F.; Rosen, M. J. *Langmuir* , **2002**, 18(6), 2205–2215

[52] Hill, R. M. "*Specialist Surfactants*", Robb, I. D. ed., Blackie Academic and Professional, **1997**, London

[52] Adams, J. W. "*Surface Phenomena and Additives in Water-Based Coatings and Printing Technology*", Sharma, M. K. ed., Plenum Press, **1991**, New York, pp.73–86

[53] Vick, S. C. *"Soap/Cosmetics/Chemical Specialties",* May, **1984**, p. 36

[54] Floyd. D. *in Cosmetic and Pharmaceutic Applications of Polymers*, C. Gebelein et al. Ed., Plenum Press, **1991**, New York, pp.49–62

[55] DiSapio, A.; Fry, C.; Zellner, D. *Preprints 17th IFSCC Congress*, Yokahama, **1992**, pp.334–341

[56] Floyd, D.; Jenni, K. *CRC Handbook on Polymers*, CRC Press, **1998**, Boca Raton, FL

[57] Schaefer, D. *Preprints 15th IFSCC Congress 1*, **1988**, London, p.103

[58] Newmann, W.; Cohen, G.; Hayes, C. J. Soc. Cosmet. Chem. **1973**, 24, 773–784

[59] Garcia, M.; Diaz, J. *J. Soc. Cosmet. Chem.* **1976**, 27, 379–387

[60] Niak, A., Rego, V.; Cot, J. Preprints 14th IFSCC Congress 2, **1986**, Barcelora, pp.993–999

[61] Yahagi, K. *Int. J. Cosmet. Sci. I*, **1991**, 13, 221–227

[62] Suzuki, Y.; Yahagi, K. Perprints 31st SCCJ Congress, **1991**, Tokyo, pp.1–9

[63] Sabia, A. J. *American Dyestuff Reporter* May, **1982**, pp.45–57

[64] Callaghan, I. C. *"Defoaming, Theory and Industrial Applications"* ed. Garrett, P. R.; Marcel Dekker, New York, Surfactant Sci. Ser. **1993**, 45, pp.119–145

[65] Leece, D. R.; Dirou, J. F. *Commun. Soil Sci. Plant Anal.* **1977**, 8, 169–174

[66] Greenberg, J.; Monselise, S. P.; Goldschmidt, E. E. *J. Am. Soc. Hortic. Sci.*, **1987**, 112, 625–628

[67] Adams, A. J.; Fenlon, J. S.; Palmer, A. *Ann. Appl. Biol.* **1988**, 112, 19–31

[68] Green, C. F.; Rowe, L.; Penner, D.; Burow, R. F.; Ekeland, R. A.; Petroff, L.J. *Proceeding of the Brighton Crop Protection Conference, Weeds*, **1989**, 219–224

[69] Knoche, M.; Tamura, H.; Bukovac, M. J. *HortScience*, **1991**, 26, 1948–1950

[70] Stevens, P. J. G. *Pestic. Sic.* **1993**, 38, 103–114

[71] Demes, H.; Gaudchau, M.; Burow, R. F. Pestic. Sci., **1993**, 38, 278–280

[72] Murphy, D. S. *PCT Int. Appl.*, **1994**, 29–33

[73] Gradzielski, M.; Hoffmann, H.; Robisch, P.; Ulbricht, W. *Tenside Surf. Det.*, **1990**, 27, 366–371

[74] Schwarz, E. G.; Reid, W. G. *Ind. Eng. Chem.*, **1964**, 56, 26–35

[75] Bailey, D. L.; Petersen, I. H.; Reid, W. G. In *Chem. Phys. Appl. Surface Active Substances Proc 4th Int Congr*, **1967**, 1, 173–182

[76] Kanner, B.; Reid, W. G., Petersen, I. H. *Ind. Eng. Chem. Prod. Res. Dev.*, **1967**, 6, 88–92

[77] Bailey, D. L. U.S. Patent 3,299,112 **1967**

[78] Bailey, D. L. U.S. Patent 3,359,212 **1967**

[79] Hill, R. M. *Current Opinion in Colloid and Interface Sci.* **1998**, 3, 247–254

[80] Marmur, A. *Adv. Colloid Interface Sci.* **1983**, 19, 75–81

[81] Zabkiewicz, J. A.; Gaskin, R. E. *Adjuvants and Agrochemicals, Vol. 1, Mode of Action and Physiological Activity* (Chow, N. P.; Grant, C. A.; Hinshalwood, A. M. and Simmundsson, E. eds.) CRC Press, **1989**, Boca Raton, FL, , pp.141–156

[82] Gaskin, R. E.; Kirkwood, R. C. Adjuvants and Agrochemicals, Vol. 1, Mode of Action and Physiological Activity (Chow, N. P.; Grant, C. A.; Hinshalwood, A. M. and Simmundsson, E. eds.) CRC Press, **1989**, Boca Raton, FL, pp.129–140

[83] Knoche, M.; Tamura, H.; Bukovac, M. *J. Agric. Food Chem*, **1991**, 39, 202–211

[84] Ananthapadamnabhan, K. P.; Goddard, E. D.; Chandar, P. *Colloids Surface*, **1990**, 44, 281–288

[85] Goddard, E. D.; Ananthapadamnabhan, K. P. "*Adjuvants Agrichem.*" Foy, C. L. ed., CRC Press, **1992**, New York, pp.373–384

[86] Zhu, X. Ph.D. Thesis, University of Minnesota, **1992**

[87] C. G. M. Marangoni, *Annln Phys.* (Poggendrof), **1871**, 143, 337

[88] Lin, Z.; Hill, R. M.; Davis, T. D.; Ward, M. D. *Langmuir*, **1996**, 12, 345–351

[89] Stoebe, T.; Hill, R. M.; Ward, M. D.; Davis, H. T. *Langmuir*, **1997**, 13, 7270–7275

[90] Stoebe, T.; Hill, R. M.; Ward, M. D.; Davis, H. T. *Langmuir*, **1997**, 13, 7276–7281

[91] Everett, D. H. *Pure Appl. Chem*, **1972**, 31, 579–590

[92] Gibbs, J. W. *The Collected Works of J. W. Gibbs* , Vol. I, , Longmans, Green, New York, **1931**, p.219

[93] Defay, R.; Prigogine, I.; Bellemans, A.; Everett, D. H. *Surface Tension and Adsorption*, **1966**, John Wiley & Sons, New York, p.62

[94] Gibbs, J. W. *Trans. Com. Acad. III (1876), Collected Works*, Vol. I, Longmans, Green, New York, **1931**

[95] Guggenheim, E. A.; Adam, N. K. *Proc. Roy. Soc.* London, Ser. A, **1933**, 139, p.218

[96] Rosen, M. J. "*Surfactants and Interfacial Phenomena*" 2nd ed., John Wiley and Sons, **1989**, New York, pp.39–41

[97] Wakamatsu, T.; Fuerstenau, D. W. In *Adsorption from Aqueous Solution*, ed. by W. J. Weber, Jr. and E. Matijevic, ACS, Washington DC, **1968**, pp.161-172

[98] Dick, S. G.; Fuerstenau, D. W.; Healy, T. W. *J. Colloid Interface Sci.*, **1971**, 35, 595

[99] Giles, C. H.; D'Silva, N. D.; Easton, I. A. *J. Colloid Interface Sci.*, **1974**, 47, 766

[100] Giles, C. H.; Mac Ewan, T. H.; Nakhwa, S. N.; Smith, D. *J. Chem. Soc.*, **1960**, 3973

[101] Giles, C. H.; Smith, D.; Huitson, A. *J. Colloid Interface Sci.*, **1974**, 47, 755

[102] Rybinski, W. V.; Schwuger, M. In *Nonionic Surfactants-Physical Chemistry*, Schick, J. M. ed.; Surfactant Sci. Series 23; Marcel Dekker, New York, **1987**; p.49

[103] Adamson, A. W.; Gast, A. P. "*Physical Chemistry of Surfaces*", 6th ed.; John Wiley and Sons, New York, **1997**, pp.393–397

[104] Rosen, M. J. "*Surfactants and Interfacial Phenomena*" 2nd ed., John Wiley and Sons, New York, **1989**, pp.44–46

[105] Clunie, J. S.; Ingram, B. T. In *Adsorption from Solution at the Solid/Liquid Interface*, Parfitt, G. D.; Rochester, C. H. ed. Academic Press, **1983**, New York, pp.116–117

[106] Corkill, J. M.; Goodman, J. F.; Tate, J. R. *Trans. Faraday Soc.* **1966**, 62,979

[107] Klimenko, N. A.; Permilovskaya, A. A.; Koganovskii, A. M. *Kolloidn. Zh.*, **1974**, 36, 788

[108] Corkill, J. M.; Goodman, J. F.; Tate, J. R. In *Wetting*, S.C.I. Monograph, No. 2; *Soc. Chem. Ind.*, London, **1966**, p.363

[109] Corkill, J. M.; Goodman, J. F.; Tate, J. R. *Trans. Faraday Soc.* **1967**, 63,2264

[110] Volkov, V. A. *Kolloidn. Zh.*, **1974**, 36, 641

[111] Volkov, V. A. *Kolloidn. Zh.*, **1976**, 36, 135

[112] Bartell, F. E.; Donahue, D. J. *J. Phys. Chem.*, **1952**, 55, 665

[113] Bartell, F. E.; Thomas, T. L.; Fu, Y. *J. Phys. Colloid Chem.*, **1951**, 55, 1456

[114] Kuno, H.; Abe, R.; Tahara, S. *Kolloid-Z.*, **1964**, 198, 77

[115] Barclay, L. M.; Ottewill, R. H. *Spec. Discuss. Faraday Soc. I*, **1970**, 138, 164

[116] Schott, H. *Kolloid-Z.*, **1964**, 199, 158

[117] Schott, H. *J. Colloid Interface Sci.*, **1967**, 23, 46

[118] Van Voorst Vader, F. *Trans. Faraday Soc.*, **1960**, 50, 1078

[119] Rösch, M. In *Nonionic Surfactants*, Schick, J. M. ed.; Marcel Dekker, New York, **1967**; Ch. 22, p.753

[120] Tanford, C.; Nozaki, Y.; Rohde, M. F. *J. Phys. Chem.*, **1977**, 81, 1555

[121] Rosen, M. J.; Gu, B. *Colloids and Surfaces*, **1987**, 23, 119–135

[122] Skange, A.; Spitzer, J. J.; *J. Phys. Chem.*, **1983**, 87(13), 2398

[123] Gillap, W. R.; Weiner, N. D.; Gibaldi, M. J. *Phys. Chem.*, **1968**, 72, 2218

[124] Tamaki, K. *Bull. Chem. Soc. Japan*, **1967**, 40, 38

[125] Naifu, Z.; Gu, T. *Sci. Sinica*, **1979**, 22, 1033

[126] Spitzer, J. J.; Heerze, L. D. *Can. J. Chem.* **1983**, 61, 1067

[127] Rosen, M. J.; Aronson, S. *Colloids Surf.* **1981**, 3, 201

[128] Rosen, M. J. "*Surfactants and Interfacial Phenomena*" 2nd ed., John Wiley and Sons, **1989**, New York, pp.44–46

[129] Rubingh, D. N. In *Solution Chemistry of Surfactants*, Mittal, K. L. ed., Vol. 1, Plenum Press, New York, **1979**, pp.337–354

[130] Rosen, M. J.; Hua, X. Y. *J. Colloid Interface Sci.*, **1982**, 86, 164

[131] Hua, X. Y.; Rosen, M. J. *J. Colloid Interface Sci.*, **1982**, 90, 212

[132] Hua, X. Y.; Rosen, M. J. *J. Colloid Interface Sci.*, **1988**, 125, 730

[133] Schlachter, I.; Feldmann-Krane, G. In *Novel Surfactants* Holmberg, K. ed.; Surfactant Sci. Series 74; Marcel Dekker, New York, **1998**; p.232

[134] Schonhorn, H. *Nature*, **1966**, 210, 896

[135] Schonhorn, H.; Ryan, F. W. *J. Phys. Chem.* **1966**, 70, 3811

[136] Zettlemoyer, A. C. *J. Colloid Interface Sci.* **1968**, 28, 343

[137] Petke, F. D.; Ray, B. R. *J. Colloid Interface Sci.* **1969**, 31, 216

[138] Tadros, M. E.; Hu, P.; Adamson, A. W. *J. Colloid Interface Sci.* **1974**, 49, 184

[139] Tsubouchi, M.; Yamasaki, N.; Yanagisawa, K. *Anal. Chem.* **1985,** 57, 783

[140] O'Connell, A. W. *Anal. Chem.* **1986,** 58, 669

[141] Skoog, D. A.; Leary, J. "Principles of Instrumental Analysis" 4th Ed. Harcout Brace College Publishing, New York, **1992**, p.127

[142] Rosen, M. J.; Zhu, Z. H.; Gu, B.; Murphy, D. S. *Langmuir*, **1988**, 4(6), 1273–1277

[143] Hill, R. M. in "Silicone Surfactants" Hill, R. M. ed. Surfactant Sci. Ser. 86, **1999**, p.20

[144] Rosen, M. J. "*Surfactants and Interfacial Phenomena*" 2nd ed., John Wiley and Sons, **1989**, New York, p.401

[145] Hua, X. Y.; Rosen, M. J. *J. Colloid Interface Sci.*, **1982**, 87, 469

[146] Marmur, A.; Lelah, M. D. *Chem. Eng. Commun.* **1981**, 13, 133–143

[147] Cachile, M.; Cazabat, A. M. *Langmuir*, **1999**, 15, 1515–1521

[148] Radigan, W.; Ghiradella, H.; Frisch, H. L.; Schonhorn, H.; Kwei, T. K. *J. Colloid Interface Sci.*, **1974**, 49, 241

[149] Couzis, A.; Maldarelli, C.; Kumar, N. Abstr. Pap. -Am. Chem. Soc., **2001**, 221st COLL–351